Glucose production in the ultrafiltration system and cell-free xanthan gum production

Sarbatly, Rosalam

Award date:
2006

Awarding institution:
University of Bath

GLUCOSE PRODUCTION IN THE ULTRAFILTRATION SYSTEM AND CELL-FREE XANTHAN GUM PRODUCTION

Submitted by Rosalam Sarbatly
for the Degree of Doctor of Philosophy (PhD)
of the University Of Bath
United Kingdom.
2006

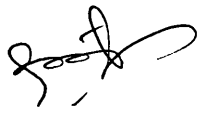

ProQuest LLC
789 East Eisenhower Parkway
P.O. Box 1346
Ann Arbor, MI 48106-1346

ACKNOWLEDGEMENTS

Firstly, I would delight to express a special thank to my wife, Mrs. Maslipah Idris, and my kids, Fatin Arisa and Mohammad Zaydan, and to all members of family.

I would like to express the gratitude to my supervisor Dr. R. England for great moral support and ideas. It is also not possible to make more than a general acknowledgement of help received from many other quarters, but I would like to express particular thanks to the following for help on specialised and technical matters: Emeritus Prof. J.A. Howell, Prof. B. Crittenden, Dr. J. Hubble, Prof. J. Chaudhuri, Prof. Z. Kurtanjek (Uni. of Zagreb, Croatia), Prof. Prof. Felix Garcia-Ochoa (Universidad Complutense, Madrid, Spain), Tan Seri Prof. Dr. Abu Hassan Othman (ex. NC, UMS), Prof. Dr. A. Bono (UMS), Prof. Dr. D. Krisnaiah (UMS), Prof. Dr. Sazali Yaacob (ex. UMS), En. Hela Ladin Mohd Dahlan (UMS), Prof. Dr. Rakmi Abdul Rahman (UKM), Mr. M. Forsyth, Mr. F. Barkley, Mr. R. Bull, Mr. J. Bishop, Mr. M. Newnes, Mr. R. Brain, and Ms. S. Baker.

Thanks also to the University of Bath, the Universiti Malaysia Sabah (UMS), and the Malaysian Government, perhaps I could get more support in the future.

ABSTRACT

The study reported in this thesis is the development and modelling of a process for the production of a continuous and clean glucose solution from tapioca starch which is then used as the raw material for production of xanthan gum. To produce a continuous and clean glucose solution ultrafiltration with a 30 kD cut off polysulfone hollow fibre cartridge was used and the conventional starch hydrolysis was replaced with low temperature simultaneous, liquefaction, gelatinisation and saccharification (SLGS). This maintained a low viscosity and low temperature throughout the process thus reducing membrane fouling and enzyme inhibition respectively. The batch SGLS was operated at 55^0C, tapioca starch at w=10 %, and 1:1 of α-amylase and Amyloglocosidase at 6 ml/litre gives a low viscosity < 2.2×10^{-3} pa-s with ~65% of starch converted into glucose. Investigation of the SLGS kinetic has confirmed the developed kinetic model. The kinetic is derived based on the Michaelis-Menten equation and the critical assumption is "the balanced reactions of gelatinisation-liquefaction and the gelatinisation rate are set as the limiting factor". Following the successful kinetic study, a continuous operation for extraction of the mixed glucose solution was carried out using the developed ultrafiltration system at 55^0C and 0.5 bar. The system was operated within the critical flux region, giving a constant flux of ~14.5 liter/m^2-h, and a glucose solution of ~64g/liter concentration. The 30kD membrane also effectively retained the high degree polysaccharides giving a permeate of >98% glucose purity after 30 minutes operation and was at a steady state over 8 hours continuous operation. The produced glucose solution was used for production of cells-free xanthan gum. The results showed that the xanthan gum kinetic has effectively the same biomass accumulation, glucose consumption and xanthan gum production as that produced using pure glucose under standard procedures.

LIST OF FIGURES

Fig. 1-1: Various processes for hydrolysis of starch.

Fig. 1-2: A combined of continuous, sterile and clean glucose production with xanthan gum process

Fig. 2-1: Conversional starch hydrolysis process

Fig. 2-2: The amount of glucose, maltose, maltotrios, maltoheptaose, maltopentaose and maltotetraose (as weight % of total) as a function of the dextrose equivalent for the hydrolysis of amylopectin potato starch (10% w/w) with B.licheniformis α-amylase at different temperature.

Fig. 2-3: Effect of temperature on conversion during batch hydrolysis of starch (pH=5.8, $71<\theta<87^0$C, S_o=100g/dm^3, E_{01}=0.2cm^3/dm^3)

Fig. 2-4: Effect of temperature on saccharification of barley starch by 0.15 ml α-amylase and 0.15 ml glucoamylase per litre

Fig. 2.5: A Schematic diagram of the concentration polarisation

Fig. 2.6: Dope solution agitated by the mechanical roller.

Fig. 2-7: Cross-sectional SEM morphology of blend asymmetric membrane, pure PAN (0 wt%), 10, 30, and 40 wt% of PAN-r-SAPS respectively

Fig. 2-8: A typical of schematic diagram of dry-wet spinning process.

Fig. 2.9: Morphology Structure of Ceramic Membrane

Fig. 2-10: Outline of the conventional and the alternative processes

Fig. 2.11: Structure unit of xanthan gum

Fig. 2-12: Entner-Doudoroff Pathway

Fig. 2-13: The Trycarborxylic Acid Cycle

Fig. 2-14: Flow sheet of xanthan production in conventional stirred tank fermentor.

Fig. 3-1: pH changes against intervals time during SGLS of tapioca starch ($\gamma_{S_0} = 100$ g/litre, $\sigma_{E_0^{mix}} = 0.9$ ml/litre, and T=60^{0}C).

Fig. 3-2: Glucose concentrations at different enzymes concentration. $\gamma_{S_0} = 100$ g/litre and T=55 ^{0}C.

Fig. 3-3: Glucose conversion at different starch concentrations and at 6ml/lkg enzymes to starch ratio, and T=55^{0}C.

Fig. 3-4: Temperature effects on the rate of glucose production. $\gamma_{S_0} = 100$ g/litre , and $\sigma_{E_0^{mix}}$ =0.9 was used.

Fig. 3-5: Relative productivity curves ($\psi^{relative}_{productivity}$) of the SGLS process at T=55^{0}C

Fig. 3-6: Plots of (a) the obtain a half of maximum glucose production (τ), and (b) τ/γ_{S_0} against the concentration of enzymes ($\sigma_{E_0^{mix}}$)

Fig. 3-7: The enzymes and starch concentrations effects on (a) Γ_{max}, and (b) $\Gamma_{max}/\gamma_{S_0}$ at T=55^{0}C.

Fig. 3-8: Plots of enzymes activity at T=55^{0}C

Fig. 3-9: Graph showing the relationship of the $\sigma_{E_0^{mix}}$ to the $\alpha^{max}_{55^0C}$.

Fig. 3-10: **(a, b, c, d):**

Comparison plots of the rate of glucose formation with the developed models at different concentrations of the enzymes and a fixed starch concentration at 100g/liter. The enzyme concentration; (a) 0.3 ml/liter, (b) 0.6 ml/liter, (c) 0.9 ml/liter and (d) 1.2 ml/liter.

Fig. 3-11 (a, b):

Plots of the *m* values obtained experimentally against t/τ at T=55^{0}C for (a) fixed starch concentration of 100g/litre and (b) fixed ratio of enzyme to starch concentration of 6 ml/kg.

Fig. 3-12: Plots of the *m, m/B* and *B* at $\gamma_{S_0} = 100$ g/litre, $\sigma_{E_o^{mix}} = 0.9$ ml/litre and T=55^{0}C

Fig. 3-13 (a, b, c, d):

Comparison experimental rate of glucose formation versus value predicted by model with consideration of enzymes decay.

Fig. 3-14: Comparison of the kinetic obtained from (a) experiments and (b) the developed kinetic model of Equation 3-69. $\gamma_{S_0} = 100$ g/litre and T=55^{0}C.

Fig. 3-15: Plots of m_t at different temperature. $\gamma_{S_0} = 100$ g/litre, and $\sigma_{E_0^{mix}} = 0.9$ ml/litre.

Fig. 3-16: Temperature effect on the kinetic of Glucose production

Fig. 4-1 : The process flow diagram of the ultrafiltration process

Fig. 4-2: The Reactor Diagram Unit

Fig. 4-3: The Settling Tank Diagram Unit

Fig. 4-4: The Membrane Module Diagram Unit

Fig. 4-5: Pictures of (a) a 30 kD hollow fibre membrane module (b) ceramic membranes and casing.

Fig. 4-6: A Picture of the Laboratory Reactor Unit

Fig. 4-7: The layers of the polymers inside the cylinder column mounted on the settling tank

Fig. 4-8: The HPLC spectrum (a) after 30 minute operation (b) when steady state, after 300 minute.T_R=55^{0}C, T_M =50^{0}C and P=0.5 bar.

Fig. 4-9: UV-Visible spectrophotometer transmitted spectrums

Fig. 4-10: Plots of the glucose concentration and flux at T_R=55^{0}C, T_M =50^{0}C and P=0.5 bar.

Fig. 4-11: Plots of (a) the glucose concentration and (b) the progress of fluxes at T=55^{0}C, $\sigma_{E_0^{mix}} = 0.6$ ml/litre, and $\gamma_{S_0} = 100$ g/litre

Fig. 4-12: Plots of (a) the glucose concentration and (b) the fluxes at P=1bar $\sigma_{E_0^{mix}} = 0.6$ ml/litre, and $\gamma_{S_0} = 100$ g/litre

Fig. 4-13: Comparison of the glucose concentration by batch process in the Flask and the Ultrafiltration System. T_R=55^{0}C, $\gamma_{S_0} = 100$ g/litre, and $\sigma_{E_0^{mix}} = 0.6$ ml/litre.

Fig. 5-1: Curves of Xanthan gum, glucose, and biomass during Batch Fermentation. (a) Using packed matrix support and the glucose was purchased from Fisher Scientific, (b) Using unpacked matrix support and the glucose was purchased from Fisher Scientific (c) Free-cell fermentation using the glucose was produced in-situ and (d) Free cell fermentation (control experiment) using the glucose was purchased from Fisher Scientific.

Fig. 5-2: Comparison curves side by side for (a) glucose, (b) biomass and (c) xanthan gum.

Fig. 6.1: Schematic Representation of Experiment setup. (1). Mixing tank with magnetic stirrer (2) Packed-bed bioreactor (3) Sterilized air (4) Inoculums (5) Membrane filter (6) Concentrated cell- free xanthan gum (7) Permeate substrate and medium recycled stream (8), (9). Water in and out and, (10) Air out.

Fig. 6.2: Example of the proposed bioreactor.

LIST OF TABLES

Table 2-1: Properties of starch from various sources

Table 2-2: Impurity Levels in Native Granular Starches

Table 2-3: Summary of enzymes used in starch hydrolysis

Table 2-4: Value of ε and θ for different experiments

Table 2-5: Effect of temperature on activity decay and reactor performance during continuous experiments

Table 2-6: Some optimum pH and activation energies (Ea) of Bacillus α-amylase

Table 2-7: Some of polymeric membranes prepared by several authors

Table 2-8: Compositions of the support slips

Table 2.9: Some examples of xanthan gum in food applications

Table 2-10: Comparison of nutrients composition by different authors

Table 2-11: Effect of carbon sources

Table 3-1: Shear stress, shear rate and viscosity of the SGLS hydrolysis with $\gamma_{S_0} = 100$ g/litre, $\sigma_{E_0^{mix}} = 0.9$ ml/litre, and incubated at T=55^{0}C.

Table 3-2: Shear stress, shear rate and viscosity of the control experiment with $\gamma_{S_0} = 100$ g/litre and incubated at T=55^{0}C.

Table 3-3: Summary of glucose production at different concentration of the enzymes. $\gamma_{S_0} = 100$ g/litre and T=55^{0}C

Table 3-4: Summary of glucose production rates at different starch concentrations and at $\sigma_{E_0^{mix}} / \gamma_{S_0} = 6$ ml/kg and T=55^{0}C.

Table 3-5: Summary of the glucose production rate by two temperatures when $\gamma_{S_0} = 100$ g/litre, and $\sigma_{E_0^{mix}}$ =0.9 ml/litre.

Table 3-6: The fitted value when $\gamma_{S_0} = 100$ g/litre, and T=55^{0}C

Table 3-7: The Kinetic Parameters at different temperature when $\gamma_{S_0} = 100$ g/litre and $\sigma_{E_0^{mix}} = 0.9$ ml/litre.

Table 4-1: The technical specifications of the physical unit operations of the Ultrafiltration System

Table 4-2: The material and the experiment conditions

Table 4-3: Percentage of transmitted wavelengths. (A 30kD hollow fibre membrane, T_M=room temperature, and P=1bar).

Table 4- 4: Protein passing through a 5kD ceramic Membrane

Table 4- 5: The effect of the applied pressure on the glucose concentration and the flux.

Table 4- 6: Summary of the glucose concentration in batch process carried out in the flask and the ultrafiltration System. T_R=55^{0}C, $\gamma_{S_0} = 100$ g/litre, and $\sigma_{E_0^{mix}} = 0.6$ ml/litre.

Table 4- 7: Comparison summary of batch and continuous processes carried out in the Ultrafiltration System. T_R=55^{0}C, $\gamma_{S_0} = 100$ g/litre, and $\sigma_{E_0^{mix}} = 0.6$ ml/litre.

NOMENCLATURES

A	First order coefficient-constant equation
B	First order coefficient-constant equation (hr^{-1})
C	First order coefficient-constant equation (g-substrate/hr)
D	Diffusion coefficient
F	Filtrate flow (m^3/s)
M	Molecular weight
N	Stirrer speed (RPM)
R	Hydraulic resistance/gas constant
V	the filtrate volume (m^3),
A_m	Membrane area (m^2)
A_1	Empirical constants
A_2	Empirical constants
A_3	Empirical constants
C_b	Concentration in bulk (g/litre)
C_g	Gel layer concentration
C_w	Wall layer concentration
D_t	Tube diameter (m)
D_h	Hydraulic diffusivity (m^2/s).
E_1	α-amylase (termamyl),
E_2	amyloglosacidase (AMG),
E_1S_1	First intermediate product,
E_2S_2	Second intermediate product,
E_{diss}	Dissipated rate of energy consumption (J/s)
$E_{activity}$	Enzymes activity
J_V	Flux (litre/m^2-h)
J_V^{ss}	Steady state flux (litre/m^2-h)

N_S	Number of data
K_S	Saturation or Monod constant (g/litre)
K_m	Michealis-Menten constant
P_M	Overall permeability coefficient
P_n	The product
R_C	Cake Resistance
R_{bl}	Boundary layer resistance
R_{true}	True rejection
R_m	Membrane resistance
R_O	Experimental data of observed rejection
R_{obs}	Rejection coefficient
S	Starch
S_1	Gelatinised starch
S_2	Hydrolysed starch
Sh	Sherwood number,
d_h	Hydraulic diameter of flow channel,
T_B	Water bath temperature (^{0}C)
T_R	Reactor temperature (^{0}C)
T_M	Membrane temperature (^{0}C)
V_R	Total volume of the ultrafiltration system (litre)
$Y_{P/S}$	Product yield coefficient based on substrate
$Y_{O_2/X}$	Oxygen used base on biomass
$Y_{X/N}$	Biomass yield coefficient based on nitrogen
V_S	Superficial air-flow rate (ms^{-1})
$\sum V_{E_0^{mix}}$	Total volume of enzymes (ml)
$\sum w_{glucose}$	Total weight of glucose (gram)
$\psi^{relative}_{productivity}$	Relative productivity (g-glucose/ml-enzymes-h)

Γ_{max}	Maximum production rate (g/litre.hr)
Γ_X	Rate of biomass production, (g-cell/hr)
Γ_p	Production rate (g-product/hr)
Γ_S	Substrate utilisation rate (g-substrate/hr)
dP	Pressure different (bar)
ΔP	Pressure drop (bar)
$\Delta\pi$	Osmotic pressure drop across the membrane
f	Function particular to the system used
t	Time (s),
k	Mass transfer coefficient (kg/m^{2}h),
k_X	Maximum specific growth rate (l g N^{-1} g X^{-1} h^{-1}),
k_P	Maximum specific production rate (l g S^{-1} g X^{-1} h^{-1})
$k_L a$	Oxygen mass transfer coefficient (s^{-1})
k	The rate constant, g-product per hour (g-hr^{-1})
k_1^{gel}	Zero order gelatinization rate velocity (g/hr)
k_2^{gel}	First order gelatinization rate velocity (hr^{-1})
k_1^{liq}	Forward liquefaction velocity (hr^{-1})
k_{-1}^{liq}	Reverse liquefaction velocity (hr^{-1})
k_2^{liq}	Forward liquefaction velocity (hr^{-1})
k_1^{sac}	Forward saccharification velocity (hr^{-1})
k_{-1}^{sac}	Reverse liquefaction velocity (hr^{-1})
k_2^{sac}	Forward liquefaction velocity (hr^{-1})
k_E	Kinetic constant (h^{-2})
k_g	Kinetic constant (h^{-1})
k_S	Kinetic constant (-)
m_l	Mass liquid (kg)
m	A new constant that determine the τ
m_{final}	The final value of m (-)

m_s	Biomass maintenance coefficient (g S^{-1} g X^{-1} h^{-1})
m_{O_2}	Dissolved oxygen consumption coefficient (molO_2 g$X^{-1}h^{-1}$)
m_t	Time decreasing of the *m* value (-)
n	A new constant that giving the production rate at an hour hydrolysis (g/hr)
t_{SS}	Steady state time (h)
x_A	Product conversion
$x_{glucose}$	Glucose conversion
γ_{P_n}	Product concentration (g/litre)
γ_{CO_2}	Oxygen concentration
γ_N	Nitrogen concentration (g/litre)
$\gamma_{P_{glucose}}$	Glucose concentration (g/litre)
$\gamma_{P_{glucose}^{max}}$	Maximum glucose concentration, fixed 10%(w/v) starch strength (g/litre)
γ_{Poison}	Poison concentration (g/litre)
γ_{S_0}	Initial substrate concentration (g/litre)
γ_S	Substrate concentration (g/litre)
$\gamma_{S_0^{lim}}$	Initial substrate concentration after zero order gelatinisation reaction (g/litre)
γ_{S_1}	Gelatinised starch concentration (g/litre)
γ_{S_2}	Liquefied starch concentration (g/litre)
γ_U	By-products and non-productive substrate (g/litre)
γ_X	Biomass concentration (g/litre)
γ_{X_m}	Maximum concentration of biomass (g/litre)
γ_ξ	Other special adverse components or inhibitors concentrations (g/litre)

$\gamma_{E_1S_1}$	Intermediate concentrations of bonded α-amylase (termamyl) enzyme and substrate (g/litre)
$\gamma_{E_2S_2}$	Intermediate concentration of bonded AMG enzyme and substrate (g/litre)
$\gamma_{glucose}^{ss}$	Steady state glucose (g/litre)
$\gamma_{O_2}^{*}$	Saturated oxygen concentration
μ	critical thermal increment
μ_m	Growth specific rate (h^{-1})
ε	Dimensionless constant.
υ	Kinematics viscosity (m^2/s)
η	Viscosity of fluid (pas)
δ	Distance (m)
σ	Reflection coefficient
$\rho_{E_0^{mix}}$	Density of the mixed 1:1 ratio of Termamyl and AMG (g/litre)
ρ_s	Density of solid
ρ_l	Density of liquid
$\sigma_{E_{01}}$	Initial α-amylase concentration (ml/litre)
$\sigma_{E_{02}}$	Initial Amyloglocosidase (AMG) concentration (ml/litre)
σ_{E_1}	α-amylase concentration (ml/litre)
σ_{E_2}	Amyloglocosidase (AMG) concentration (ml/litre)
$\sigma_{E_0^{mix}}$	Volume of the enzymes added over the total reactor volume occupied at 1:1 ratio of termamyl and AMG (ml/litre).
$\sigma_{E_{act}^{mix}}$	Active concentration of the enzymes of termamyl and AMG (ml/litre)
θ	Index of inhibitory effects
α	Unproductive to productive ratio
$\alpha_{55^0C}^{max}$	Maximum unproductive to productive ratio at 55 ^oC

τ	Time that is required to obtain half of the max production (h)
$\tau_{residence}$	Residence time (h)
φ	Operating time required to obtain the total weight of glucose

ABBREVIATIONS

AGUs	Anhydroglucopyranose units
ADP	Adenosine di-phosphate
AMG	Amyloglocosidase
ATP	Adenosine tri phosphate
BLA	B. lichemiformis α-amylase
BAA	B. amyloliquefacines α-amylase
BO	Botanone
CRMR	Continuous recycle membrane reactor
CFBMR	Continuous fluidised bed membrane reactors
CPBMR	Continuous packed bed membrane reactors
CPBR	Centrifugal packed-bed reactor
CSR	Cake specific resistance
EC	Enzymes class number
EE	Diethyl ether
EELMR	Enzyme emulsion liquid membrane reactors
EGMA	Ethylene glycol monomethyl ether
EMR	Enzyme membrane reactors
EMP	Embden-Meyerhop
EOR	Enhanced oil recovery
EPs	Extracellular polysaccharides
DE	Degree of Equivalent
DMAc	Dimethyl acetamide
DMF	Dimethylformamide
DMSO	Dimethylsulfoxide
DNA	Di nucleic acid
DSMZ	Deutsche Sammlung von Mikroorganismen und Zellkulturen GmbH
DP	Concentration of oligosaccharides polymerisation

HF	Hollow fibre
HPLC	High performance liquid chromatography
NF	Nano Filtration
NHO	non hydrolysable oligosaccharides
NMP	*N*-methylpyrrolidone
IO	Intermediately oligosaccharides
kD	Kilo Dalton
mt	Metric tonne
PAN	Polyacrylonitrile
PAN-*r*-SAPS	poly(acrylonitrile-*r*-3-sulfoproyl acylate potassium salt)
PEG	Polyethylene glycols
PEI	Poly (ether imide)
PEO	Polyethylene oxide
PVP	Polyvinylpyrrolidone
Re	Reynolds number
RID	Refractometer index detector
RNA	Ribo nucleic acid
RO	Reverse osmosis
RPM	Rotation per minute
THF	Tetrahydrofuran
TiO_2	Titanium dioxide
TMP	Trans-membrane pressure
SEM	Semi electron microscope
SLGS	Simultaneous, gelatinisation, liquefaction and saccharification
SPPESK	Sulfonated poly, phthalazinone ether sulfone ketone
U	Recalcitrant polymers
UF	Ultrafiltration
USEPA	United State Environmental Protection Agency

CONTENTS OF THE THESIS

		Pages
Author declaration		i
Acknowledgements		ii
Abstract		iii
List of figures		iv
List of tables		viii
Nomenclatures		x
Abbreviations		xvi
Contents of the thesis		xviii
CHAPTER 1: OVERVIEW OF THE RESEARCH		
1-0	INTRODUCTION	1
1-2.	SIMULTANEOUS, GELATINISATION, LIQUEFACTION, AND SACCHARIFICATION (SGLS)	2
1-3	ULTRAFILTRATION IN THE STARCH HYDROLYSIS PROCESS	5
1-4	APPLICATION IN CONTINUOUS XANTHAN GUM MANUFACTURING PROCESS	8
1-5	RESEARCH OBJECTIVES	11
CHAPTER 2: LITRETURE SURVEY		
2-0	INTRODUCTION	13
2-1.	REVIEW OF THE STARCH HYDROLYSIS	14
2-1.1.	Development of the Starch Hydrolysis	14
2-1.2.	Tapioca Starch	16
2-1.3.	Starch Properties	17

2-1.4. Conversional Starch Hydrolysis Processing 19
2-1.5. Enzymes In Starch Hydrolysis 20
2-1.6. Enzyme Activity And Inhibitions 23
2-1.7. Kinetics of Starch Hydrolysis 27
2-1.7.1 Inhibitions Consideration 27
2-1.7.2 Enzyme Decay 28
2-1.7.3 Temperature Effect 29
2-1.7.4 pH Effect 30
2-1.7.5 Evaluations of oligosaccharides 31
2-1.8. Simultaneous Starch Hydrolysis at Low Temperature 33

2-2. REVIEW OF TRANSPORT MECHNASIM AND PREPARATIONS OF THE ULTRAFILTRATION MEMBRANE 38
2-2.1 History and Developments of The Membrane Process 39
2-2.2 Transport Mechanisms in Ultrafiltration Membrane 40
2-2.2.1 Dead-End Filtration Process 41
2-2.2.2 Continuous Tangential Filtration Process 42
2-2.2.3 Gel Layer Model 44
2-2.2.3.1 Prevention of the Gel Layer 47
2-2.2.4 Osmotic Pressure Model 48
2-2.2.5 Mass Transfer Coefficient Correlation 49
2-2.2.5.1 Mass Transfer of Empty Tubes in Turbulent Regime 49
2-2.2.5.2 Mass Transfer of Fluidised Bed Membrane 50
2-2.2.6 The Flux Decrease with Time 51
2-2.2.7 Experiment Evaluation: The Critical Flux 52
2-2.3 Preparations of The Ultrafiltration Membrane 53
2-2.3.1 Polymeric Organic Membrane Preparation 55
2-2.3.2 Thin Layer Flat Sheet Membrane 56
2-2.3.3 Hollow Fibre Membrane 58
2-2.3.4 Inorganic Membrane Preparation 64

2-2.3.5 Coating the Membrane 66

2-3. REVIEW OF XANTHAN GUM 68
2-3.1. Application of Xanthan Gum 69
2-3.2 Chemistry of Xanthan Gum 71
2-3.3. Strain of X. camprestris Sp. 75
2-3.4. Nutrients 77
2-3.5. Batch against Continuous Process 82
2-3.6. Xanthan Gum Kinetics 83
2-3.7. Commercial Productions Processes. 89
2-3.8. Recent Developments of Xanthan Gum Production 91

CHAPTER 3: KINETICS MODELLING AND OPTIMISATION OF THE SIMULTINEOUS, GELATINISATION, LIQUEFACTION AND SACCHARIFICATION (SGLS)

3-0 INTRODUCTION 93
3-1. THE PRINCIPLES OF THE SLGS 94
3-1.1 Reaction Involve 95
3-1. 2 Evaluation of the Increased Viscosity 96
3-1.3 Evaluation of Glucose Formation 98
3-2. MATERIALS AND METHODS 103
3-2.1. Simultaneous Batch Hydrolysis 103
3-2.2. Viscosity Test 104
3-2.3. Glucose Determination by HPLC 105
3-2.4. Data Analysis 106
3-3. RESULTS 106
3-3.1 Viscosity of the SGLS 106
3-3.2. The pH during SGLS 107
3-3.3. Effects of the Enzymes Concentration 109
3-3.4. Effects of the Starch Concentration 111

3-3.5. Effects of Temperature 112
3-4. DISCUSSION 114
3-4.1. The Relative Productivity Analysis 114
3-4.2. The Time to Obtain Half of the Maximum Production 116
3-4.3. The Maximum Production Rate 118
3-4.4. Enzymes Activity 122
3-4.5. The constant *n* 123
3-4.6. The Fraction of the Maximum Unproductive Starch 125
3-4.7. The Constant *m* 126
3-4.8. Consideration of Enzymes Activity Decay in Constant *m*
3-4.9. The Kinetic of Glucose Production 131
3-4.10. Temperature Effect on the Kinetic Model Parameters 138
3-4.11. Error Evaluations on the Models 141
3-5. CONCLUSION 144
145

CHAPTER 4: DEVELOPMENT OF THE ULTRAFILTRATION SYSTEM FOR CONTINUOUS SEPARATION OF THE GLUCOSE SOLUTION

4-0. INTRODUCTION
4-1. MATERIALS AND METHODS 149
4-1.1 The Physical Unit Operations 150
4-1.2 Operation of the Ultrafiltration System 150
4-2. ANALYSIS METHODS 156
4-2.1. Membrane Restoration and Pure Water Test 158
4-2.2. Glucose Concentration and Rejection of High 158
Polysaccharides Analyses 159
4-2.3 Protein Permeation Analysis
4-3. RESULTS AND DISCUSSION 160
4-3.1 The Ultrafiltration System Performance 161
4-3.1.1 Reactor 161

4-3.1.2 Settling Tank 162
4-3.1.3 Membrane Module 163
(a) Polysaccharide Permeation Test 164
(b) Protein Permeation Test 164
4-3.1.4. The Performance of the Continuous Ultrafiltration System 166
168
4-3.2. Effect of the Applied Pressure
4-3.3 Effect of the Temperature 170
4-3.4 Comparison of Batch Processes in the Flask over the Ultrafiltration System: Effects of the Pre-heated Substrate 172
175
4-3.5 Comparison of Batch Process with Continuous Process in the Ultrafiltration System 177
4-4 CONCLUSION
180

CHAPTER 5: IN-SITU GLUCOSE PRODUCTION AND A PACKED BED BIOREACTOR FOR CELL FREE XANTHAN GUM PRODUCTION

5.0 INTRODUCTION
5-1 WHY NEW BIOREACTOR IS REQUIRED 183
5-2. MATERIALS AND METHODS 184
5-2.1 Bacterial Strain 186
5-2.2 Inoculums Preparation 186
5-2.2 Preparation of Packed of Cotton Fibre 186
5-2.3 Batch Fermentation of Packed and Unpacked Supports 187
5-2.5 Cell Density Measurement and Xanthan Gum Recovery 187
5-2.6 Glucose Analysis 188
5-3. RESULTS AND DISCUSSION 188
5-3.1 Sources of Glucose 188
5-3.2 Glucose Consumption 188
5-3.2 Adsorption of Cells 189

5-3.3 Xanthan Gum Production 190
5-4 CONCLUSION 191
5-5 FUTURE RESEARCH IN XANTHAN GUM PRODUCTION 194
195

CHAPTER 6: CONCLUSION AND FUTURE STUDIES

6-1 CONCLUSION
6-2 FUTURE STUDIES 197
203

REFERENCES

APPENDIX 1 *: A STANDARD CALIBRATION CURVE FOR GLUCOSE DETERMINATION BY HPLC*

APPENDIX 2: ERROR ESTIMATION OF THE SAMPLING AND THE FLOW RATE DURING EXPERIMENTS.

APPENDIX 3: *RELATED LISTS OF PUBLISHED, SUBMITTED, WAITING LIST, PROCEEDING PAPERS AND PRESENTATIONS*

CHAPTER 1:

OVERVIEW OF THE RESEARCH

1-0 INTRODUCTION

While starch used to be primarily looked upon as a major source of energy in human diet, its significance as a polysaccharide lending itself to breakdown into sugars has only been discovered in the last two to three decades. In this era, extensive developments in biotechnology products should lead to increase in sugar demand as the raw material. Studies of cell cultures, tissue cultures, fermentations, food supplements, and medical products and applications are the examples and the key issues that are applicable to the whole world. In the wake of this development in which the quality of the produced product relies critically on the quality of raw materials, a significant increase in demand for high standard of raw materials has occurred. Currently, the starch industry has paid great attention to find alternative ways to refine the raw starch syrup carried out after the starch hydrolysis process and before the evaporation of the final product [Hinkova, *et al.* 2004; Slominska and Grzeskowiak-Przywecka, 2004].

Glucose, the raw material that is frequently used in many biotechnology processes, is industrially produced via breakdown of starch-borne polysaccharides into monomeric and/or oligomeric components. The common rule of sugar industries aiming to mass produce products is to compromise the quality. This is not applicable for many processes in

biotechnology industry as the final product would critically rely on the raw material quality making raw material quality one of the uncompromised values. In this respect, the mass production raw material (glucose) by a conventional process has to be further refined to achieve certain standards which also reflect on the higher price that has to be paid.

By narrowing down the application of glucose for fermentation and pure culture processes, sterilisation is a necessary process to obtain sterile media but cleanliness and pure substrate is only controlled by regular quality checking. Generally, increasing the number of unit operations will increase the production cost. Furthermore, although the supplied glucose is described as having a high standard, some uncertainty may require re-processing of the raw material. Thus, this suggests that the industry that critically relies on the raw material should look at producing their glucose at a reasonable investment cost but fully controlling the quality.

1-2. SIMULTINEOUS GELATINISATION, LIQUEFACTION, AND SACCHARIFICATION (SGLS)

One of important areas in biochemical and bio-processing engineering are studies involving enzymes, yeasts, and microbes used to produce valuable products. These materials may be developed or isolated from genetically modified microbes to release certain compounds that are able to fulfil certain process requirements. For example, many enzymes react and are stable at ambient temperature or slightly higher, but because of the process require high temperature, microbes would be genetically modified to produce enzymes stable at high temperatures. These strategies, which may change the natural behaviour, have been used and transferred into industry for mass production. The product may have been distributed worldwide.

Conventionally, glucose production is carried out in three separate steps called gelatinisation, liquefaction and saccharification. Gelatinisation reaction usually is carried out in an extruder or mixing tank at high temperature to completely gelatinise the starch within a short residence-time. This process is energy intensive especially for agitation and pumping. When gelatinisation and liquefaction reactions are carried out simultaneously, high viscosity and high temperature will decrease interactions of enzymes with the substrate, increase enzyme decay, and also be limited to use certain thermo stable enzymes which can be extracted from genetically modified microbes or plants.

A summary of the starch hydrolysis by various methods and various products is given in Fig. 1-1. The processes of (a), (b), (c), and (d) require rapid gelatinisation reaction at temperature more than 80 ^{0}C. The simultaneous, gelatinisation, liquefaction and saccharification (SGLS) indicates by process (e). The consecutive reaction order of the three steps starch hydrolysis carried out at the optimum reaction temperatures respectively are gelatinisation (~140 ^{o}C, ~2 hours) > liquefaction (~80-90^{0}C, ~24 hour) > saccharification (55-60^{0}C, ~48 hours). When the reaction temperature is lowered to a temperature between 55-60^{0}C, gelatinisation reaction rate is affected more as the temperature is reduced by ~85^{0}C, while liquefaction reaction rate is reduced by ~30^{0}C, but the saccharification reaction rate stays constant. The gelatinisation rate is decreased exponentially, while liquefaction rate decreases about 2-3 times for every 10^{0}C temperature step [Rosalam and England, 2004].

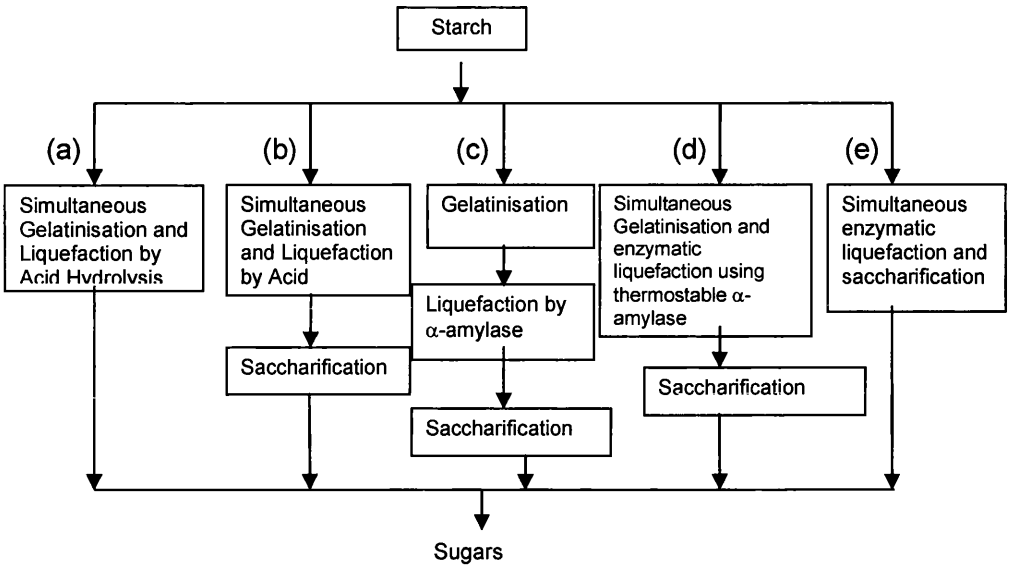

Fig. 1-1: Various processes for hydrolysis of starch

Studying the required reaction time, it should be that at certain fixed temperature the rate of reactions would achieve equilibrium. Thus, the low temperature SGLS is proposed that at the optimum temperature of the saccharification, the reactions can achieve equilibrium. This simultaneous reaction would have the advantages of overlapping the reactions to shorten the reaction time, and would maintain control over formation of the gelatinised starch at a particular time.

Although the SGLS could be an ideal and flexible technique, the gelatinisation reaction can not occur for certain type of starches or retain a high fraction of recalcitrant polymers. However, the literature review supports the SGLS in that the gelatinisation of the tapioca starch and many other starch sources can occur at 55-60^{0}C but at low rates. The conversion can also as high as 70% [Linko & Javanainen 1996; Marchal *et al.* 1999]. This may be the key point on the success of the SGLS.

1-3 ULTRAFILTRATION IN THE STARCH HYDROLYSIS PROCESS

Membrane technology has become a mature separation technology over the past few decades. The main force of membrane technologies is the fact that it works without the addition of chemicals, with relatively low energy requirements, is a relatively simple process, a green process, and known process conductions. Slominska and Grzeskowiak-Przywecka, [2004] mentioned that the application of a vacuum filter that requires precoating has a high maintenance cost, but replacing it with a microfiltration system eliminates the filter aid as well as all problems such as purchasing, handling and disposing of its filter cake. Membrane filtration was also reported to improve the quality of hydrolysates.

Enzymatic starch hydrolysis to produce glucose is a time consuming process. In conventional processes, gelatinisation requires the starch to be heated to 105^0C and held for 5 minutes, then followed by liquefaction at 80-95^0C for ~2 hour, and finally saccharification at 55-60 ^{0}C for ~72 hour [Rosalam and England, 2004]. It implies that if an ultrafiltration membrane is to be used for SGLS, a low flux is required so that the process will have sufficient residence time for the reactions. Because the required flux is very low to guarantee enough residence time during the SGLS reaction, a membrane with small pore sizes and using low trans-membrane pressures (TMP) should be applied, thus it could completely reject the enzymes and high degree of oligosaccharides, and allows a slow release of the product. Low flux would produce a high concentration of glucose, and high flux would produce low concentration of glucose in the permeate stream.

There are many design strategies for the ultrafiltration processes that can be used to perform as the membrane reactor, which could potentially be applied to starch hydrolysis. They are; a) continuous recycle membrane reactors (CRMR) [*Paolucci*-Jeanjean *et al.* 1999; 2000a; Kawai *et al.* 2001],

b) continuous fluidised bed membrane reactors (CFBMR) where immobilised enzyme is fluidised, c) continuous packed bed membrane reactors (CPBMR) where immobilised enzyme particles are used as a packed bed, d) enzyme membrane reactors (EMR) [Giorno *et al.* 2001; Calabro *et al.* 2002; Bayramoglu *et al.* 2004] where enzymes are immobilised onto the membrane surface, and e) enzyme emulsion liquid membrane reactors (EELMR) [Pala *et al.* 2002]. The applications of CFBMRs and CPBMRs for starch hydrolysis have not yet been found in the literature. However, these two types of reactors have been used in the study of other applications such as waste water treatments and fermentation. The CFBMRs and CPBMRs may have a possible use in starch hydrolysis processes.

Based on the literature review, an ultrafiltration membrane that has a pore size in range 2-50nm should be suitable for glucose separation in the SGLS. Sugars that have molecular weights less than 400 and diameters that range from 0.8-1 nm [Bailey and Ollis, 1986] would easily pass through ultra-membrane, whilst the oligosaccharides polymers, unconverted starch, and active amylase enzymes which have molecular weights varying from 10 kD to 210 kD [Gupta R., *et al.* 2003] should be retained in the reactor.

Ultrafiltration processes have been used for continuous separation of hydrolysed starch, they retain high degree polysaccharides, and enables reuse of the enzymes. Enzymes reuse is done by two strategies, a] recycling [Paolucci-Jeanjean *et al.* 2000 and b] immobilising the enzymes onto the membrane surface [López-Ulibarri and Hall, 1997; Sims *et al.* 1992; Bayramoglu *et al.* 2004], depending on the mw cut off and the membrane type. Paolucci-Jeanjean *et al.* [2000b] used the Carbosep M4 membranes (molecular weight cut-off: 50 kD; Orelis, France) to carry out a study on a single step starch hydrolysis using Termamyl enzyme in the CRMR at TMP = 1 bar and T = 80^0C and claimed to be able to completely reject the enzyme and non-hydrolysed starch and pass the hydrolysates. The CRMR for

simultaneous hydrolysis of tapioca starch suggested by Paolucci-Jeanjean *et al.* [2000b] has several disadvantages; flexibility in selection the membrane, a pre-hydrolysis stage to reduce viscosity, and starch milk mass is limited to about w = 10 % to avoid overloading by gelatinised starch due to imbalance reactions between gelatinisation and liquefaction of which might cause heavy fouling to the membrane. The other problems are accumulation of higher degree oligosaccharides in the recirculation in the system and the enzymes decay. The product obtained is a mixture of polysaccharides of several low degree of polymerisations (DPs) with the composition mainly the DP>7. Although the 50kD of the Carbosip membrane is said to be able to reject the Termamyl enzyme, there is no clear evidence to confirm the result e.g. such as protein analysis. The CRMR proposed by Paolucci-Jeanjean *et al.* [2000b] clearly needs improvement for prevention of imbalanced reactions of gelatinisation and liquefaction which may help to prevent flux decline.

Advantages of the membrane system have been identified as having great potential in the starch industry, particularly for continuous extraction of the produced glucose by the SGLS. Flux decline is a major problem discussed in membrane technology. Many strategies have proposed including membrane material modifications [Dai *et al.*2001; Malaisamy *et al.* 2002; Khayet *et al.* 2002; Xu *et al.*2003; Qin *et al.* 2004; Jung 2004]. But, the proposal in the field of membrane bioreactors where the residence time is critically defined by the flux has been proposed by Howell *et al.* [1995]. The proposal has introduced a new terminology called the critical flux [Howell *et al.* 1995; Field *et al.* 1995; Wu, *et al.* 1999]. The proposal philosophy used in determining the critical flux that is used in the membrane reactor is that a constant required residence time would define the flux. This is an inverse objective to conventional filtration which attempts to reach high flux.

The proposal of a balanced reaction of gelatinisation and liquefaction in the simultaneous gelatinisation, liquefaction, and saccharification (SGLS) could be a promising strategy. There are limitations of flux decline and temperature that should be addressed before the system can be a success. However, the SGLS operated at low temperature appears to be a suitable approach to use of the membrane, but the decline in flux would change the residence time and affect the continuous steady state concentration of glucose in permeate stream. The SLGS, carried out at low temperature which needs long residence times to achieve high conversion and low applied pressure to increase the residence time, could be operated at a constant flux within a critical flux regime.

Other than viscosity of solute, build-up of the high degree biopolymers and the un-reacted starch may also increase fouling. Studies by many authors on the simultaneous hydrolysis at low temperature between 37-80^{0}C reveal that the starch can be converted by enzymatic means into the hydrolystates with the final conversion between 60-80 % [Linko & Javanainen, 1996; Marchal *et al.* 1999; Paolucci-Jeanjean *et al.* 2000a; 2001]. These results suggest that not only extraction of the glucose is required but some of the by-products in the form of recalcitrant polymers have to be removed if a continuous operation is required. Hence, a settling tank is included in the ultrafiltration system that should be able to retain the by-products and it also can be used to discard the by-products by pumping them from the system.

1-4 APPLICATION IN CONTINUOUS XANTHAN GUM MANUFACTURING PROCESS

Polymers are important materials used in broad range of industries. Polymers may be produced, collected or synthesised from three sources;

petrochemical, plants or animals. The Biopolymers derived from animals and plants could have similar properties to the petrochemical polymers. Ironically petrochemical polymers were dominant in the global market but nowadays, biopolymers that are renewable, biodegradable, and greener have become more acceptable and are the choice in many applications e.g. personal care products, household products, and an oil recovery. Although biopolymers have many advantages, the increasing the cost for collection and extraction and volatile market prices have encouraged manufacturers to find alternatives to industrially produce the biopolymer.

Xanthan gum is a product industrially produced as ingredient in food consumption, and also having many other applications. Xanthan gum is the preferred product for emulsifying and for suspensions due to the chemical reproducibility and relatively easy supply. In 1969, the FDA gave a final approval for the use of xanthan gum in the food product. The applications of xanthan gum have been spreading in many industries such as in foods, toiletries, oil recovery, cosmetics, in water-based paints, etc. Market demand of xanthan gum has steadily increased at approximately 5-10% every year [Lo *et al.* 1997a]. The price of the processed xanthan gum in the year 2002 was USD 8,000/mt F.O.B for food grade and USD 6,000/mt F.O.B for the industrial grade at the sea port of china [China National United Oil Corporation].

Due to increasing demand and its utilisation, researchers have been studying the use of specific abundant raw materials found worldwide for use in the xanthan gum production. These raw materials are hydrolysed rice, barley and corn flour [Glicksman, 1975]. Acid whey [Charles and Radjai, 1977] sugarcane molasses [El-Salam *et al.* 1993; Kalogiannis *et al.* 2003], mixture of mannose and glucose [Jean-Claude *et al.* 1997], waste sugar beet pulp [Yoo and Harcum, 1999], and peach pulp [Papil *et al.* 1999]. Yields and quality of xanthan gum have been reported to be competitive,

however, glucose as the raw material still gives better product yield [Leela and Sharma, 2000; Becker *et al.* 1998; Harding *et al.* 1995;], constancy of supply, and product quality [Davidson, 1978]. Some of the possible reasons which could cause low yield and quality of xanthan gum manufactured by different substrates are;

i. Deficiency of certain functional groups in utilising carbon sources, resulting in different metabolic pathway reactions being followed. Subsequently, the synthesis produced slightly different structures of extracellular polysaccharides (EPs), or
ii. The nutrient composition varies by different carbon sources; hence the quality of produced xanthan gum would not be as required.
iii. Formation of other by-products.
iv. Components or/and chemical variants in the unmodified starch could be inhibitors.
v. A low yield caused by high concentration of non-reacted compounds would lower the quality, thus post purification processes is required.

In this respect, starch hydrolysis by the ultrafiltration process that produces clean and sterile glucose could be an ideal process for utilising universally available raw materials such as starches. Integrating the ultrafiltration process with the xanthan gum production could lead to solutions of the deficiency stated above. Fig. 1-2 shows the flow diagram of the strategy of the integration process proposed in this thesis.

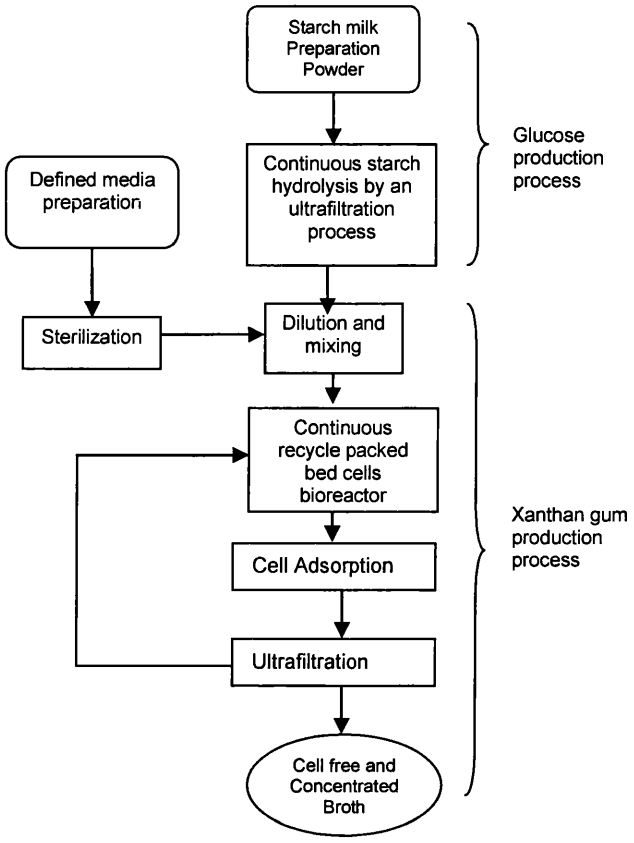

Fig. 1-2: A combined of continuous, sterile and clean glucose production with xanthan gum process

1-5 RESEARCH OBJECTIVES

Fig. 1-2 shows the research proposal. As can be seen, the major contributions in this thesis are; the development of the SGLS and ultrafiltration system used to produce continuous, sterile and clean glucose solution. After the SGLS process in the ultrafiltration has successfully been developed, the SGLS in the ultrafiltration system will be integrated with the xanthan gum production. In this thesis, the integration is limited to the xanthan gum production, but the SGLS process in the ultrafiltration system

could also be done to other biotechnology processes that utilise glucose solution as the substrate.

A few of the objectives of the batch SGLS are outlined here; (1) to develop a mathematic model based on Michaelis-Menten equation, (2) to define certain limitations, (3) to determine the optimum conditions and (3) to verify the developed kinetic model and determine the kinetic parameters.

The next stage after the batch SGLS is, to develop the ultrafiltration system for continuous separation of the glucose solution. The development of the ultrafiltration system will require fulfilling few objectives; (1) to determine the suitable membrane (2) to see the effect of the operational conditions (e.g. applied pressure, temperature, and preheating of the substrate) on the membrane performance and the produced glucose concentration, and (3) to compare the efficiency between the ultrafiltration system and the batch process.

Following development of the ultrafiltration system in producing the clean and pure glucose solution, the process will be integrated with a specific application; in this case the xanthan gum production. Integration of the xanthan gum production with the in-situ glucose production requires a bridge to connect both processes. Thus, comparison studies of two sources of glucose, pure glucose purchased from a local chemical supplier and the glucose produced by the ultrafiltration process, is required, thus studies will provide some information for process integration. As the xanthan gum to be produced has to be high quality which requires significant investigation, only fundamental studies are proposed in this thesis. The study will serve as a basis on the future development of the continuous packed bed recycle bioreactor for xanthan gum production.

CHAPTER 2:

LITERATURE SURVEY

2-0. INTRODUCTION

This literature survey will look in depth at the reaction and technology of the starch hydrolysis, the ultrafiltration membrane process for continuous production of glucose, and the xanthan gum production. Although glucose is being used in many applications, the xanthan gum process has been chosen to be tested for benefiting from the advantage of the proposal of in-situ continuous glucose production due to its current price and increasing demand [Lo *et al.* 1997b]. The SGLS in the ultrafiltration membrane system has huge potential in the next generation processes for manufacturing of pure, clean and sterile glucose for use by many biotechnology industries due to several reasons discussed in the Chapter 1 of this thesis. Despite this, utilisation of membranes has been reported to suffer from the accumulation of high degree polysaccharides when operated at the conventional norm of the starch hydrolysis process at high temperature [Paolucci-Jeanjean *et al.* 2000 a and b]. Additionally, specific membranes would have to be used to withstand the high temperature. It is clear that the standard conventional hydrolysis process is not the appropriate method if membrane processing is to be used. Low temperature SGLS suggested in this work might be an appropriate choice and could provide a solution to the current problem of the starch hydrolysis in the ultrafiltration system as it has been proposed to limit the viscosity throughout the process. This strategy should also minimise

fouling, and low operating temperature would give flexibility for selecting the membrane.

Some important aspects in ultrafiltration membranes, transport mechanism and membrane preparations, will be covered to provide an understanding when designing and operating the membrane system. Furthermore, in the literature survey the review of xanthan gum production, a proposal on a new technique on xanthan gum fermentation may help to prevent the problems of mass transfer and cell viability.

2-1. REVIEW OF THE STARCH HYDROLYSIS

Starch has been an important raw material for the sugar industry in which for centuries the consumer has relied on sugar beet for production of the natural sweeteners. Starch, the carbohydrate resource and food reserve that sustains the initial plant grow of the entire plant, is found in the vegetative parts of the plant, such as in tubers, in living cells of the pith, and in cortex of roots and stems. Although starch from other sources have an academic interest in the study of the problems involved in starch chemistry, only those that can be obtained in high yield from plants which grow or are cultivated in abundance, such as tubers, roots, and cereal grains, are of industrially importantance at present.

2-1.1. Development of the Starch Hydrolysis

There are two methods the starch hydrolysis; the acid and the biocatallyst reactions. Acid hydrolysis of starch that had been widely used in the past randomly cleaves the polymers of anhydroglucopyranose units (AGUs).. This old method was first discovered by a German's chemist,

Gottlied Sigmund Constantin Kirchoff in 1811. Nowadays, bio-catalytic hydrolysis by amylolytic enzymes or debranching enzymes, which had originally been extracted by French chemists, *Payen* and *Persoz* in 1833, has generally replaced the acid method. Amyollytic enzymes that are isolated from active fraction of malts, containing a mixture of α and β amylases which react specifically with certain bonds. These have made it possible to control and design required products.

The heat-stable bacterial α-amylase produced from *Bacillus subtilis*, which is active up to about 90 ^{0}C, was introduced in 1960s. The application of the thermo-stable enzyme has been utilised for the simultaneous reaction of gelatinisation and saccharification. However, the enzyme is insufficiently stable at high temperatures for complete gelatinisation (~140 ^{0}C), thus it could be a good reason for the starch industry to reject of its utilisation. In 1973, a more thermo-stable α-amylase derived from *Basillus licheniformis*, which active up to ~110 ^{0}C was introduced. This temperature is high enough for effectively completion of the gelatinisation reaction, making both high temperature stages of gelatinisation and α-amylase additions by a prior enzymatic liquefaction process unnecessary [Reeve, 1992].

Beginning in the 1811 in Germany to 1970s, the starch industry saw discoveries and developments on acid and enzymatic processes used exclusively for sugars production for human consumption and for increasingly demand on the sweeteners as a raw material for downstream industries. The 1980-1990s saw minor developments in starch technology however the strategy to combine the starch hydrolysis and the production of down stream products was started [Linko and Javanainen, 1996]. Recently, low temperature starch hydrolysis strategies were introduced [Marchal *et al.* 1999; Rosalam and England 2004]. The use of membrane technology has also been brought into the starch industry [Houng *et al.* 1992; Paolucci-Jeanjean *et al.* 1999; 2000 a and b; Hinkove *et al.* 2002; Slominska and

Grzeskowiak-Przywecke 2004; Bayramoglu *et al.* 2004; Rosalam and England 2004] but the proposed technology for fully utilising membranes is still in the laboratory stage.

Generally, commercial sugar industry uses membrane filtration in final purification of products. Some research in membrane technology has recently been devoted to the starch industry by developing a process for continuous production of hydrolysed starch [Houng *et al.* 1992; Paolucci-Jeanjean *et al.* 1999; 2000 a and b; Bayramoglu *et al.* 2004]. The proposal of the continuous recycle membrane bioreactor system (CRMR) seems to require major research and attention for process optimisation and commercialisation. Problems of the membrane process for carrying out the starch hydrolysis are flux decline due to viscosity, recalcitrant starch grains, and intermediate high molecular weight of oligosaccharides. Use of high temperature also would restrict operation to specific membranes. This indicates that the conventional norm of starch hydrolysis may not be appropriate for membrane processing systems but reconsideration of the operating parameters process could make it possible.

2-1.2. Tapioca Starch

In Borneo, a lot of starch sources of tropical origin can be considered for potential industrial development. The products that most likely to be commercially successful are; tapioca, sweet potato, sago, and yam [Krisnaiah and Rosalam, 2002]. In this thesis, tapioca or cassava crop which is easy to grow, and the powder flour which is readily available will be used as the raw material and discussed here.

Tapioca starch, isolated from the tuberous rood of the *Manihot* plant, grows mainly in equatorial climates. Depending on regions of growth, plants

may be known as mandioca, yucca, cassava, or tapioca. There are two general varieties of the plant, *Manihot utilissima* and *Manihot palmate*, the former contains a higher percentage of starch thus it is cultivated in plantations to supply the more modern and progressive mills. Tuberous roots may be bitter or sweet depending on the present of a β-D-glucoside that decomposes to hydrogen cyanide. A glucoside called phaseolunatin appears in tubers and concentration can vary from 0.01 to 0.04 % depends on many factors such as variety, soil, cultivation, climate, and age of plants during harvesting but the processing would reduce cyanide to acceptable levels [Reeve, 1992]. Hard water containing high calcium or/and iron ions used for processing of the starch would react with trace amounts of hydrocyanic acid in the starch to give low starch viscosity and a greyish colour respectively. The tapioca granule is round or oval shape with an indentation on one side, and the granule size varies from 5 to 35μm with an average of 20μm.

2-1.3. Starch Properties

Regardless of the source of starch, they are virtually identical in terms of chemical, physical and organoleptic properties; therefore the starch industry can produce the down stream products from a wide variety of raw materials. Starch is build up of polymers of anhydroglucopyranose units (AGUs) with a general formula of $(C_6H_{10}O_5)_n$. The AGU units are joined by α-glucosidic linkages. AGU is composed of two distinct fractions called amylose and amylopectin; both are homopolymers of D-glucose. In amylose, AGU units are joined exclusively in α-1,4 position to produce linear polymer molecules, while amylopectine units are predominately joined in α-1,4 positions added with branches points resulting from α-1,6 links. The molecular weight and the relative fraction would determine the difference of the granule structure, the rheological property and the gelatinisation

temperature. Table 2-1 shows compositions of the amylose and amylopectine by various sources of starches.

Table 2-1: Properties of starch from various sources [Reeve, 1992]

Starch	Amylose (%)	Amylopectine (%)	Gelatinisation temperature (^{0}C)
Maize	26	74	62-74
Potato	24	76	56-69
Wheat	25	75	52-64
Tapioca	17	83	52-64
Waxy maize	1	99	63-72
Amylomaize	50-75	25-50	>140

Plant sources would also give rise to trace impurities such as lipids, nitrogen, ash, and phosphorus in starch granules. The starch impurity indicated range from about 0.5 to 1.5% [Reeve, 1992]. Nominal levels of selected impurities are shown in Table 2-2.

Table 2-2: Impurity Levels in Native Granular Starches [Reeve, 1992]

Starch	Impurities (wt % db)			
	Lipids	Protein	Ash	Phosphorus
Maize	0.75	0.35	0.1	0.02
Waxy maize	0.25	0.30	0.1	0.01
Milo Maize	0.75	0.30	0.1	
Wheat	0.80	0.35	0.3	0.05
Rice	0.80	0.45	0.5	
Potato	0.15	0.08	0.4	0.08
Tapioca	0.20	0.10	0.2	0.01
Sago	0.15	0.10	0.2	

Starches are not entirely composed of carbohydrate. Some starches, such as potato, contain molecules of amylopectin which are esterified by phosphoric acid. Other starches such as corn contain non-carbohydrate residues, *e.g.* fatty acids, so closely associated with the carbohydrate. Therefore, normal processing of starches or laboratory extraction by common solvents would not be able to extract such substances [Kerr, 1968].

2-1.4. Conventional Starch Hydrolysis Processing

Industrially, various manufacturers use different approaches for starch liquefaction but the principles are the same; the starch granular is slurried at 30-40% (w/w) with cold water containing 20-80 ppm Ca^{2+} at pH 6.0-6.5, and the enzyme added via a metering pump. The α-amylase is usually supplied at high activities of about 0.5-0.6 kg/tonne of starch (about 1500 U/kg dry matter).

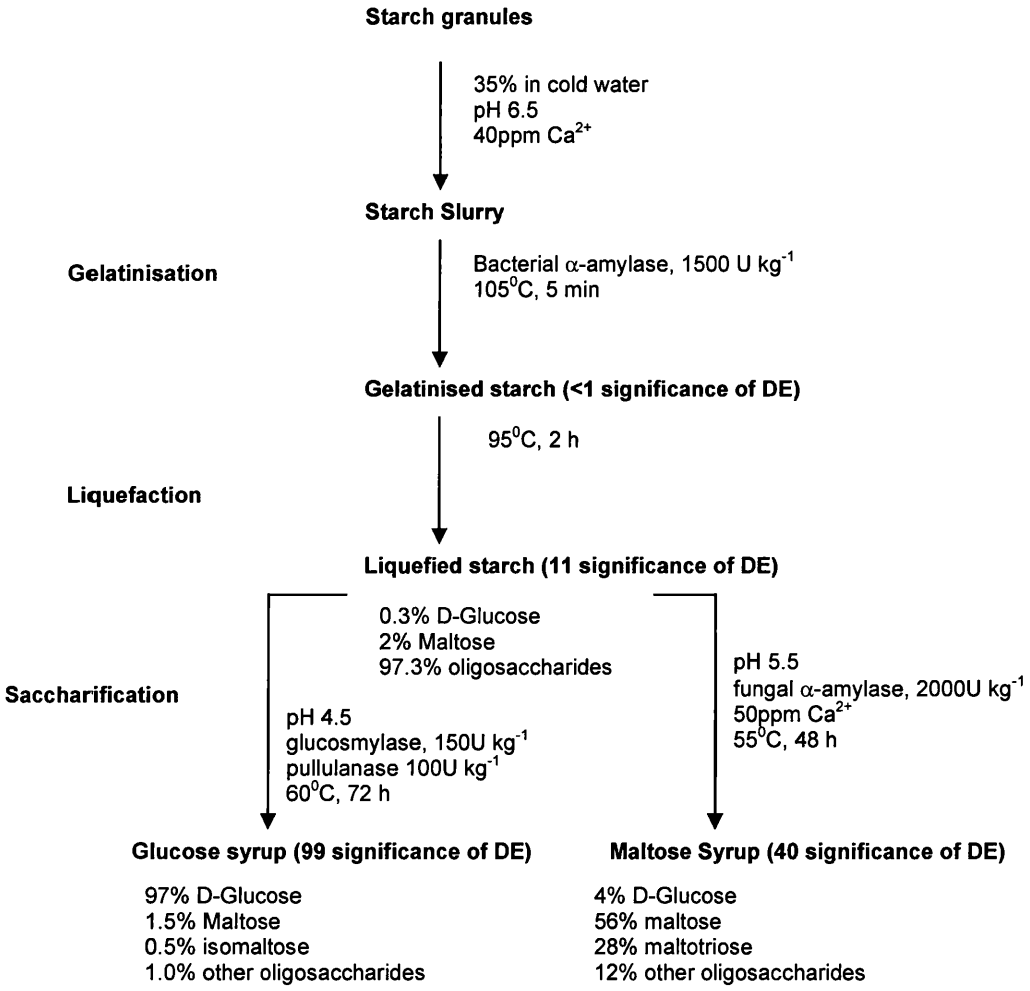

Fig. 2-1: Conventional starch hydrolysis process

When Termamyl is used, the starch slurry plus enzyme is pumped continuously through a jet cooker, heated to 105°C by live steam. Gelatinisation occurs very rapidly, and the enzymatic activity combined with the high shear forces begins the hydrolysis. The residence time in the jet cooker is very brief. The partly gelatinised starch is passed into a series of holding tubes, maintained at 100-105°C and held for 5 min to complete the gelatinisation process. Hydrolysis to the required DE is completed in holding tanks at 90-100°C for 1 to 2 h. These tanks contain baffles to discourage back-mixing. A similar process is used with *β-amyloliquefaciens* and α-amylase but the maximum temperature of 95°C will not be exceeded. This has the drawback that the final 'cooking' stage must be introduced when the required DE has been attained in order to gelatinise recalcitrant starch grains present in some types of starch which would otherwise cause cloudiness in solutions of the final product. Fig. 2-1 shows conventional starch hydrolysis processes.

2-1.5. Enzymes In Starch Hydrolysis

Nomenclature of enzymes for starch hydrolysis used commercially for the starch hydrolysis is summarised in Table 2-3. Each enzyme is given the nomenclature of the EC number, although they are somewhat confusing as sometimes the nomenclature system lumps together the enzymes with subtlely different activities.

The α-amylases (1, 4-α-D-glucan glucanohydrolases) are endohydrolases by which would cleave 1, 4-α-D-glucosidic bonds. It can bypass but cannot hydrolyse 1, 6-α-D-glucosidic branch-points. Commercial enzymes used for industrial hydrolysis of the starch are produced by *Bacillus amyloliquefaciens* supplied by various manufacturers, and by *B. licheniformis*, supplied by Novo Industri A/S as Termamyl. They differ

principally in their tolerance to high temperatures. Termamyl retains more activity at up to 110°C in presence of the starch than the *B. amylofquefaciens* α-amylase. The maximum dextrose of equivalent (DE) obtainable using the bacterial α-amylases is around 40, but prolonged treatment leads to the formation of maltulose (4-α-D-glucopyranosyl-D-fructose), which would resistant to hydrolysis by glucoamylase and α-amylases. The DE value of 8 to12 is used in most commercial process where further saccharification would occur. The principal requirement for liquefaction to this extent is to reduce the viscosity of gelatinised starch thus will ease subsequent processing.

Table 2-3: Summary of enzymes used in starch hydrolysis [Rosalam and England, 2005]

Enzyme	EC number	Source	Action
α-Amylase	3.2.1.1	*Bacillus amyloliquefaciens*	Only α-1,4-oligosaccharide links are cleaved to give α-dextrins and predominantly maltose (DP2), DP3, DP6 and DP7 oligosaccharides
		B. licheniformis	Only α-1,4-oligosaccharide links are cleaved to give α-dextrins and predominantly maltose, DP3, DP4 and DP5 oligosaccharides
		Aspergillus oryzae, *A. niger*	Only α-1,4 oligosaccharide links are cleaved to give α-dextrins and predominantly maltose and DP3 oligosaccharides
Saccharifying α-amylase	3.2.1.1	*B. subtilis* (*amylosacchariticus*)	Only α-1,4-oligosaccharide links are cleaved to give α-dextrins with maltose, DP3, DP4 and up to 50% (w/w) glucose
β-Amylase	3.2.1.2	Malted barley	Only α-1,4-links are cleaved, from non-reducing ends, to give limit dextrins and β-maltose
Glucoamylase	3.2.1.3	*A. niger*	α-1,4 and α-1,6-links are cleaved, from the nonreducing ends, to give β-glucose
Pullulanase	3.2.1.41	*B. acidopullulyticus*	Only α-1,6-links are cleaved to give straight-chain maltodextrins

2-1.6. Enzyme Activity And Inhibitions

Sometimes in many publications the glossary's terms of inhibition and deactivation seem ill defined, thus discussions and explanations of the enzyme activity is obscure. These could result in misunderstandings, and in many cases no effort has been taken to prevent and reduce enzymes inactivation.

This thesis will start with basic explanations of the enzymes inactivation. Deactivation and inhibition are two different mechanisms, but the results are the same; inactivation of the enzymes would contribute to the reduction of the overall enzymes activity. Enzyme deactivation may be defined as reactions where active enzymes molecules undergo chemical changes into inactivate forms that are so called decay. Active enzymes may turn inactivate under certain denaturing conditions which would be influenced by many factors, i.e. pH, temperature, viscosity, and mechanical agitation [Ozbek *et al.* 2001]. Denaturing of the enzymes may be reversible or irreversible; all depend on the load of denaturing conditions that have been experienced. The assessment of enzyme deactivation may be done by exposing the enzyme to be studied to the denaturing conditions over a certain time interval without adding the substrate, then the initial rate activity is assayed by returning the deactivated enzyme solution to the standard condition with substrate.

There are three types of inhibition behaviour of the enzyme-catalysed reactions; competitive, uncompetitive, and non-competitive. Inhibition may be defined as when the enzyme-substrate reaction(s) is/are are destabilised or reduced by inhibitors. Inhibitors can be chemical substances of; inerts which are introduced with the feed materials (substrates, enzymes, and water), or/and the by-products which might form wilt enzyme-substrate reactions, or/and the products themselves, or/and the enzyme(s) itself. Loss

of the enzyme activity may either be reversible, which could be restored by removal of inhibitor(s) or irreversible where loss of the enzyme activity is time dependent and can not be restored during the time scale of interest. If the inhibited enzyme has totally been inactivated, irreversible inhibition would behave as time dependent loss, (i.e lower the fastest production velocity (g/litre.hr), Γ_{max}), in other cases, that involving incomplete inactivation, they could be time-dependent changes in both Γ_{max} and Michealis-Menten constant (K_m).

In case of enzymatic hydrolysis of the starch, inhibitor substances may be as follows:- many alcohols, ascorbic acid, lactose, oxalate, phosphates, sucrose, dextrin, maltose and glucose, and their inhibition effect can be non-competitive, uncompetitive or competitive [Schwimmer, 1950; Atikinson and Mavituna, 1991; Akerberg, *et al.* 2000; MacGregor *et al.* 2002; Lim *et al.* 2003]. Other inhibitors that might be introduced along with the feed materials that are also known as inert substances are heavy-metal ions (e.g. mercury and lead). Heavy metals are the most crucial inhibitors as they usually cause irreversible reactions by binding strongly into the amino acid backbone. However, some inorganic ions such as Ca^{2+}, Mg^{2+}, Sr^{2+}, and Zn^{2+} are required to act as coenzymes by which would enhance the enzyme stability, although the concentration required may vary according to source of the enzyme. Lim *et al.* [2003] have reported that Ca^{2+} ions would help in stabilising the tertiary structures of α-amylase. Since enzymes are highly charged proteins, use of the soluble enzyme might also result in some sort of enzyme-enzyme inhibition [Ozbek *et al.* 2001] caused by ionic disturbances between a pair of enzyme molecules, thus reducing the ability of active sites to bind the starch particles effectively.

Ozbek *et al.* [2001] have investigated the effect of pH, temperature, viscosity, the added amount of the enzyme during preparation, impeller speed, quantity of the hydrolysates, and processing time. They reported that

the optimum condition is a temperature of 60°C, 300rpm impeller speed, and a pH of 6.5. At these conditions, α-amylase enzyme has lost 48% of the initial activity, and the degree of wheat starch hydrolysis is only 40% over 30 min of hydrolysis. Paolucci-Jeanjean *et al.* [2000 a and b] studied enzyme activities of the Termamyl in the retentate by the continuous recycle membrane reactor (CRMR). They have found that the enzyme activity has followed an exponential decay law as below;

$$\sigma_{E_1}(t) = \sigma_{E_{01}} e^{-\varphi t/\tau_{av}} \qquad (2\text{-}1)$$

where $\sigma_{E1}(t)$ and $\sigma_{E_{01}}$ are the running and the initial activity in the retentate (g cm^{-3} min^{-1}), τ_{av} is the average space time while ϕ (see Table 2-4) is the dimensionless constant which is much similar to ε, is a dimensionless constant, and is effectively linked to the loss of enzyme activity in their model. They also have indicated that loss of the enzyme activity has underlined the similarity between the production of small oligosaccharides in the batch reactor and the continuous membrane reactor.

Table 2-4: Value of ε and θ for different experiments [Paolucci-Jeanjean *et al.* 2000b]

$\sigma_{E_{01}}$ (cm^3dm^{-3})	1.8	2.7	3.7	5.5
ε	0.32	0.30	0.31	0.29
θ	-	-	0.29	0.28

[a] θ = 80°C, pH = 5.8, γ_{S_0} = 100 gdm^{-3}, V_R = 6dm

In latest publication, Paolucci-Jeanjean *et al.* [2001] have re-investigated the enzyme activity loss using the same conditions as given in Table 2-4 above. The expression given for the enzyme activity is slightly changed although it still relates to the exponential decay law as described above. The relationship is given below;

$$\sigma_{E_1}(t) = \sigma_{E_{01}} e^{-\alpha t} \qquad (2\text{-}2)$$

where, α (h^{-1}) is the constant equal to 0.27 specified for the certain condition. When the temperature has been changed from 71 to 82 ^{0}C, initial enzyme activity was reported to remain constant, but with no detectable active enzymes after 6 hrs hydrolysis at 87 ^{0}C. The effect of temperature by Paolucci-Jeanjean *et al.* [2001] on the activity decay is presented below.

Table 2-5: Effect of temperature on activity decay and reactor performance during continuous experiments (pH=5.8, γ_{S_0} = 100g/dm^3, $\sigma_{E_{01}}$ = 1.8cm^3/dm^3, u=3m/s, V_R = 9dm^3) [Paolucci-Jeanjean *et al.* 2001].

	Temperature ^{0}C	
	70	80
α (h^{-1})	0.20	0.27
Half time (h)	3.5	2.6
Average permeate flux (dm^3 h^{-1} m^2)	78	95
Average conversion (%)	65	70
Productivity (g h^{-1} dm^{-3})	46	57

From both results, for batch and continuous operations, the loss of enzyme activity is similar by which it could be concluded that, in the continuous operation, addition of the fresh enzyme is required to replace the inactivated enzyme; hence the process could be maintained at maximum performance. The accumulation of the inactivated or non-productive enzymes in the re-circulation system may also lyse to form small compounds which could cause problems for certain process, thus a prevention method may be necessary. The proposed prevention method for the ultrafiltration system will be discussed later in the review of the ultrafiltration system.

2-1.7. Kinetics of Starch Hydrolysis

Kinetics of the starch hydrolysis production would be determined by types of the enzymes (Table 2-3) and the starch origins. Many of the enzymatic reactions fit the classical enzymatic model, the Michaelis-Menten equation;

$$\Gamma = \frac{\Gamma_{max}\gamma_S}{K_m + \gamma_S} = \frac{k\gamma_E\gamma_S}{K_m + \gamma_S} \qquad (2\text{-}3)$$

where

Γ = the production rate (g $dm^{-3}h^{-1}$)

γ_E = enzyme concentration (g dm^{-3})

γ_S = substrate concentration (g dm^{-3})

Γ_{max} = maximum production rate (g $dm^{-3}h^{-1}$)

K_m = Michaelis-Menten constant (g dm^{-3})

k = the kinetic constants (g $cm^{-3}h^{-1}$)

The best fitting values of Γ_{max}, K_m and k may be found by batch or continuous process experiments. However in many cases, the basic Michaelis-Menten model would need modifications to consider correctly more complex reactions. The complexity of the model for starch reactions could be due to the substrates origins, inert components, deactivations, inhibitions, and the physical properties of substrates and enzymes, as well as experimental designs [Nakajima *et al.* 1992; Ahmet *et al.* 2003].

2-1.7.1 Inhibitions Consideration

In order to take into account product inhibition, the following equation is used [Nakajima *et al.* 1992; Ahmet *et al.* 2003],

$$\Gamma^{app} = \frac{\Gamma_{max}^{app} \gamma_S}{K_m^{app}(1+\gamma_P / K_i)+\gamma_S} \qquad (2\text{-}4)$$

γ_P = the product concentration (g dm^{-3})

K_i = inhibition constant (g dm^{-3})

Γ^{app} = apparent production rate (g $dm^{-3}h^{-1}$)

Γ_{max}^{app} = maximum apparent of the production rate (g $dm^{-3}h^{-1}$)

K_m^{app} = apparent Michaelis-Menten constant

Using this model, the kinetic constants have been studied in batch and membrane reactor systems by Nakajima *et al.* [1992], and in packed bed immobilised enzyme reactors by Ahmet *et al.* [2003]. The kinetic model above has actually considered mixed inhibitions in the starch hydrolysis [Schwimmer, 1950; Atkinson 1991; Akerberg *et al.* 2000; MacGregor 2002; Lim *et al.* 2003].

2-1.7.2 Enzyme Decay

Houng *et al.* [1992] have proposed the following Equation 2-5 used for starch hydrolysis for maltose production by a CRMR as;

$$\Gamma^{app} = \frac{\Gamma_{max}^{app} e^{(-\alpha t+\beta t^2)} \cdot \gamma_S}{K_m^{app}(1+\gamma_P / K_i)+\gamma_S} \qquad (2\text{-}5)$$

where α (h^{-1}) and β (h^{-2}) are two new constants. The equation describes the enzyme activity related to the enzyme decay or enzyme stability as the enzyme deactivation is linked with time, thus the constants should vary for different processes (batch or continuous), systems and experimental designs.

As given in Equation 2-1, Paolucci-Jeanjean *et al* [2000a and b] have proposed the enzyme activity decay rate of the Termamyl enzymes to follow the exponential law. By combining the Equation 2-1 and Equation 2-4 for consideration of the enzymes decay rate in continuous process and a long time operation and , a new kinetic model is obtained hence;

$$\Gamma^{app} = \frac{\Gamma_{\max}^{app} e^{-dt/\tau_{av}} \cdot \gamma_S}{K_m^{app}(1+\gamma_P / K_i)+\gamma_S} \qquad (2\text{-}6)$$

The Equations 2-5 and 2-6 are similar but differ in the enzymes decay model over the time space.

2-1.7.3 Temperature Effect

Rates of the chemical reaction increasing with temperature are best described by the Arrhenius Equation as below;

$$\ln\frac{k_1}{k_2} = \frac{\mu}{R}\left[\frac{1}{T_1} - \frac{1}{T_2}\right] \qquad (2\text{-}7)$$

where T_1 and T_2 are the absolute temperature corresponding to reaction velocities k_1 and k_2, R is the gas constant, and μ is the *critical thermal increment* of the constant that would characterise the particular reaction. When this relationship holds, an easier measure can be calculated as;

$$Q_{10} = k_{t+10} / k_t, \qquad (2\text{-}8)$$

where k_t is the rate at temperature t, and k_{t+10} is the rate at 10° C higher. The term $\gamma_{S_0} Q_{10}$ would simply tell us by what factor a rate increases for every 10 ^{0}C rise in temperature.

In biochemical process that are often composed of a complex pathway of many intermediate reactions, the μ and Q_{10} would only be a constant over a limited temperature range, which might be smaller than that under study. A change in temperature may change which of the steps in the pathway is the rate-limiting one, resulting in a sharp change in μ and Q_{10} at particular temperatures. In practice, the interaction of several potentially rate-limiting processes (physical as well as chemical) can lead to gradual, rather than sharp changes in μ with temperature. Even for a single biochemical reaction, the rate increase with temperature may fall off as temperature increases, presumably because of the destruction of the enzymes on which they depend [Yapp, 1970]. Nevertheless, the Arrhenius relationship holds for many biological phenomena under temperature ranges of interest. The slope of the linear relationship between the log of the rate of most biological reactions and the reciprocal of the absolute temperature is the Arrhenius μ divided by approximately 4.6, with μ is defined by the limiting step. For thermo-chemical (enzymatic) reactions, Q_{10} in typically somewhere between 2 and 3: they often go about twice as fast for every 10 ^{o}C rise in temperature [American Physiological Society, Handbook of Physiology, 1964].

2-1.7.4 pH Effect

Marchal *et al.* [1999] have reported that varying the pH from 5.1, to 6.2, and 7.6 at 70^{0}C would not significantly influence the composition of saccharides obtained during B. *licheniformis* α-amylase hydrolysis, although the optimum pH should be used as there is a certain pH that would produce high productivity by giving high enzyme activity.

Table 2-6: Some optimum pH and activation energies (Ea) of Bacillus α-amylase [Marchal *et al.* 1999].

E_a [kJ/mol]	Enzyme	pH	T=^{0}C	Substrate
32.75	Termamyl	6.9	37-90	1% NaBH4 Potato Starch
28.65	Termamyl	6.9	37-90	1% NaBH4 Cassava Starch
25	BLA M27	7	52-85	0.5% Soluble starch
12	BLA BLM 1777	6	30-60	1% Linear soluble starch
30	BLA	8.2	55-85	1% Starch
42	BLA MY10	6	50-75	1% Soluble starch
11.4	BAA K	5.8	26-90	1% Starch

Notes: BLA = *B. lichenformis* α-amylase, BAA = *B. amyloliquefacines* α-amylase. Termamyl is industrial *B. licheniformis* α-amylase as sold by Novo Nordisk (Denmark).

2-1.7.5 Evaluations of Oligosaccharides

Oligosaccharides are categorised into non hydrolysable oligosaccharides (NHO) of DP 1-3 and intermediately oligosaccharides (IO) of DP 4-7. The concentration of NHO with respect to time is given as [Paolucci-Jeanjean *et al.* 2000b];

$$\gamma_{P(t)} = \frac{at^2}{b^2 + t^2} \qquad (2\text{-}9)$$

Gaouar *et al.* [1997] have proposed a similar equation for maltose and glucose production starting from liquefied starch using Maltogenase® for saccharification;

$$\gamma_{p(t)} = \gamma_{P(0)} + \frac{a't}{b'+t} \qquad (2\text{-}10)$$

where $\gamma_{P(0)}$ is the initial product concentration (g.dm^{-3}), *a'* (g.dm^{-3}) and *b'* (min) two constants. As suggested by Paolucci-Jeanjean *et al.* [2000a], IO concentration cannot, however be fitted by a simple equation. After an initial delay, concentration would increase to a maximum and then decrease until a constant value is reached. The new equation may be written as;

$$\gamma_{P(t)} = \frac{at^2}{b^2 + t^2} - \frac{\gamma_c t^4}{d^4 + t^4} \qquad (2\text{-}11)$$

where γ_c (g.dm^{-3}), and *d'(h)* two new constants.

The tapioca starch hydrolysis kinetics by the termamyl enzyme at 80 ^{0}C in a batch and CRMR could be described by a semi-empirically equation in Equation 2-12 [Paolucci-Jeanjean *et al.* 2000b]. The empirical model would describe the concentration of oligosaccharides polymerisation (DP) ranging from 1 to 5 throughout the cassava starch hydrolysis.

$$\gamma_{P(n)} = k_n \left(\sum_{i-m_n}^{\infty} \gamma_i - \sum_{i-m_n}^{\infty} \gamma_i \lim \right) \sigma_E \qquad (2\text{-}12)$$

where $\gamma_{P(n)}$ is the production of oligosaccharide (g dm^3 h^{-1}), γ_i the concentration of the oligosaccharide with a DP equal to *i* (in the retentate for CRMR) (g dm^{-3}), $\gamma_i \lim$ the limit concentration of the oligosaccharide with a DP equal to *i* (in the retentate for the CRMR) (g dm-3), m_n corresponds to the DP of the smallest oligosaccharide leading to the production of a sugar with a DP equal to *n*, $\sigma_{E_{act}}$ the concentration of active enzymes (cm^3 dm^{-3}), always equal to the initial concentration in the batch reactor or continuously decreasing according to $\sigma_E = \sigma_{E(0)} e^{-\varepsilon t / \tau_{av}}$ in the CRMR, k_n a constant (dm^3 cm^{-3} h^{-1}). The values of k_n are similar in both reactors, whereas final

concentrations are different due to retention of high molecular weight products by the membrane and limited reaction yield in the CRMR.

2-1.8. Simultaneous Starch Hydrolysis at Low Temperature

Very few studies of simultaneous gelatinisation liquefaction and saccharification (SGLS) have been found in the literature. Marchal *et al.* [1999] have investigated the simultaneous gelatinisation and liquefaction hydrolysis of amylopectin potato starch to produce low-molecular weight products at different temperatures of 50, 70, 90 ^{0}C by Bacillus *licheniformis* α-amylase. They found that changing the temperature would not significantly increase the glucose concentration but it would effectively increase the concentration of high degree polysaccharides. The temperature effect is shown in Fig. 2-2 below:

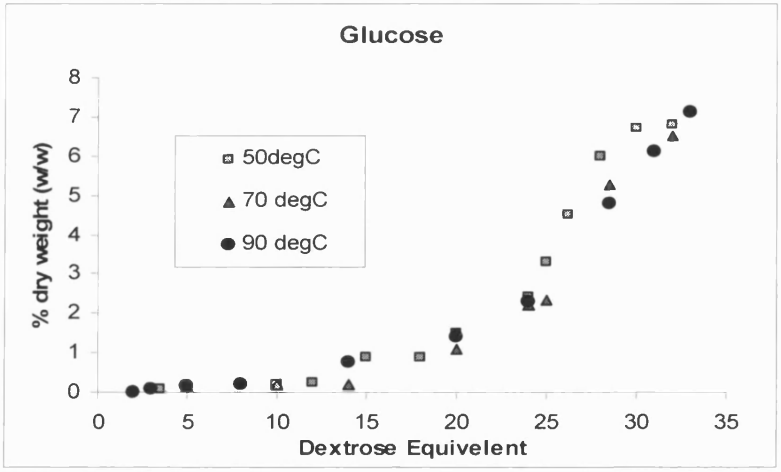

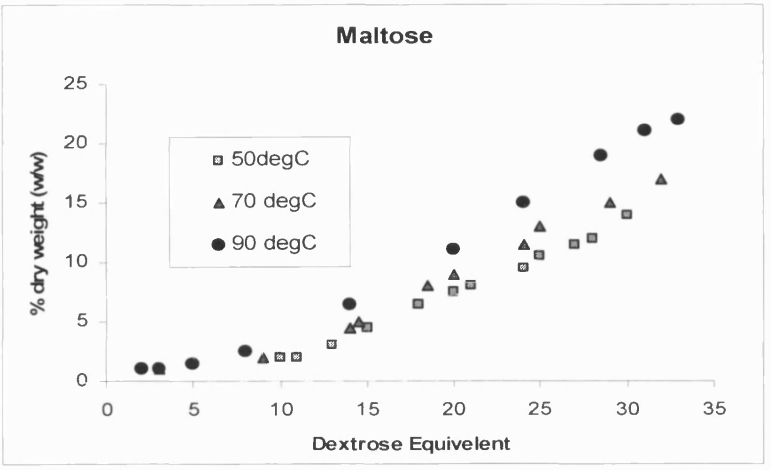
Maltose
% dry weight (w/w)
25
20
15
10
5
0
0
5
10
15
20
25
30
35
Dextrose Equivelent
50degC
70 degC
90 degC

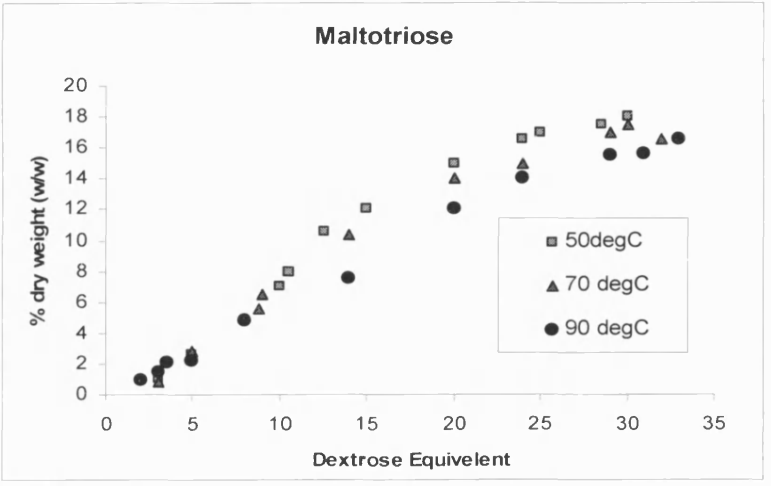
Maltotriose
% dry weight (w/w)
20
18
16
14
12
10
8
6
4
2
0
0
5
10
15
20
25
30
35
Dextrose Equivelent
50degC
70 degC
90 degC

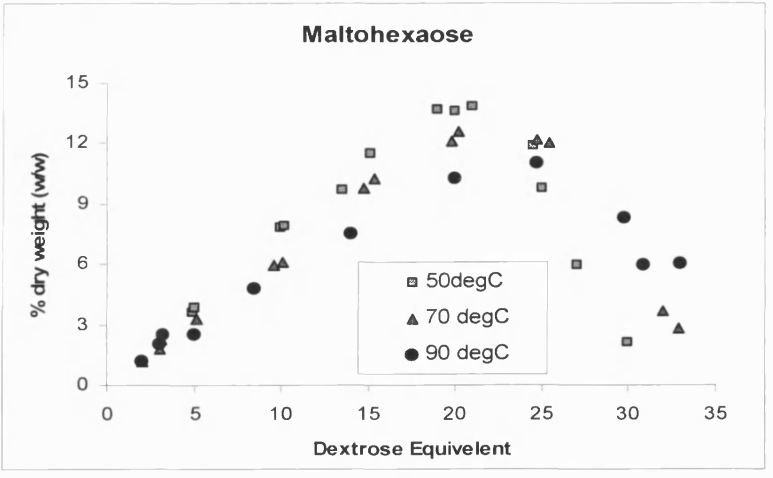
Maltohexaose
% dry weight (w/w)
15
12
9
6
3
0
0
5
10
15
20
25
30
35
Dextrose Equivelent
50degC
70 degC
90 degC

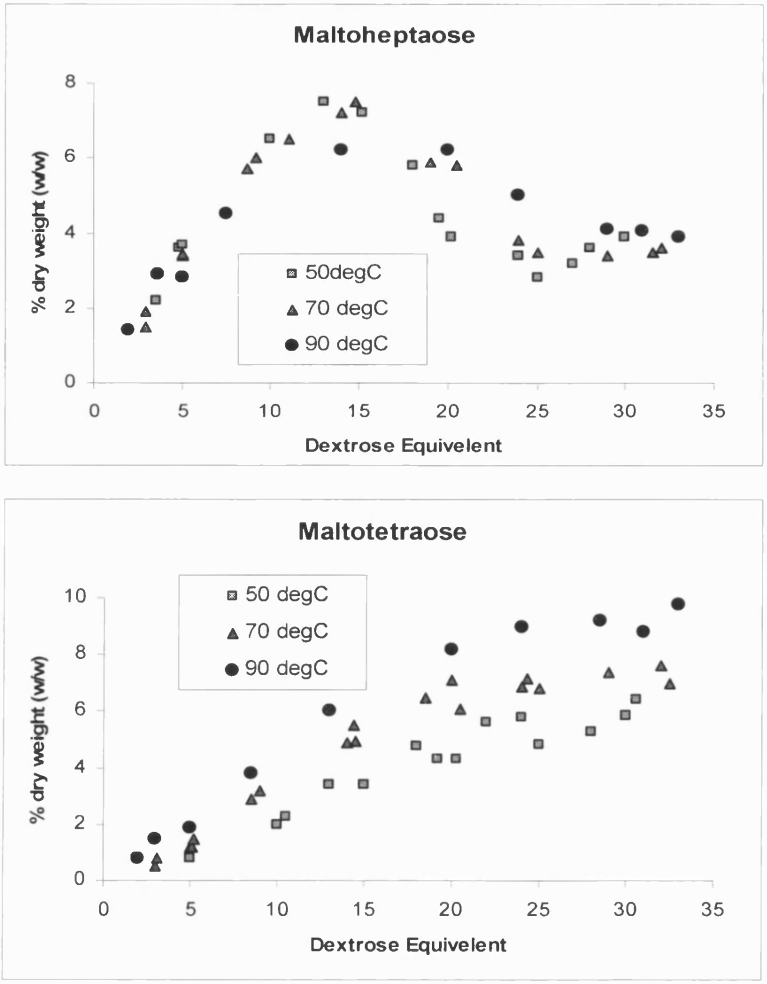

Fig. 2-2: The amount of glucose, maltose, maltotriose, maltoheptaose, maltopentaose and maltotetraose (as weight % of total) as a function of the dextrose equivalent for the hydrolysis of amylopectin potato starch (10% w/w) with B.licheniformis α-amylase at different temperature [Marchal *et al.* 1999].

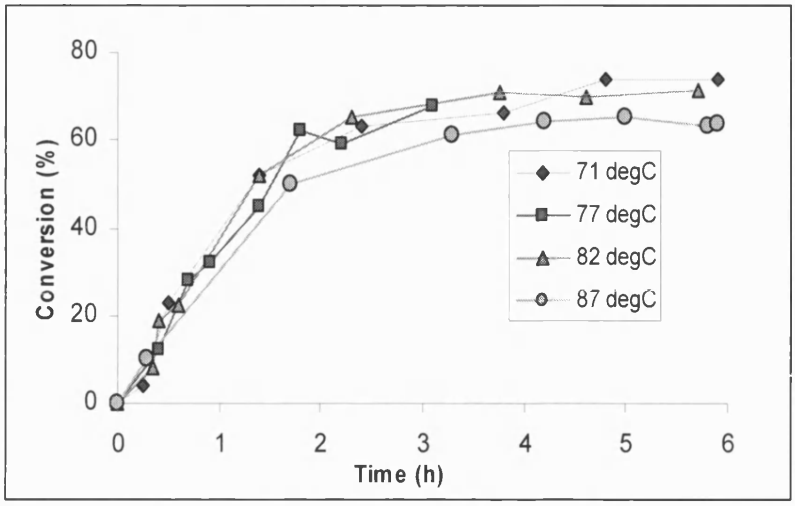

Fig. 2-3: Effect of temperature on conversion during batch hydrolysis of starch (pH=5.8, $71<\theta<87^0$C, S_o=100g/dm^3, E_{01}=0.2cm^3/dm^3) [Paolucci-Jeanjean *et al.* 2001]

A simultaneous hydrolysis of gelatinisation and liquefaction by the Termamyl (B. lichenformis α-amylase) has also been studied by Paolucci-Jeanjean *et al.* [2001]. They have investigated the temperature effect on conversions during batch hydrolysis. The result of the temperature effect is given in Fig. 2-3. The conversion of the tapioca starch to liquefied starch is ~60% over the period studied.

Linko and Javanainen [1996] have investigated the simultaneous liquefaction, saccharification and acid lactic fermentation on barley starch. They reported that the process was successfully carried out without prior gelatinisation reaction. The result is shown in Fig. 2-4 below;

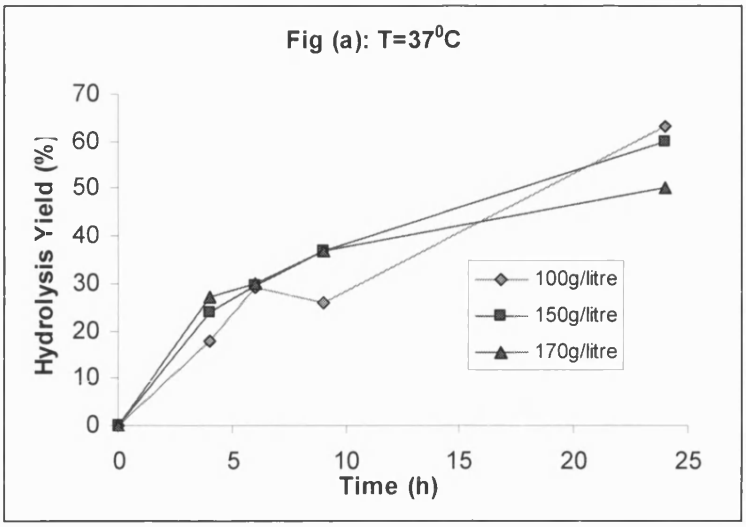

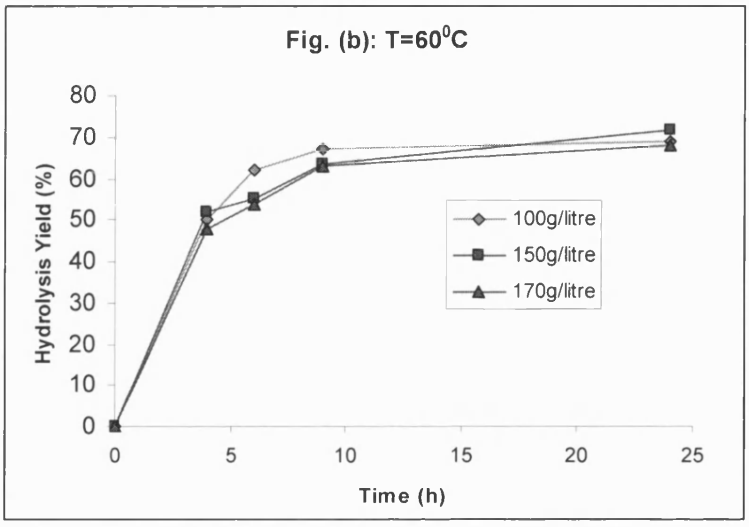

Fig. 2-4: Effect of temperature on saccharification of barley starch by 0.15 ml α-amylase and 0.15 ml glucoamylase per litre [Linko and Javanainen, 1996]

The study carried out by Linko and Javanainen [1996], Marchal *et al.* [1999], and Paolucci-Jeanjean *et al.* [2000a; 2001] show that simultaneous starch hydrolysis by temperature above 60^0 C but below 90^0 C has effectively the same conversion of 60-70%. According to the literature review done so far, the present information found on low temperature simultaneous gelatinisation, liquefaction, and saccharification (SGLS) is very limited, therefore a comprehensive investigation is needed.

2-2. REVIEW OF TRANSPORT MECHNASIM AND PREPARATIONS OF THE ULTRAFILTRATION MEMBRANE

Basically, liquid system separation membranes are categorised as reverse osmosis (RO), nano-filtration (NF) and ultra-filtration (UF), and micro-filtration (MF). RO is a highly-efficient technique used almost exclusively for ultra-pure water production for industrial use, wastewater treatment, municipal drinking water production and seawater desalination. It has the ability to concentrate all dissolved and suspended solids, and the permeate stream contains very low concentrations of dissolved solids. Nano-filtration falls between RO and ultrafiltration and it would be used when both RO and ultrafiltration are not a correct choice for separation. Applications of the nano-filtration are in demineralisation, colour removal, and desalination. Micro-filtration is the low-pressure cross-flow membrane process for separating colloidal and suspended particles in the range 0.05-10 microns, and it is frequently used for concentrating the tomato puree etc, and for fermentation, broth and biomass clarification, and solvent recovery.

Ultra-filtration membranes that have a pore size in range 2-50nm has been used for variety of applications. Several strategies have been employed to improve the flux performance. [Sims and Munir 1992; Prazeres and Cabral, 1994; Attafuah and Hall, 1995; Perea and Ugalde 1996; Buchtmann, *et al.* 1997; López-Ulibarri and Hall, 1997; Schreyer and Coughlin, 1999; Lee and Min, 1999; Paolucci-Jeanjean *et al.* 1999, 2000a,b; Nagpal *et al.* 2000; Giorno *et al.* 2001; Kawai *et al.* 2001; Noordman *et al.* 2002; Pala *et al.* 2002; Rosalam and England 2004; Saffaj *et al.* 2004; Atra *et al.* 2005; Feins and Sirkar, 2005; Akoum *et al.* 2005; Martin Lo *et al.* 2005]. Ultrafiltration concentrate suspended solids and solutes of molecular weight greater than 1,000, and the permeate stream has low-molecular-weight organic solutes and salts. In specific application, ultrafiltration is widely used in the fractionation of milk and whey, and in protein fractionation

[Atra *et al.* 2005; Akoum *et al.* 2005]. Other uses include production of ultra pure water, egg and animal blood processing, clarification of juice, downstream processing, membrane bioreactors, treatment of bleach plant effluents, and recovery of lignin compounds in the pulp and paper industry.

Fouling basically causes flux decline, and the cost of an ultrafiltration system would rise by the need for cleaning. Fouling phenomena is one of the subjects studied by researchers in the membrane technology area. Many strategies have been proposed including membrane material modifications [Dai *et al.* 2001; Malaisamy *et al.* 2002; Khayet *et al.* 2002; Xu *et al.*2003; Qin *et al.*2004; Jung 2004]. One of the significant proposasl in the field of membrane bioreactor in which the residence time is critically defined by the flux is that of Howell *et al.* [1995]. The study proposal is the concept of the critical flux [Howell *et al.* 1995; Field *et al.* 1995; Wu, *et al.* 1999]. The philosophy used in critical flux is the residence time defines the flux, which is the inverse of the conversional filtration which attempts to reach high flux.

2-2.1 History and Developments of The Membrane Process

Membranes were first prepared as a commercial product in the form of symmetric micro-filtration membranes in the late 1920s for bacteriological laboratory use. Until the end of 1960s, the used of ultrafiltration membranes were limited only to use in laboratories. The notion that salt could be removed from seawater without a phase change was suggested by Dr. Sourirajan in the late 1950's. The actual invention of the reverse osmosis (RO) membrane started in his laboratory at UCLA around 1960 [Loeb and Sourirajan, 1963]. The polymeric hollow membrane was first mentioned in 1966 by Mohon. Despite early findings, full commercialisation of the RO, ultrafiltration (UF) and crossflow technologies only occurred in early 1970's. The 1970s saw rapid development of ultrafiltration processes by the dairy

industry, and also many plants were developed for whey protein concentration and the electro-coat paint industry. Since then, membrane technology had diversified in applications. In the 1980's, the cross-flow membrane process has become well accepted by industry for medical applications. Today many industries such as waste treatment and water purification rely on the cross-flow membrane for cost-effective separations.

2-2.2 Transport Mechanisms in Ultrafiltration Membranes

Ultrafiltration is a selective fractionation process using pressures up to 10 bar with a pore size in range 2-50nm. Basically the filtration rate or the flux can be expressed by the Darcy equation as;

$$F = \frac{dV}{dt} = A_m \frac{dP}{\eta R} \qquad (2\text{-}13)$$

$$J_v = \frac{F}{A_m} = \frac{dP}{\eta R} \qquad (2\text{-}14)$$

Where F is the filtrate flow (m^3/s), V the filtrate volume (m^3), t is the filtrate time (s), A_m is the filter area (m^2), dP is the pressure different across the membrane module (bar), η is the dynamic viscosity of the filtrate (Pa-s), R is the total hydraulic resistance (m^{-1}), and J_v is the flux (m^3/m^2-s). When pure water is used but without adding solutes and at a constant temperature the flux would be proportional to the applied pressure. The membrane resistance (R_m) that replaces the hydraulic resistance is a constant value when different operating temperature is used. When solute is added, and when the applied pressure is above the critical flux [Field *et al.* 1995; Wu, *et al.* 1999], the flux model will change. Parameters that will influence the flux are pressure, cross-flow velocity, solute concentration and temperature, the time, the interaction between solute and membrane, and the characteristics of the solute. Therefore, the general Darcy equation model has to be extended to

consider not only the membrane resistance and the applied pressure, but also would require consideration of the concentration polarisation of the solute at the membrane. Since pressure is used to drive the permeate through the membrane, the solute having a larger size than the pore will be retained on the surface of the membrane.

2-2.2.1 Dead-End Filtration Process

In the dead-end filtration process, continuous filtration would accumulate the solute onto the membrane surface in the form of a solid cake which would increase the hydraulic resistance. From the beginning of experiment, the pressure increases due to increase in cake resistance. Below the specified pressure, the flow rate would be kept constant by providing pumping. When the specified pressure is reached, the pump may be controlled to a pressure constant. During the constant pressure, the flux would gradually reduce and finally when the cake resistance is higher than the applied pressure, no filtrate can pass through the membrane. In the case of the cake filtration, the total hydraulic resistance can be separated to cloth resistance (R_m) and cake resistance (R_c). Heertjes, [1964] has suggested the cake resistance increases during filtration as;

$$R_c = \alpha C \frac{V}{A_m} \qquad (2\text{-}15)$$

where α is the cake specific resistance (CSR, m/kg) and C the total concentration of solid matter (kg/m^3). The CSR may depend on the pressure if the cake is compressible and generally can be expressed by an empirical relation [*Meindersma et al.* 1997]. Fig. 2.5 shows the schematic diagram of concentration polarisation. Providing the concentration of solid is constant a combination of equations (2-13) and (2-15) gives at a constant pressure give a modified form of the Darcy equation as:

$$F = \frac{dV}{dt} = \frac{A_m{}^2 \Delta P}{\eta(\alpha CV + AR_m)} \qquad (2\text{-}16)$$

$$J_v = \frac{A_m \Delta P}{\eta(\alpha CV + A_m R_m)} \qquad (2\text{-}17)$$

2-2.2.2 Continuous Tangential Filtration Process

In a continuous filtration system, the applied pressure, or TMP usually can be keep constant from the beginning of operation but the flux would reduce when the concentration polarisation and the gel layer of the solute that develops on the interacted surface of the membrane during filtration has gradually increased.

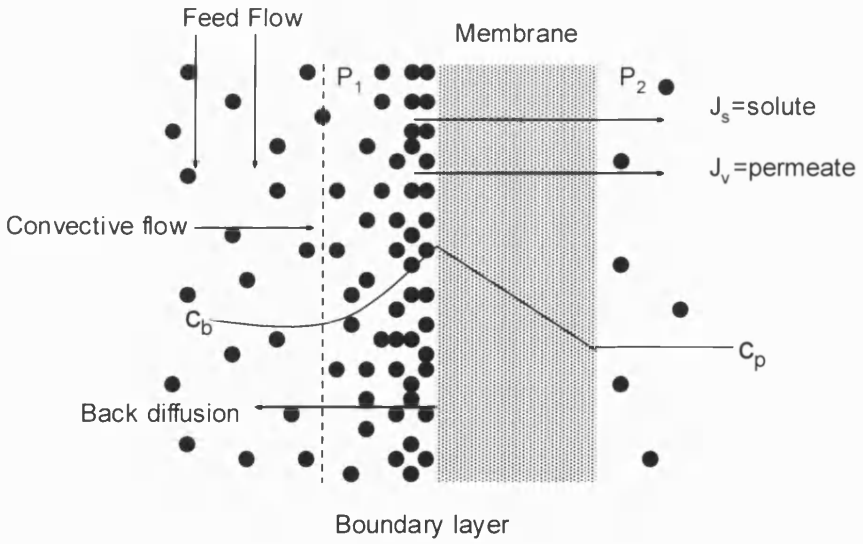

Fig. 2.5: A Schematic diagram of the concentration polarisation [Sablani *et al.* 2001];

To study the transport phenomena of ultrafiltration, firstly the system without added solute is examined. In this case, the flux will change if one of

two parameters of the pressure difference ($P_1 - P_2$) and/or the total hydraulic resistant (R) is changed. At certain operating conditions, the pressure difference and hydraulic resistance are constant. However, when solute is added, depending on the interaction of the membrane surface and solute, the flow pattern (e.g. laminar or turbulent) along the membrane, and the applied pressure, the gel layer may form which would accumulate on the surface of the membrane. If the applied pressure is kept constant, the hydraulic resistance *(R)* becomes the parameter that solely determines the flux. Many authors separate the total hydraulic resistance into two; the membrane resistance (R_m), and the boundary layer resistance (R_{bl}) [Chudacek and Fane, 1984; Aimar, *et al.*1988; Espinasse *et al.* 2002].

$$R(t) = R_m + R_{b1} \qquad (2\text{-}18)$$

Thus, the modified Darcy equation after taking consideration the increased boundary layer resistance becomes;

$$J_v(t) = \frac{\Delta P}{\eta\left(R_m + R_{b1}\right)} \qquad (2\text{-}19)$$

From the beginning of operation of the cross flow filtration system until the system reaches the steady state condition by which the boundary layer resistance becomes constant, and ultrafiltration system is operated at the pressure that gives a flux that falls within a critical flux value, the cake resistance (R_c) suggested by Heertjes, [1964] is used to replace boundary layer resistance (R_{bl}), the flux should reach a plateau after initial exponential decay, hence,

$$R_c = R_{bi}(t) = \alpha C \frac{V}{A} \qquad (2\text{-}20)$$

Hence;

$$\frac{dV}{dt} = \frac{A_m \Delta P}{\eta\left(R_m + \alpha C V / A_m\right)} \qquad (2\text{-}21)$$

If a solute concentration is held constant, re-arranging and integrating with initial conditions $V=V_0$ and $t=t_0$,then;

$$\alpha C \frac{(V - V_0)(V + V_0)}{2} + A_m R_m (V - V_0) = \frac{A_m{}^2 \Delta P (t - t_0)}{\eta} \qquad (2\text{-}22)$$

$$\left(\frac{t - t_0}{V - V_0}\right) = \frac{\alpha C \eta}{2 A_m{}^2 \Delta P}(V + V_0) + \frac{\eta R_m}{A_m \Delta P} \qquad (2\text{-}23)$$

2-2.2.3 Gel Layer Model

Another model used to describe the flux decay is the gel layer model, which also is the first model proposed to explain the gel polarisation [Porter 1972; Nakao *et al.* 1984]. The flux may be decreasing at the beginning but would reach a relatively constant value if the system is operated at a critical flux. During the steady state condition, the diffusion of the solvent in the x-direction is described as;

$$J_v = -D\frac{dC}{dx} \qquad (2\text{-}24)$$

Integrating of the diffusion model at a specified boundary condition, $x_0=0$, $C=C_b$ and $x=\delta$, $C=C_g$, the gel layer model becomes;

$$J_v = \frac{D}{\delta} \ln\left(C_g / C_b\right) \qquad (2\text{-}25)$$

$$J_v = k \ln\left(C_g / C_b\right) \qquad (2\text{-}26)$$

$$k = \frac{D}{\delta} \qquad (2\text{-}27)$$

Equation 2-26 is usually applicable and is a common phenomenon in protein solution filtration by ultrafiltration where the solute is completely rejected. The diffusion coefficient D can be calculated by the equation:

$$D = 8.34 \times 10^{-15} \frac{T}{\eta M^{1/2}} \qquad (2\text{-}28)$$

where M is the molecular weight (Da) and T, temperature (^{0}C), and η, dynamic viscosity (pas), k the mass transfer coefficient (kg/m^{2}h), C_g concentration in the gel layer, C_b is concentration in the bulk system. Depending on the membrane system, the thickness of the gel layer may be a self regulated process. This equilibrium could be attained due to the fact the applied pressure increases the gel layer, while the cross flow velocity gives a drag force to diffuse the solute in reverse direction thus decreasing the gel layer and so to surface polarisation. However, the reverse diffusion by the drag force to reduce the gel layer mainly depends on the particle size, density of solute, the velocity, and the liquid viscosity. Therefore, at certain operating condition below the critical flux, there should exist a relationship between the drag force, the applied pressure and the reverse diffusion, thus the gel layer may reach a constant value, and the flux will reach a constant value after initially decaying.

In the case of ultrafiltration where the flux is driven by the pressure gradient, considering the back diffusion in equation (12), the steady state mass balance over the liquid boundary layer can be written as:

$$J_v C = J_V C_p - D\frac{\partial C}{\partial x} \tag{2-29}$$

Integrating the steady state mass balance at a specified boundary condition, $x_0=0$, $C=C_b$ and $x=\delta$, $C=C_w$, a well known concentration polarisation equation is obtained.

$$J_v = k \ln\left(\frac{C_w - C_p}{C_b - C_p}\right) \tag{2-30}$$

where C_w is the concentration of solute at the membrane surface, k the mass transfer coefficient, C_p permeate concentration, C_b boundary concentration. The degree of separation of solute is expressed by rejection coefficient as;

$$R_{obs} = 1 - \frac{C_p}{C_b} \tag{2-31}$$

The true rejection (R_{true}) influences the rejection coefficient (R_{obs}), the true rejection is defined as;

$$R_{true} = 1 - \frac{C_p}{C_w} \tag{2-32}$$

Combining with the mass balance equation across the ultrafiltration system, hence;

$$\ln\left(\frac{1-R_{obs}}{R_{obs}}\right) = \frac{J}{k} + \ln\left(\frac{1-R_{true}}{R_{true}}\right) \tag{2-33}$$

At low permeate flux, R_{true} increases with increasing the flux. At high flux, R_{true} approaches a constant value, while R_{obs} decreases with increasing the

flux that may due to the concentration polarisation effect [Noordman *et al.* 2002].

2-2.2.3.1 Prevention of the Gel Layer

The drag force to reduce gel layer formation has been used by Noordman *et al.* [2002] by using the particles such as glass and steel at different sizes to promote turbulent flow in a fluidised bed. This method would lead to reduction of the velocity of forming the turbulent regime but also reduce the pressure drop across the membrane compared with when high velocity to promote turbulence is used. As result, the flux and rejection has been improved significantly over the ultra-filtration system in their study. They also reported that particle fluidisation is the best method for use with higher viscosity liquids; otherwise the membrane may be subjected to the potential risk of damage. Chiu and James [2005] have studied the critical flux of the non-circular multi-channel ceramic membrane by using TiO_2 particle as suspensions. They have reported that increasing the cross-flow velocity from 0.5 to 1.0ms^{-1} (Re = 2313) has led to an increase in the critical flux by a factor of 4.

Another factor that may increase or decrease the concentration polarisation and the gel layer formation is the interaction of the membrane and solutes. Interactions between the membrane surface and the components can be adsorption of compounds onto the membrane surface, pore blocking and depth fouling (by particulates getting trapped in the porous structure), concentration polarisation retained in membrane surfaces, fouling layer (gel/cake), and osmotic pressure [Rosalam and England, 2004]. Interaction in-terms of hydrophobicity and hydrofilicity properties of the membrane, solute, and solvent are a part of the subject that have been vastly discussed for formulation of the membrane to improve the flux [Malaisamy *et al.* 2002; Qin *et al.* 2004; Jung 2004].

2-2.2.4 Osmotic Pressure Model

Another model used to determine the flux limit is the osmotic pressure model [Wijmans *et al.* 1984; 1985]. The increased osmotic counter-pressure produced by a high concentration of the rejected solute near the membrane surface will limit the flux. One of the frequently used model based on the osmotic pressure model is the Spiegler-Kedem and solution-diffusion model. The equations of this model are;

$$J_v = L_p(\Delta P - \sigma\Delta\pi) \qquad (2\text{-}34)$$

$$R_{true} = \sigma\frac{(1-F)}{(1-\sigma F)} \qquad (2\text{-}35)$$

$$F = \exp(-J_v a_2) \qquad (2\text{-}36)$$

$$a_2 = \frac{(1-\sigma)}{P_M} \qquad (2\text{-}37)$$

where R_{true} is the true rejection, ΔP is the pressure drop across the membrane, $\Delta\pi$ is the osmotic pressure drop across the membrane, σ is the reflection coefficient which represents the rejection capability of the membrane, (i e , σ = 0 means no rejection and σ = 1 means 100% rejection), and P_M is the overall permeability coefficient. Combining the Equations (2-34) to (2-37) with the film theory model in Equation (2-25) results in

$$\frac{R_0}{1-R_0} = a_1[1-\exp(-J_v a_2)]\exp(-J_v / k] \qquad (2\text{-}38)$$

where $a_1 = \sigma/(1-\sigma)$. The membrane parameters σ , P_M, and k can be estimated simultaneously with experimental data of observed rejection (R_0) and solvent flux (J_v) at constant σ with a pressure, feed rate and

concentration by using the nonlinear parameter estimation method. The osmotic pressure model however is irrelevant for solutes having a molecular weight greater than 100 kDa [Vilker, 1984] and is insufficient to explain the decrease of the slope of flux vs. pressure [Meindersma *et al.* 1997].

2-2.2.5 Mass Transfer Coefficient Correlation

Most of the models used in characterization of RO or UF membranes, such as the three parameter of the osmotic-pressure model (Spiegler-Kedem model), and the (gel) concentration polarization model, make use of a mass transfer coefficient correlation in order to calculate the concentration at the membrane wall, C_g. This correlation has the empirical form based on the Chilton-Colburn analogy.

$$Sh = \frac{kd_h}{D_t} = A_1 \mathrm{Re}^{A_2} Sc^{A_3} \qquad (2\text{-}39)$$

where Sh is the Sherwood number, d_h, the hydraulic diameter of flow channel, A_1, A_2, and A_3 empirical constants, Re the Reynolds number, D_t is tube diameter, and Sc is the Schmidt number Based on the Chilton-Colburn and Deissler analogies.

2-2.2.5.1 Mass Transfer of Empty Tubes in Turbulent Regime

If the flow in empty tubes operated in the turbulent regime, the mass transfer coefficient k in the liquid boundary layer can be calculated by means of the Dittus-Boelter correlation.

$$Sh = \frac{kd_h}{D_t} = 0.023 \mathrm{Re}^{0.8} Sc^{0.33} \qquad (2\text{-}40)$$

2-2.2.5.2 Mass Transfer of Fluidised Bed Membrane

If operated within the fluidised bed regime, more complicate empirical relations would be involved as the fluidisation correlates with the particle size, shape, and molecular weight and event though when interaction of the bed particle and fluid is involved. Noordman *et al.* [2002] have compared the experimental results to the mass transfer relations suggested by Smith and King [1975] and Yasunishi *et al.* [1988]. The relationship of Smith for larger particles (diameter ratio d_p/D_t<0.06) is:

$$Sh = 0.455\mathrm{Re}^{0.56}\, Sc^{0.33} \qquad (2\text{-}41)$$

where Re_h is equal to $\rho(v_{sf}/\varepsilon)d_h/\eta$ and d_h is defined as:

$$d_h = \frac{D_t\varepsilon}{1+1.5(1-\varepsilon)(D_t/d_p)} \qquad (2\text{-}42)$$

Yasunishi *et al.* [1988] relates the Sh number to the rate of energy consumption in the fluidised bed:

$$Sh = 0.13\left(\frac{E_{diss}^{1/3}D_t^{4/3}}{m_l^{1/3}\upsilon}\right)^{3/4} Sc^{1/3} \qquad (2\text{-}43)$$

The energy dissipation due to the presence of the fluidised particles;

$$E_{diss,fb} = \frac{\pi}{4}D_h^2 v_{sf} gH(1-\varepsilon)(\rho_s - \rho_l) \qquad (2\text{-}44)$$

The energy dissipation due to the presence of the wall fraction;

$$E_{diss,w} = \frac{\pi}{4} D_h^2 v_{sf} \Delta P_w \qquad (2\text{-}45)$$

$$\Delta P = 4f \frac{1}{2} \rho_l v_{sf}^2 \frac{H}{D_h} \qquad (2\text{-}46)$$

Where m_l is mass liquid (kg), E_{diss} dissipated rate of energy consumption (J/s), υ kinematics viscosity (m^2/s), v_{sf} superficial velocity (m/s), H high of fluidised bed (m) and D_h the hydraulic diffusivity (m^2/s).

2-2.2.6 The Flux Decrease with Time

The flux decrease with time has also been described empirically. A well known empirical model that can describe the flux decreases with time, found in a review paper by Meindersma *et al.* [1997].

$$J_v(t) = J_0 \left(t / t_0 \right)^a \qquad (2\text{-}47)$$

where J_0 is the maximum flux at $t=t_0$. The maximum flux can be obtained from the maximum slope obtained from the graph of the volume of filtrate verses filtration time. The Darcy equation can also be combined with the gel layer model, hence;

$$J_v(t) = k \ln \left(C_g / C_b \right) = \frac{\Delta P}{\eta (R_m + R_{bi})} \qquad (2\text{-}48)$$

Combining the concentration polarisation given by Equation 2-30;

$$J_v(t) = k \ln \left(\frac{C_w - C_p}{C_b - C_p} \right) = \frac{\Delta P}{\eta (R_m + R_{bi})} \qquad (2\text{-}49)$$

When the empirical equation replaces the flux;

$$R_{bl}(t) = A\frac{\Delta P}{\eta J_v}\left(\frac{t_0}{t}\right)^a - R_m \qquad (2\text{-}50)$$

The membrane resistance (R_m) can be estimated by pure water tests at certain pressure and temperature, while the boundary layer resistance can be determined by adding the solutes thereafter. The flux changes with time can be obtained experimentally. The Darcy equation, the gel layer model, and the empirical equation mentioned above could be used to predict the gel layer thickness and so flux.

2-2.2.7 Experiment Evaluation: The Critical Flux

The elementary transport mechanism is not insufficient in delivery methods to prevent fouling due to different membrane and operating conditions. The method suggested by Noordman *et al.* [2002] is also quite aggressive and may risk damage to the membrane. Howell *et al.* [1995] have proposed the fouling prevention method by studying the optimum operation condition of the flux or so called critical flux. The critical flux is described as the flux below which the ratio (J/TMP) is constant. There are two types of the critical flux, the strong and weak forms. The strong form of the critical flux exists if the flux of the suspension is identical to the clean water flux at a certain range of TMP. The weak form of critical flux exists if the relationship between TMP and flux is linear but the slope differs from the clean water flux. Hence, a new system operated for certain applications has to be used to determine the critical flux. The critical flux approach is very useful especially if the process is carried out for long residence times and continuous operation.

Wu, *et al.* [1999] have described how to successfully measure the critical flux for two colloidal silica suspensions, BSA solution and a baker's yeast suspension by a 50k MWCO membrane. Another strategy to measure the critical flux is by changing the TMP and it is changed step by step by alternate positive and negative pressure changes [Espinasse *et al.* 2002].

2-2.3 Preparations of The Ultrafiltration Membrane

Generally, an ultrafiltration membrane is built up asymmetrically. It has three layers; the porous support, the intermediate layer, the top layer, with pore sizes in the range 2-50 nm. The top layer can be modified by deposition of a phase inside the pores to further decrease the pore size or to add a certain function to the membrane (for example, a catalyst). The actual separation process takes place at the top layer. The support provides mechanical strength to the membrane. The intermediate layer acts as a transition phase, preventing the top layer from penetrating into the pore structure of the support. In polymeric membranes, the intermediate layer that includes macrovoids, pores and micropores is governed by many variables in the polymer dope solutions such as concentration, temperature, and organic and inorganic additives [Jung, 2004]. For ceramic membranes, the support and intermediate layer can be used as a microfiltration membrane, which is mainly for separation of microscopic particles (0.1-1.0 μm) [Lindqvist and Liden, 1997]. Ceramic membranes with the top layer casting can be used for ultrafiltration for separations of macromolecules and colloidal particles. The top layer of ceramic membranes may be cast by tape or dip casting by different configurations.

Ultrafiltration membranes may also be classified by the molecular weight cut-of or the pore size, the material used for membrane preparation, functional groups such as hydrophobicity and hydrophilicity or electric

charges, and the preparation techniques such as tubular, hollow fibre, capillary, flat sheet membrane, and monolithic membranes. All configurations are commonly prepared by various techniques. The materials used for preparations of membranes could be organic, inorganic or a composite of several chemicals and additives. Moreover, the material used in preparation of the membrane may be classified into ceramic, polymer, composite polymer or composite ceramic. Membrane selections for some specific applications differ greatly according to the chemical and physical properties of substances exposed to the membrane, and the operating conditions. Compared to organic, the inorganic membranes offer several advantages such as superior thermal and chemical resistance and so better mechanical strength. These have made them suitable for applications in which high temperature and corrosive or organic media are present [Lindquvist and Liden, 1997; Saffaj *et al.* 2004]. Polymeric membranes also may change properties along with the changes of their chemical structure after they are used for long period.

The favoured geometry of ceramic membranes is tubular shapes or tubes. They are combined to form a honeycomb structure. The honeycomb structure is effective because of a relatively large membrane area can be obtained in a small volume. Flat membranes are not as common as the tubular-shaped, but a large membrane area can be achieved by stacking layers of the flat membrane and the 'dead volume' is minimised. Tubular shapes and honeycomb structures are mostly used for liquid separation processes while the flat shape is more suitable for gas separation, low-pressure liquid processes and catalytic processes. Flat membranes can be prepared by several forming methods. Slip casting, calendering and tape casting are all examples of forming methods suitable for making flat shapes. Unfortunately most ceramic membranes are too expensive for applications like waste water treatment. Hence a low cost of TiO_2 (50%)-$ZnAl_2O_4$ (50%) composite ceramic membrane formed by deposition on an artificial cordierite

support was developed [Saffaj *et al.* 2004]. Although the ceramic membrane can be prepared by low cost manufacturing, in most biotechnology applications where membrane are not exposed extreme process conditions (pressure, temperature, and pH) but knowledge of the interaction of the membrane and the substances are more desirable, polymeric membrane are normally used [Atra *et al.* 2005; Feins and Sirkar, 2005; Akoum *et al.* 2005; Martin Lo *et al.* 2005]. Furthermore, when functional groups are needed for the enzyme immobilisation, polymeric membranes are favoured as it can relatively easy to chemically modify the structure. [Godjevargove *et al.*1999; Giorno *et al.* 2001; Calabro *et al.* 2002;].

2-2.3.1 Polymeric Organic Membrane Preparation

The phase inversion process is a well-known method to fabricate most asymmetric flat sheet and hollow fibre membranes. In the laboratory, basically the process for making the membrane is started with mixing a selected polymer, solvents, and additives in an airtight glass bottle to form a dope solution as shown in Fig. 2.6. Table 2.7 shows some polymers and additives conventionally used that would give different properties such as thermo-stable [Dai *et al.* 2001], high flux [Qin *et al.* 2004], hydrophilic [Jung 2004] and hydrophobic, and some functional group required for certain applications.

The dope solution is kept agitated for several hours for complete dissolution. The most frequently used solvents are *N*-methylpyrrolidone (NMP), dimethyl acetamide (DMAc), dimethylformamide (DMF), dimethylsulfoxide (DMSO), γ-butyrolactone and ε-caprolactam [Chaturvedi *et al.*2001; Liu *et al.* 2003]. In the particular case such as synthesising the polyacrylonitrile and poly(acrylonitrile-*r*-3-sulfoproyl acylate potassium salt) PAN-*r*-SAPS) for hydrophilic polyacrylonitrile blend membranes, nitrogen

gas is used to purge the dissolve oxygen out of the reaction vessel [Jung *et al.* 2004] otherwise vacuum may be used to purge out the air bubble that can increase the defect of the membrane. After complete dissolution, additives are subsequently added and solution is homogenised and is kept for de-aeration. Additives are used to design the membrane structure which would create a spongy structure by prevention the macrovoid formation, enhance the pore formation, improve pore interconnectivity, and/or to introduce hydrophilicity [Liu *et al.* 2003].

Fig. 2.6: Dope solution agitated by the mechanical roller.

The coagulation bath is often water or a mixture of water and solvent. Hydrophilic structures are obtained by adding hydrophilic materials, e.g. polyvinylpyrrolidone (PVP) [Liu *et al.* 2003]. Other frequently used additives are: glycerol, alcohols, dialcohols, water, polyethylene glycols (PEG), polyethylene oxide (PEO), LiCl and $ZnCl_2$ [Liu *et al.* 2003].

2-2.3.2 Thin Layer Flat Sheet Membrane

The dope solution obtained after agitation is spread over a smooth glass plate with the help of a knife edge. The thickness of the membranes can be controlled by varying the thickness of adhesive tapes at the sides of

the glass plate. The glass plate is kept in an environment of controlled temperature and humidity during membrane casting. The glass plate is subsequently immersed in a gelling bath, which is generally demineralised water maintained at a certain temperature. Immediately phase inversion starts and after few minutes a thin polymeric film membrane separates out from the glass. The membrane is then repeatedly washed with demineralised water and wet stored to avoid over drying that can damage the membrane [Chaturvedi *et al.* 2001].

The side runner's thickness determines the thickness of membrane films, but the actual thickness is measured by using a micrometer. The manufactured membrane films are characterised using pure water flux measurement, retention measurement usually using polysaccharides, scanning electron microscopopy (SEM) to see the micropores and microvoid (Fig. 2.7) , and mechanical properties by a tensile machine [Chaturvedi *et al.* 2001; Liu *et al.* 2003; Xu *et al.* 2003; Jung *et al.* 2004]. When a small pore size is required, a tape casting process will be used.

Some typical examples found in literature on the preparation of the flat sheet membranes is summarised in Table 2-7. Dai *et al.* [2001] prepared the ultrafiltration membrane from sulfonated poly, phthalazinone ether sulfone ketone (SPPESK) and *N*-methyl-2-pyrrolidinone (NMP) as the solution cast it onto glass at a temperature of 18^0C and relative humidity of 35%. A recent paper published by the same group on preparation of the composite nano-filtration membrane is slightly changed by adding the ethylene glycol monomethyl ether (EGMA) in the dope solution [Zhang *et al.*2005]. The evaporation time is 15 seconds in air. The cast solution is then immersed into water at 6^0C for 36 hours. Longer time is required to provide a sufficient time for solvent to replace the non-solvent water. The membrane sheets are then rinsed with water. The SPPESK concentrations of 10, 12, 14, 16 and 18 wt% were used. The additives used are butanone, ethelene

glycol dimethyl ether, and tetrahydrofuran at concentrations of 12, 15 and 18 wt% respectively.

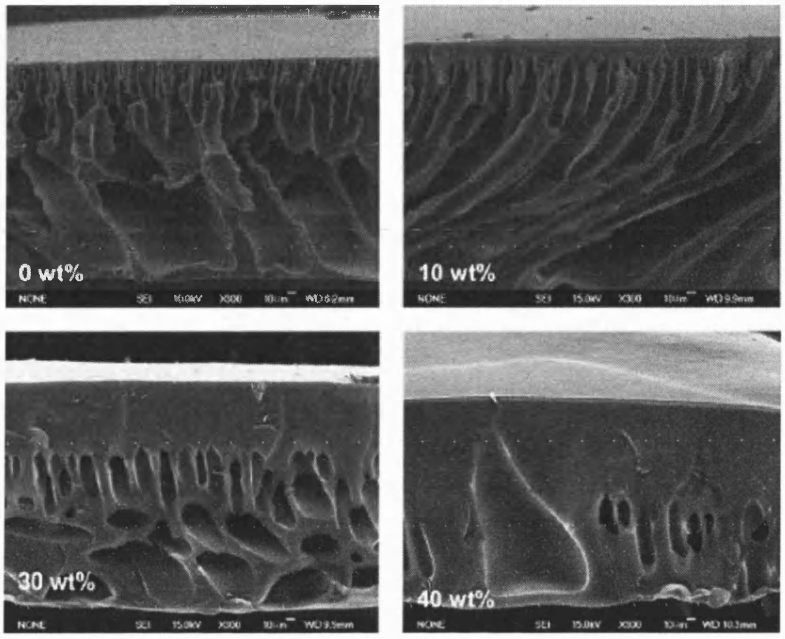

Fig. 2-7: Cross-sectional SEM morphology of blend asymmetric membrane, pure PAN (0 wt%), 10, 30, and 40 wt% of PAN-r-SAPS respectively [Jung *et al.* 2004]

2-2.3.3 Hollow Fibre Membrane

Basically preparations of the dope solution of the hollow fibre membrane are similar as that preparation of the dope solution for flat sheet membrane. After mixing of the dope solution, the mixture is poured into a vessel, pumped through the filter into the spinneret and the hollow fibre membrane is formed out of the spinneret. Nitrogen gas is applied to pressurised vessel that is also commonly used to push the dope solution out from the vessel (Fig. 2-8). The spinneret that is mounted at the bottom of the vessel at which the bore liquid is pumped through the orifice tube produces

the nascent hollow fibre membrane [Li *et al.* 1994]. The orifice tube and the nozzle sizes greatly determine the thickness of the nascent hollow fibre membrane. The nascent hollow fibre may be cured by two methods called dry—wet (Fig. 2-8) or wet-wet spinning processes. Only a few of the hollow fibre membranes are prepared by wet–wet or dual bath spinning process [Van't Hof *et al.* 1992; Li *et al.* 1994].

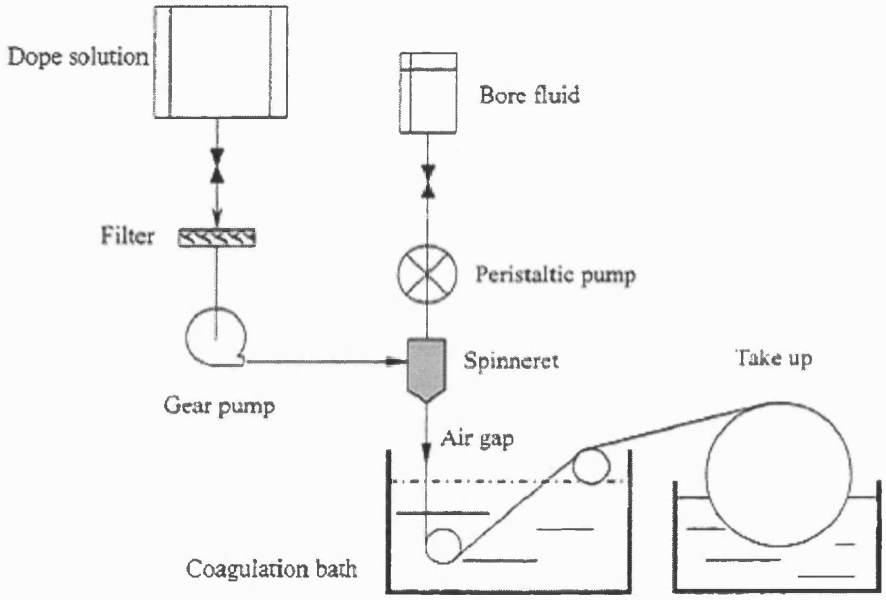

Fig. 2-8: A typical of schematic diagram of dry-wet spinning process.

The term of dry-wet spinning is used because the nascent fibre is extruded by the bore solution (normally deionise water), while at outside of the nascent fibre is left opened to air. The tube-in-orifice spinneret is normally applied in the dry–wet spinning process. Basically the air gap length and environment of the air gap (humidity, temperature, presence of organic vapour), spinning rate of the dope solution emerges out to form the nascent fibre, flow rate of the bore liquid, the bore liquid and the coagulant bath compositions are studied as these affect the property of the hollow fibre membrane and hence determine of the ultimate structure of the produced fibre. Generally only deionised water is used as a bore liquid and

coagulation bath, but some researcher used a mixture of water and organic solvent/non-solvent in both [Xu *et al.* 2003; Khayet *et al.* 2002]. Inside surface structure is mainly controlled by the bore liquid composition. Preferably one would like to have a spongy membrane structure without macrovoids, which normally results in mechanically more stable membranes.

Macrovoid formation in phase separation occurs from freshly formed of nuclei of the diluted phase when the composition in front of the nuclei remains stable for relatively long period of time [Smolders, *et al.* 1992; Boom *et al.* 1992]. Due to diffusion of the solvent expelled from the surrounding polymer solution, the macrovoids will grow. Macrovoids are generally formed in systems where instantaneous de-mixing takes place, except when the polymer additive (e.g. PVP) concentration and/or the non-solvent concentration in the polymer solution exceeds a certain minimum value [Smolders, *et al.* 1992; Boom *et al.*1992; Lai *et al.* 1996; Kimmerle and Strathmann 1990]. Therefore, a dope composition close to the bi-nodal composition favours the formation of spongy structures.

The wet–wet spinning process is well applied for controlling the shell side surface structure [Li *et al.* 1994]. In this process the nascent fibre is brought into brief contact with the first coagulant, after which the fibre enters the coagulation bath (second coagulant). When the weak non-solvent is applied, such as glycerol, completely dense skin layers can be obtained, and supported by a porous sub-structure, which makes the membrane suitable for gas separation and pervaporation [Van't Hof *et al.*1992; Li *et al.*1994]. In this case, diffusion of the solvent out of the nascent fibre is much higher than the diffusion of non-solvent into the nascent fibre. When a mixture of solvent and strong non-solvent, e.g. *N*-methylpyrrolidone and water is applied, extremely open surface layers can be obtained [Wienk *et al.*1993]. The solvent/non-solvent composition is a strong parameter influencing the pore

size of the membrane. The diffusion of solvent out of the nascent fibre is retarded by the presence of solvent in the coagulation bath. When the solvent concentration in the coagulation bath is higher than in the nascent fibre solvent, it might even diffuse into the nascent fibre, diluting the polymer concentration prior to phase separation. Proper application of the wet–wet spinning process requires a triple-layer spinneret; the bore liquid composition controls the inside structure, while the outside liquid composition controls the structure of the shell side [Li et al. 1994, Wienk *et al.* 1993, Liu *et al.* 2003].

Hollow fibre (HF) configurations produced by spinning technique is more advantageously used for membrane reactor because of its high surface-to-volume ratio that permits to obtain high biocatalyst in a small reactor volume. The typical device of a bundle of parallel polymeric hollow fibres is assembled in a cylindrical shell. The reactor is divided into luminal and shell side by the porous membrane wall that will act as a selective barrier with respect to the transport of the involved species. Although diffusion is a primary mass transfer mechanism, membrane bioreactors may be even operated with ultrafiltration flux across the membrane wall. These fluxes are generally promoted by significant trans-membrane pressure (TMP), and when the TMP is achieved the mass transfer rate would be enhanced by the addition of a convective component to the diffusive mass transfer mechanism [Calabro *et al.* 2002].

Table 2-7: Some of polymeric membranes prepared by several authors

Authors	*Ultrafiltration Membrane types*	*Polymers used*	*Solvents*	*Additives*	*Post-treatment/Coagulant*	*Water flux litre-m^{-2}-h^{-1}-Pa^{-1}*	*Nominal molecular weight cut-off (NMWCO)*	*Remarks*
Qin *et al.*[2004]	Hollow fibre	Polyethersulfone (PES) and poly(vinyl pyrrolidone)(PVP) K90	N-dimethylacetamide (DMA) and 1,2-propanediol (1,2-PD)	-	Soaked with hypoclorite	$1565x10^{-5}$	~100kDa	High flux
Xu *et al.*[2003]	Hollow fibre	Poly(ether imide) (PEI)	N, N-dimethylacetamide (DMAc)	Acetic acid	Adding DMAc in coagulant changes inner fibre to more porous structure	No given	-	
Khayet *et al.*[2002]	Hollow fibre	Polyvinylidene fluoride (PVDF)	N, N-dimethylacetamide	Varies ethylene glycol	Water + ethylene glycol / ethanol added in both external and internal coagulation bath			Increased ethylene glycol/ethanol in spinning increase gas permeation

Cont. **Table 2-7**

Jung [2004]	Thin sheet	Polyacrylonitrile (PAN) and poly(acrylonitrile-r-3-sulfoproyl acylate potassium salt) (PAN-r-SAPS)	DMSO	Ammonium persulfate,	Solvent evaporated in oven, 60^{0}C, 3 hrs	Varies (please refer to the original paper)	65-69kDa	Hydrophilic
Malaisamy *et al.*[2002]	Thin sheet	Polyurethane and sulfonated polysulpone (80/20)	N,N'-dimethylformamide (DMF)	Polyethylene glycol (PEG) 600 (sodium saly form)=7.5wt%	2.5% (v/v) DMF+o,2wt% sodium lauryl sulphate in distilled water	19-77kD		PEG improve the flux
Dai *et al.*[2001]	Thin sheet	Poly(phthlazinone ether sulfone ketone) (PPESK)	Chloroform, N-methyl-2-pyrrolidinone (NMP), butanone (BO), ethylene glycol dimethyl ether (EGME), diethyl ether (EE), tetrahydrofuran (THF)	Fuming sulphuric acid – increase hydrophylicity	The casting membrane immersed into water at 6^{0}C for 36 hrs	Varies (please refer to the original paper)	-varies -	Thermo-stable

2-2.3.4 Inorganic Membrane Preparation

Conventionally, the preparation of ultrafiltration ceramic membrane requires three main steps; preparation of porous support, intermediate layer, and the top layer. Commercial membranes supplied distributed in the present market are asymmetric multilayer configuration [Seffaj *et al.*2005]. Generally, the ceramic membrane preparation uses a conversional method. At the University of Bath, the spinning process is used to produce the untreated ceramic membrane. The first steps is to prepare the dope solution by mixing the solvents, binder, dispersing agent, additives in air tights bottle, the same procedure as that the preparation of the dope solution for making the polymeric membrane. Instead of polymers, α-alumina is used as the main ingredient, but some polymer is necessary act as binder and pore maker. Different ceramic supports materials are currently used, but α-alumina supports are the most common [Luyten *et al.*1997; Gestel *et al.*2002; Saffaj *et al.*2004; Seffaj *et al.*2005]. Starch like rice has also been used in the slip and tape casting of ceramic membranes to create the pore after firing [Lindquvist and Liden, 1997]. Examples of compositions of the support slip is given in Table 2-8

Table 2-8: Compositions of the support slips [Lindquvist and Liden, 1997]

Material	Slip casting, weight (g)		Tape casting, weight(g)	
Al_2O_3	100	100	298.5	298.5
Starch rice	24.6		73.5	
Starch corn		19.9		59.4
Dispersing	1.2	1.2	3.7	3.7
agent	33.3	33.3	94.6	94.6
Water	4.5	4.5	107.7	98.6
Binder				

After dope mixing, the spinning process by dry-wet method is carried out; the same equipment used as that for making the hollow fibre membrane. Preparation of the hollow fibre membrane may be stopped after soaking in the defined bath solution, but the ceramic membrane is still in the beginning of the process as the produced nascent have to be cured by burning off the organic compounds and sintered the α-alumina. The sintering process is normally conducted in the high temperature oven, by which the membrane would be gradually heated for certain period. The temperature may be burnt by certain temperature rate increment up to certain temperatures and then left to cool at ambient temperature. The cooling temperature may also be controlled at a certain cooling rate.

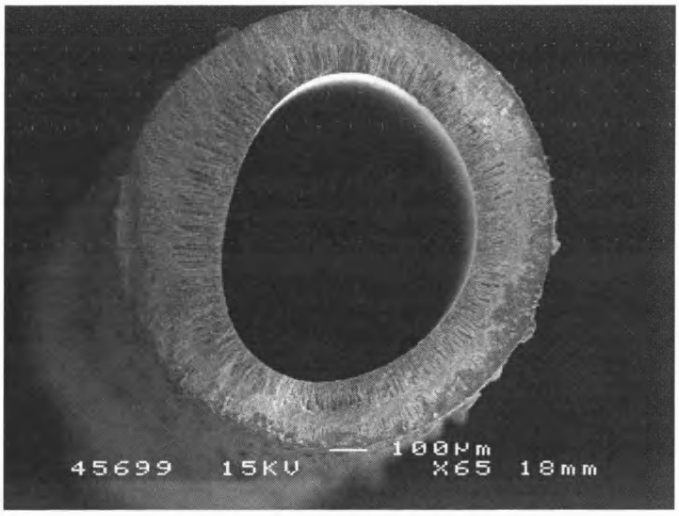

Fig. 2.9: Morphology Structure of Ceramic Membrane

Fig.2-9 shows SEM pictures of the morphology structure of the ceramic membrane. The method of burning the ceramic membrane differs by some author as the membrane may be burn at initially up to 500-600^{0}C and the temperature is held constant. Holding the temperature at 500-600^{0}C may be used to burn off organic materials before sintering process at high temperature is proceed at ~1500^{0}C [Luyten *et al.* 1997; Lindquvist and Liden, 1997; Gestel *et al.* 2002; Saffaj *et al.* 2004; Seffaj *et al.* 2005]. In fact,

the commercial support made of artificial materials is the important part of high price of the ceramic membranes. Some authors have developed the preparation of low coast supports made of natural raw materials such as clays [Weir *et al.* 2001; Rakib *et al.* 2001].

2-2.3.5 Coating the Membrane

An intermediate layer prepared by dip coating is used to reduce the pore size to a certain required level, and also to repair some defect that may be occurred during casting or spinning process, and during sintering process. Although precautions to remove agglomerates and entrapped air by a wet sieved through a 31.5 μm cloth [Lindquvist and Liden, 1997], some unwanted inert particles entrapped in the dope solution and cracking during sintering process makes the dip coating is necessary and it provides double precautions to eliminate the defect. Selectivity of the membrane is obtained by deposition of the thin porous layer on the surface of the support. Significant research efforts have been devoted to preparations such porous layers made by TiO_2, SiO_2 and ZrO_2 by sol–gel route [Luyten *et al.* 1997; Gestel *et al.* 2002; Saffaj *et al.* 2004; Seffaj *et al.* 2005].

The sol-gel technique is commonly used to obtain the desired pore sizes on the top layer of the membrane. The pore size is dependent on the particle size in the sol, which means that fine particulate sols are required to obtain the pore in nano-meter ranges. The polymeric sol has a potential of giving a smaller pore size than the particulate sol as the obtained gel layer is formed by the polymeric network. The polymeric sol can be prepared by partial hydrolysis of the metal alkoxide. The hydrolysis is often the fast reaction which can be very difficult to control and subsequent drying of the gel layer has to be carried out in very carefully to avoid cracking. The top layer is usually applied by the dip coating. Fig. 2-10 shows two alternatives

for making ceramic membranes, conventional and alternative process as proposed by Lindquvist and Liden, [1997].

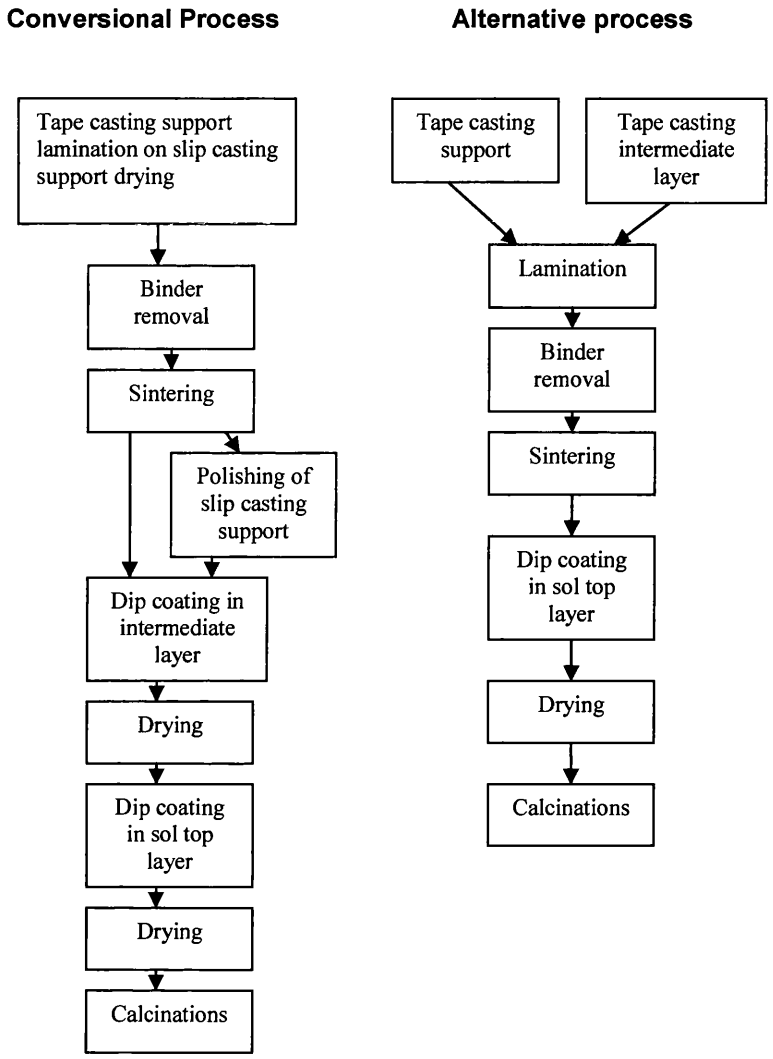

Fig. 2-10: Outline of the conventional and the alternative processes [Lindquvist and Liden, 1997].

2-3. REVIEW OF XANTHAN GUM

In response to environmental concerns, some industries which have previously used non-degrading polymers in their products and raw materials have looked closely at the possibilities of using materials that are "greener" and environmentally friendly. Polymers can be manufactured from petrochemicals, plants or animals based raw chemicals. Petrochemical based polymers are the less preferable choice compared to biopolymers collected or manufactured from plant or animal sources especially for use in consumer products. Despite the increasing collection and extraction costs, and volatile market prices of plant and algal gums (biopolymers) it is suggested that the industrially produced biopolymers (e.g. modified starches, celluloses, and microbial polysaccharides) could be a suitable alternatives.

Xanthan Gum has discovered in the late 1950's by US Scientists and is the first biopolymer produced industrially. The natural source of the polysaccharide came from a cabbage plant bacterium, known as *Xanthomonas campestris*. It was not until 1969 that the FDA issued the final approval for the use of xanthan gum in food products. The demand for xanthan gum produced by Xanthomonas campestris sp. has increased steadily every year and is estimated to grow continuously at an annual rate of 5% - 10%. Commercial production of xanthan gum uses glucose as the substrate, and generally batch production instead of continuous production due to the batch process having been proven to work successfully. However, increasing market price and demand suggests that glucose may no longer economic for the raw material, while using batch processes may also limit the capacity. In is therefore the purpose of this review to investigate alternatives to economically produce xanthan gum.

2-3.1. Application of Xanthan Gum

Xanthan gum is widely used in a broad range of industries such as in foods, toiletries, oil recovery, cosmetics, as water-based paints, etc., due to its superior rheological properties and is used as a rheological control agent in aqueous systems and as stabiliser for emulsions and suspensions. The important properties of the xanthan gum is the ability to form high viscosity solution at low shear forces, highly pseudoplastic, and may also display a viscosity yield value [Yoshida and Tanner, 1993]. The xanthan solution is stable over a wide range of salt concentrations (up to 150 g/litre NaCl), temperatures (up to 90 ^{0}C) and pH (2-11) [Lee, 1996].

The superior properties of xanthan gum have enabled it to compete with most natural gums, and also become the preferred material due chemical reproducibility and relatively easy supply. Xanthan gum applications have diversified its commercial value and now become one of widely used ingredients in food products. As can be seen in Table 2-9, the concentration of xanthan gum used in food products is very small to enable it to confer the required properties without affecting the taste of the final product.

In the agriculture industry, xanthan has been used to improve the flow-ability in fungicides, herbicides, and insecticides formulations by uniformly suspending the solid component [Flickinger and Drew, 1999]. The unique rheological properties of the xanthan gum solution also reduce drift, and increase pesticide cling and permanence. Recently, various "tolerance exemptions" were issued by U.S. Environmental Protection Agency for use of xanthan gum as the surfactant in pesticide formulations. Because of its ability to disperse and hydrate rapidly, is non-polluting and gives a good colour yield, xanthan gum is also used in jet injection printing. Recently, in the formulation of new generations of thermo-set coatings, xanthan gum has

been introduced to meet the challenges of producing environmental friendly products.

Table 2-9: Some examples of xanthan gum in food applications [Imeson and Alan, 1997]

Applications	Uses/Benefits	%
Beverages	Provides enhanced body and quality to the reconstituted drink.	0.05-0.15
Instant Soups	Provide high viscosity in instant soups at both acid and neutral pH.	0.30-0.50
Salad Dressing	Ideal stabiliser for pourable no-oil, low-oil, and regular salad dressings.	0.15-0.50
Cake Mixes	Contributes smoothness; air incorporation and retention.	0.05-0.25
Sauces	Provide high viscosity in sauces and gravies.	0.10-0.30
Relish	Improves the drained weight and virtually eliminates the loss of liquor during handling.	0.10-0.25

In the petroleum industry, xanthan gum is used in oil drilling, fracturing, pipeline cleaning and work-over and completion. Due to xanthan gum's excellent compatibility with salt and resistance to thermal degradation it is also useful as an additive in drilling fluids. The pseudoplasticity of its solutions provide low viscosity at the drill bit where the shear rate is high and high viscosity in the annulus where shear is low. Therefore, xanthan serves a dual purpose by allowing faster penetration at the bit and suspending cuttings in the annulus. For every barrel of oil produced, approximately two remain in the ground. Therefore, enhanced oil recovery (EOR) will be an important use of xanthan gum in the next decades. The basic principle

applied is to improve the separation of water and oil thereby increase oil recovery. However, the concentration of xanthan gum is a critical consideration as high impurities would increase the difficulty when refining the oil. Xanthan gum is used in micellar-polymer flooding as a tertiary oil recovery operation. In this application, polymer-thickened brine is used to drive the slug of the surfactant through porous reservoir rock to mobilise residual oil; the polymer prevents bypassing of the drive water through the surfactant band and ensures good area sweeping [Byong, 1996]. In both applications, the function of polymers is to reduce the mobility of injected water by increasing its viscosity.

The other specialty applications employing xanthan gel are in removing rust, welding rods, wet slag, and cleaning other debris from gas pipelines. Many more application of xanthan gum could be expected to be developed. These wide range of applications of xanthan gum may be summarised due to it superior properties of (1) non-Newtonian behavior, (2) high viscosity yield even at low concentrations (600-2000 ppm), (3) low sensitivity of viscosity to salinity changes, (4) resistance to mechanical degradation, (5) stable with respect to temperature (up to 90 ^{0}C) and (6) a biodegradable material and hence an environmental friendly product, [Malik and Sridhar, 1992].

2-3.2 Chemistry of Xanthan Gum

Xanthan gum is a complex microbial exo-polysaccharide industrially produced from glucose via fermentation by the plant – pathogenic bacterium, *Xanthomonas campestris* pv. campestris. The molecular weight of xanthan gum is approximately 2 million but it can go as high as 13-50 million [Becker *et al.* 1998]. As shown in Fig. 2-11, xanthan gum consists of D – glucosyl, D – mannosyl, and D – glucuronyl acid residues in a molar ratio of 2:2:1 and

variable proportions of *O* – acetyl and pyruvyl residues. Xanthan gum is an acidic polymer made up of pentasaccharide subunits, forming a cellulose backbone with trisaccharide side – chains composed of mannose (β1,4) glucuronic acid (β1,2) mannose attached to alternate glucose residues in the backbone by α -1,3 linkages. On approximately half of the terminal mannose residues is a ketal linkage joined by a pyruvic acid moiety. Acetyl groups are often present as 6 – *O* substituents on the internal mannose residues. Some external mannoses contain a second 6 – *O* – acetyl substituent [Becker, *et al*, 1998].

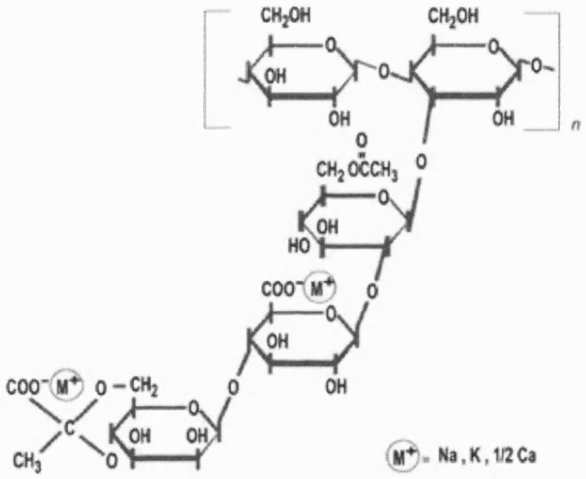

Fig. 2-11: Structure unit of xanthan gum [Sutherland, 1977]

The synthesis of xanthan gum is believed to be similar to exopolysaccharide synthesis by other Gram-negative bacteria [Harding *et al.* 1995]. The synthetic pathway can be divided into three parts:

1. Uptake of simple sugars and conversion to necleotidal derivatives.
2. Assembly of pentasaccharide subunits attached to an isopentyl pyrophosphate carrier.

3. Polymerisation of pentasaccharide repeats units and their secretion.

The xanthan backbone is formed by successive additions of D-glucose-1-phosphate and D-glucose from two moles of UDP-D-glucose. Thereafter, D-mannose and D-glucoronic acid are added from GDP-mannose and UDP-glucoronic acid, respectively. O-Acetyl groups are transferred from acetyl-CoA to the internal mannose residue, and pyruvate from phosphoenolpyruvate is added to the terminal mannose. Each of these steps requires specific substrates and specific enzymes for completion. If either the substrate or the enzyme is absent, the step will be blocked.

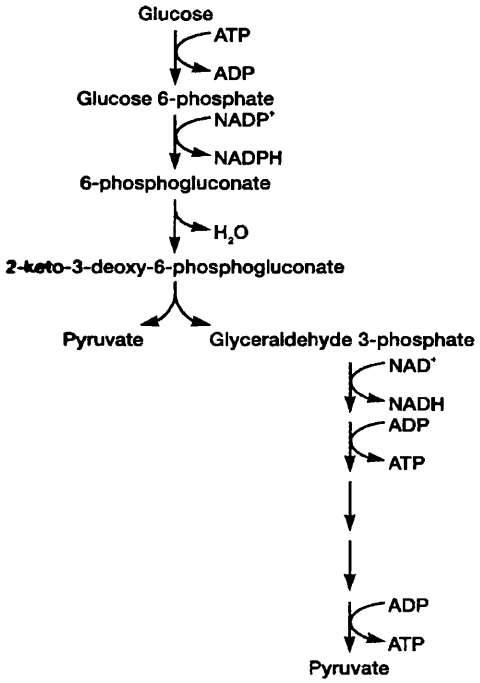

Fig. 2-12: Entner-Doudoroff Pathway [Flickinger and Drew, 1999].

In *X. campestris*, the Entner-Doudoroff pathway in conjunction with the tricarboxylic acid cycle pathway is the predominant mechanism for glucose catabolism (Fig. 2-12). A small portion of glucose is routed via the pentose phosphate pathway. For glucose uptake, two discrete systems exist.

The biosynthesis of xanthan, as in most polysaccharide-producing bacteria, utilises various activated carbohydrate donors to form the polymer on an acceptor molecule. The oligosaccharide repeated units of xanthan are constructed by sequential additions of monosaccharides from sugar nucleotide diphosphates to isoprenoid lipid acceptor molecules. At the same time, acyl substitutes are added from appropriate activated donors. It has been suggested that the construction of the exopolysaccharide follows a "tail – to – head" polymerisation [Flickinger and Drew, 1999]. After the pentasaccharide repeated unit is formed, oligomers are formed by transfer to other lipid intermediates. Oligomer construction normally involves the addition of the longer oligosaccharide sequence to the isoprenoid lipid diphosphate. The inactive lipid carrier is dephosphorylated to yield isoprenyl phosphate, which can then re-enter the biosynthetic sequence.

The structure of repeating units is determined by the sequential transfer of different monosaccharides and acyl groups from their respective donors by highly specific sugar transferases, the polymerase enzyme responsible for polymerisation of the pentasaccharides into a macromolecule. The final stages of exopolysaccharide secretion from the cytoplasmic membrane involve passing across the periplasm and the outer membrane and finally excreted into the extracellular environment. This mechanism must exist in all polysaccharide – producing bacteria for releasing polymer from the isoprenoid lipid prior to transport to its final destination (Fig. 2-13). The process requires an energy source and may be analogous to the of export lipopolysaccharide to outer membrane in which ATP is the energy supplier [Flickinger and Drew, 1999].

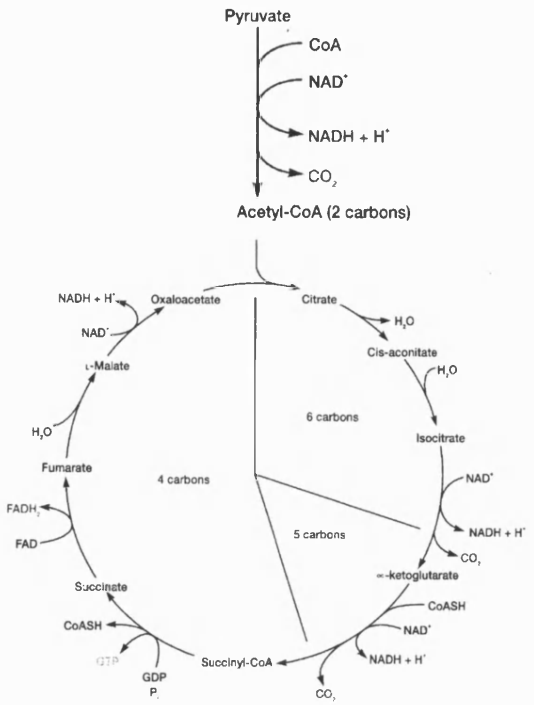

Fig. 2-13: The Trycarborxylic Acid Cycle [Flickinger and Drew, 1999].

2-3.3. Strain of X. camprestris Sp.

The strains for xanthan gum production are selected and improved by several conventional methods. The purpose of genetic modification could be to have improvements of the properties as required by the down stream application, or to suit with the medium supplied, or to improve the product yield, or to improve the performance by reducing the fermentation time, or to simplify the recovering and purification in following processes.

Attempts of mutation of specific genes involved in the xanthan gum synthesis have been made to simplify the repeating unit structure, however the xanthan gum yield was much lower as than that produced from wild-type strains. Betlach *et al.* [1987] have constructed a mutant lacking the glucuronic acid residues and the pyruvate. As result, the xanthan gum solution produced by this strain is highly viscous. Another strategy to alter the structure of xanthan gum is by postsynthetic enzymatic treatment, such

as removal of the terminal β-D-glucuronosyl residue from xanthan gum eliminating the mannosyl side-chain terminus. This truncated xanthan gum missing the terminal disaccharide is more viscous than the original xanthan gum [Betlach *et al.* 1987]. The method of increasing xanthan gum production but varying of the quality of the product of xanthan gum to some extant has been successfully described by Pollock and Thorne [US patent 233019A2, 1987].

A method of increasing xanthan gum production by some extent was successfully described. Despite positive strain developments, the overall increase of xanthan gum yield by new strains still seems to be unlikely [Becker *et al.* 1998]. It may be concluded that modification the of the microbial strains to increase the xanthan gum yields is not necessary since the synthetic production for xanthan gum is very efficient with high conversion of carbon sources into a product (50-85%) [Linton 1990; Amanullah *et al.*1998]. This may suggest that improvement of xanthan yield and quality could be achieved by improving the fermentor and process design, changing the composition of the medium, and the media feeding strategy.

Due to differing supply of particular raw materials in various part of the world, other attempts have been made by researchers to extend the range of the substrates that can be efficiently used for xanthan gum production. *X. campestris* sp generally does not use lactose efficiently because of the low level of β-galactosidase activity in the organism. Fu and Tseng [1990] had introduced a plasmid carrying β-galactosidase-encoding gene into *X. campestris*. The resulting strain is able to produce xanthan gum in whey-containing medium, but the plasmid is not stable. It was concluded that the unmodified starch used as carbon source in producing xanthan gum may not be a correct method.

2-3.4. Nutrients

In order to grow and be reproductive, cells must ingest nutrients necessary to manufacture membranes, proteins, cell walls, chromosomes and other components. The fact that different cells employ different carbon and energy sources shows clearly that all cells do not posses the same internal chemical machinery. Different growth phase and alteration of the growth medium, for example by using different substrate and limiting nutrients, do not influence the primary backbone structure, but do affect the structure of side-chains, the molecular mass, and the yield, thus xanthan gum produced from a batch culture process would represent a mixture produced at different grow phases and may vary with different culture conditions [Davidson 1978]. As different cultures would require different media and optimum conditions, many studies on nutrients required for the purpose of product side-chain variation and optimisation in xanthan gum biosynthesis have been reported [Evans *et al.* 1967; Davidson 1978; Souw and Demain, 1979; Vashitz and Sheintuch, 1991; Zhang and Greasham, 1999; Garcia-Ochoa *et al.* 1992, 2000; Letisse *et al.* 2001].

Davidson [1978] has demonstrated that by limiting magnesium or phosphate it resulted in the production of low pyurate containing xanthan gum (Embden-Meyerhop or EMP). In ammonia-deficient media, high xanthan gum production can be observed. Because of the conventional effects of medium compositions on xanthan gum fermentation, the present industrial xanthan gum production is usually carried out in the medium that provides a compromise between the concentrations needed for cell growth and for xanthan gum formation.

Letisse, *et al.* [2001] performed the fermentation using *X.Camprestris* ATCC 13951 and sucrose as the carbon source. They reported that two

nitrogen sources containing either NH_4Cl or $NaNO_3$ (at 0.055% nitrogen equivalent) showed a slower cell growth rate at 0.07/h than ammonium at 0.13/h. Yet, the xanthan gum production rates has been increased by nitrate at 0.79 mmol/g.cells.h c.f. ammonium at 0.52 mmol/g.cells.h, although the organic acid content (acetate and pyruvate) of the xanthan gum remained constant at 6.0% and 4.6% respectively. Ammonium is therefore a better substrate for biomass accumulation, while xanthan gum yields are higher with nitrate used as the nitrogen source. The growth initiation is poor for each of the mineral nitrogen sources, but could be improved using organic nitrogen (e.g. soybean flour hydrolysate). Using mixtures of ammonium and nitrate salts show that ammonium salts are depleted first. Hence, the sequential consumption of the nitrogen sources (soybean hydrolysates, ammonia and nitrate salt) can be used for further optimisation of the medium. Letisse, *et al.* [2001] also mentioned the biomass accumulation and found that it is limited by phosphate availability. A xanthan gum yield of more than 60% (grams of xanthan gum per gram of sugar) can be obtained with constant acetyl content of the xanthan gum. However, pyruvyl substitution would decrease as the growth rate declines due to the metabolic constraints specific to the phosphate depletion. High rates of carbon conversion into xanthan gum can be observed throughout the course of the culture, and the ATP/ADP ratio is not affected by the decline in the specific growth rate. Souw and Demain [1979] have reported that sucrose is better substrate for xanthan gum production. They have found that succunate and 2-oxoglutarate have stimulatory effects on xanthan gum production in sucrose-based medium.

Garcia-Ochoa *et al.* [1992] conducted the nutritional study of *X. Camprestris* NRRL B-1459 for xanthan gum production as a factorial design of experiments and use a statistical tool to deal with optimisation. The concentrations of other nutrients were fixed e.g. sucrose, calcium, iron, zinc, and citric acid, and the concentration the nutrients nitrogen, magnesium,

phosphorus, and sulphur were varied. They found that the xanthan gum concentration over 24 hours fermentation time is 10g/litre, higher than usual case of ~ 7 g/litre over the same period reported by other authors [Davanson 1978; Souw & Demin 1979; Tait *et al.* 1986; De Vuyst *et al.* 1987]. The optimum summary results are shown in Table 2-10 along with the other findings on the media compositions of four nutrients;

Table 2-10: Comparison of nutrients composition by different authors [Garcia-Ochoa *et al.* 1992]

Nutrient (g/litre)	Davidson [1978]	Souw and Demain, [1979]	Tait *et al.* [1986]	De Vuyst *et al.* [1987]	Garcia-Ochoa *et al.* [1992]
Nitrogen	0.66	0.21	0.66	0.21	0.20
Phosphorus	3.49	3.49	3.49	3.49	2.01
Magnesium	0.02	0.02	0.02	0.02	0.13
Sulphur	0.52	1.50	0.84	1.54	0.07

Casas *et al.* [2000] have studied the effects of temperature, initial nitrogen concentration and oxygen mass transfer rate. They have found that the degree of pyruvilation and acetylation and the average molecular weight of the xanthan gum increases with fermentation time for any operating conditions. The highest average molecular weight of xanthan gum molecules are obtained at a 25°C operating temperature, but acetate and pyruvate radical concentrations are the lowest. Nitrogen concentration seems to have no clear effect on the average of the xanthan molecular weight over the conditions studied.

Leela and Sharma [2000] studied various types of sugars used as the carbon sources during fermentation of the wild type of *X. camprestris* GK6. The obtained xanthan gum yield given as the declining order is glucose, sucrose, maltose and soluble starch. The result is shown in Table 2-11.

Table 2-11: Effect of carbon sources [Leela & Sharma, 2000]

Carbon sources	Xanthan yield (g/litre)
Glucose	14.744
Sucrose	13.234
Maltose	12.321
Fructose	5.232
Xylose	5.531
Arabinose	10.958
Galactose	7.129
Lactose	1.008
Inositol	1.502
Sarbitol	1.401
Soluble Starch	12.10
Potato Starch	9.754

Lo *et al.* [1997a] showed that the preferred course for xanthan gum production is by the two stage batch fermentation using glucose and yeast extract at initial low of 2.5% glucose / 0.3% yeast extract for the initiation/exponential phase to a higher level of 5% by adding 2.5% of the glucose during of the steady state phase. There was no further addition of yeast extract. They also reported that by adding the glucose periodically over the course of the fermentation in five equal parts, the yields are poor giving only 18g/litre of xanthan gum. However, using the two stage fermentation technique by a single addition of the additional glucose after 34 h ferrmentation the yield can reach up to 40g/litre of xanthan gum. The fermentation cycle also takes only 100 h instead of about 120 h using the technique of glucose addition only at the start. Amanullah *et al.* [1998] have extended the sequence feeding approach by introducing the glucose in a series of pulses after the supplied nitrogen had been exhausted in a conversional agitated fermentor. They have found that the yield improved significantly. These two results suggest that a high glucose concentration should be introduced after microbial growth has reached the stationary phase, and although a high glucose concentration is required after reaching the stationary phase the glucose concentration must be controlled at a level that avoids inhibition by the high concentration of the substrate.

Partially hydrolysed starches that have been utilised in xanthan gum production are from hydrolysed rice, barley and corn flour [Glicksman, 1975]. Acid whey [Charles and Radjai, 1977] sugarcane molasses [El-Salam *et al.* 1993; Kalogiannis *et al.* 2003], a mixture of mannose and glucose [Jean-Claude *et al.* 1997], waste sugar beet pulp [Yoo and Harcum, 1999], and peach pulp [Papil *et al.* 1999]. Yields and qualities of xanthan gum have been reported to be competitive, however, glucose still give the best in terms of product yield [Leela and Sharma, 2000; Becker *et al.* 1998; Harding *et al.* 1995;], constancy of supply, and product quality [Davidson, 1978]. Some of the possible reasons that could cause low yield and quality are;

i. The deficiency of certain functional groups in the carbon sources, resulting in different metabolic pathway reactions being followed. Subsequently, the synthesis produced slightly different structures of extra-cellular polysaccharide (EPs), or
ii. The nutrients composition vary due different carbon sources used, hence the quality of produced xanthan gum cannot be obtained as required.
iii. Formation of other by-products.
iv. The components or/and chemical variants in the unmodified starch might become inhibitors.
v. A low yield caused by high concentration of non-reacted compounds and lower quality and the post purification process becomes more complicated.

It is concluded that the important findings on nutrients studies are outlined as: a relatively high nitrogen concentration is required for fast cell growth, the type of salt supplied as a source of nitrogen such as ammonium or nitrate or undefined nitrogen sources resulting in different bacterial growth rates, continuous feeding of the carbon source at certain concentration after

microbial reach a steady state growth phase would improve yield, and glucose is a preferable substrate.

2-3.5. Batch against Continuous Process

Although batch culture is commercially preferred having fewer parameters to be controlled and well understood, a problem of operation in batch culture is that the environment for cell growth keeps changing throughout the "growth cycle" and could give adverse conditions such as toxic products or extreme pH and exhaustion of nutrients. While in continuous culture, the growth medium is continuously supplied to the culture vessel, extreme conditions will not occur as medium is continuously diluted and removed from the vessel. Becker *et al.* [1998] have also pointed out that continuous process shows reasonably high conversion rates of substrate to polymer of 60-70%, but also mention problems of maintaining the sterility and the risks of emergence of fast-growing mutants that do not produce the desire product, xanthan gum. Nevertheless, the continuous process gives a cost competitive system, and with suitable growth conditions considerable yields of polysaccharides can be maintained for more than 2000 hours [Evans, *et al.* 1967], thus the continuous process could be the choice rather than the batch mode.

Although conventional methods can be improved by continuous fermentation, there is still a classic problem that the product contain cells and cell debris, which gives lower the filterability of the xanthan solution and limits its application. The production of cell-free xanthan gum is therefore desirable. In 1966, Esso Production Research Company found that continuous film fermentation reactions can be readily carried out by a continuously depositing a suitable substrate on the surface of a rotating drum or moving belt or similar device, and applying a culture containing

selected microorganisms to the film, and then continuously removing the fermentation product after sufficient residence time has elapsed. Tests have shown that such a process makes it possible to use the substrate in higher concentrations, permits surprisingly effective utilisation of the substrate, reduces the time required for carrying out the fermentation reaction, minimises variation in product quality, and simplifies recovery of the fermentation products [Glicksman, 1975].

2-3.6. Xanthan Gum Kinetics

Selection and development of the appropriate kinetic models particularly for certain micro-organisms should begin with understanding of the behaviour and habitat of the micro-organisms. Two main options are available for kinetic developments, batch or continuous operation as the time course of the microbial growth would differ in each operation.

Studies of the unstructured kinetic and the structured kinetics models have been described in a batch process [Luong and Mulchandani, 1988; Garcia-Ochoa, *et al.* 1995, 1998; 2004]. Many authors used the unstructured kinetic model to describe the synthesis of xanthan gum by *X. camprestris sp.* [Moraine and Rogovin, 1971; Weiss and Ollis 1980; Luong and Mulchandani, 1988; Garcia-Ochoa, *et al.* 1995]. These unstructured kinetics would include a balance on the cells mass (γ_X), the product concentration (γ_P), and the substrates concentration (γ_S).

A more comprehensive kinetic model could also include the mass transfer limitation caused by increased viscosity, mechanical design of equipment, and variation of the adverse conditions with time such as cell population density, which would contribute to increasing cells stress and endogenous rate. Garcia-Ochoa *et al.* [1998] have proposed the metabolic structured kinetic model for xanthan gum production by *X. camprestris* which is based on the assumptions studied by Pons *et al.* [1989]. The proposed

kinetic model is able to describe xanthan gum production at different temperatures and take into account variations in model parameters when the kinetic equations are first order for dissolved oxygen. The latest study by this group [Garcia-Ochoa *et al.* 2004] proposed a chemical structured kinetic model by involving both carbon source metabolism and nitrogen metabolism into cells. This model considers eight lumped reactions (synthesis of amino acids, both non forming and forming bases, nucleic acids synthesis, both RNA and DNA synthesis, xanthan production, total sugar metabolism, oxidative phosphorylation and maintenance energy) and eight key compounds (biomass, ammonium, RNA, DNA, intracellular proteins, xanthan gum, sucrose and dissolved oxygen). The model more closely describes the experimental results and it able to predict the behaviour of the system when some operational conditions are changed, e.g. temperature, initial nitrogen concentration, and also different oxygen transport rates, thus predicting different xanthan production rates by depending on the operational conditions and medium composition (nitrogen source concentration).

As many authors use unstructured kinetic models and batch processing, the kinetic discussed here is limited to the most used of the kinetic models. In this case, interest is centred on the population growth rather than the substrate utilisation and the xanthan gum production as both relate to the microbial growth factor. Other than substrates and nutrients that would limit the microbial reproductive are reactor design, agitation rates, and changes of viscosity [Casas *et al.* 2000]. The general form of microbial growth kinetics may be expressed by Equation 2-39.

$$\Gamma_X = \frac{d\gamma_X}{dt} \propto f\left(\gamma_X, \gamma_S, \gamma_P, \gamma_N, \gamma_{O_2}, \gamma_\xi\right) \qquad (2\text{-}39)$$

where Γ_X is the biomass growth rate, f the function particular to the used system, γ_X the biomass concentration, γ_S the concentration of substrate i, γ_P the product concentration, γ_N the nitrogen concentration, γ_{O_2} the oxygen concentration, and γ_ξ other special adverse components or inhibitors concentrations e.g. $\gamma_{CO_2}, \gamma_{poison}$.

Weiss and Ollis, [1980] have expressed growth rate as a function of biomass by the logistic equation which is also known as the Verlhurst-Pearl or so called autonomous equation. The equation can be written as;

$$\Gamma_X = \mu_m \gamma_X \left(1 - \frac{\gamma_X}{\gamma_{X_m}}\right) \qquad (2\text{-}40)$$

The modified logistic growth kinetics that describe the batch kinetic of the microbial growth during biosynthesis of extra- and intra-cellular polymers proposed by Mulchandani *et al.* in the paper published by Luong and Mulchandani, [1988] is given as;

$$\Gamma_X = \mu_m \gamma_X \left(1 - \left(\frac{\gamma_X}{\gamma_{X_m}}\right)^\theta\right) \qquad (2.41)$$

The relationship is valid as long as $\left[1-\left(\gamma_X / \gamma_{X_m}\right)^\theta\right]$ in non-negative, i.e., $\theta > 0$. The constant θ could be defined as an index of inhibitory effects that accounts for the deviation of growth from the exponential growth. For a very large θ, the generalised logistic equation kinetic approaches the exponential growth equation:

$$\Gamma_X = \mu_m \gamma_X \tag{2.41}$$

Luong and Mulchandani [1988] proposed a combination of Monod and logistic or modified logistic as follow;

$$\Gamma_X = \mu_m \frac{\gamma_S}{K_S + \gamma_S}\left(1 - \frac{\gamma_X}{\gamma_{X_m}}\right)\gamma_X \tag{2.42}$$

Two substrates are expressed in term of stoichiometric coefficients [Garcia-Ochoa *et al.* 1995).

$$\Gamma_S = \frac{d\gamma_S}{dt} = -\frac{1}{Y_{P/S}}\Gamma_P \tag{2.43}$$

$$\Gamma_N = \frac{d\gamma_N}{dt} = -\frac{1}{Y_{X/N}}\Gamma_X \tag{2.44}$$

Where $Y_{P/S}$ is the product yield coefficient based on substrate, $Y_{X/N}$ is the biomass yield coefficient based on nitrogen. Unfortunately for the biomass in xanthan gum production, the rate is not of the Monod type, therefore the equation proposed by Luong and Mulchandani [1988] is not suitable to represent the synthesis of xanthan gum. Garcia-Ochoa *et al.* [1995] have proposed the rates as follows:

$$\Gamma_X = k_X \gamma_N \gamma_X \tag{2.45}$$

$$\Gamma_P = \frac{d\gamma_P}{dt} = k_P \gamma_S \gamma_X \tag{2.46}$$

The logistic equation is given from the combination of equations (2.41) an (2.42).

$$\Gamma_X = k_X \frac{\gamma_{X_m}}{Y_{X/N}} \cdot \gamma_X \cdot \left(1 - \frac{\gamma_X}{\gamma_{X_m}}\right) \tag{2.47}$$

When nitrogen is the limiting factor, microbial growth has ceased after the nitrogen source had exhausted, therefore the parameter γ_{X_m} is replaced by;

$$\gamma_{X_m} = \gamma_{X_0} + Y_{X/N}\gamma_{N_0} \tag{2.48}$$

$$\Gamma_X = k_X \left(\frac{\gamma_{X_0}}{Y_{X/N}} + \gamma_{N_0}\right) \cdot \gamma_X \cdot \left(1 - \frac{\gamma_X}{\gamma_{X_0} + Y_{X/N} + \gamma_{N_0}}\right) \tag{2.49}$$

Carbon source is used for maintenance and for growth, thus;

$$\Gamma_S = \frac{d\gamma_S}{dt} = -m_S \cdot \gamma_X - \frac{1}{Y_{X/S}} \cdot \frac{d\gamma_X}{dt} \tag{2.50}$$

Dissolve oxygen is described by the following equation;

$$\frac{d\gamma_{O_2}}{dt} = k_L a \cdot \left(\gamma^*_{O_2} - \gamma_{O_2}\right) - \left(m_{O_2} \cdot \gamma_X + \frac{1}{Y_{O_2/X}} \cdot \frac{d\gamma_X}{dt}\right) \tag{2.51}$$

Where the oxygen mass transfer coefficient is given as;

$$k_L a = 3.08 \cdot 10^{-4} \cdot V_S^{0.43} \cdot N^{1.75} \cdot \eta^{-0.39} \qquad (2.52)$$

So far for the unstructured kinetics models that have been reviewed, no authors have evaluated the microbial growth caused by adverse conditions e.g. carbon dioxide contents and other inhibit chemicals produced by the microorganism itself. However, a modification of the combination of logistic and Monod kinetics, given by Luong and Mulchandani [1988], (shown in equation 2-42) represents the cell growth kinetics of *A. eutrophus* sp, and describes the effect of substrate concentration on the growth rate. Consideration of inhibition effects proposed by Mulchandani *et al.* reported in a published paper by Luong and Mulchandani [1988], could partially describe adverse conditions, and if so, a combination of the substrate concentration effect (equation 2-53) and inhibition effects (equation 2-54) into the microbial kinetic suggested by Garcia-Ochoa *et al.* [1995] could completely describe the adverse conditions effect on microbial growth rate. In xanthan gum fermentation, high substrate concentrations would inhibit microbial growth.

$$r_X = \mu_m \frac{\gamma_S}{K_S + \gamma_S}\left(1 - \frac{\gamma_S}{\gamma_{S_m}}\right)^{\delta} \gamma_X \qquad (2\text{-}53)$$

$$\Gamma_X = \mu_m \frac{\gamma_S}{K_S + \gamma_S}\left(1 - \left(\frac{\gamma_X}{\gamma_{X_m}}\right)^{\theta}\right)\gamma_X \qquad (2\text{-}54)$$

$$\Gamma_X = k_X\left(\frac{\gamma_{X_0}}{Y_{X/N}} + \gamma_{N_0}\right) \cdot \gamma_X \cdot \left(1 - \left(\frac{\gamma_X}{\gamma_{X_0} + Y_{X/N} + \gamma_{N_0}}\right)^{\theta}\right) \cdot \left(1 - \frac{\gamma_S}{\gamma_{S_m}}\right)^{\delta} \gamma_S \qquad (2\text{-}56)$$

In this kinetic review, it is proposed that the function of microbial growth is given by Equation (2-38). The effects of (a) carbon source is given by Equations (2-45) and (2-50), (b) biomass is given by Equation (2-48), (c) nitrogen source is given by equation (2-48), (d) oxygen is given by Equation (2-1), and (e) the proposed Equation (2-56) which has considered other adverse conditions and substrate inhibition.

2-3.7. Commercial Productions Processes.

Most commercial production of xanthan gum uses glucose or invert sugars, and most industries prefer batch instead of continuous [Garcia-Ochoa *et al.* 1992 Leela, and Sharma, 2000, Harding *et al.* 1995]. Quality assurance and easer of control are reasons why the xanthan gum production uses invert sugars, instead of polysaccharides, and batch processes instead of continuous operation.

A typical commercial production process starts with inoculums of *X. campetris* that are prepared in a suitable fermentation medium in conventional batch processing using mechanically agitated vessels. The aerated culture that undergoes the aerobic process is held at the following operating conditions: temperature approximately T=28-30^{0}C, pH~7, the aeration rate must higher than 0.3 v/v, and the specific power input for agitation higher than 1 kW/m^3 [Flickinger and Draw 1999]. The fermentation process is carried out for about 100 h and converts an approximately 50% of the glucose into the product. Inoculums preparation includes several stages which require a set of reactors ranging from 10 litres for the initial seed up to 100 m^3 in production stage by which the volume is usually enlarged 10 fold. As the fermentation evolves, cells would grow exponentially resulting in rapid consumptions of the nitrogen source. After fermentation stage, multi steps downstream processes would follow. Fig. 2-14 shows an example of the

xanthan gum process used by industry that includes multi steps of downstream process.

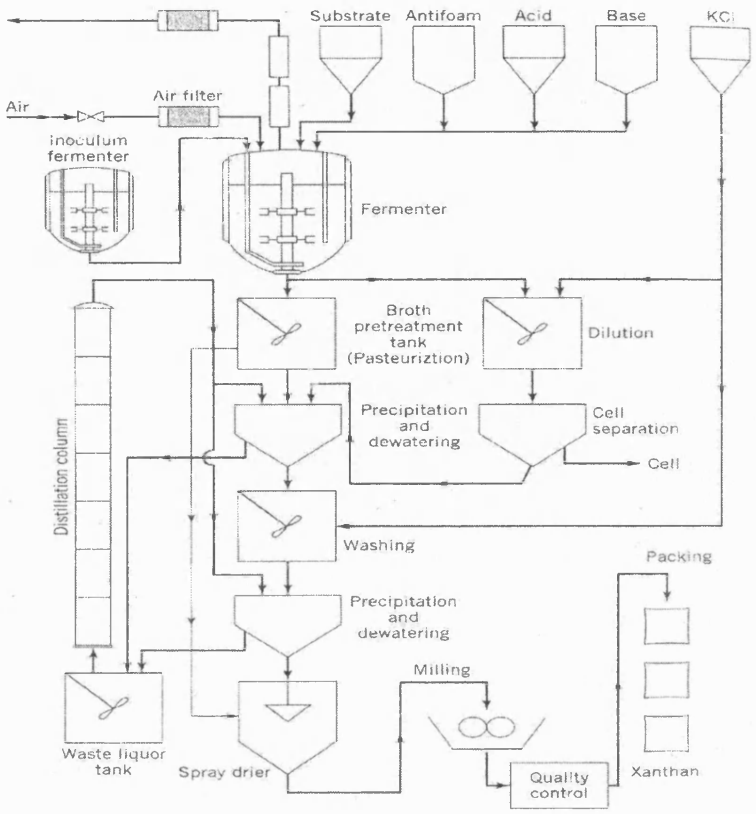

Fig. 2-14: Flow sheet of xanthan production in conventional stirred tank fermentor [Flickinger and Drew, 1999]

When industrial grade xanthan is required, the post fermentation process treatment may be started with pasteurisation on the fermented broth to sterile the bacterial and to deactivate the enzymes. This process usually uses a large amount of alcohol to precipitate the xanthan gum, and the precipitated xanthan gum is then sprayed dry or maybe re-suspended on the water and then re-precipitated. When cell-free xanthan gum is required, cells centrifugation is facilitated by diluting the fermentation broth to improve the cell separation.

The cell separation by the dilution process from highly viscous xanthan solution is a cost-intensive process [Balows and Truper, 1991]. A favoured method is by adding alcohol and salt to improve precipitation by creating reverse effect charges. The xanthan gum obtained in wet solid form undergoes dewatering and washing to obtain the final purity required. Alcohol used for xanthan precipitation is recovered by distillation. Washing may be carried out to improve the quality of product as it would entirely remove particulate matters such as cell debris, microgels, organic residues and pigments. Concentrated xanthan gum is then re-dissolved and washed with water/KCl to reduce viscosity, precipitated and dewatered again until required is obtained. Finally, the precipitated xanthan gum is spray-dried in batch or continuous driers. The dry xanthan gum is milled to the desired mesh sizes for control of disperse ability and dissolution rate as well as to easier handling.

2-3.8. Recent Developments of Xanthan Gum Production

Developments and improvements have been studied for the xanthan production by Lo, *et al.* 1997a; Amanullah, *et al.* 1998; and Garcia-Ochoa, *et al.* 2000. In the last few years, membrane processes have been increasingly used for concentrating highly viscous broth [Pritchard, *et al.* 1995; Lo, *et al.* 1996; 1997b; Howell, *et al.* 1996]. Ultra-filtration was also reported to save up to 80% the energy is required for recovering of xanthan gum from the fermentation by conventional means [Lo, *et al.* 1997b].

Lo, *et al.* [1996] studied the performance of the ultrafiltration system of the whole fermentation broth, introducing heat treatment before exposing the broth to ultrafiltration, and the cell free broth collected from immobilised cells fermentation. Results revealed that the membrane was heavily fouled by cells when the whole broth was introduced. When heat treatment was

introduced in the first place to lyses the cells, ultra-filtration performance was improved but cell debris still contributed to significant membrane fouling. This could also become a major problem in long-run operation. The cell free xanthan broth did not significantly foul the membrane during the entire period [Lo *et al.* 1996]

As cell free xanthan gum would eliminate membrane fouling, Yang *et al.* [1996] have developed a novel of centrifugal packed-bed reactor (CPBR) used for viscous xanthan gum production. *X. campestris* cells were immobilised in a rotating fibrous matrix by natural attachment to the fibre surfaces. Continuously pumping and circulating the medium broth through the rotating fibrous matrix would ensure a good transfer of the gas and liquid with the cells. The fibrous matrix support would give a good separation of the xanthan gum from the cells as most cells are immobilised onto the fibre surfaces. Yang *et al.* [1998] have also studied a system for cells adsorption using a matrix support. Studying four different woven materials; cotton towel, cotton fabric, and 50% cotton and 50% polyester, the result showed that cotton with rough surfaces was the preferred material. Cell adsorption to cotton was also reported faster than polyester fibres, and almost all cells have been removed from the fermentation broth. They also found that cells adsorption is not efficient in the absence of xanthan gum [Yang, *et al.* 1998]. The CPBR and cells adsorption method have potential to be developed further for continuous operation.

Other developments are the axial-flow hollow fibre cell culture bioreactors [Brotherton and Chau, 1996], the fibrous-bed bioreactor for continuous production of developmental endothelial locus-1 by osteosarcoma cells [Chen, *et al.* 2002], and the ceramic membrane reactor which could possibly help in development of continuous xanthan gum production.

CHAPTER 3:

KINETICS MODELLING AND OPTIMISATION OF THE SIMULTINEOUS, GELATINISATION, LIQUEFACTION AND SACCHARIFICATION (SGLS)

3-0. INTRODUCTION

The aim of this chapter is to develop the kinetic model of the simultaneous, gelatinisation, liquefaction and saccharification (SGLS) at low temperature, to optimise the SGLS, to see the effect of some operational conditions, and also to validate and verify the SGLS kinetic model. The balanced reactions of gelatinisation, liquefaction, and saccharification carried out simultaneously at low temperature below < 60^0C proposed in this study is a new development in the starch hydrolysis technology which could be an alternative for future processing of glucose in the field of biotechnology. The main purpose of the SGLS carried out at low temperature is for development of the ultrafiltration process for production of pure, clean and sterile glucose solution [Rosalam & England, 2004]. Thus, this study may lead to a better understanding of the low temperature SGLS kinetic in batch hydrolysis processes and will also serve as a basis for a study of continuous production in an ultrafiltration system. Development of the ultrafiltration process as a working system for the SGLS will be considered in chapter 4.

The kinetic of some starch hydrolysis processes were found to be reasonably modelled [Nakajima *et al.* 1992; Ahmet *et al.* 2003; Paolucci-Jeanjean 2000a and c; Houng *et al.* 1992; Brandam *et al.* 2003]. The kinetic

models have been discussed in the literature survey in Chapter 2, but the proposed equilibrium kinetic for the SGLS was not sufficient. Thus, this chapter will discuss a proposed kinetic model for SGLS which is derived based on the Michaelis-Mentan kinetic model. Determination of the proposed kinetic parameters and model verification are performed using the batch hydrolysis processes. Viscosity has also been monitored to confirm the model assumption that it is remained consistently low throughout the entire SGLS process.

3-1. THE PRINCIPLES OF THE SLGS

Conventionally the consecutive reaction order carried out at the optimum reaction temperatures respectively are gelatinisation (~140 ^{o}C, ~2 hours) > liquefaction (~80-90^{0}C, ~24 hour) > saccharification (55-60^{0}C, ~48 hours). When the reaction temperature is lowered to a certain setting temperature between 55-60^{0}C, gelatinisation reaction rate is affected more as the temperature reduced by ~85^{0}C, while liquefaction reaction rate is reduced by ~30^{0}C. But the saccharification reaction rate would stay constant. The gelatinisation rate decreases by exponential pattern, while liquefaction rate decreases about 2-3 times for every 10^{0}C temperature step [Rosalam and England, 2004].

Studying the required reaction time, it could be that at a certain fixed temperature, the reactions would achieve equilibrium. Thus, the low temperature SGLS is proposed by hoping that at the optimum temperature of the saccharification, the reactions would achieve equilibrium. This simultaneous reaction scheme should consume less reaction time by overlapping the reactions, and should also permit control over formation of the gelatinised starch at a certain particular time. This means that the

gelatinisation rate of reaction is set as the limiting factor in the low temperature SGLS reaction.

Although the SGLS seems the ideal technique and flexible, the gelatinisation reaction can not occur for a certain type of starches or may retain a high fraction of recalcitrant polymers. However, the literature review supports the SGLS hypothesis that the gelatinisation of the tapioca starch and many other starch sources can occur within 55-60^{0}C but at a low rate. The conversion can also as high as 70% [Linko & Javanainen 1996; Marchal *et al.* 1999]. This may be the key point on the success of the SGLS.

Giving a priority to limit viscosity, in the batch process, the viscosity would change from initially low to a slightly higher value and then remain constant at equilibrium. At equilibrium, the gelatinised starch concentration is considered to be unchanged (a quasi steady state), until finally the productive starch concentration approaches zero. The remaining unconverted starch, so called the unproductive substrate, represents the quantity of higher molecular weight polysaccharides in the system. In the continuous process, the equilibrium reaction would remain constant as a quasi steady state condition, provided there is continuous or sequential supply of the starch and enzymes required and by-products of higher molecular weight polysaccharides need to be removed.

3-1.1 Reactions Involve

In order to develop the reaction kinetic model, we assume the SGLS reactions as below;

$$S \xrightarrow{k_1^{gel}} S_1 \quad \text{(Initial zero order gelatinisation)} \qquad (3\text{- }1)$$

$$S \xrightarrow{k_2^{gel}} S_1 \quad \text{(First order gelatinisation reaction)} \qquad (3\text{-}2)$$

$$S_1 + E_1 \underset{k_{-1}^{liq}}{\overset{k_1^{liq}}{\Leftrightarrow\!\Rightarrow}} E_1S_1 \xrightarrow{k_2^{liq}} +E_1 + S_2 + U \quad \text{(Liquefaction)} \qquad (3\text{-}3)$$

$$S_2 + E_2 \underset{k_{-1}^{sac}}{\overset{k_1^{sac}}{\Leftrightarrow\!\Rightarrow}} E_2S_2 \xrightarrow{k_2^{sac}} +E_2 + P_n \quad \text{(Saccharification)} \qquad (3\text{-}4)$$

Where S is the starch, S_1 the gelatinised starch, S_2 the hydrolysed starch, U the recalcitrant polymers, E_1 the α-amylase (termamyl), E_2 the amyloglosacidase (AMG), E_1S_1 the first intermediate product, E_2S_2 the second intermediate product, P_n the product, k_1^{gel} zero order gelatinisation rate velocity, k_1^{gel} first order gelatinisation rate velocity, k_1^{liq}, k_{-1}^{liq} and k_2^{liq} the liquefaction reaction rate velocities, and k_1^{sac}, k_{-1}^{sac} and k_2^{sac} the saccharification reaction rate velocities.

3-1.2. Evaluation of the Increased Viscosity

If only the gelatinisation reaction occurs at a certain condition, e.g. constant temperature and pressure, the gelatinisation reaction is initially zero order then followed by first order. At $0 \le t \le t_1$;

$$\frac{d\gamma_s}{dt}\Big|_{t=0}^{t=t_1} = -k_1^{gel} \qquad (3\text{-}5)$$

$$\gamma_S = k_1^{gel} t \qquad (3\text{-}6)$$

$$\gamma_{S_1}(t \le t_1) = k_1^{gel} t \qquad (3\text{-}7)$$

Where γ_S and γ_{S_1} are the concentration of starch and gelatinised starch (g/litre) respectively and t_1 (hr) the time after zero order gelatinasation. When gelatinasation is first order kinetics $t > t_1$;

$$\frac{d\gamma_S}{dt}\Big|_{t_1}^{t} = -k_2^{gel}\gamma_S \qquad (3\text{-}8)$$

At $t > t_1$, $\gamma_{S_0} - k_1^{gel} t\Big|_{t=0}^{t=t_1} = \gamma_{S_0^{lim}}$ a constant value. Combining both kinetic stages;

$$\gamma_S = \gamma_{S_0^{lim}} \cdot \left(\exp\left(-k_2^{gel}(t - t_1)\right)\right) \qquad (3\text{-}9)$$

Where γ_{S_0} is the initial starch concentration (g/litre), and $\gamma_{S_0^{lim}}$ the starch concentration after zero order gelatinisation. The gelatinised starch produced after $t \geq t_1$ is:

$$\gamma_{S_1}(t \geq t_1) = \gamma_{S_0} - \gamma_{S_0^{lim}} + \gamma_{S_0^{lim}}\left(1 - \exp\left(-k_2^{gel}(t - t_1)\right)\right) \qquad (3\text{-}10)$$

When applying simultaneous reactions, the gelatinised starches would instantaneously convert to products. The Michealis-Menten model would be ideal to represent the liquefaction rate;

$$\frac{d\gamma_{S_1}}{dt} = \frac{\Gamma_{max}\gamma_{S_1}}{K_m + \gamma_{S_1}} \qquad (3\text{-}11)$$

Combining the formation of gelatinised starches and the utilisation rate by the liquefaction reaction, the first order coefficients-constant equation demonstrates the net rate changes is of γ_{S_1} is obtained.

$$\frac{d\gamma_{S_1}}{dt} + \frac{\Gamma_{max}\gamma_{S_1}}{K_m + \gamma_{S_1}} - (k_1^{gel} + k_2^{gel}\gamma_{S_0^{lim}}) = 0 \qquad (3\text{-}12)$$

The maximum formation of gelatinised starches is given when $\frac{d\gamma_{S_1}}{dt} = 0$, hence;

$$\gamma_{S_1} = \frac{(k_1^{gel} + k_2^{gel}\gamma_{S_0^{lim}})K_m}{\Gamma_{max} - (k_1^{gel} + k_2^{gel}\gamma_{S_0^{lim}})} \qquad (3\text{-}13)$$

At certain conditions yet to be identified, the equation given above would be able to calculate the concentration of γ_{S_1} and predict the increased viscosity, provided the relationship between γ_{S_1} and increased viscosity is known.

3-1.3 Evaluation of Glucose Formation

The formation rates of each component in batch systems can be given as;

$$\frac{d\gamma_{S_1}}{dt} = k_1^{gel} + k_2^{gel}\gamma_S + k_{-1}^{liq}\gamma_{E_1S_1} - k_1^{liq}\gamma_{E_1}\gamma_{S_1} \qquad (3\text{-}14)$$

$$\frac{d\gamma_U}{dt} = k_2^{liq}\gamma_{E_1S_1} \qquad (3\text{-}15)$$

$$\frac{d\gamma_{E_1S_1}}{dt} = -(k_{-1}^{liq} + k_2^{liq})\gamma_{E_1S_1} + k_1^{liq}\gamma_{E_1}\gamma_{S_1} \qquad (3\text{-}16)$$

$$\frac{d\gamma_{S_1}}{dt} = k_2^{liq}\gamma_{E_1S_1} + k_{-1}^{sac}\gamma_{E_2S_2} - k_1^{sac}\gamma_{E_2}\gamma_{S_2} \qquad (3\text{-}17)$$

$$\frac{d\gamma_{E_2S_2}}{dt} = -(k_{-1}^{sac} + k_2^{sac})\gamma_{E_2S_2} + k_1^{sac}\gamma_{S_2}\gamma_{E_2} \qquad (3\text{-}18)$$

$$\frac{d\gamma_{P_n}}{dt} = k_2^{sac}\gamma_{E_2S_2} \qquad (3\text{-}19)$$

Where $\gamma_{E_1S_1}$ and $\gamma_{E_2S_2}$ are the intermediate concentration of the bonded enzyme and substrate (g/litre). As the gelatinisation reaction has been set to

be the limiting factor, in this condition, no significant accumulation of the gelatinised starch can occurred in the system. Therefore;

$$\frac{d\gamma_{E_1S_1}}{dt} \approx 0 \text{ and } \frac{d\gamma_{E_2S_2}}{dt} \approx 0,$$

$$\gamma_{E_2S_2} = \frac{k_1^{sac}\gamma_{E_2}\gamma_{S_2}}{k_{-1}^{sac} + k_2^{sac}} \quad (3\text{-}20)$$

$$\gamma_{E_1S_1} = \frac{k_1^{liq}\gamma_{E_1}\gamma_{S_1}}{k_{-1}^{liq} + k_2^{liq}} \quad (3\text{-}21)$$

$$\frac{d\gamma_{S_1}}{dt} = k_1^{gel} + k_2^{gel}\gamma_S + k_{-1}^{liq}\gamma_{E_1S_1} - k_1^{liq}\gamma_{S_1}\gamma_{S_1} \approx 0 \quad (3\text{-}22)$$

$$\gamma_{S_1} = \frac{k_1^{gel} + k_2^{gel}\gamma_S + k_{-1}^{liq}\gamma_{E_1S_1}}{k_1^{liq}\gamma_{E_1}} \quad (3\text{-}23)$$

By describing the gelatinised and liquefied starches as intermediate substrates, controlling the gelatinisation rate has increased the ratio of intermediate substrate concentrations to enzymes. Thus, allowing instantaneous conversion of the substrates into products.

$$\frac{d\gamma_{S_2}}{dt} = k_2^{liq}\gamma_{E_1S_1} + k_{-1}^{sac}\gamma_{E_2S_2} - k_1^{sac}\gamma_{E_2}\gamma_{S_2} \approx 0 \quad (3\text{-}24)$$

$$\gamma_{S_2} = \frac{k_2^{liq} + k_2^{liq}\gamma_{E_1S_1} + k_{-1}^{sac}\gamma_{E_2S_2}}{k_1^{sac}\gamma_{E_2}} \quad (3\text{-}25)$$

$$\gamma_{E_2S_2} = \frac{k_2^{liq}\gamma_{E_1S_1}}{k_2^{sac}} \quad (3\text{-}26)$$

$$\gamma_{E_1S_1} = \frac{k_1^{gel} + k_2^{gel}\gamma_S}{k_2^{liq}} \quad (3\text{-}27)$$

$$\gamma_{E_2S_2} = \frac{k_1^{gel} + k_2^{gel}\gamma_S}{k_2^{sac}} \quad (3\text{-}28)$$

$$\frac{d\gamma_{P_n}}{dt} = k_1^{gel} + k_2^{gel}\gamma_S \quad (3\text{-}29)$$

The mass balance of the substrate and enzymes is;

$$\gamma_{S_0} = \gamma_S + \gamma_{S_1} + \gamma_{S_2} + \gamma_{E_1S_1} + \gamma_{E_2S_2} + \gamma_{P_n} + \gamma_U \qquad (3\text{- }30)$$

$$\gamma_{E_{01}} = \gamma_{E_1} + \gamma_{E_1S_1} \qquad (3\text{- }31)$$

$$\gamma_{E_{02}} = \gamma_{E_2} + \gamma_{E_2S_2} \qquad (3\text{- }32)$$

Where $\gamma_{E_{01}}$ is the initial α-amylase concentration (mg/litre), $\gamma_{E_{02}}$ the initial AMG concentration (mg/litre), γ_U the by-product and non-productive substrate, and γ_{P_n} the product concentration (g/litre) mainly glucose (95-99.9%)

In many cases, the enzymes concentration is very small compared to the substrate concentration (≈ 0), thus;

$$\gamma_{S_0} = \gamma_S + \gamma_{S_1} + \gamma_{S_2} + \gamma_{P_n} + \gamma_U \qquad (3\text{- }33)$$

Relating unproductive products and the substrate;

$$\gamma_U = \alpha(\gamma_{S_0} - \gamma_S) \qquad (3\text{- }34)$$

Hence;

$$\gamma = \gamma_{S_0} - \frac{\gamma_{S_1} + \gamma_{S_2} + \gamma_{P_n}}{(1-\alpha)} \qquad (3\text{- }35)$$

Where, α is the fraction of the recalcitrant starch over the productive hydrolysed starch. As γ_{S_1} and γ_{S_2} are instantaneously converted into products and by-products, then γ_{S_1} and $\gamma_{S_2} \approx 0$. The equations 3-29 and 3-35 become;

$$\frac{d\gamma_{P_n}}{dt} = k_1^{gel} + k_2^{gel}\left(\gamma_{S_0} - \frac{\gamma_{P_n}}{1-\alpha}\right) \qquad (3\text{-}36)$$

Rearranging the first order linear homogenous coefficients-constant equation gives;

$$\frac{d\gamma_{P_n}}{dt} + k_2^{gel}\left(\frac{\gamma_{P_n}}{1-\alpha}\right) - \left(k_1^{gel} + k_2^{gel}\gamma_{S_0}\right) = 0 \qquad (3\text{-}37)$$

and setting;

$$A = 1;\ B = \left(\frac{k_2^{gel}}{1-\alpha}\right);\ \text{and}\ C = k_1^{gel} + k_2^{gel}\gamma_{S_0} \qquad (3\text{-}38)$$

Hence;

$$A\frac{d\gamma_{P_n}}{dt} + B\gamma_{P_n} - C = 0 \qquad (3\text{-}39)$$

The maximum production is when $\frac{d\gamma_{P_n}}{dt} = 0$, hence;

$$\gamma_{P_n^{max}} = \frac{C}{B} \qquad (3\text{-}40)$$

The best-fit equation obtained from experiment results was;

$$\gamma_{P_n} = t^m \cdot e^n \qquad (3\text{-}41)$$

$$\frac{d\gamma_{P_n}}{dt} = mt^{(m-1)} \cdot e^n \qquad (3\text{-}42)$$

If equation 3-41 is one of the solutions to the linear homogenous coefficients-constant, direct substitution into equation 3-39 gives

$$\left(mt^{(m-1)} \cdot e^{n}\right) + B\left(t^{m} \cdot e^{n}\right) - C = 0 \qquad (3\text{-}43)$$

$$t^{m} \cdot e^{n}\left(\frac{m + Bt}{Ct} - \frac{1}{t^{m} \cdot e^{n}}\right) = 0 \qquad (3\text{-}44)$$

The equation 3-44 gives two solutions;

$$\left(\frac{m + Bt}{Ct} - \frac{1}{t^{m} \cdot e^{n}}\right) = 0 \qquad (3\text{-}45)$$

$$\gamma_{P_n} = \frac{Ct}{m + Bt} = t^{m} \cdot e^{n} \qquad (3\text{-}46)$$

At $m = Bt$, then $t = \tau$

$$\gamma_{P_n} = \frac{C}{2B} = \frac{\gamma_{P_n^{max}}}{2} \qquad (3\text{-}47)$$

$$\tau = \left(\frac{\gamma_{P_n^{max}}}{2e^{n}}\right)^{1/m} = \frac{m}{B} \qquad (3\text{-}48)$$

Where, $\gamma_{P_n^{max}}$ is the maximum product concentration (g/litre). Introducing the initial starch concentration (γ_{S_0}) into the equation 3-46;

$$\frac{\gamma_{P_n}}{\gamma_{S_0}} = \frac{\gamma_{P_n^{max}} t}{\gamma_{S_0}(\tau + t)} = \frac{t^{\pi B} \cdot e^{n}}{\gamma_{S_0}} \qquad (3\text{-}49)$$

A linear form of the first solution becomes;

$$\frac{\gamma_{S_0}}{\gamma_{P_n}} = \frac{1}{x_A} = \frac{\tau\gamma_{S_0}}{\gamma_{P_n^{max}} t} + \frac{\gamma_{S_0}}{\gamma_{P_n^{max}}} \qquad (3\text{-}50)$$

A linear form of the second solution becomes;

$$\ln\frac{\gamma_{P_n}}{\gamma_{S_0}} = \ln x_A = \tau B \ln t + n - \ln\gamma_{S_0} \qquad (3\text{-}51)$$

3-2. MATERIALS AND METHODS

Commercial tapioca starch isolated from *Manihot* plant supplied by the Thai World Import and Export Co., Ltd was used throughout the experiment. Commercial enzymes of α-amylase (EC3.2.1.1) and amyloglocosidase (AMG) was prepared and supplied by Nova Nordisk, derived from *Basillus licheniformis* and *Aspergillus niger* (EC 3.2.1.3) respectively.

3-2.1. Simultaneous Batch Hydrolysis

The effect of the enzymes concentration in the batch process on the productivity, enzymes activity, and the glucose formation kinetics was determined by varying the enzymes concentration and fixing the starch concentration at w=10%. Starch milk was prepared by mixing 10 grams of the tapioca starch powder in 100 ml RO water containing 50 ppm of the calcium chloride dehydrate in 250 ml Erlenmeyer flasks. Calcium ion is used to enhance stability of the enzymes. Various concentrations of enzymes were added into the starch milk solution;

1) $\sigma_{E_{01}} = 0.30$ ml/litre of the termamyl,
2) A ratio of 1:1 of enzymes of the α-amylase and amyloglucosidase, $\sigma_{E_{01}}$ and $\sigma_{E_{02}}$ = 0.15, 0.30, 0.45 and 0.60 ml/litre each enzymes or can be written as $\sigma_{E_0^{mix}}$ = 0.3, 0.60, 0.90, 1.20 ml/litre, and
3) Control experiment with no enzymes added.

All flasks were covered with aluminium foil, incubated for 28 hours at 55 ^{0}C, and agitated at 350 RPM. At intervals during courses of the hydrolysis process, 1 ml aliquots were withdrawn using pipettes.

Experiments were repeated by fixing the ratio of enzymes to starch concentrations ($\sigma_{E_0^{mix}} / \gamma_{S_0}$) at 6 ml-enzymes per kilogram-starch, thus the enzymes concentration in the system is kept consistent as in the first experiment for comparison. W= 5, 10, 15, and 20% of the starch concentration, i.e. equivalent to γ_{S_0} = 50, 100, 150, and 200 g/litre and the enzymes concentration were $\sigma_{E_0^{mix}}$=0.30, 0.60, 0.90, and 1.20 ml/litre respectively. All other conditions were fixed. To determine the temperature effect, the SGLS batch experiment was repeated at T=60^{0}C, starch concentration, $\gamma_{S_0} = 100$ g/litre , and $\sigma_{E_0^{mix}} = 0.90$ ml/litre. In all experiments, pH was monitored throughout.

3-2.2. Viscosity Test

Aliquots collected from the batch SGLS and control experiments at T=55^{0}C were submerged into a cooled glycol solution (T < 4 ^{0}C) to stop further enzymatic reaction and starch swelling. Viscosity of samples was determined using a Bohlin CS Rheometer machine, type BR CS-50 at a

constant temperature (30^0C), and a cone spindle of 4^0 cone angle and a standard diameter of 20 mm.

3-2.3. Glucose Determination by HPLC

SGLS samples collected from the flask were diluted to 1/10 ratio using hydrochloric acid (*HCl*) solution that was initially set at pH 3-3.5 and T < 4^0 C. This sample treatment should effectively stop further gelatinisation and enzymatic reactions, and permanently inhibit the enzymes over a sufficient contact time. The treated samples were kept in a cool room (T<4^0C) for not less then 3 hours before being analysed by HPLC. Samples were neutralised with sodium hydroxide solution to pH 6-8, filtered through a 0.2μm nylon filter using a syringe into vials. The Shimadzu HPLC analysis machine coupled with the refractometer index detector (RID-10A) and the sodium column with a guard was used. The column operating temperature was maintained at 80 ^{0}C, and reverse osmosis water containing 0.05% sodium azide at the flow rate of 0.3 ml/min was used as eluent.

To validate the analytical method, comparison was made with the glucose concentration produced when the samples was filtered by the 30kD polysulphone membrane. The sample was not treated either with acid or temperature. The permeate stream containing glucose was diluted with RO water, and was analysed by HPLC, the same procedure and conditions applied as mention above. The results obtained using this method were compared. Since both results obtained were effectively the same, the first method using acid and temperature treatment was used for the rest of the samples.

3-2.4. Data Analysis

The Least-square linearization and non-linearization method is used for data analysis to obtain the most suitable reaction parameter. To combine both methods, the parameter obtained from least-square linearization is used as an initial trial and error value for the least-square non-linearization data analysis. In nonlinear absolute least square analysis, trial and error was used to find the value that minimise the sum of squares of the differences between the measured values and the calculated value for all data points. The Microsoft excel spreadsheet was used to solve the equation and to obtain the most suitable kinetic parameters.

3-3. RESULTS

3-3.1 Viscosity of the SGLS

The observed result showed that hydrolysed starch products produced by the SGLS with $\gamma_{S_0} = 100$ g/litre, $\sigma_{E_0^{mix}} = 0.9$ ml/litre, and T=55^{0}C apparently low viscosity throughout the process. However, the control experiment with $\gamma_{S_0} = 100$ g/litre showed formation of a liquid gel appeared after ~10 minutes operation.

The sample's viscosity determined by rheometery is given in Table 3-1. As can be seen, viscosity of the SGLS analysed at a constant shear stress of 0.181 pa and fixed sample temperature of T=30^{o}C showed that effectively constant over the period studied. The average shear rate was 83 /s and the average viscosity was 2.2 x 10^{-3} pa-s. Table 3-2 shows viscosity of the control experiment over the period studied. The result showed that the viscosity had increased but the shear rate reduced over a constant heating

process. Comparison on both results suggests that the SGLS has buffered viscosity over the entire period of the SGLS hydrolysis process in space.

Table 3-1: Shear stress, shear rate and viscosity of the SGLS hydrolysis with $\gamma_{S_0} = 100$ g/litre, $\sigma_{E_0^{mix}} = 0.9$ ml/litre, and incubated at T=55^{0}C.

Time (min)	Shear Stress (pa)	Shear Rate (1/s)	Viscosity pa-s
0	0.181	80.7	2.24×10^{-3}
30	0.181	82.8	2.18×10^{-3}
105	0.181	93.3	1.94×10^{-3}
230	0.181	88.7	2.04×10^{-3}
390	0.181	69.1	2.62×10^{-3}
Avg.		82.9	2.20×10^{-3}

Table 3-2: Shear stress, shear rate and viscosity of the control experiment with $\gamma_{S_0} = 100$ g/litre and incubated at T=55^{0}C.

Time (min)	Shear Stress (pa)	Shear Rate (1/s)	Viscosity pas
0	0.181	99.6	1.81×10^{-3}
15	5.05	4	1.26
30	5.05	2.13	2.38
110	5.05	1.98	1.97
250	5.05	0.50	10.1

3-3.2. The pH during SGLS

Fig. 3-1 shows change of pH with time by the SGLS with $\gamma_{S_0} = 100$ g/litre, $\sigma_{E_0^{mix}} = 0.9$ ml/litre, incubated at T=55^{0}C, and carried out without adding buffer solutions or neutraliser. As can be seen, during the initial process until ~3 hours (A-A' line), the pH remained unchanged. It then

gradually decreased to a plateau giving a pH 4.3 after 25 hours (B-B' line) of hydrolysis time. Fixing the pH using the buffer solution would have the effect of giving a pH between the optimum pH values required for the liquefaction and gelatinisation reactions. The α-amylase (*B.licheniformis*) requires pH ~6.5 for optimum conditions whilst β-amylase (*A. Niger*) requires pH ~4.5 for optimum reaction. As the liquefaction by α-amylase is faster than the saccharification reaction by β-amylase, and from observations of the un-control pH result recorded in Fig. 3-1, adding the buffer to control the pH at a certain compromise value might not be ideal.

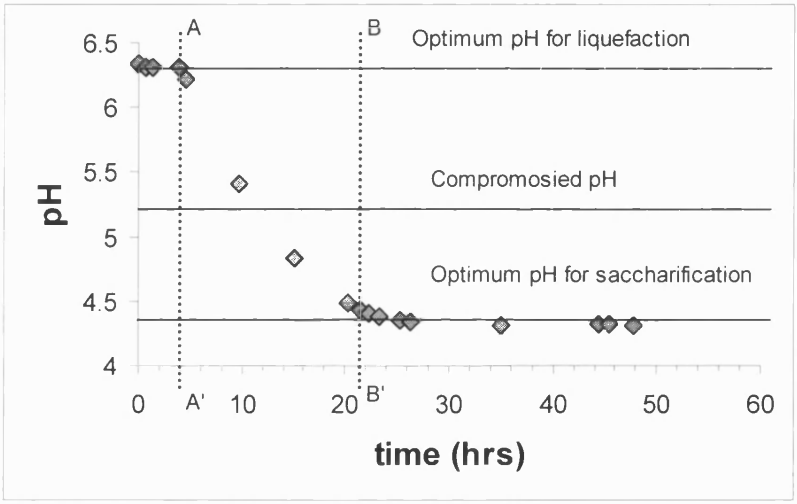

Fig. 3-1: pH changes against intervals time during SGLS of tapioca starch ($\gamma_{S_0} = 100$ g/litre, $\sigma_{E_0^{mix}} = 0.9$ ml/litre, and T=60^{0}C).

In the early stage process, the pH should be optimised for fast liquefaction reactions to buffer increased viscosity. When the substrate has depleted, the pH of the system should be optimised for saccharification reactions to rapidly convert the liquefied starch into products therefore reduces the hydrolysis time. Nevertheless, permitting the pH to be uncontrolled showed that the pH was naturally optimised (for the liquefaction and saccharification) at a particular time suggesting a buffer solution is not required. However, uncontrolled pH should not be applied for reactions of

liquefaction and saccharification when separated, as the pH should be fixed separately for each reaction for optimisation.

3-3.3. Effects of the Enzymes Concentration

As shown in the kinetic model derivation in Equations 3-37 and 3-38, the first order linear homogenous coefficients-constant below is used to describe the glucose production rate. Since the glucose is the intended product and at a concentration > 98% of the product composition, it is assumed that;

$$\gamma_{P_n} = \gamma_{P_{Glucose}} + \gamma_{P_{glucose}^{initial}} \qquad (3\text{-}52)$$

$$\frac{d\gamma_{P_{glucose}}}{dt} + k_2^{gel}\left(\frac{\gamma_{P_{glucose}} + \gamma_{P_{glucose}^{initial}}}{1-\alpha}\right) - \left(k_1^{gel} + k_2^{gel}\gamma_{S_0}\right) = 0 \qquad (3\text{-}53)$$

Where the $\gamma_{P_{glucose}^{initial}} \sim 0.65$ g/litre is the initial glucose concentration.

Fig. 3-2 shows glucose concentrations during the batch SGLS in progress. As can been seen, the glucose concentration produced by $\sigma_{E_0^{mix}}$ = 0.6, 0.90, and 1.20 ml/litre reached an effectively the same limiting glucose concentration at $\gamma_{P_{glucose}^{max}} \sim 65$ g/litre, despite that it was lower of $\gamma_{P_{glucose}^{max}} \sim 28$ g/litre when $\sigma_{E_0^{mix}} = 0.3$ ml/litre was used. Nevertheless, high enzymes concentration decreased the time is required to obtain the maximum glucose concentration. These results suggest that high enzymes concentration would reduce the time to complete the reaction but the maximum conversion of the starch into glucose is effectively the same level over the period studied. Additionally, the result also suggests that the enzymes concentration in the system may have an optimum value for a fixed

starch concentration. The optimum concentration could be limited by the gelatinised starch under a certain period due to low temperature reaction was used. Thus, optimisation of the enzymes at certain fixed starch concentration can be explained by considering the final conversion, the required time to complete the reaction, and also the higher enzyme activity. Table 3-3 shows the summary of the kinetic parameters obtained from Fig. 3-2.

Using the Termamyl enzyme individually without adding a saccharifying enzyme gave the lowest maximum glucose concentration at less than 2 g/litre, thus saccharifying enzyme requires for the glucose formation is confirmed.

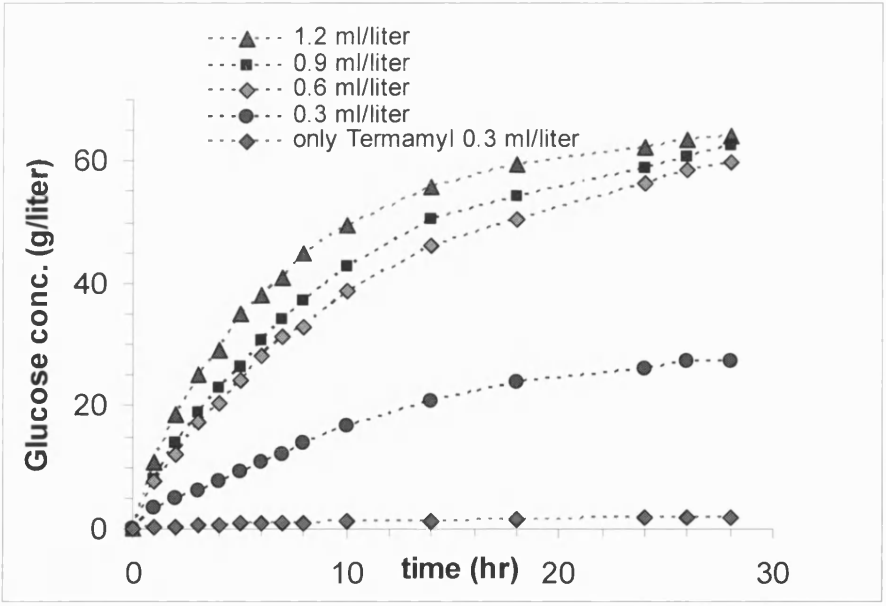

Fig. 3-2: Glucose concentrations at different enzymes concentration. $\gamma_{S_0} = 100$ g/litre and T=55 ^{0}C.

Table 3-3: Summary of glucose production at different concentration of the enzymes. $\gamma_{S_0} = 100$ g/litre and T=55^{0}C

	$\sigma_{E_{01}} = 0.3$	$\sigma_{E_0^{mix}} = 0.3$	$\sigma_{E_0^{mix}} = 0.6$	$\sigma_{E_0^{mix}} = 0.9$	$\sigma_{E_0^{mix}} = 1.2$
$\gamma_{P_{glucose}^{max}} / \gamma_{S_0}$	0.018	0.27	0.61	0.64	0.65
$\tau(hr)$	7.2	8	7	6.1	5
Γ_{max}	0.27	2.88	6.67	8.89	10.8

3-3.4. Effects of the Starch Concentration

Fig. 3-3 shows the effect of different starch concentrations on the starch conversion into glucose. In this study, the enzymes to starch ratio was fixed at 6 ml/kg, and the hydrolysis temperature was fixed T=55^{0}C.

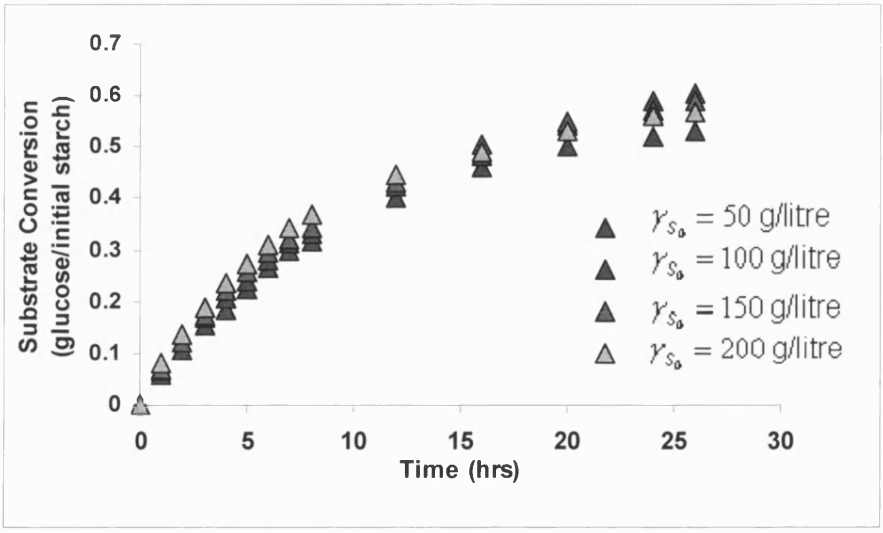

Fig. 3-3: Glucose conversion at different starch concentrations and at 6ml/lkg enzymes to starch ratio, and T=55^{0}C.

Table 3-4: Summary of glucose production rates at different starch concentrations and at $\sigma_{E_0^{mix}}/\gamma_{S_0} = 6$ ml/kg and T=55^{0}C.

	$\gamma_{S_0} = 50$	$\gamma_{S_0} = 100$	$\gamma_{S_0} = 150$	$\gamma_{S_0} = 200$
$\gamma_{P_{glucose}^{max}}/\gamma_{S_0}$	0.53	0.61	0.60	0.58
$\tau(hr)$	6	7	6.5	5.5
Γ_{max}	2.81	6.67	10	12.8

As can be seen, 50g/litre substrate gave slightly low final conversion at 0.53 than the other experiments which reached effectively the same final conversion at ~0.6 over the period studied. These results suggest that within a certain range of the enzymes and starch concentrations but at a fixed ratio of enzymes to starch, the final conversion will be effectively the same. Furthermore, lowering the starch and enzymes concentrations lead to a low in the final conversion. Very high enzymes and starch concentrations should lead in producing a low final conversion which could be due to mass transfer limitations, enzymes-enzymes inhibition [Ozbek *et al.* 2001], product inhibition [Lim *et al.* 2003], and insufficient water content for starch swelling and gelatinisation [Tester and Sommerville, 2000]. Table 3-4 shows a summary of the glucose conversion at different starch concentrations at a fixed ratio of 6 ml-enzymes per kilogram starch.

3-3.5. Effects of Temperature

Fig. 3-4 shows the glucose production by SGLS at T=55 ^{0}C and 60 ^{0}C. The initial starch concentration was fixed at 100 g/litre, and the enzymes to starch ratio was fixed at 0.9 ml/litre. As can be seen, initially the glucose concentration of T=60^{0}C was high and reached faster the maximum glucose concentration at $\gamma_{P_{glucose}^{max}}$ ~ 65 g/litre than when T=55^{0}C was used. However, the maximum glucose concentration effectively reached the same level.

Similar results were reported by other authors but different operating conditions were used [Linko & Javanainen, 1996; Paolucci-Jeanjean *et al.* 2001]. These results suggest that a higher temperature increases the enzymes activity and the initial starch conversion rate to gelatinised starch, but the maximum gelatinised starch conversion not changes with small changes of temperature, thus the maximum glucose concentration reaches an effectively the same level. Table 3-5 gives the summary of the kinetic values obtained at the two different temperatures studied.

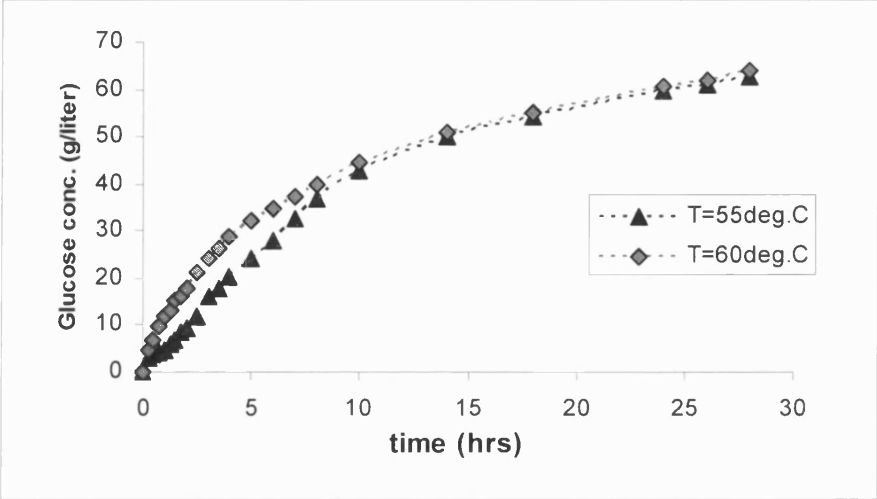

Fig. 3-4: Temperature effects on the rate of glucose production. $\gamma_{S_0} = 100$ g/litre , and $\sigma_{E_0^{mix}}$ =0.9 was used.

Table 3-5 Summary of the glucose production rate by two temperatures when $\gamma_{S_0} = 100$ g/litre , and $\sigma_{E_0^{mix}}$ =0.9 ml/litre.

	55 ^{0}C	60 ^{0}C
$\gamma_{P_{glucose}^{max}} / \gamma_{S_0}$	0.63	0.64
$\tau(hr)$	6.1	5
Γ_{max}	8.89	13.3

3-4. DISCUSSION

3-4.1. The Relative Productivity Analysis

As shown in Fig. 3-2 and Fig. 3-3, when sufficiently high enzymes concentration was used, the maximum substrate conversion to glucose over the period studied has slightly changed ranging from 0.58-0.64. This conversion might not represent the final conversion as a longer reaction time is required to complete the hydrolysis. Therefore, relative productivity that considers the required time to obtain half of the maximum conversion and a half of the maximum production within the period of studied is used. It should be sufficient for optimisation and comparison in batch processes. The efficiency analysis considers enzymes concentrations as the subject while product or conversion and the time required to complete the reaction are the objectives. Additionally, optimisation analysis has to follow the specific targets such as viscosity and enzymes decay.

Since the SGLS is developed for use by a membrane bioreactor system, ideally the unconverted starch concentration and the viscosity throughout the process should be at a low controlled value. Meanwhile, the conversion has to be high and the required operation time should be low with low enzymes concentration. Therefore, the relative productivity describe here can be written by Equation 3-54. A higher value indicates a more efficient process.

$$\text{Relative Productivity} = \psi^{relative}_{productivity} = \frac{\gamma^{\max}_{glucose}}{2 \cdot \tau \cdot \sigma_{E_0^{mix}}} \qquad (3\text{-}54)$$

Fig. 3-5 shows two calculated curves of the relative productivity at (1) 100 g/litre starch, and (2) varying the starch and the enzymes at 6 ml-

enzymes per kilogram starch of fixed ratio. As can be seen, at 100 g/litre starch concentration, the relative productivity was optimised when 0.6 ml enzymes was used. When $\sigma_{E_0^{mix}} / \gamma_{S_0}$ was fixed at 6 ml-enzymes per kg-starch, increasing the starch concentration increased the relative productivity compared to when the starch concentration was fixed. This result suggests that by keeping the enzymes to starch ratio, increasing the starch and enzymes concentrations increases the relative productivity. Despite that, by increasing the enzymes and starch concentrations beyond a certain limit will decrease the productivity which could be due to insufficient water content for starch swelling and gelatinisation [Tester and Sommerville, 2000], and products and enzymes-enzymes inhibitions [Ozbek *et al.* 2001; Lim *et al.* 2003].

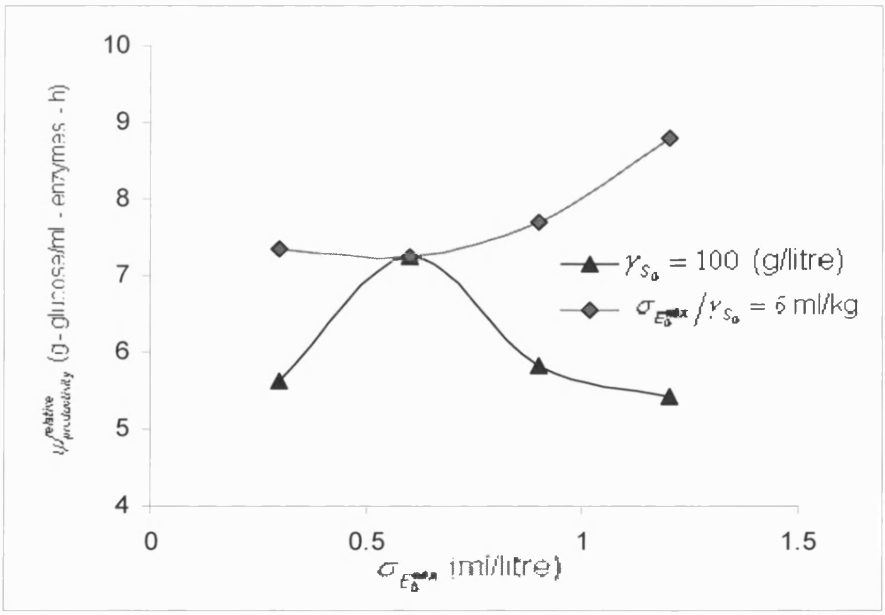

Fig. 3-5: Relative productivity curves ($\psi^{relative}_{productivity}$) of the SGLS process at T=55^{0}C

The relative productivity discussed here is useful to serve as an indicator for optimisation and comparison studies on the overall performance

in batch reaction processes when different systems and procedures are used. Furthermore, the relative productivity is also a useful tool as a basis for comparison studies between the batch and continuous processes in the ultrafiltration system, however, slight modifications may be necessary. The relative productivity could also be of importance when used as a guideline when upgrading the reactor system.

3-4.2. *The Time to Obtain Half of the Maximum Production* (τ)

Fig 3-6 (a) shows the relationship of the time to obtain a half of maximum production at T=55^{0}C given by (1) fixing the starch concentration at 100g/litre and (2) varying the concentration of enzymes. As can be seen, when the starch concentration was fixed at 100 g/litre, the time to obtain a half of maximum production proportionally decreased when the concentration of enzymes was increased. The result has suggested that increasing the concentration of enzymes increases the glucose production rate, thus reduces the time to reach half of the maximum production. Furthermore, the result also suggests that the time to reach half of the maximum production will reach a plateau when the gelatinised starch concentration limits the reaction.

When the starch concentration was changed from 50-200 g/litre and the enzymes concentration was fixed to 6ml per kilogram of starch, the τ showed a curve with an initially low value, then increased to a maximum value when $\gamma_{S_0} = 100$ g/litre, and then decreased again when $\gamma_{S_0} > 100$ g/litre. The time to obtain a half of the maximum glucose production was low when 50 g/litre starch was used is due to low the final substrate to glucose conversion at 0.53. This result may be corresponding to a low gelatinised starch and enzymes concentrations in the system therefore has reduced the effective time and the chances of enzymes and substrates

to contact for the reactions to occur. Despite that, extending the reaction time should lead to an increase in conversions to an effectively the same level, but τ would also increase. When the starch and enzymes concentrations were increased > 100g/litre and 0.6 ml/litre respectively, the time to obtain half of the maximum production also decreased. This result may be due to the ratio of the gelatinised starch to active enzymes is within a sufficient range to avoid the mass transfer limitations, but the high remaining concentration of enzymes and depleting the gelatinised starch over the hydrolysis in progress has led to an increase in the ratio of enzymes to starch. Nonetheless, it is expected that the minimum value would be reached with certain concentrations of enzymes and starch and would increase again when the water content is insufficient, and the time has almost reached the effective contact time for enzymes to complete the reaction.

To further evaluate the effect of the initial starch concentration, the graph of τ/γ_{S_0} against $\sigma_{E_0^{mix}}$ was plotted. As can be seen in Fig. 3-6 (b), fixing the starch concentration had reduced the time to reach half of maximum production in a linear fashion. When the time of the half of maximum production is divided by initial starch concentration, the plot obtained shows an exponential decrease initially high and then reducing to lower values than when the starch concentration was fixed. If the starch concentration is not affecting τ, the same shape of graph should be obtained. However, the plot obtained rejects this hypothesis, thus it is concluded that both the concentrations of enzymes and starch in the system influences the time to reach half of the maximum production rate is confirmed.

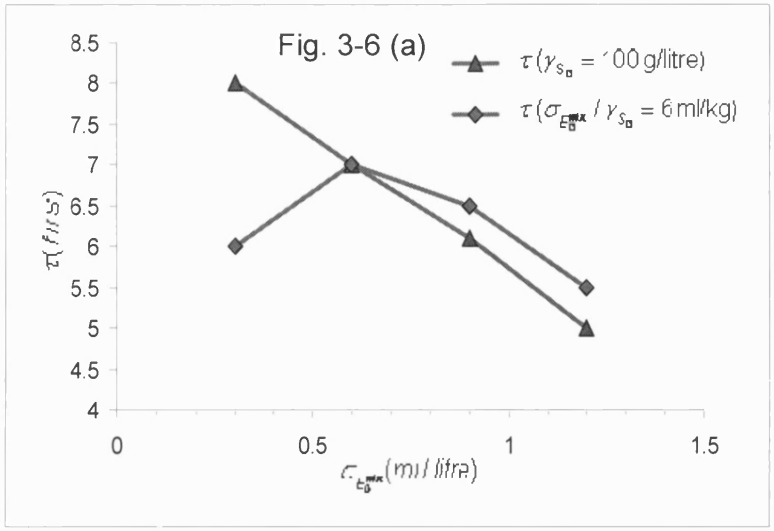

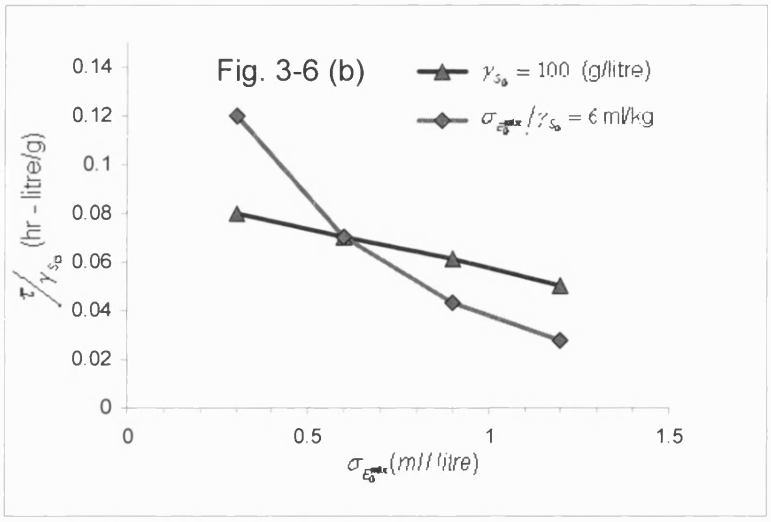

Fig. 3-6: Plots of (a) time to obtain half of the maximum glucose production (τ) and (b) τ/γ_{S_0} against the concentration of enzymes.

3-4.3. The Maximum Production Rate (Γ_{max}),

The maximum production rate is described as the highest rate glucose can be produced over a short period of the reaction time. If the assumption that the gelatinised starch limits the reaction is valid, the production rate should be controlled by the concentration of gelatinised

starch within a certain period of operation. Otherwise the production rate would be determined by the liquefaction or saccharification rates whichever would be the limiting factor of the production rate. In low temperature SGLS, gelatinised starch concentration may be determined by the initial starch concentration, the operating temperature, and the water content, while the reaction time is divided into two; the time for the enzymes to move from one substrate to another, and the bonding time required to complete the reaction, both times also so called the effective reaction time.

Fig. 3-7 (a) shows the effect of enzymes and starch concentrations on the maximum production rate (Γ_{max}) at T=55^{0}C. As can be seen, when γ_{S_0}=100 g/litre was fixed, increasing the concentration of enzymes from $\sigma_{E_0^{mix}}$=0.3 to 1.2 ml/l increased the maximum production rate. This result suggests that increasing the enzymes molecules number in the system increases the substrate conversion rate. The production rate would reach the upper limit which may be limited by the gelatinised starch concentration, and the effective time to complete the reaction.

When the ratio of enzymes to starch was fixed to 6 ml/kg, increasing the starch concentration 50 to 100 g/litre increased the production rate with the same reaction rate as shown by a fixed starch concentration at 100g/litre. When a starch concentration > 100 g/litre was used, the production rate obtained was higher than by fixing the starch at 100g/litre. These results suggest that when less than 0.6 ml/litre of the enzymes used in the system, the production rate may be determined by the mass transfer limitation, but when > 0.6 ml/litre of the enzymes is used, the reaction may be determined by the ratio of the enzymes to productive substrates. When the enzymes concentration is too high, the production rate would be limited by the concentration of the gelatinised starch at a particular time. The effect of the gelatinised starch limiting the reaction rate may be explained by

studying the effect of the pre-heating process for the substrate before being fed into the reactor which will be discussed in Chapter 4.

Fig. 3-7 (b) shows the re-plotted graph that includes the effect of initial starch concentration on the production rate. When the enzymes to starch ratio was fixed to 6 ml/kg, increasing the starch concentration from 50 to 100 g/litre increased the $\Gamma_{max} / \gamma_{S_0}$, however after $\gamma_{S_0} > 100$ g/litre, the $\Gamma_{max} / \gamma_{S_0}$ is effectively constant at ~0.07h^{-1}. The result of $\gamma_{S_0} > 100$ g/litre is explained that by fixing the ratio of enzymes to starch and increasing the concentrations of enzymes and starch at 6 ml/kg does not increase the maximum production rate. This is consistent with earlier suggestion that the ratio of the productive substrate to enzymes determine the maximum reaction rate. To explain further the findings, the reactions are discussed below.

In the SGLS, glucose production rate relies on the concentration of the liquefied starch, and the liquefaction reaction relies on the concentration of the gelatinised starch. As the gelatinised starch is set as a limiting factor by the low reaction temperature, fixing the initial starch concentration and increasing the concentration of the enzymes would increase the ratio of Termamyl enzyme to gelatinised starch. Increasing the rate of liquefaction would also increase the saccharification reaction. Hence it would increase the overall production rate. However, increasing the concentration of enzymes but fixing the starch concentration would increase the maximum production rate up to the upper limit which the gelatinised starch may be the limiting substrate in the system. If the gelatinised starch is not a limiting factor, the production rate may be limited by the saccharification reaction, but the HPLC spectrum at the beginning of the SGLS showed that the product was >98% of glucose hence rejecting this hypothesis, but the low viscosity throughout the experiment suggests that the gelatinisation reaction

is the limiting factor. This result is also parallel with the assumption made in the kinetic development of the SGLS.

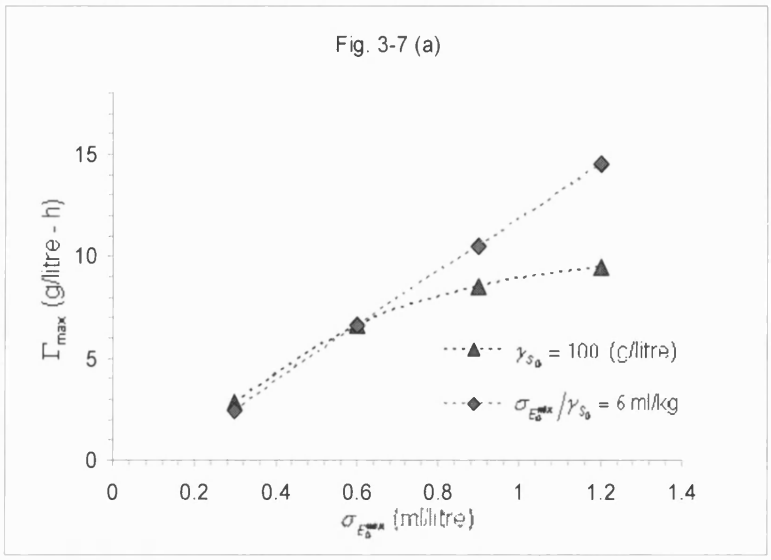

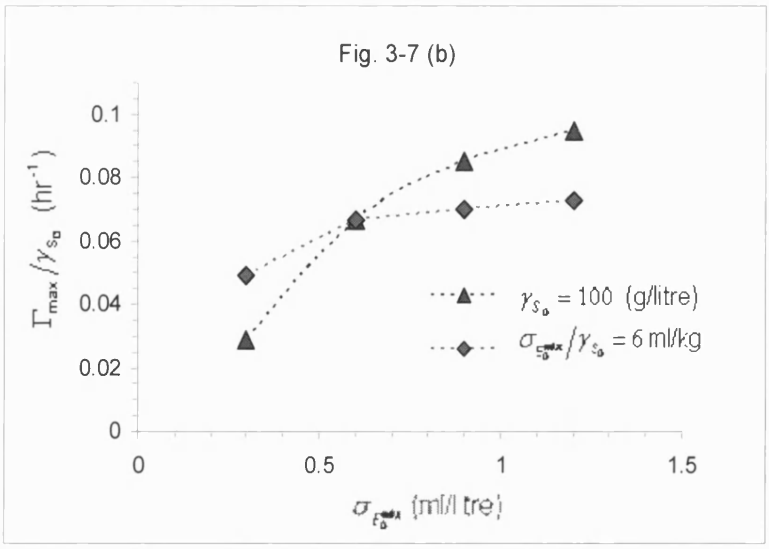

Fig. 3-7 (a, b): The enzymes and starch concentrations effects on (a) Γ_{max} , and (b) $\Gamma_{max}/\gamma_{S_0}$ at T=55^{0}C.

If the ratio of the enzymes to productive substrate has been optimised, the other limiting factor of the maximum production rate as

mentioned earlier is the effective reaction time. The effective reaction time may be reduced by increasing the reaction temperature. The temperature effect on the effective reaction time will be discussed separately.

3-4.4. Enzymes Activity

Although increasing the ratio of enzyme to starch can significantly increase the production rate and reduce the reaction time, enzymes activity analysis may be useful to particularly look at the productivity of the enzymes at molecule level. The highest specific molecule productivity may be the best term to describe the highest enzymes activity, and it is relative to the highest glucose produced over a short period of time by every millilitre of the enzymes, which can be calculated by Equation 3-55. This analysis should give the optimum volume of enzymes that gives a high enzymes activity.

$$\text{Enzymes Activity} = \frac{\Gamma_{max}}{\sigma_{E_0^{mix}}} \qquad (3\text{- }55)$$

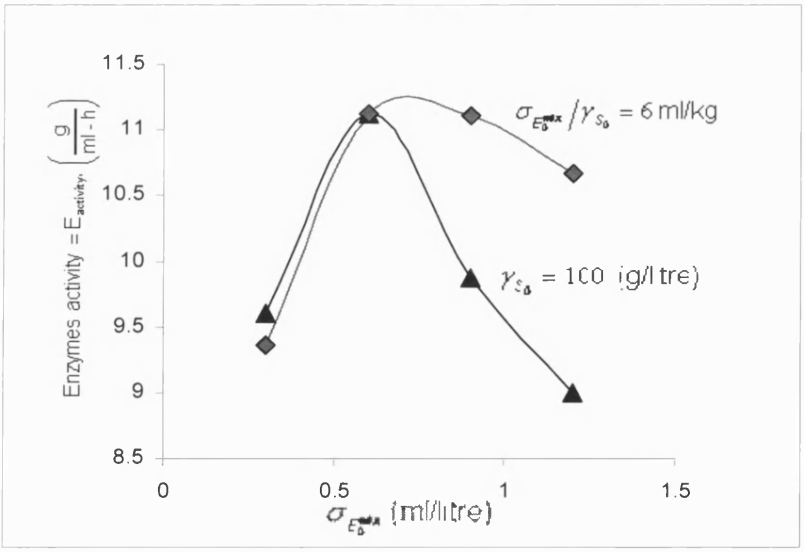

Fig. 3-8: Plots of enzymes activity at T=55^{0}C

As can be seen in Fig 3-8, when the starch concentration was fixed at 100g/litre, the ratio of 3ml-enzymes per kilogram substrate gave low enzyme activity of 9.6 g/ml-h. The enzymes activity was increased to the highest value of 11.12 g/ml-h when the ratio was 6 ml/kg, and then decreased again when more than 6 ml/kg to the lowest value of 9 g/ml-h when the ratio of 12 ml/kg was used. When the ratio of enzymes to starch was fixed at 6 ml/kg, enzymes, activity was low when 0.3 ml/litre of the enzymes and 50 g/litre of the substrate were used. The enzyme activity increased to the highest value of 11.12 g/ml-h when the enzymes concentration fell within the range $0.6 > \sigma_{E_0^{mix}} > 0.9$ ml/litre and the substrate within 100 to 150 g/litre. Enzymes activity is then decreased to 10.67 g/ml-h when $\sigma_{E_0^{mix}} = 1.2$ ml/litre of enzymes and 200g/litre of substrate was used. As discussed before, low activity of the enzymes when less than 0.6 ml/litre of enzymes is used may be due to mass transfer limiting the contact time between the enzymes and substrate. When the starch concentration was fixed and the enzymes concentration was increased, the enzymes activity could be reduced due to insufficient supply of the gelatinised starch in the system. However, when the ratio of the enzymes to substrate was fixed, increasing the enzymes and substrate concentrations should give a constant activity, but the enzymes activity was slightly lower which may be due to insufficient water content in the system., It might also be due to enzymes-enzymes inhibition. The enzymes activity analysis suggests that at T=55^{0}C and a one to one ratio of the amylase and AMG, the SGLS is optimised when the concentration of the enzymes ranges between $0.6 \leq \sigma_{E_0^{mix}} < 0.9$ ml/litre and the starch concentration ranges between $100 \leq \gamma_{S_0} \leq 150$ g/litre.

3-4-5. The constant n

Having said that within a certain range of the enzymes and starch concentrations the ratio of $\sigma_{E_0^{mix}} / \gamma_{S_0}$ determines the optimum enzymes

activity, and also the higher the ratio the higher the production rate will be. The mathematical model can be used to explain the relationship. In Equation 3-42 the production rate is given as;

$$\frac{d\gamma_{P_n}}{dt} = mt^{(m-1)} \cdot e^n \qquad (3\text{-}56)$$

The production rate of the SGLS could change as a result of many factors such as the substrate concentration, the concentration of enzymes, the product concentration, the unproductive product or by-products, inhibitions [Nakajima *et al.* 1992; Ahmet *et al.* 2003], and temperature. The production rate is generally represented by Equation 3-57 below;

$$\frac{d\gamma_{P_{glucose}}}{dt} \propto \mathrm{f}\left(\gamma_S, \gamma_P, \gamma_U, \sigma_{E^{mix}_{active}}, \mathrm{T}\right) \qquad (3\text{-}57)$$

Where, the $\sigma_{E^{mix}_{active}}$ is the active enzymes concentration (ml/litre), γ_S the substrate concentration (g/litre), γ_P the product concentration (g/litre) and γ_U the unproductive starch concentration (g/litre). At this point, the discussion concentrates only on the maximum production rate and enzymes activity. Since the value of $m < 1$, according to Equation 3-42, the Γ_{max} can be reached when

$$mt^{m-1} = 1 \text{ and } \Gamma_{max} = \exp(n) \qquad (3\text{-}58)$$

Hence, the Γ_{max} would represent the exp(n). The relationship of the maximum production rate, enzymes activity, and enzymes concentration can be obtained by using Equations 3-55, 3-56, and 3-58, hence,

$$\frac{d\gamma_{P_{glucose}}}{dt}\Big|_{max} = \Gamma_{max} = E_{activity} \times \sigma_{E_0^{mix}} = \exp(n) \qquad (3\text{-}59)$$

Since the maximum production rate occurs during the earlier stage of the process, it should depend upon the enzymes concentration, the substrate concentration, and the reaction temperature. If all other side effects such as inert is neglected, hence,

$$\Gamma_{max} = E_{activity} \times \sigma_{E_0^{mix}} = \exp(n) = f\left(\left\langle \sigma_{E_0^{mix}} \right\rangle, \left\langle \gamma_{S_0} \right\rangle, T\right) \qquad (3\text{-}60)$$

If in the condition that the water content and temperature profile are sufficient within the appropriate range [Tester and Sommerville 2000], and other experimental conditions are held constant, the effect of the concentrations of enzymes and starch to the maximum production rate can be evaluated by using Equation 3-60.

3-4.6. The Fraction of the Maximum Unproductive Starch ($\alpha_{55^0C}^{max}$)

To explain the effect of enzymes concentration on the value of α, we have to limit the discussion to a fixed starch concentration ($\gamma_{S_0} = 100$ g/litre) and a temperature which would produce a constant value of k_2^{gel}. Giving the definition of $\alpha_{55^0C}^{max}$ as the mass fraction of unproductive products after achieving the steady state product concentration at T=55^{0}C,then;

$$\alpha_{55^0C}^{max} = \left(1 - \frac{\gamma_{P_{glucose}^{max}}}{\gamma_{S_0}}\right)_{max} \qquad (3\text{-}61)$$

The effect of the enzymes concentration to the fraction of the unproductive starch ($\alpha_{55^0C}^{max}$) is given in Fig. 3-9. At initial starch concentration of

$\gamma_{S_0} = 100$ g/litre, increasing enzymes concentration reduced the $\alpha_{55^0C}^{max}$ to an asymptote line at ~0.26. Reducing the $\sigma_{E_0^{mix}}$ < 0.3 ml/litre has decreased $\alpha_{55^0C}^{max}$ to 1. The $\alpha_{55^0C}^{max}$ value is equal zero indicates all substrate has fully converted to the product (glucose), while when the $\alpha_{55^0C}^{max}$ value is equal to one that indicates no product is produced. A more complex curve of the $\alpha_{55^0C}^{max}$ is found when the concentrations of starch and enzymes were simultaneously varied but the starch to enzymes ratio was fixed to 6 ml/kg. This result could be explained by considering mass transfer limitations, water profile in the system, and also enzymes inhibition.

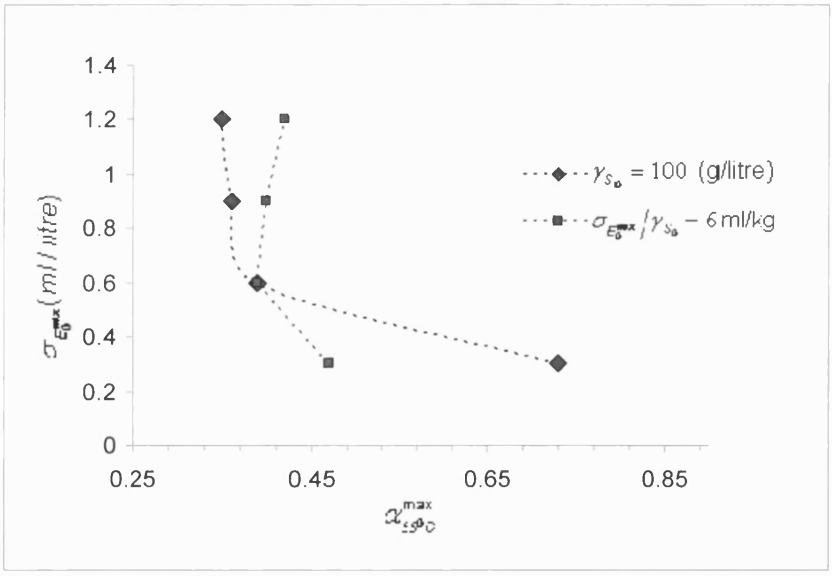

Fig. 3-9: Graph showing the relationship of the $\sigma_{E_0^{mix}}$ to the $\alpha_{55^0C}^{max}$.

3-4.7. The Constant m

The constant m is described in Equation 3-46 as; $m = \pi B$, where $B = \left(\frac{k_2^{gel}}{1-\alpha}\right)$., hence, there are two possibilities for the value of m with respect to changes with the reaction time;

i. change of the k_2^{gel} values,

ii. changeof the value of *(1-α)*.

For constant reaction temperature at T=55^{0}C, the gelatinisation rate value (k_2^{gel}) should be constant as the gelatinisation and swelling rates are controlled by the water content in the system, and the reaction temperature. Tester and Sommerville [2000] explained this phenomenon in their study on the swelling and enzymatic hydrolysis of starch in low water containing systems. Three major factors were outlined for changing of the rate of the gelatinisation and swelling. Firstly, water content in the system and the reaction temperature. Secondly, when the water content and the reaction temperature profile are sufficient to permit the gelatinisation and the starch hydrolysis by *alpha*-amylase, swelling may be restricted as the starch becomes amorphous its ability to hydrate and expanding of the starch is restricted. Thirdly, the botanical origin and the composition of starches moderate their response to gelatinisation, and hydrolysis in limiting water conditions. Thus these facts show that there must be at least one existing correlation between *m* value with the value of *(1-α)*. If gelatinisation rate and *(1-α)* value are both constant throughout the hydrolysis, the *m* value can be calculated by Equation 3-48 or alternatively by the slope of the linearised model of Equation 3-51 and therefore should be ideal to estimate the rate of glucose formation.

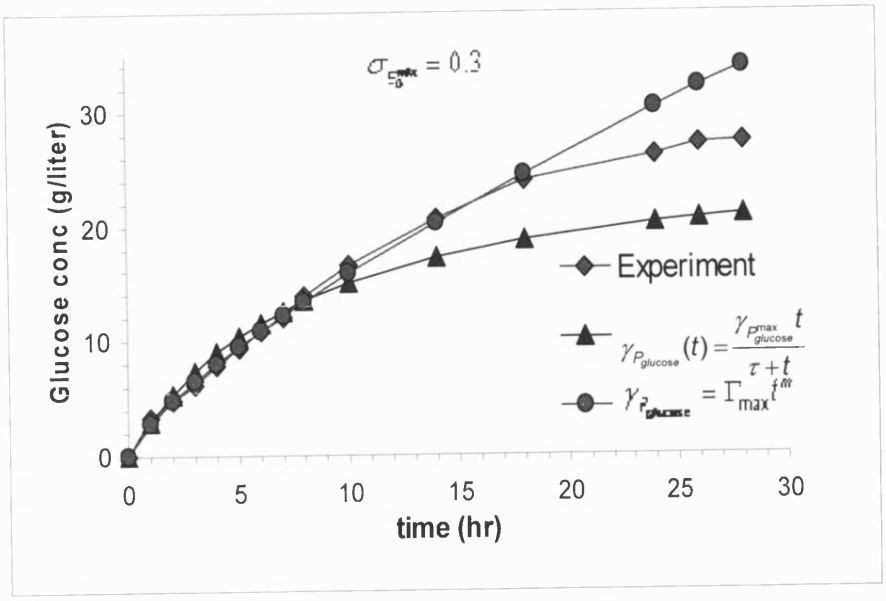
$\sigma_{\varepsilon_0^{max}} = 0.3$
Glucose conc (g/liter)
0
10
20
30
0
5
10
15
20
25
30
time (hr)
Experiment
$\gamma_{P_{glucose}}(t) = \frac{\gamma_{P^{max}_{glucose}} t}{\tau + t}$
$\gamma_{P_{glucose}} = \Gamma_{max} t^{m}$

(a)

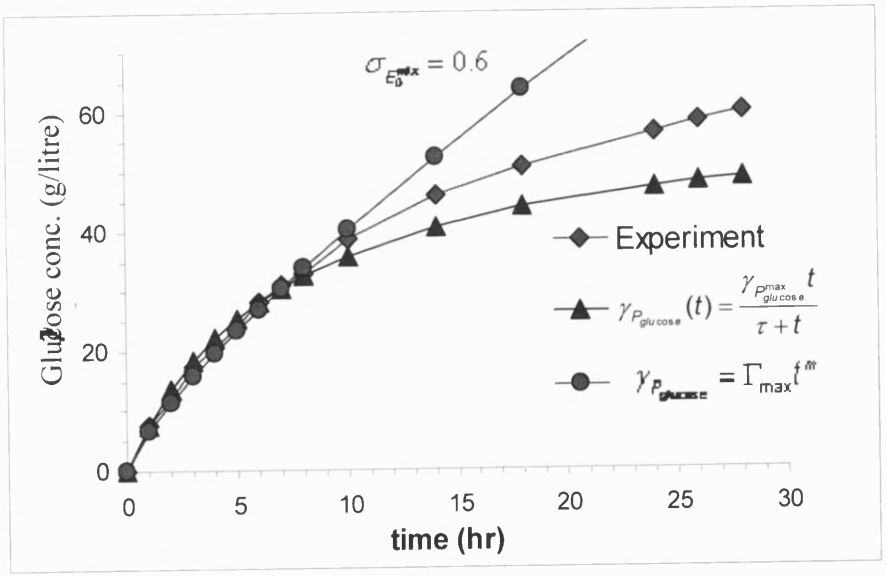
$\sigma_{\varepsilon_0^{max}} = 0.6$
Glucose conc. (g/litre)
0
20
40
60
0
5
10
15
20
25
30
time (hr)
Experiment
$\gamma_{P_{glucose}}(t) = \frac{\gamma_{P^{max}_{glucose}} t}{\tau + t}$
$\gamma_{P_{glucose}} = \Gamma_{max} t^{m}$

(b)

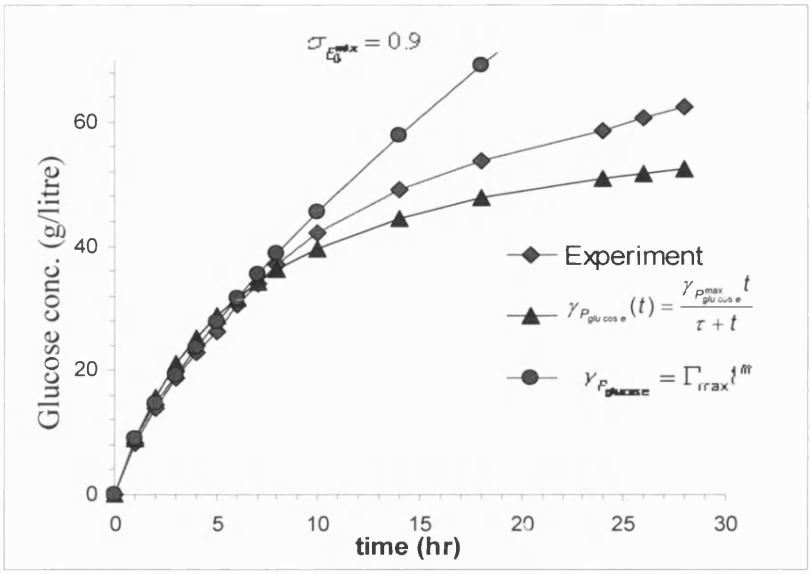

(c)

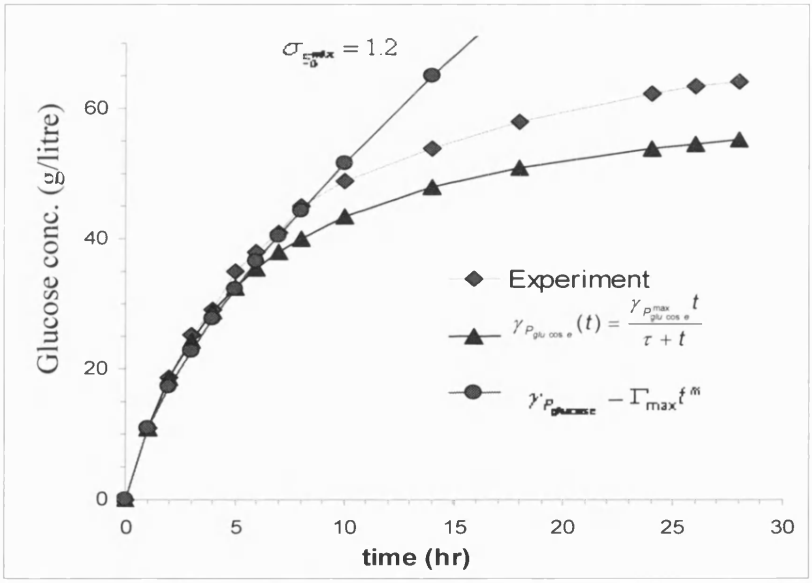

(d)

Fig. 3-10: (a, b, c, d). Comparison plots of the rate of glucose formation with the developed models at different concentrations of the enzymes and a fixed starch concentration at 100g/liter. The enzyme concentration; (a) 0.3 ml/liter, (b) 0.6 ml/liter, (c) 0.9 ml/liter and (d) 1.2 ml/liter.

However, as shown in Fig. 3-10, comparison between the experiment and the two models of $\gamma_{P_{glucose}}(t) = \Gamma_{\max} t^{m}$ and $\gamma_{P_{glucose}}(t) = \frac{\gamma_{P^{\max}_{glucose}} t}{\tau + t}$ demonstrate that both models closely describe the rate of glucose formation until a half of the maximum glucose concentration is achieved, but later $\gamma_{P_{glucose}}(t) = \Gamma_{\max} \frac{t^{\tau B}}{\tau B}$ gives over-estimation and the $\gamma_{P_{glucose}}(t) = \frac{\gamma_{P^{\max}_{glucose}} t}{\tau + t}$ estimates less than the experimental value. As shown in Equation 3-49, both models have constant values of $\Gamma_{\max}$ and $\gamma_{P^{\max}_{glucose}}$, while $\left(\frac{t^{\tau B}}{\tau B}\right)$ and $\left(\frac{t}{t+\tau}\right)$ are shown to change with hydrolysis time. When $t \to \infty$, $\frac{t^{\tau B}}{\tau} \to \infty$ and $\left(\frac{t}{t+\tau}\right) \to 1$. This gives clear proof that the first model would estimate higher than the experiment value when t is large, and also would produce an infinite value when $t \to \infty$. While the second model would estimate lower than the experiment value and will only reach the maximum glucose concentration when $t \to \infty$. If the gelatinisation rate value (k_2^{gel}) is held constant [Tester and Sommerville, 2000], according to Equation 3-46 the m value should not be constant but rely on the (1-α) value which changes with the hydrolysis time. Furthermore, in Equations 3-34 and 3-35 the relationship between the *(1-α)* value and the intermediate and the product concentration are determined by the active concentration of the enzymes $\left(\sigma_{E^{mix}_{act}}\right)$ and the concentrations of gelatinised and liquefied starch. Since the gelatinised starch formation rate is constant, then within a certain range of starch concentration, in which mass transfer limitation is avoided, the constant m would be influenced by the active concentration of the enzymes $\left(\sigma_{E^{mix}_{act}}\right)$.

3-4.8. Consideration of Enzymes Activity Decay in Constant m

In order to determine the true value of *m*, a trial and error method was employed. The $\gamma_{P_{glucose}}(t) = \Gamma_{max} t^m$ has been used to obtain the m value which only relies on the maximum production rate. The second model $\gamma_{P_{glucose}} = \frac{\gamma_{glucose}^{max} \cdot t}{m/B + t}$ is more complex as it relies on $B = \left(\frac{k_2^{gel}}{1-\alpha}\right)$ and $C = k_1^{gel} + k_2^{gel}\gamma_{S_0}$, however the relationship of $\gamma_{P_{glucose}} = \frac{\gamma_{glucose}^{max} \cdot t}{m/B + t}$ can be used to obtain the true value of m/B.

Fig. 3-11 (a and b) show the changes of *m* value that were obtained by trial and error, determined by minimisation of the absolute sum of square of the *m* value against t/τ. As can be seen, when t/τ < ~1 the change of *m* value for all experiments is inconsistent. Generally, the value of *m* when t/τ < ~1 was increased. When t/τ > ~1, all experiments gave the *m* value decreasing exponentially with time. The *m* value influenced by the active enzymes concentration which also relates to the enzymes activity has been discussed earlier and is shown in Fig. 3-10 (a, b). Assuming that the gelatinisation rate is constant, hence, the most significant reasons the *m* value varies (the average value that slightly increased when t/τ < ~1) are due to variation of the gelatinised starch concentration over certain initial reaction period, which could be due to zero and first order gelatinisation rates. Also, the enzymes may be deactivated and the system is operated in the unsteady state. When t/τ > ~1, the steady state condition is achieved (e.g. operating temperature). However the enzymes activity and the denaturing of the enzymes, which are influenced by the substrate concentration and the pH, would reduce the production rate. These would

give the decreasing value of *m*. The value of *m* decreasing with reaction time may also be partly due to decreasing enzymes activity by product inhibition as reported by Nakajima *et al.* [1992] and Ahmet *et al.* [2003]. In the literature survey in Chapter 2, most factors that increase the enzymes decay and the enzymes inhibition has been discussed.

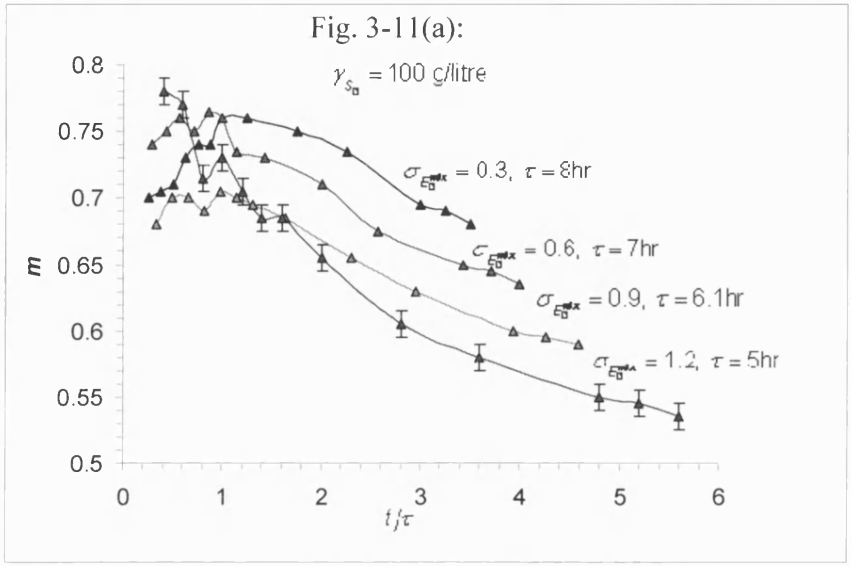

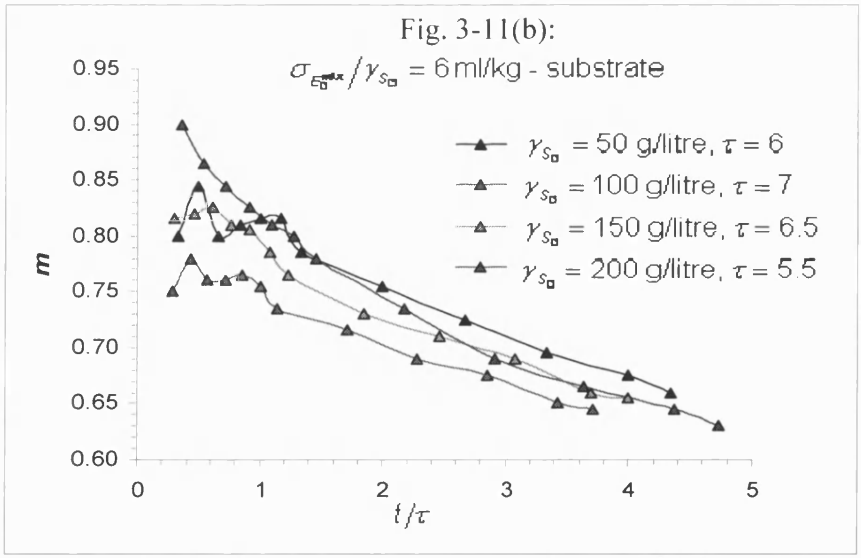

Fig. 3-11 (a, b): Plots of the *m* values obtained experimentally against t/τ at T=55^{0}C for (a) fixed starch concentration of 100g/litre and (b) fixed ratio of enzyme to starch concentration of 6 ml/kg.

Fig. 3-12 shows the plot of *m*, *m/B* and *B* when $\gamma_{S_0} = 100$ g/litre, $\sigma_{E_o^{mix}} = 0.9$ ml/litre and T=55^{0}C. The value of *B* was obtained by dividing the value of *m* obtained from the first model over *m/B* obtained from the second model. However, the plot does not give any significant conclusion due to the fact that there are still two parameters, gelatinisation rate velocity and the percentage of unproductive starch, remaining unidentified. Nonetheless, it does show that the value of $B = \left(\frac{k_2^{gel}}{1-\alpha} \right)$ was high when t/τ < ~1, making the value of *m* low and consistently decreased with the hydrolysis time with slightly low gradients as compare to the gradient produced by the value of *m*.

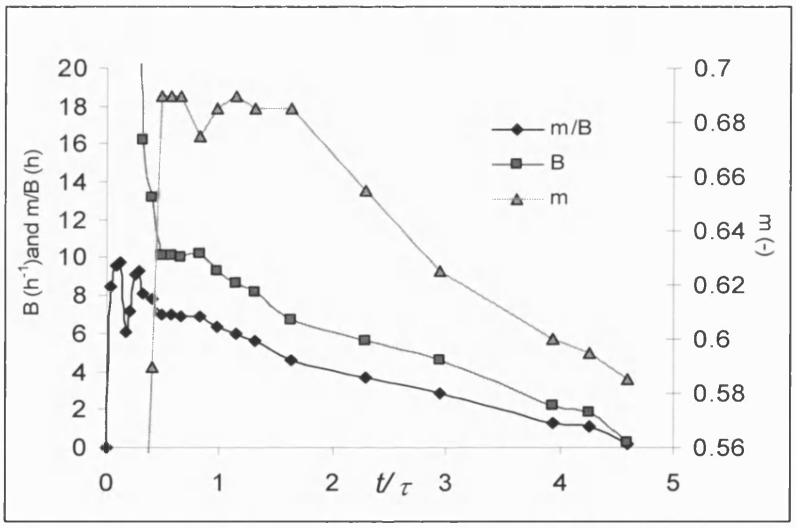

Fig. 3-12: Plots of the *m*, *m/B* and *B* at $\gamma_{S_0} = 100$ g/litre, $\sigma_{E_o^{mix}} = 0.9$ ml/litre and T=55^{0}C

Having said that the *m* value is influenced by the concentration of the active enzymes, while the gelatinisation rate value (k_2^{gel}) is assumed constant [Tester and Sommerville, 2000], if no substrate and enzymes are added during the SGLS experiment, while other conditions are held constant, the general relationship can be expressed as;

$$m \propto f\left(\gamma_S, \gamma_{S_1}, \gamma_{S_2}, \sigma_{E_{act}^{mix}}, \mathrm{T}\right) \qquad (3\text{-}62)$$

where the $\sigma_{E_{act}^{mix}}$ is the active concentration of the enzymes. If the temperature is kept constant and the initial starch concentration is fixed, this would produce effectively the same product inhibition effect and $\gamma_{S_1}, \gamma_{S_2}$~0, hence the general relationship can be reduced to;

$$m \propto f\left(\sigma_{E_{act}^{mix}}\right) \qquad (3\text{-}63)$$

As shown in Equation 2-2, the decay rate of the termamyl enzyme was studied by Paolucci-Jeanjean *et al.* [2001]. They proposed that the enzymes would decay exponentially with the hydrolysis time. Houng *et al.* [1992] proposed Equation 2-5 which is used for starch hydrolysis into maltose in a CRMR, which also considers the enzymes decay as an exponential function. In this study, it was found that the value of *m*, which relates to the active enzymes concentration, is closely described by Equation 3-64 below;

$$m_{(t)} = m_{final} + k_s e^{k_g(t\tau) - k_E(t)^2} \qquad (3\text{-}64)$$

Where the k_S (-), k_g (h^{-1}), and k_E (h^{-2}) are constants that rely on the operating condition and the system. To find the best fitting value of the constant k_S, k_g, and k_E, least square linearisation was used.

$$\ln(m_t) = \ln(m_{final}) + (k_g \tau t - k_E t^2)\ln K_S \qquad (3\text{-}65)$$

$$Y_i = \ln(m_t),\ X_i = \ln K_S,\ a = \ln(m_{final}),\ b = k_g \tau \cdot t - k_E t^2$$

$$\sum_{i=1}^{N} Y_i = Na + b\sum_{i=1}^{N} X_i \qquad (3\text{-}66)$$

$$\sum_{i=1}^{N} X_i Y_i = a\sum_{i=1}^{N} X_i + b\sum_{i=1}^{N} X_i^2 \qquad (3\text{-}67)$$

The value calculated by least square linearisation was used to calculate the glucose production rate. The calculated glucose formation rate was compared with the measured glucose formation rate, and trial and error estimation was stopped when the smallest absolute error was obtained. Table 3-6 shows the best fitted result obtained.

$$\sigma^2 = \frac{s^2}{N_S - K} = \sum_{i=1}^{N_S} \frac{(|Measured - Calculated|)^2}{N_S - K} \qquad (3\text{-}68)$$

Where

N_S = number of date

K = number of parameter to be determined

Table 3-6: The fitted value when $\gamma_{S_0} = 100$ g/litre, and T=55^{0}C

	$\sigma_{E_0^{mix}}$=0.3	$\sigma_{E_0^{mix}}$=0.6	$\sigma_{E_0^{mix}}$=0.9	$\sigma_{E_0^{mix}}$=1.2
$E_{activity}$ (g/ml-hr)	9.6	11.12	9.88	9
$\tau(hr)$	8	7	6.1	5
m_{final}	0.68	0.635	0.59	0.535
k_S	0.04	0.15	0.116	0.181
k_g	0.017	0.0055	0.0048	0.004
k_E	0.007	0.0028	0.0054	0.0054

Therefore, after taking into consideration the enzymes decay and the glucose formation rate model in Equation 3-46, the model combined with Equation 3-64 becomes;

$$\gamma_{P_{glucose}} = E_{activity} \cdot \sigma_{E_0^{mix}} \cdot t^{m_{final} + k_s e^{k_g t - k_E t^2}} \quad (3\text{-}69)$$

or $$\gamma_{P_n} = \Gamma_{max} \cdot t^{m_{final} + K_s e^{k_g (t - k_E t^2}} \quad (3\text{-}70)$$

Fig. 3-13 shows comparison of the glucose production rate between the experiment and the corrected model after taking into consideration enzyme decay. As can be seen, the simulated glucose production rate is effectively the same as the experiment result with the percentage error in each points < 2 %.

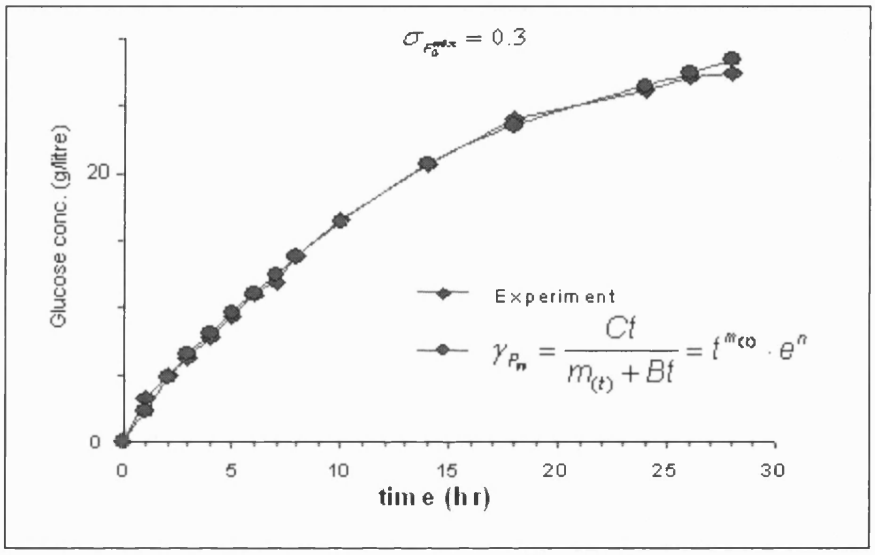

(a)

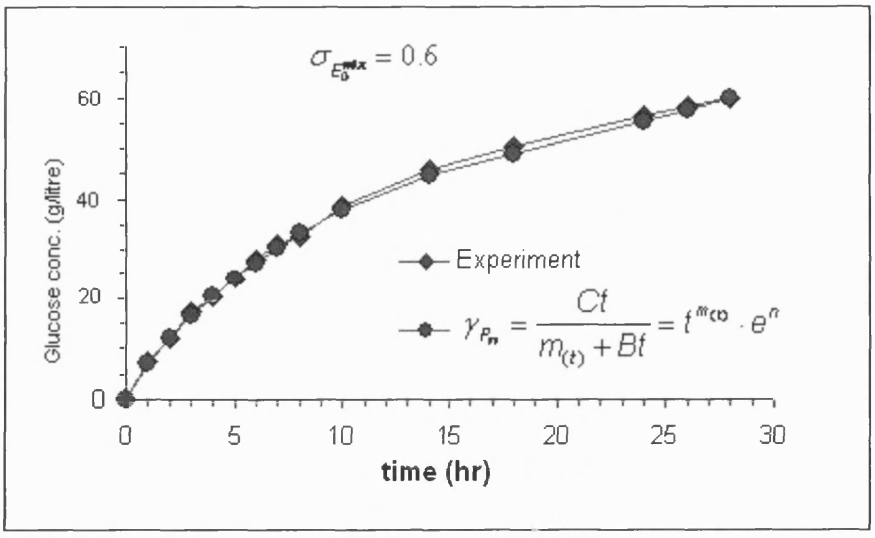
$\sigma_{E_0^{max}} = 0.6$
Glucose conc. (g/litre)
60
40
20
0
0
5
10
15
20
25
30
time (hr)
Experiment
$\gamma_{P_n} = \frac{Ct}{m_{(t)} + Bt} = t^{m\infty} \cdot e^{n}$

(b)

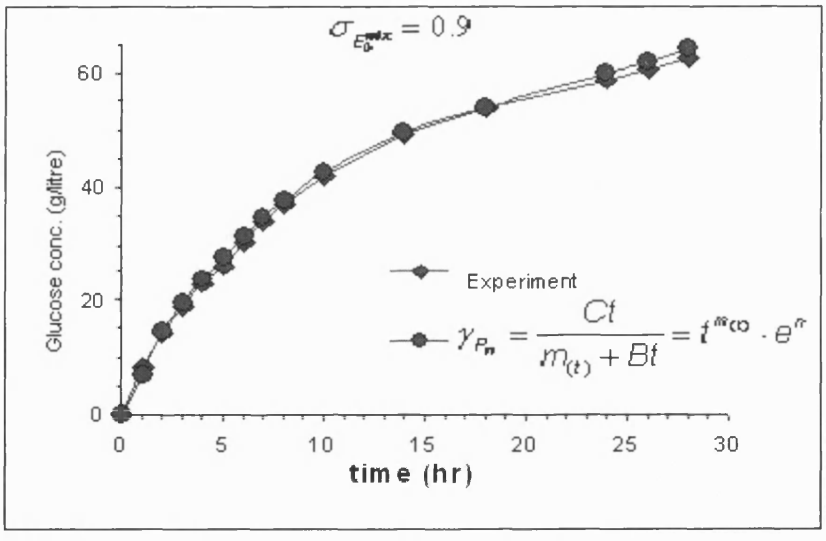
$\sigma_{E_0^{max}} = 0.9$
Glucose conc. (g/litre)
60
40
20
0
0
5
10
15
20
25
30
time (hr)
Experiment
$\gamma_{P_n} = \frac{Ct}{m_{(t)} + Bt} = t^{m\infty} \cdot e^{n}$

(c)

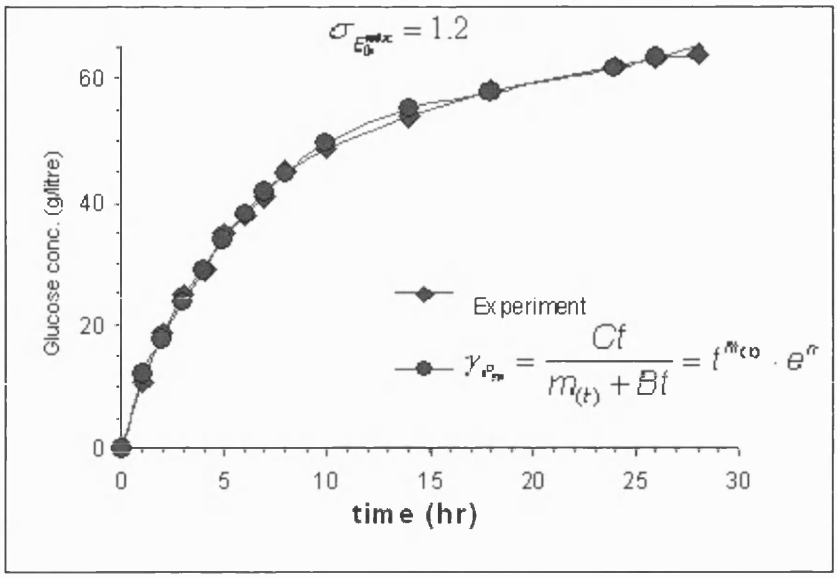

(d)

Fig. 3-13 (a,b,c,d): Comparison experimental rate of glucose formation versus value predicted by model with consideration of enzymes decay.

3-4.9. The Kinetic of Glucose Production

The kinetic for glucose production is given in Equation 3-42. When enzymes decay in Equation 3-64 is considered, the kinetic for glucose production become;

$$\frac{d\gamma_{P_{glucose}}}{dt} = \Gamma_{\max} \cdot \left(m_{final} + k_S e^{k_g t - k_E t^2}\right) \cdot t^{\left(m_{final} + k_S e^{k_g t - k_E t^2}\right)-1} \qquad (3\text{-}71)$$

From the experiments at different enzymes concentrations, with the starch concentration fixed at 100 g/litre and T=55^{0}C, the m_{final} value has linear relationships with the initial enzymes concentration which can be represented by Equation (3-72) below;

$$m_{final} = 0.73 - 0.16\sigma_{E_0^{mix}} \qquad (3\text{-}72)$$

Combining Equation 3-71 and 3-72, a semi empirical kinetic model for $\gamma_{S_0} = 100$ g/litre and T=55^{0}C was found as;

$$\frac{d\gamma_{P_{glu\cos e}}}{dt} = \left[E_{activity} \cdot \sigma_{E_0^{mix}} \left(0.73 - 0.16\sigma_{E_0^{mix}}\right) + k_s \sigma_{E_0^{mix}} E_{activity} \cdot e^{k_g \pi t - k_E t^2}\right] \cdot t^{\left(0.73 - 0.16\sigma_{E_0^{mix}} + k_s e^{k_g \pi t - k_E t^2}\right) - 1}$$

---------(3- 73)

In Equation 3-46, the t^m can be written as;

$$t^{m_t} = \frac{\gamma_{P_{glu\cos e}^{max}} t}{\Gamma_{max}\left(\frac{m_t}{B} + t\right)} \qquad (3\text{-}74)$$

By replacing the t^{m_t}, the semi empirical kinetic model in Equation 3-73 becomes;

$$\frac{d\gamma_{P_{glu\cos e}}}{dt} = \frac{\gamma_{P_{glucose}^{max}}}{\left(\frac{0.73 - 0.16\sigma_0^{mix} + k_S \cdot e^{k_g \pi t - k_E t^2}}{B} + t\right)} \left[\left(0.73 - 0.16\sigma_{E_0^{mix}}\right) + k_s \cdot e^{k_g \pi t - k_E t^2}\right]$$

.....(3- 75)

or

$$\frac{d\gamma_{P_{glu\cos e}}}{dt} = \frac{B\gamma_{P_{glucose}^{max}}}{\left(\left(0.73 - 0.16\sigma_{E_0^{mix}}\right) + k_s \cdot e^{k_g \pi t - k_E t^2} + tB\right)} \left[\left(0.73 - 0.16\sigma_{E_0^{mix}}\right) + k_s \cdot e^{k_g \pi t - k_E t^2}\right]$$

.....(3- 76)

Fig 3-14 (a) show the plot of the glucose production kinetic obtained from the experiment,in which the production rate of each point was calculated by;

$$\frac{dp}{dt} \sim \frac{\Delta(\gamma_{t_2} - \gamma_{t_1})}{\Delta(t_2 - t_1)} \qquad (3\text{-}77)$$

and Fig. 3-14 (b) shows plots of the simulated kinetic by the model given in Equations 3-73 or 3-76.

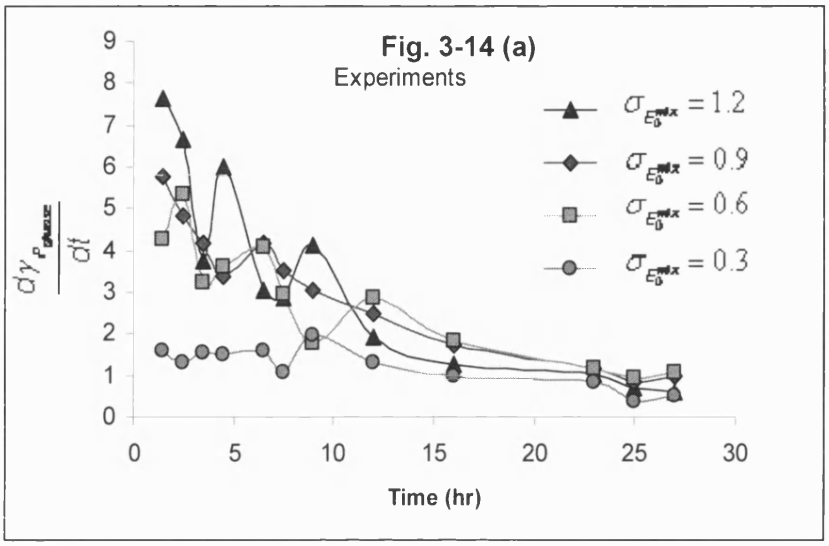

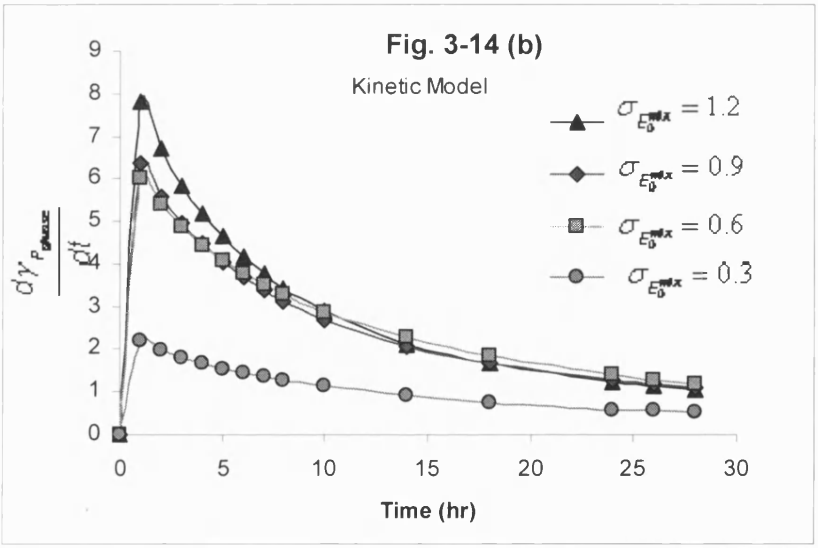

Fig. 3-14: Comparison of the kinetic obtained from (a) experiments and (b) the developed kinetic model of Equation 3-69. $\gamma_{S_0} = 100$ g/litre and T=55^{0}C.

3-4.10. Temperature Effect on the Kinetic Model Parameters

The temperature effect on the maximum reaction rate, the substrate conversion and τ value is shown in Table 3-7. The relationship's expression of the τ value with the maximum reaction rate is given by the Equation 3-48. As shown in Table 3-7, when the $\gamma_{S_0} = 100$ g/litre and the $\sigma_{E_0^{mix}} = 0.9$ ml/litre was fixed, increasing the temperature from T=55^{0}C to 60^{0}C has reduced the τ value from 6.1 to 5 hr. The relative productivity has increased from 5.74 (g-enzymes/ml-enzymes-h) to 7.11(g-glucose/ml-enzymes-h) and is about a 23 % increase but the final glucose concentration remained effectively the same. The highest enzymes activity was also increased from 8.89 g/ml-hr to 14.78 g/ml-hr. According Equation 3-48, it is clear that the reduction of the τ value, and the increasing of the relative productivity is due to the increased enzymes activity. This phenomenon is best described by the Arrhenius relationship (Equation 2-7), which can be written in the form:

$$\ln\frac{k_1}{k_2} = \frac{\mu}{R}\left[\frac{1}{T_1} - \frac{1}{T_2}\right]$$

Where T_1 and T_2 are the absolute temperatures corresponding to reaction velocities k_1 and k_2, R is the gas constant, and μ is the *critical thermal increment*: a constant characterising the particular reaction. When this relationship holds, a more friendly measure can be calculated: $Q_{10} = k_{t+10} / k_t$, where k_t is the rate at temperature t, and k_{t+10} is the rate at 10° C higher. The $\gamma_{S_0} Q_{10}$ simply determines what factor a rate increases for a 10 °C rise in temperature. For enzymatic reactions, Q_{10} is typically somewhere between 2 and 3: the rate increases by 100% for every 10°C rise in temperature [Rosalam & England, 2004]. This phenomenon has been explained in the literature review (Chapter 2).

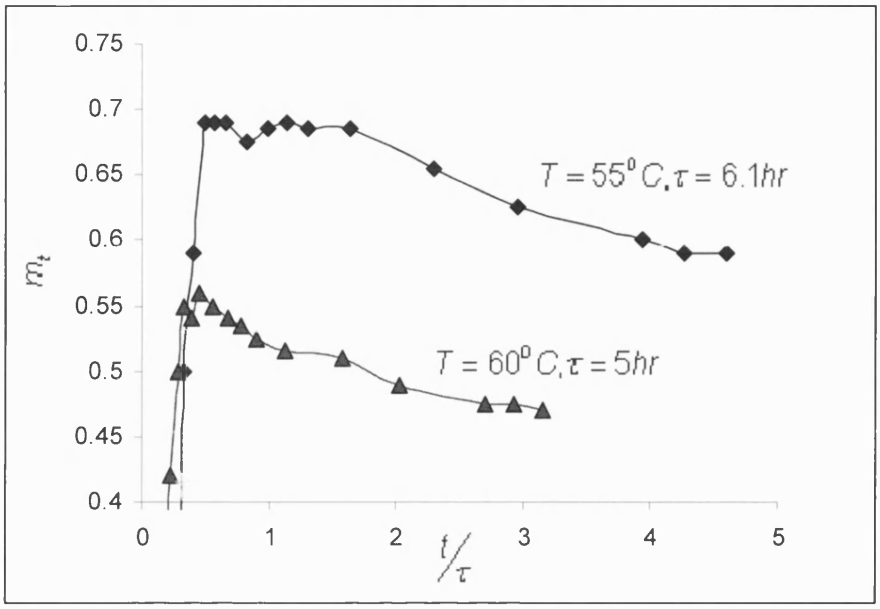

Fig. 3-15: Plots of m_t at different temperature. $\gamma_{S_0} = 100$ g/litre, and $\sigma_{E_0^{mix}} = 0.9$ ml/litre.

Table 3-7: The Kinetic Parameters at different temperature when $\gamma_{S_0} = 100$ g/litre and $\sigma_{E_0^{mix}} = 0.9$ ml/litre.

	T=55^{0}C	T=60^{0}C
$\psi_{productivity}^{relative}$ (g/ml-h)	5.74	7.11
$E_{activity}^{max}$ (g/ml-hr)	9.88	14.78
τ (hr)	6.1	5
m_{final}	0.59	0.47
k_S	1.16×10^{-1}	5.1×10^{-2}
k_g	4.8×10^{-3}	1.64×10^{-2}
k_E	5.4×10^{-3}	7×10^{-3}

Fig. 3-15 shows the temperature effect on the value of m_t. Considering m_t only when the reaction was steady state (t/τ > ~1), increasing the temperature from T=55 to 60^{0}C decreased the value of m_t by ~20%. Although the enzymes activity was increased, by increasing the temperature the enzymes decay should also be increased. Nevertheless, as shown in Fig. 3-15, the reduction (t/τ > ~1) of the m value at T=60^{0}C was similar to the slope obtained by T=55^{0}C. This indicates that increasing the operating temperature does not significantly increase the rate of enzymes decay but increases significantly the activity of the enzymes.

Fig. 3-16 shows the temperature effect on the glucose formation kinetic. As can be seen, increasing the temperature has increased the enzymes activity. However, due to depleting the substrate, the specific glucose production kinetic rate was reduced to lower value than when low temperature was used.

A very important finding obtained from a step increment of the temperature from 55 to 60^{0}C is that the overall efficiency has increased by reducing the hydrolysis time, and that the viscosity also kept low when hydrolysis was in progress. The temperature was not increased beyond 60^{0}C as it limits the flexibility of membrane selection, and could significantly increase the enzymes decay rate, and could also increase the viscosity by increasing the gelatinisation rate.

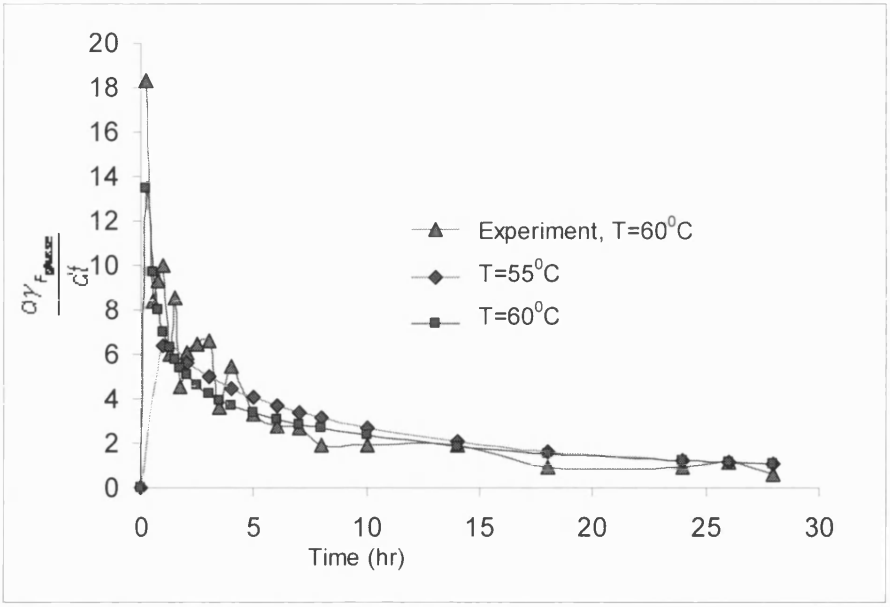

Fig. 3-16: Temperature effect on the kinetic of Glucose production

3-4.11. Error Evaluations on the Models

Other than experimental errors which were minimised by repeating the experiment and taking more frequent samples during the SGLS (appendix 2), the other possible error is from linearization of Equation 3-78 to obtain constants. The mathematical models of Equation 3-65 are linearised by taking logarithms of both sides of the equations respectively.

$$\ln(m_t) = \ln(m_{final}) + (k_g \tau t - k_E t^2)\ln k_S \qquad (3\text{-}78)$$

Making a change of variable, we have;

$$\zeta = \lambda\psi + const\,, \qquad (3\text{-}79)$$

Where, $\zeta = \ln m_t$, ,and $const = k_g \tau \cdot t - k_E t^2$. The constant values of λ and $const$ is obtained from equation as below;

$$\lambda = \frac{\sum \zeta \psi - \sum \zeta \sum \psi / N}{\sum \psi^2 - \left(\sum \psi\right)^2 / N} \qquad (3\text{-}80)$$

$$const = \zeta - \lambda \psi \qquad (3\text{-}81)$$

It should be noted that constant parameters obtained in this manner do not give the least value of m_t. However, least square analysis used is to minimise the deviation of ζ. Since the variants were employed, the error can be reduced. Smith *et al.* 1970 has pointed out that for most of engineering analysis this method is sufficient.

3-5. CONCLUSION

The optimisation and the kinetic model of the SGLS of the tapioca starch at 1:1 ratio of α-amylase to Termamyl enzymes and low temperature below 60^0C was successfully studied. At the optimum operation condition, the SGLS hydrolysis can convert 65% of tapioca starch. The viscosity of the SGLS has been kept consistent below 11pas throughout the course of the hydrolysis. When pH was monitored, the SGLS has naturally optimised the pH at a particular hydrolysis time, thus it optimises the enzymatic reactions as required by the α-amylase and AMG.

The relative productivity of the SGLS was also studied at different concentrations of the starch and the enzymes. When the starch concentration was fixed to 100g/litre, the relative productivity was optimised at 0.6 ml/litre of enzymes. The relative productivity can be increased by increasing the concentration of the initial starch and fixing the concentration of the enzymes. However, it is believed that at certain starch concentrations, the relative productivity could be reduced that due to mass transfer limitations and the starch to water ratio becoming insufficient [Tester and

Sommerville, 2000]. However, the relative productivity is not so important when studying the kinetic and optimisation of the enzymes activity; the maximum reaction rate and the conversion rate has clearly described the kinetic and the optimised condition, but it is a useful tool for comparison studies and economic analysis when different systems and procedures are employed.

When the enzyme activity was analysed, the study found that the enzymes activity at T=55^{0}C and with a one to one ratio of the amylase and AMG, a high activity was obtained when the concentration of the enzymes lies between $0.6 \leq \sigma_{E_0^{mix}} < 0.9$ ml/litre and the starch concentration lies between $100 \leq \gamma_{S_0} \leq 150$ g/litre.

The developed kinetic study of the SGLS based on the basic Michalies-Menten kinetic Equation has a critical assumption used to mathematically derive the kinetic model, i.e. "**the balanced reactions of the gelatinisation and liquefaction and the gelatinisation is the limiting factor"**. Furthermore, the reaction temperature must be low so that the saccharyfing enzymes of the AMG can be mixed and react simultaneously. When the balanced reaction between the gelatinisation and the liquefaction is assumed to occur during the SGLS hydrolysis, the intermediate substrates concentration of the gelatinised and liquefied starches should be low, and have been considered negligible, thus the rate of the glucose formation should just rely on the gelatinisation rate or on the saccharifying rate, thus two rate of glucose formation models has been found. The first model is based on the maximum production rate and the second model is based on the maximum glucose formation. As both the maximum production rate and the maximum glucose production are constant within certain specified conditions as mention above, both models must have a time function which decreases with hydrolysis time. This time function is found to change with the enzymes and substrate concentration, thus it is probably representing

the decrease of the enzymes activity as enzymes activity has been shown to change with the enzymes and starch concentration. In order to calculate the glucose formation models, three parameters are required; (1) the maximum production rate, (2) the time to obtain a half of the maximum glucose production, and (3) the maximum conversion.

To further evaluate the kinetic models, two new parameters of the *n* and *m* have also been introduced by which both depend on the concentration of the enzymes and the starch concentration. From the mathematical derivation shown in the kinetic model development, the exp(*n*) is the maximum production rate by which it is controlled by the concentration of enzymes in the system but the starch concentration must be kept at a value to avoid the mass transfer limitation due to insufficient water to starch ratio [Tester and Sommerville 2000]. The value of *m* after the transient phase (t/τ > ~1) that describes the enzymes activity is also affected by the starch concentration, meaning that both the active enzymes and the starch concentrations affect the value of *m*. The experiment results have also shown that high initial enzymes activity gave low values of *m*. The *m* value after transient phase was also found to decrease with time and has followed the enzymes decay model. In this study, the value of *m* changes with time has been modelled but three unknown parameters of $k_S, k_g,$ and k_E have been introduced. These three constants value is determined by the statistical methods of linearization least square analysis, and non-linearization least square analysis. Finally, the kinetic of the glucose production has been successfully developed as it has been shown in Fig. 3-14, a comparison of the glucose kinetic between the experiment and the simulated value gives good agreement.

The temperature effect on the kinetic of the SGLS was also investigated. When the temperature was increased from T=55 to 60^0C, the relative productivity and the enzymes activity significantly increased by 24%

and 50% respectively. Despite the fact that productivity and enzymes activity increased, the temperature cannot be increased beyond 60^0C as it will limit the flexibility for membrane selection, could significantly increase the enzymes decay rate, and should also increase the viscosity due to an imbalance in the rate of the gelatinisation and liquefaction reactions.

The value of m has the relationship shown in Equation 3-49. However, the relationship uses the assumption that the m is a constant thus it does not change by the hydrolysis time. This assumption might not be ideal as the Equation 3-48 of $m = B\tau = \frac{k_2^{gel}}{(1-\alpha)}\tau$ shows that it depends upon the gelatinisation and the unproductive fraction. However, this Equation needs the evaluation of the α value changes with the hydrolysis time. Moreover, the kinetic model development of the glucose production uses the assumption that the first order gelatinisation rate velocity (k_2^{gel}) is a constant throughout the course of hydrolysis as suggested by Tester and Sommerville [2000]. However, as different systems and processes were used, the k_2^{gel} may differ, thus the low temperature kinetic of the gelatinisation reaction which is a part of the combined simultaneous hydrolysis has to be separately studied. A complete evaluation on those uncertainties should reveal an empirical relationship of the m value with the variable parameters such as the enzymes activity, the starch concentration, and the pH which changes with time. Nevertheless, it is believed that the value of m represents the enzymes activity and enzymes decay. Knowing the relationship for the m value, the future model of the m value should be more universal and may simplify the model. The most important objective is to reduce the number of unknown kinetic parameters, hence reducing the dependency on the linearization least square analysis and non-linearization least square analysis as currently applied.

CHAPTER 4:

DEVELOPMENT OF THE ULTRAFILTRATION SYSTEM FOR CONTINUOUS SEPARATION OF THE GLUCOSE SOLUTION

4-0. INTRODUCTION

The low temperature SGLS discussed in Chapter 3 appears to be reliable for production of a glucose solution, but the glucose is mixed with the by-products and enzymes and has to be extracted. Moreover, product inhibition requires a continuous extraction process [Atikinson & Mavituna, 1991; Akerberg, *et al.* 2000; MacGregor *et al.* 2002; Lim *et al.* 2003; Rosalam & England, 2004]. Development of the ultrafiltration system for continuous SGLS may fulfil the requirement of continuous separation of the glucose provided a suitable membrane system is used. The outcome of the SGLS in the ultrafiltration system could be a more efficient and competitive process in terms of productivity and quality compared to the batch process.

The aim of this chapter is to discuss the development of an ultrafiltration system that would serve as a working process for the SGLS reaction and for continuous separation of the glucose solution. Comparison studies of the SGLS carried out in batch mode with and ultrafiltration system may be of importance in explaining the efficiency and the productivity in both batch and continuous processes. The strategies of low temperature SGLS and ultrafiltration process described here should offer pure and clean glucose source, and could also serve as the basis for a pre-processing technology of raw material in biotechnology industries. The quality of glucose solution produced by the SGLS in the ultrafiltration system has prevented

exact comparison being made between the conventional process and this method.

Although the SGLS has advantages compared to the ultrafiltration process for continuous production of clean and sterile glucose, very few of the studies have been found in the literature [Paolucci-Jeanjean *et al.* 1999, 2000b,c; 2001] and none of the SGLS was carried out using an ultrafiltration system. Despite that, it was found that simultaneous hydrolysis at low temperature between 37-80^{0}C of the starch by enzymatic means without a prior gelatinisation process into the hydrolystates with the final conversion between 60-80 % can be achieved [Linko & Javanainen, 1996; Marchal *et al.* 1999; Paolucci-Jeanjean *et al.* 2000a; 2001]. A study of the SGLS carried out in this work given in Chapter 3 has shown that a starch conversion between 55-65% was obtained over 28 hour period. These results suggest that not only extraction of the glucose is required but some of the by-products in the form of recalcitrant polymers have to be removed if continuous operation is required. Hence, a settling tank is included in the ultrafiltration system which should be able to retain the by-products and it also can be used to discard the by-products by a purge from the system.

4-1. MATERIALS AND METHODS

4-1.1 The Physical Unit Operation

Fig. 4-1 shows the flow diagram of the physical unit operations of the ultrafiltration system used in this study. The system comprised of a mixing tank, a reaction tank, a settling tank, an ultrafiltration membrane module, and a storage tank. The full capacity of the ultrafiltration system excluding the mixing tank is 12.2 litres. The technical specification and the material used of the system are given in Table 4-1.

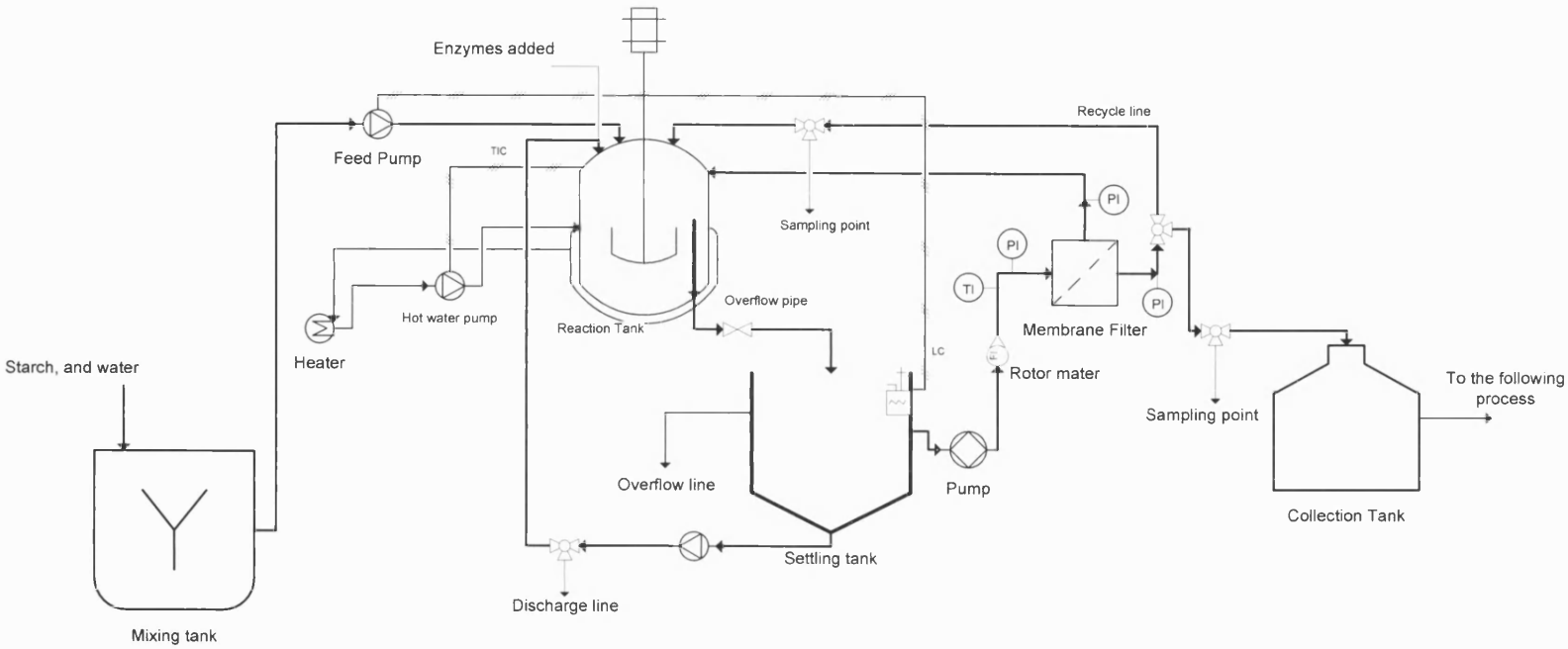

Fig. 4-1 : The process flow diagram of the ultrafiltration process.

Table 4- 1: The technical specifications of the physical unit operations of the Ultrafiltration System.

Unit operation	Specifications
Mixing tank	Max. operating capacity=25 litres, T= ambient, Stirrer, and a Watson-Marlow 501U adjustable capacity feed pump
Preheating	Water bath T~70^{0}C, a stainless steel spiral coil with $\phi_i = 6.5$ mm and $\phi_o = 3.5$ mm. Spiral diameter $\phi = 185$ mm, and spiral number 4
Reaction tank (Fig. 4-2)	A thermo couple, hot water jacket to maintain the temperature, two buffers, a heidolph stirrer model RZR 2021, impeller, and an overflow pipe with $\phi_i = 7.5$ mm. Max. operating volume=5litres
Settling tank (Fig. 4-3)	A thermocouple, a floating level control, two Millipore peristaltic pumps (capacity 6-600 rpm); for recycling the un-reacted starch back to the reactor and for intake pump of the supernatant, a transparent cylinder column mounted to the settling tank has $\phi_i = 46$ mm and high=450mm, intake pipe with $\phi_i = 3.5$ mm located inside the transparent column, and thermocouple. Max. operating volume = 7 litres

Cont. **Table 4-1**

Membrane modules (Fig. 4-4 and Fig. 4-5)	A retentate valve, two regeneration valves, a regeneration pump, a pressure relieve valve (3 bar max), two retentate pressure transducers (inflow in and outflow of the membrane module), and a pressure transducer at permeate, and a pressure gauge. Two membrane module were used; 1. A 30 kD of the polysulfone hollow fibre cartridge model no HF 1.0-43-PM30, serial number 4P3x 673 1 supplied by Romicon USA was used. The lumen diameter of the hollow fibre ϕ=0.043 inches, and the total area of the membrane was 0.1 m^2 (Fig 4-5 a) 2. A 5 kD of the ceramic membrane supplied by Oriles, France, length = 35 cm, ϕ_i = 3.5 mm, channel number =19, membrane area = 816 cm^2. (Fig. 4-5 b)
Production tank	Electronic balance, a tank

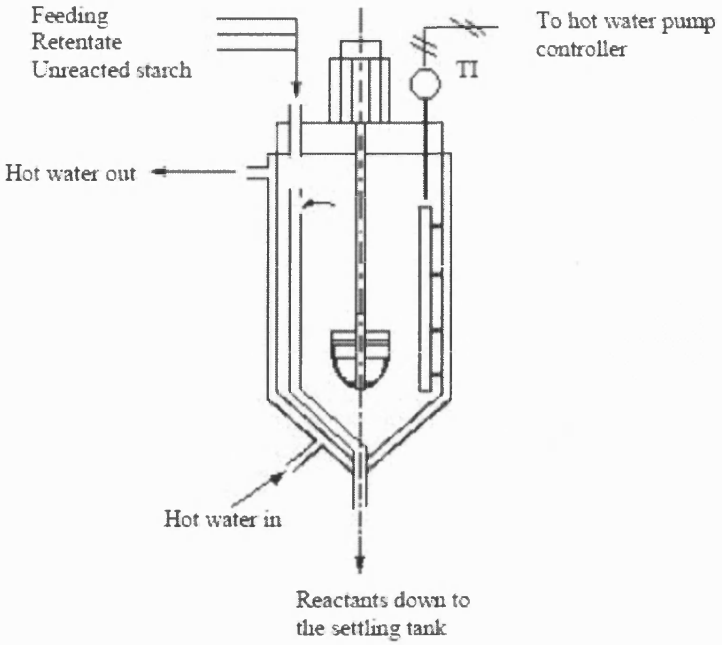

Fig. 4- 2: The Reactor Diagram Unit

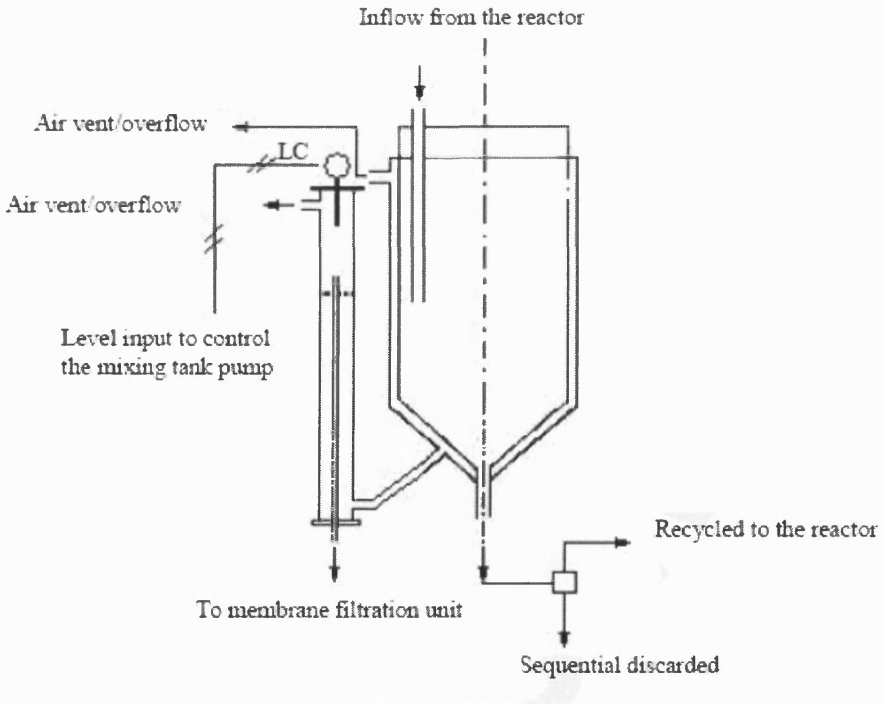

Fig. 4- 3: The Settling Tank Diagram Unit

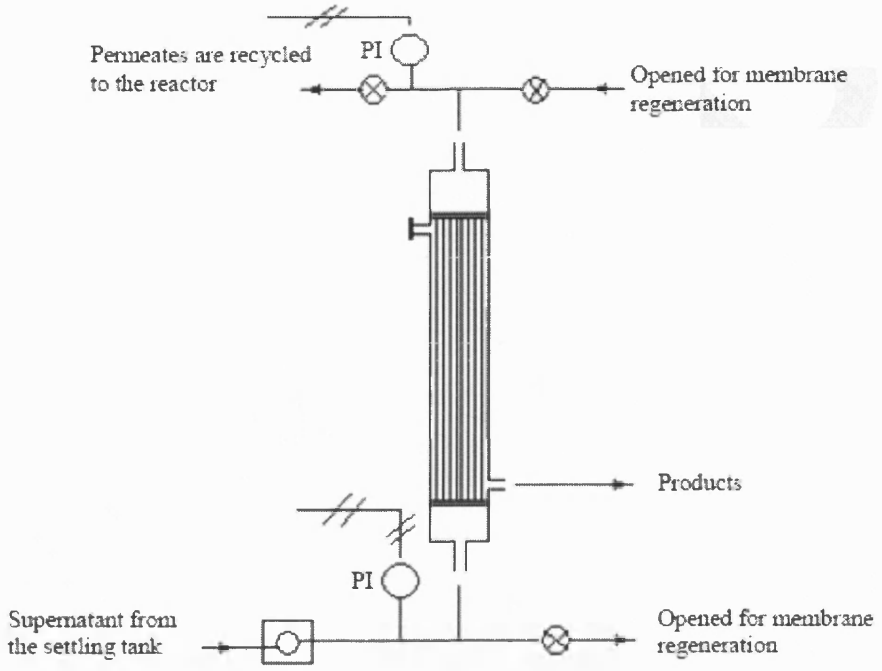

Fig. 4- 4: The Membrane Module Diagram Unit

Fig. 4-5 (a)

Fig. 4-5 (b)

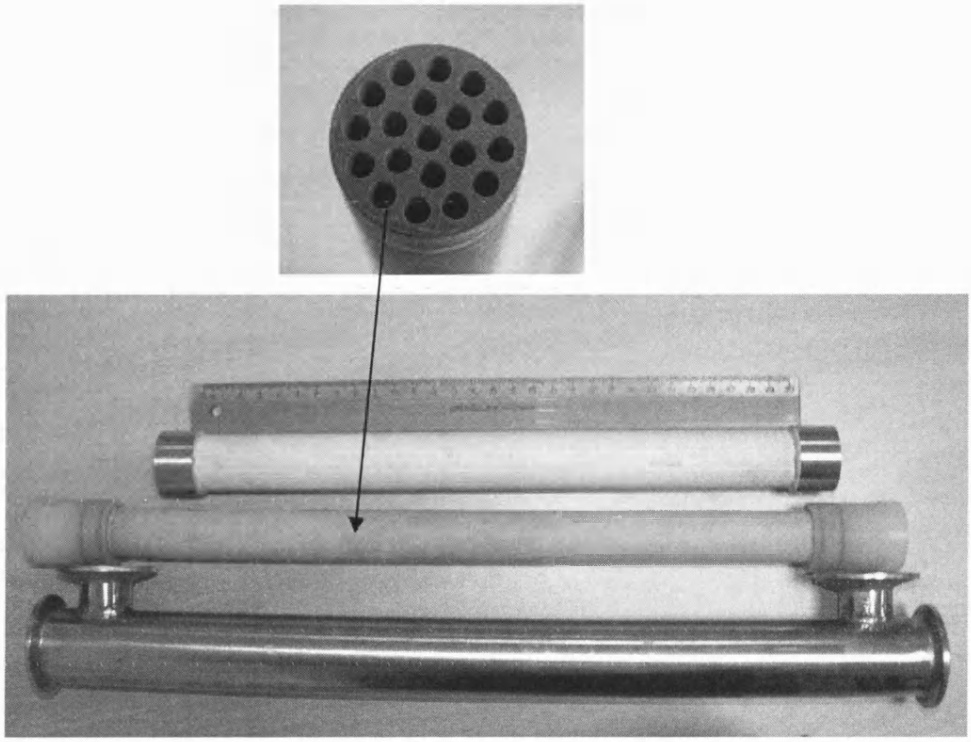

Fig. 4- 5: Pictures of (a) a 30 kD hollow fibre membrane module, (b) ceramic membranes and casing.

4-1.2 Operation of the Ultrafiltration System

Continuous Operation

Starch powder was slowly added into the mixing tank (ambient temperature, T~22^{0}C) to make a slurry with concentration of w=10% (γ_{S_0} = 100 g/litre). During mixing, 50 mg of calcium chloride per litre of water was added to enhance enzymes stability. The stirrer in the mixing tank was kept running throughout the entire process. The well-mixed slurry was pumped into the reaction tank via a heating coil spiral. The coil spiral was

submerged into hot water (T=70 ^{0}C) to pre-heat the starch slurry before being fed into the reactor. The preheating process was able to raise the slurry temperature to ~55 ^{0}C. When the reaction tank has been filled with the starch slurry, the heidolph stirrer was reset to ~350 rpm. At a certain level, the starch slurry would overflow into the settling tank through an overflow pipe installed inside the reactor. When the level reached the set level, the floating level control installed inside the cylinder column will cut the feed pump power, thus cutting the substrate supply into the reactor.

The settling tank has two outlet pipes, one for a supernatant stream at the top and one for an unproductive starch stream at the bottom. The bottom stream pump was used either to recycle the unproductive starch into the reactor or to discharge the unproductive substrate out of the system at a slow flow rate of 0.4 ml/min. The supernatant stream was pumped into a membrane module for separation of glucose solution. The intake pipe of the supernatant stream located inside the transparent column was initially adjusted to collect just the first and second layer products. This is a useful method to avoid the un-reacted starch to be contacted with the membrane module. The pumping rate of the supernatant stream was adjusted at15 litre/min and the pressure across the membrane was maintained to the setting pressure at 0.5 or 1.0 bar by adjusting the retentate valve or the retentate pump power knob.

Initially, both permeate and retentate streams were recycled into the reactor. This process was continued until the set temperature, 55 or 60^{0}C, in the reactor was reached. After reaching constant temperature (approximately 10 minutes), 3.66 ml of the α-amylase and 3.66 ml of the AMG that is equivalent to $\sigma_{E_0^{mix}} = 0.6$ ml/litre were added into the reactor. Complete recycling was used for 15 minutes to provide good enzymes distribution throughout the system. After 15 minutes, the permeate stream was switched to the production stream for product collection. The flux of the

permeate stream was measured periodically by taking the time required to produce 20 ± 0.5 ml of the sample (Figure 4-1). The permeate sample was also used for analysis of glucose concentration and other sugar components. The retentate stream was also adjusted to maintain the flow rate. The small pressures variations were recorded throughout the process, and the average was calculated and taken as the applied pressure. The pH was also monitored throughout the experiment.

Batch Operation

A complete recycling of the permeate and retentate streams were also carried out to determine the kinetic parameters of the glucose production in the ultrafiltration system and for comparison studies with the kinetic value obtained by the batch SGLS hydrolysis in the flask. The operation in batch mode of the ultrafiltration system is similar with the continuous mode except the permeate stream is returned to the reaction tank making it a complete recycle process. A complete recycle process was run for over 48 hour operating time and the sample was collected periodically. In this experiment, the $\gamma_{S_0} = 100$ g/litre and the concentration of enzymes at $\sigma_{E_0^{mix}} = 0.6$ ml/l were used. The retentate flow rate, the reactor temperature, and the applied pressure were ~15litres/hr, 55^0C, and 0.5 bars respectively.

4-2. ANALYSIS METHODS

4-2.1. Membrane Restoration and Pure Water Test

Easy, efficient cleaning of the ultrafiltration system after each run is a vital consideration when designing the system. The cleaning protocol could differ according to the membrane type, and the substances used. The

cleaning could use alternate washing with acid and base solutions and then followed with rinsing with clean water. Alkali detergents e.g. ultrasil 11 (Henkel Chemical) at T=40°C at 0.25% concentration rinsed for 1 h [Howell *et al.* 1995] can also be used. The number of cycles and the washing time rely on the degree of fouling. Pure water permeation tests at room temperature and constant pressure would give the percentage flux restoration after regeneration. In this study, back washing by rinsing with hot tap water at T ~50^{0}C, and low pressure < 0.5 bars, and flow rate ~ 30 litres/min for an approximately 3-4 hour followed by rinsing with reverse osmosis water for 30 minute was used. It was found > 98% restoration of the flux was achieved.

4-2.2 Glucose Concentration and Rejection of High Polysaccharides Analyses

Samples collected in the retentate were diluted to 1:10, and then filtered through a 0.2µm nylon filter using a syringe into vials. The sample was not treated either by the acid solution or low temperature. This is due to the fact that the membrane with a molecular weight cut-off (mw cut-off) of 30kD should allow only glucose to pass through and also retain high degree polysaccharides. It may also retain the amylase enzymes. This is based on the fact that invert sugars have molecular mass less than 400 and diameters range from 0.8-1 nm [Bailey & Ollis, 1986], while active amylase has a molecular mass varying from 10-210 kD [Gupta R., *et al.*, 2003]. Paolucci-Jeanjean *et el.*, [2000b] mentioned that the ceramic membrane with 50kD molecular weight cut off completely rejected the Termamyl enzyme and non-hydrolysed starch, and let pass the hydrolysates.

A Shimadzu HPLC analysis machine coupled with a refractometer index detector (RID-10A) and a sodium column with a guard was used for

determining the sugar concentrations. The column operating temperature was maintained at 80 ^{0}C, and reverse osmosis water containing 0.05% sodium azide at a flow rate of 0.3 ml/min was used as eluent. To validate the method, samples collected in the retentate were also assayed by acid and temperature treatment techniques as described in Chapter 3. The results shown by both methods were effectively the same. This result suggests that the 30kD polysulfone hollow fibre membrane has effectively rejected the high degree polysaccharides. The standard curve for glucose determination is given in appendix 1.

4-2.3 Protein Permeation Analysis

All enzymes are protein, thus the protein permeation test was carried out to determine the ability of the 30kD polysulfone hollow fibre membrane to retain the protein. 2 litres of the enzymes solutions were prepared by diluting Termamyl and AMG enzymes in the RO water at a concentration of $\sigma_{E_0^{mix}} = 0.6$ ml/litre each. The enzymes solutions were pumped into the membrane module. Room temperature (T~20^{0}C) and 1 bar applied pressure were used. The retentate stream was recycled while the permeate stream was collected and weighted. The experiment was stopped when half of the volume of the enzymes solution was filtered. The initial enzymes solution, the final retentate and permeate were analysed using a Shimatzu uv-visible spectrophotometer and scanned under the wave length ranging from 200-400 nm with RO water was used as a blank.

In order to obtain the reference for comparison, a 5 kD of the ceramic membrane supplied by Oriles was also used to filter a 2 litres of the enzyme solutions containing $\sigma_{E_{01}} = 0.3$ ml/litre Termamyl enzyme and $\sigma_{E_{02}} = 0.3$ ml/litre AMG. This experiment was used to verify the result that the active amylase enzymes have molecular weights varying from 10 kD to 210 kD

[Gupta R., *et al.*, 2003] and also to recheck the results of Paolucci-Jeanjean *et al.,* [2000b] that the Carbosep M4 membranes supplied by Orelis, France, with the molecular weight cut-off 50 kD rejects the Termamyl enzyme and non-hydrolysed starch but let pass the hydrolysates. Gan *et al.* [1999] used an Amicon PM10 with 10kD molecular weight cut-off found that the separation characteristics permitted a total rejection of the cellulose enzymes and zero rejection of the reducing sugar.

In this experiment, the Termamyl and AMG solutions were pumped into a 5kD ceramic membrane module separately. The initial enzyme solutions and the final retentate and permeate samples were analysed by using a Shimatzu uv-visible spectrophotometer and scanned at a 265nm wavelength. RO water was used as the blank sample. The estimation of the possible error of the experiment is attached in appendix 2.

4-3. RESULTS AND DISCUSSION

4-3.1 The Ultrafiltration System Performance

The ultrafiltration system depends on the efficiency of the unit operation in the system. Discussions to the specific function of the unit operations are given below. The overall system performance of the ultrafiltration is shown by the concentration of glucose solution and the flux rate across the membrane. In this performance analysis, the results are based on the specified conditions given in Table 4-2 below, unless stated otherwise.

Table 4- 2: The material and the experiment conditions

Slurry concentration (g/litre)	100
Concentration of enzymes (ml/litre)	0.6
Reactor temperature (T_R)	55^0C
Membrane Module	30kD polysulfone hollow fibre membrane
Membrane Temperature (T_M)	50^0C
Applied pressure across the membrane (Bar)	0.5
Duration	8.5 hours
Discarded Unproductive Product	No
Ph	Uncontrolled

4-3.1.1 Reactor

Fig. 4-2 and Fig. 4-6 show the diagram of the reactor and pictures of the reactor used in this study. The temperature was set at T_R=55^0C but a small variation of ~1^0C was observed during initial operation but then it remained effectively constant thereafter. This result indicates that the spiral coil submerged in the water bath set at T_B=70^0C used to preheat the substrate, and the thermocouple mounted to the reactor used to control the recycle flow of the hot water jacketed around the reactor body were able to maintain the set reactor temperature.

Fig. 4- 6: A Picture of the Laboratory Reactor Unit

4-3.1.2 Settling Tank

Fig. 4-7 shows a picture, taken after 5 hour operation, of the reactant layers inside the transparent column mounted on the settling tank. Observation found that four separate layers were clearly detected after ~2 to 3 hour operation, and the layers were established thereafter. As the membrane pump collected only the top first and second layers, this observation result suggests that the settling tank with 7 litres capacity, continuous recycle of the unreacted starch at ~0.4 ml/min flow rate, and retentate flow rate maintained at ~15 litre/h, is able to retain the unreacted starch and the higher molecular weight biopolymers after two to three hours of the ultrafiltration system being operated.

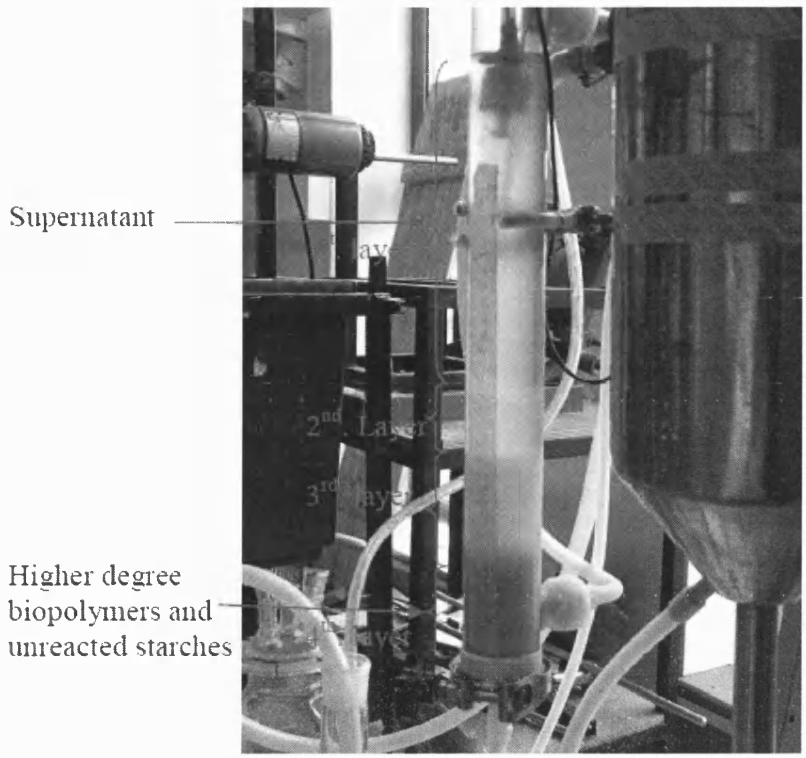

Fig. 4- 7: The layers of polymers inside the cylinder column mounted on the settling tank

4-3.1.3 Membrane Module

(a) Polysaccharide Permeation Test

Fig. 4-8 (a) shows HPLC spectrums obtained for the sample taken after 0.5 hour of the ultrafiltration system being in operation. As can be seen, glucose (concentration >98%) was the main permeate component. The rest of the component was polysaccharides with the degree of polymerisation (DP) 2-7. The glucose concentration was $\gamma_{P_{glucose}} = 24$ g/litre.

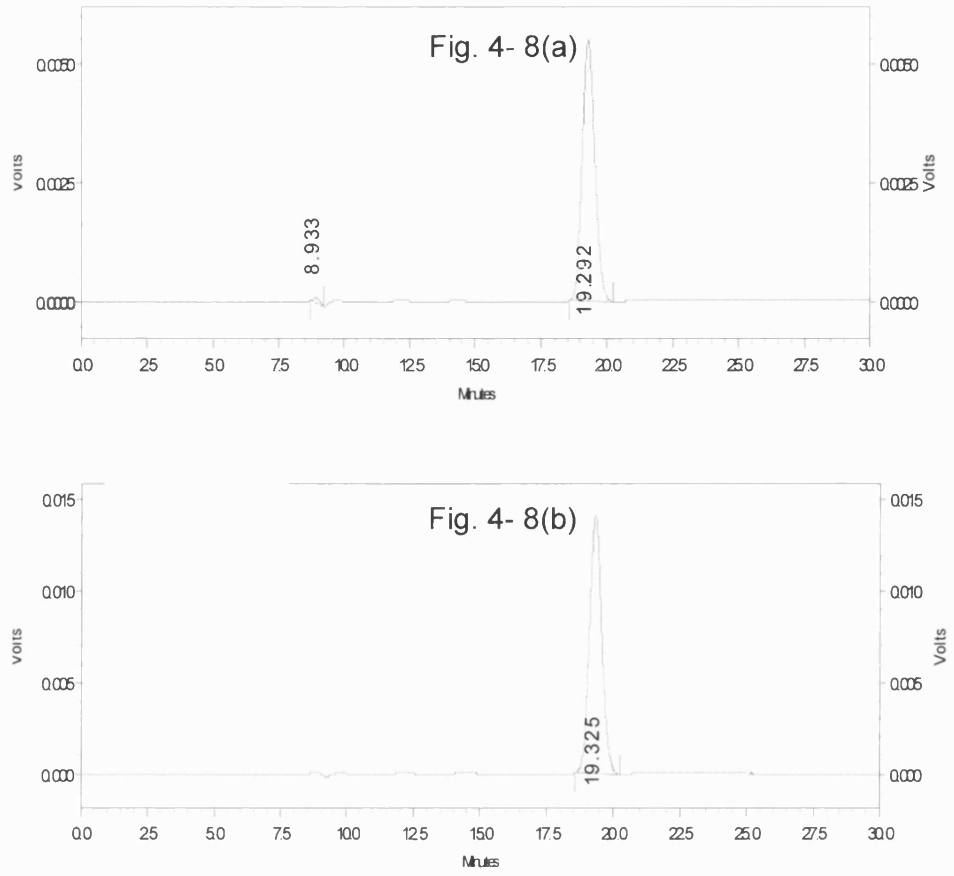

Fig. 4- 8: The HPLC spectrum (a) after 30 minute operation (b) when steady state, after 300 minute. T_R=55^{0}C, T_M =50^{0}C and P=0.5 bar.

Fig. 4-8(b) shows HPLC spectrums shown for the sample taken after 5 hours of the ultrafiltration being in operation. During steady state operation, the glucose solution purity remained consistently high, but the concentration of glucose increased to a plateau of $\gamma_{P_{glucose}} = 64$ g/litre. These results suggest that the SGLS carried out in the ultrafiltration system produces continuous and pure glucose solution at >98%, and the 30kD polysulfone membrane has effectively retained most of the high degree of polysaccharides.

(b) Protein Permeation Test

Fig. 4-9 shows the uv-visible spectrophotometer spectrums of the permeate samples shown as the transmitted wavelength percentage. The initial enzymes solution, the permeate and the retantate samples were obtained by filtering 2 litres of the $\sigma_{E_0^{mix}} = 0.6$ ml/mitre across a 30 kD hollow fibre polysulfone membrane. The result showed that all samples scanned at wavelength ranging between 200-400 nm have a maximum peak between 260-270 nm but they differed in term of the percentage of the transmitted wavelength. The typical value is shown in Table 4-3.

Activity of the enzymes in permeate stream solutions were also tested to confirm the fact that the protein passing through the membrane is the amylase enzymes by adding w=10% of the starch and heated to T_R=60^{0}C. The viscosity of the slurry remained low suggesting that the protein detected by the uv-visible spectrophotometer was active amylase enzymes. This result also clearly suggests that the 30kD polysulfone membrane does not completely reject the amylase enzymes. Despite that, the 30 kD polysulfone hollow fibre membrane has effectively rejected the high degree polysaccharides as most stream product was the glucose (>98%). Hence, a small molecular-weight cut-off membrane is proposed to be used if complete rejection of the enzymes is required.

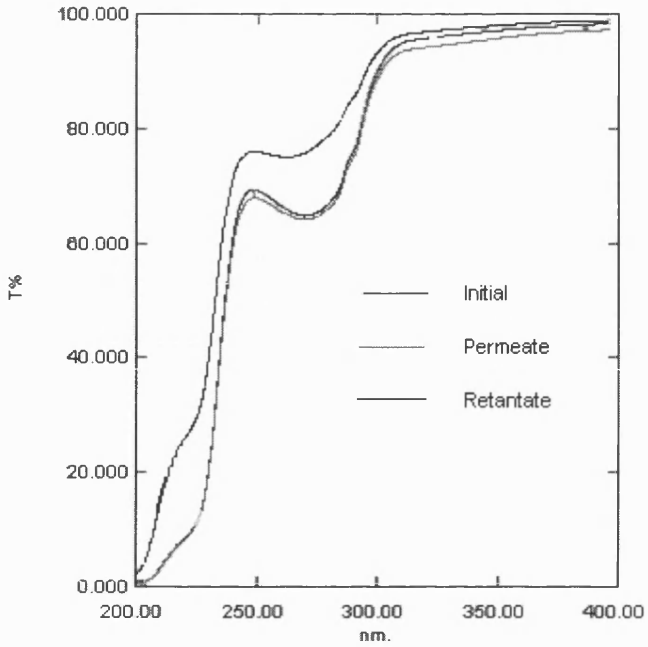

Fig. 4- 9: UV-Visible spectrophotometer transmitted spectrums

Table 4-3 Percentage of transmitted wavelengths. (A 30kD hollow fibre membrane, T_M=room temperature, and P=1bar).

Samples	*Max peak at wave length (nm)*	*Transmitted (%)*
Initial	270	65%
Retentate	270	64%
Permeate	262	75%

A 5kD ceramic membrane was tested for the ability to reject the Termamyl and AMG enzymes, which also is used to confirm the fact that the 30kD does not completely retain the amylase enzymes. When the Termamyl enzyme and the AMG enzyme solutions were filtered by a 5kD ceramic membrane at T_M=room temperature and at 1 bar applied pressure, the permeate stream showed that some trace protein was detected. Table 4-4 give a typical result of the protein permeation test. This result suggests that

the 5kD ceramic membrane is not completely rejected the protein. Furthermore, the protein detected in the permeate stream by the protein permeation test may be identified as small amylase enzymes as suggested by Gupta R., *et al.*, [2003],however, no conclusion can be made on the type of the protein in the permeate stream, as further identification tests would be necessary.

Table 4- 4: Protein passing through a 5kD ceramic Membrane

	Termamyl	*AMG*
Initial Concentration (ml/litre)	0.3	0.3
Permeate (ml/litre)	0.03	0.05
Percentage of the released protein	10%	16%

4-3.1.4. The Performance of the Continuous Ultrafiltration System

Using the conditions specified in Table 4-2 above, Fig. 4-10 shows the glucose concentration and the flux. As can be seen, the glucose concentration increased to reach to a steady state concentration of 64 g/litre after ~ 5 hours operation. The flux progress was initially high at ~21 litre/m^2-h and then decreased to a base line of the steady state flux of ~14.5 litre/m^2-h after ~3 hours operation. The flux was not recorded over 15 minute when the membrane pump was on, but the permeate stream was recycled.

As described by Darcy equation (Equation 2-13), at a constant applied pressure and during unsteady state operation (initial operation in space), the flux decay is linked to the dynamic viscosity of the solute, and the hydraulic resistance consists of the membrane, gel layer and concentration polarisation resistances. As the dynamic viscosity proportionally relates with the concentration of glucose, the recorded flux across the membrane in this study supports the fact that the flux decreased

with increasing of glucose concentration. The hydraulic resistance could slightly increase but it would not give a significant impact on decrease of the initial flux as complete recycle of the permeate stream back to the reactor was initially made for 15 minutes, and the hydraulic resistance could already have reached steady state.

When the steady state glucose concentration was reached, the flux had reached a constant value before the glucose concentration reached steady state suggesting that the dynamic viscosity and the hydraulic resistance had reached in a steady state. The flux result suggests that the ultrafiltration system was able to continuously produce glucose, and the membrane was not significantly fouled over the period being studied. Additionally, extending the operation time would not decrease the flux but it would require the unproductive product to be removed and addition of more enzymes would be necessary.

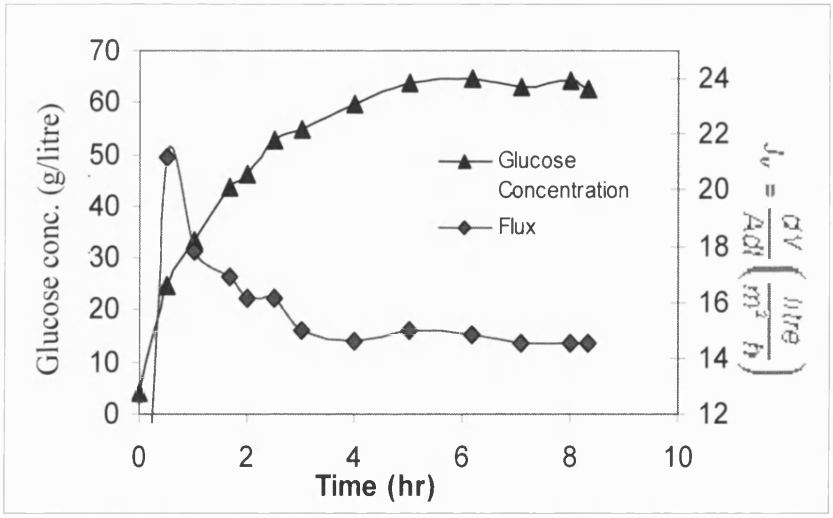

Fig. 4- 10: Plots of the glucose concentration and flux at T_R=55^{0}C, T_M =50^{0}C and P=0.5 bar.

4-3.2. Effect of the Applied Pressure

Generally, the applied pressure across the ultrafiltration module is up to 10 bars [Howell *et al.* 1993] depending greatly on the material and the type of the used membrane. Changing the pressure affects the performance of the membrane. In this case, the performance of the ultrafiltration system is considered in terms of flux, glucose concentration, and fouling. When the ultrafiltration system used as a platform for reactions, the optimum flux is determined by the residence time which gives the required conversion time of the substrate into product. However, fouling must be taken into account when choosing the substrate conversion rate due to the fact that fouling is dependent on the flux when constant pressure is applied. The ideal flux for continuous operation is a value that can give a constant residence time during the steady operation, when the dynamic viscosity of the filtrate becomes constant. The critical flux concept is the technique [Howell *et al.* 1995; Field *et al.* 1995; Wu, *et al.* 1999] that can be used to obtain the constant flux at constant applied pressure.

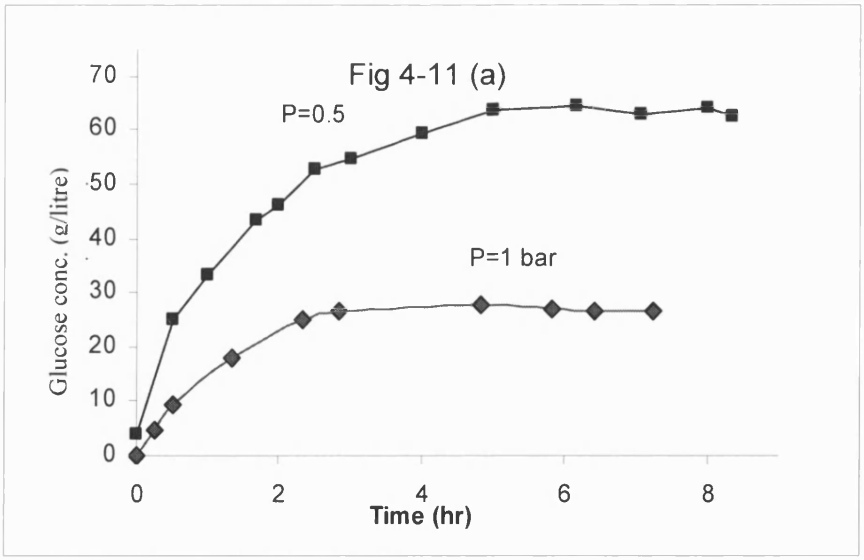

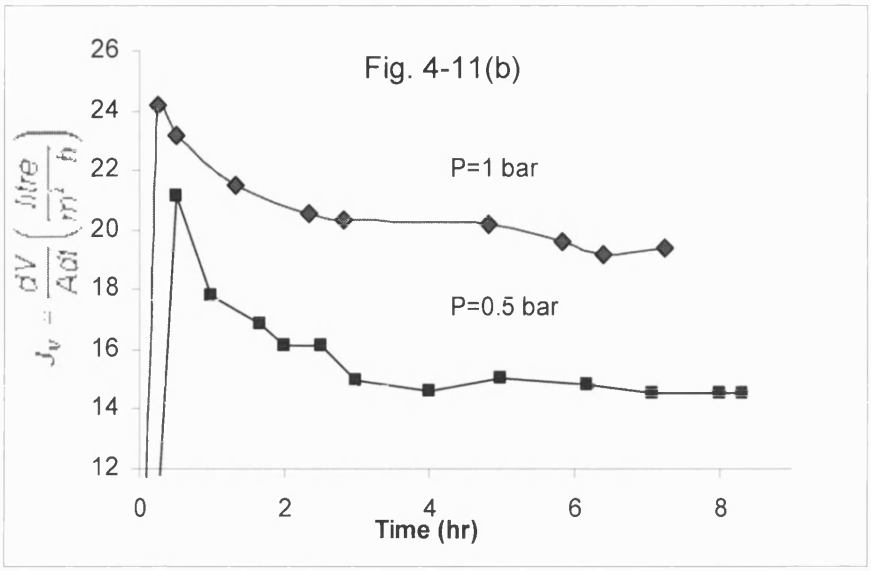

Fig. 4- 11: Plots of (a) the glucose concentration and (b) the fluxes at T=55^{0}C, $\sigma_{E_0^{mix}} = 0.6$ ml/litre, and $\gamma_{S_0} = 100$ g/litre

Table 4- 5: The effect of the applied pressure on the glucose concentration and the flux.

Pressure (Bar)	0.5 bar	1 bar
The steady state flux (litre/m^2-h)	14.5	19.5
The steady state residence time, $\tau_{residence}$ (h)	12 hr	6.2hr
The steady state glucose concentration (g/litre)	64	25

In this experiment, two different applied pressures of 0.5 and 1 bar were used across a 30 kD hollow fibre polysulfone membrane module. The other conditions were the same as that given in Table 4-4. Fig. 4-11 (a) shows the glucose concentration throughout the process. Fig. 4-11 (b) shows the flux for both pressures. As can be seen, by operating the

ultrafiltration at 1 bar and T_R=55^{0}C the concentration of the glucose in the permeate stream has reduced by 2.5 fold, which may be due to the reaction residence time being reduced by and the steady state flux increased by 35%. The result suggests that the applied pressure is generally responsive for controlling the glucose concentration in the permeate stream, but the membrane has to be relatively free from fouling. The strategy of low applied pressure controlling the glucose concentration as described here means that it may be possible to operate the process at relatively free fouling even though operation time is extended. Table 4-5 shows the effect of the applied pressure on the steady state flux, the residence times ($\tau_{residence}$), and the steady state glucose concentration.

4-3.3 Effect of the Temperature

Fig. 4-12(a) shows the glucose concentration at two different reactor temperatures (T_R) of 55^{0}C and 60^{0}C. As can be seen, the glucose concentration when T_R =60^{0}C was higher in the first three hours of operation than when T_R =55^{0}C but they both reached effectively the same maximum level. The glucose concentration at T_R =55^{0}C showed a slightly reduced value after 5 hours operation than at T_R =60^{0}C. Two reasons could affect the glucose concentration in the continuous process, the reaction temperature and the residence time. Increasing the temperature would increase the maximum reaction rate, but the maximum glucose concentration is effectively the same when steady state is reached as discussed in Chapter 3 for the temperature effect on the SGLS, while the residence time relies on the flux. Hence, the glucose concentration at T_R =55^{0}C which differed from T_R =60 ^{0}C was also due to change of the flux.

Fig. 4-12(b) shows the flux at two different reactor temperatures (T_R) of 55^{0}C and 60^{0}C. As can be seen, the flux at T_R =60^{0}C (T_M =53^{0}C) was

initially higher than when T_R =55^{0}C was used, and then it decreased and crossed the flux curve for T_R=55^{0}C at ~5 hour operation to give a lower flux thereafter than when T_R=55^{0}C was used. This result suggests that high temperature SGLS in the ultrafiltration system gives high flux but also increases the fouling rate compared to when low temperature is used. The fouling increases at high operating temperature may be due to the gelatinised starch and liquefaction rate increasing more than the saccharification rate, and it may be also due to the rapid inactivation of the enzymes. Increasing the enzymes inactivation could also increase the gelatinised starch accumulation in the system. Since Termamyl is a thermo-stable amylase, high temperature could have bigger impact on inactivation of the saccharyfing enzymes (AMG) than on the Termamyl enzyme.

The other reason may be of importance in explaining why the flux at T_R=60^{0}C was initially high but decreased to a lower value than when T_R=55^{0}C after 5 hours operation is that the membrane property changes with operating temperature and the flux at T_R =60^{0}C and at 1 bar could exceed the critical flux. Operating the SGLS in the ultrafiltration system at T_R =55^{0}C and P=1 bar produced a high steady state flux at ~19.5 litre/m^2-h but gave low glucose concentration at 25 g/litre in the permeate stream. Nevertheless, operating the SGLS in the ultrafiltration system at T_R =55^{0}C and P=0.5 bars gave a high steady state concentration of glucose at $\gamma_{Glucose} = 64$ g/litre and a steady state flux at ~14.5 litre/m^2-h after 3 hours operation, suggesting that low pressure and low temperature would give better conversion and increases the overall performance. To justify the condition that the low pressure and temperature may be still within the critical flux region, a good indication is that the flux reached the steady state after 3 hours operation, and it remained constant thereafter over the period of experiment.

It has been stated that at constant pressure, the flux would change as the dynamic viscosity and the hydraulic resistance changes. The dynamic

viscosity is affected by the glucose concentration which reaches steady state more quickly when temperature is increased. The dynamic viscosity also relies on the residence time, which is determined by the flux rate. The hydraulic resistance that consists of the gel layer and surface polarisation resistances is responsive on the flux pattern which is initially high and then decreased to a steady state. By increasing the temperature the membrane resistance would increase and stay constant, however, varying temperature would also change the reactant properties and as a result mass transfer could also change.

During imbalanced condition between diffusion and drag force, the ultrafiltration system would be operated at unsteady state, but later when reverse diffusion and drag force are in balance with the gel layer formation and the surface polarisation, a steady state hydraulic resistance would be reached. The hydraulic resistance in the SGLS reaches steady state at low temperature and could be due to the non-gelatinised starch particles having increased the drag force. However, when high temperature has been used, more gelatinised starches and high degree polymers would be formed in the system, thus this may reduce the drag force and increase the gel layer and the surface polarisation. As result, the flux would continuously decrease to reach a lower flux, and finally the membrane could completely block.

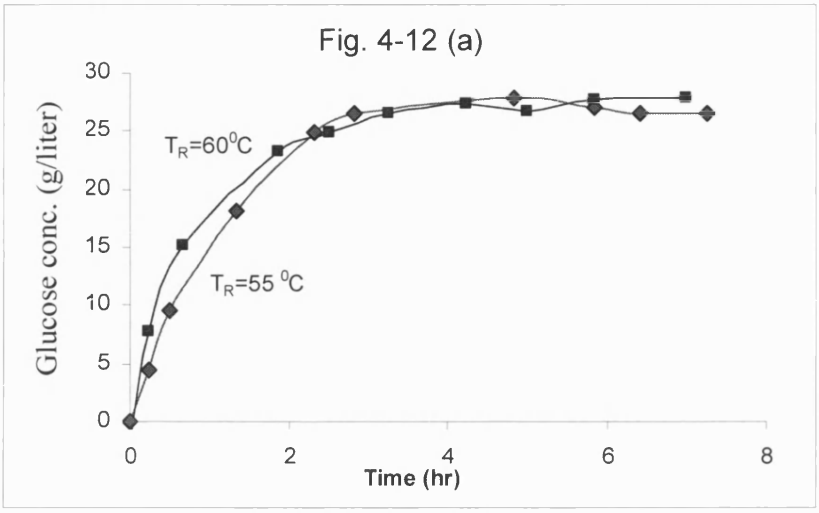

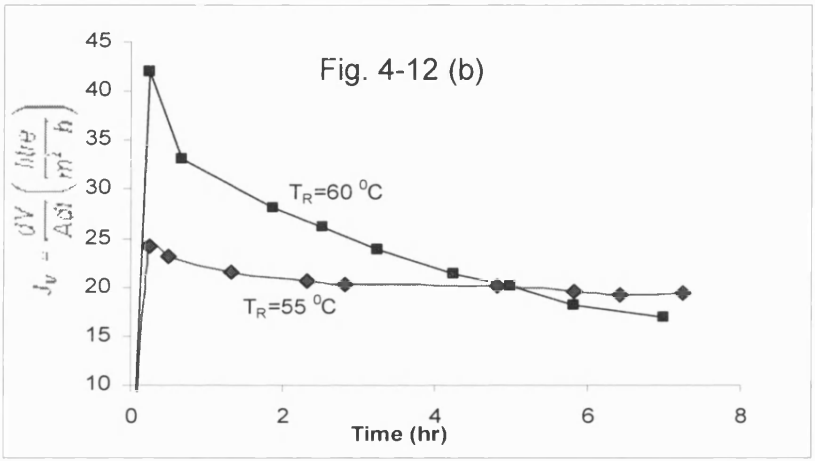

Fig. 4- 12: Plots of (a) the glucose concentration and (b) the fluxes at P=1bar $\sigma_{E_0^{mix}} = 0.6$ ml/litre, and $\gamma_{S_0} = 100$ g/litre

4-3.4 Comparison of Batch Processes in the Flask over the Ultrafiltration System: Effects of Pre-heating the Substrate

The objective of the comparison made between two batch processes carried out in flask and in the ultrafiltration system is to determine the effect of different procedures and equipment used. The batch process in 250 ml flasks experiment was discussed in chapter 3. All conditions used were the same unless stated in the operating procedures. Fig. 4-13 shows the plot of

the glucose concentration for the ultrafiltration system where the retentate and permeate streams were recycled into the reactor, and for the batch SGLS process carried out in the flask. As can be seen, the glucose concentration produced by the ultrafiltration system reached a steady state glucose concentration faster than the batch SGLS in the flask. The ultrafiltration system also produced a slightly high maximum glucose concentration over the period studied than the SGLS in the flask.

Table 4-6 shows typical comparison results for the studies. As can be seen, the maximum production rate of the SGLS in the ultrafiltration system was higher than in the flask. Increasing the maximum production rate has reduced the time to obtain half of the maximum glucose concentration by the ultrafiltration system. The maximum production rate has increased in the ultrafiltration system and is due to pre-heating the substrate before being feed into the reactor, and the enzymes were added after the reactor temperature has reached to $T_R=55^0C$. The pre-heating process would increase the gelatinised starch concentration in the system, thereby affecting the ratio of the enzymes to the productive substrate and would increase the enzymes activity. The relative productivity ($\psi^{relative}_{productivity}$) calculated by using the Equation 3-54 was higher at 68% in the ultrafiltration system than in the flask thus confirming that the preheating process will increase the performance of the SGLS.

Therefore, this result suggests that the preheating strategy by increasing the gelatinised starch concentration is useful but the reaction temperature must be optimised to avoid high viscosity in the system.

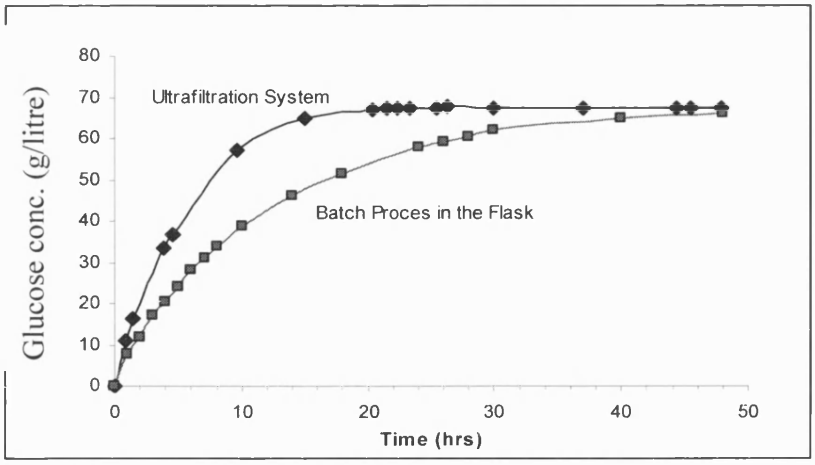

Fig. 4- 13: Comparison of the glucose concentration by batch process in the Flask and the Ultrafiltration System. T_R=55^{0}C, $\gamma_{S_0} = 100$ g/litre, and $\sigma_{E_0^{mix}} = 0.6$ ml/litre.

Table 4- 6: Summary of the glucose concentration in batch process carried out in the flask and the ultrafiltration System. T_R=55^{0}C, $\gamma_{S_0} = 100$ g/litre, and $\sigma_{E_0^{mix}} = 0.6$ ml/litre

	Ultrafiltration system	Batch process in the Flask
$\gamma_{P_{glucose}^{max}} / \gamma_{S_0}$	0.67	0.66
$\tau(hr)$	4.2	7
Γ_{max}	11.43	6.67
$\psi_{productivity}^{relative}(g/ml-h)$	13.3	7.9
Enzymes Activity $= \frac{\Gamma_{max}}{\sigma_{E_0^{mix}}}$	19.05	11.12

4-3.5 Comparison of Batch Process with Continuous Process in the Ultrafiltration System

The comparison is made between batch and continuous is to determine if there is improvement performance by continuous over batch

process. This study could also be useful as a basis for economical analysis study of the SGLS in the continuous ultrafiltration process c.f. the batch process and the conventional process for production of glucose. The experiments for the batch and continuous processes were carried in the ultrafiltration system using a 30 kD hollow fibre polysulfone membrane. All operating conditions (T_R=55^{0}C, $\gamma_{S_0} = 100$ g/litre, $\sigma_{E_0^{mix}} = 0.6$ ml/litre, P=0.5 bars) were kept constant.

As shown in Equation 3-54 discussed in Chapter 3, the relative productivity will be used as a comparison basis for this study. Modifications of the Equation 3-54 which are applied to the continuous operation are necessary to make sure a consistent comparison is made. Therefore, instead of relative productivity, the actual productivity was used which is the total weight of the produced glucose over the total enzymes quantity over the operating time, and is shown in Equation 4-1 below;

$$\text{Productivity} = \frac{\sum w_{glucose}}{\varphi \cdot \sum V_{E_0^{mix}}} \qquad (4\text{-}1)$$

The $\sum w_{glucose}$ is the total weight of glucose, $\sum V_{E_0^{mix}}$ the total volume of enzymes, and φ the operating time required to obtain the total weight of glucose. In continuous process, the total weight of glucose is calculated as;

$$\sum W_{glucose} = V_R \cdot \gamma^{ss}_{glucose} + A_m \int_0^{\varphi} J_V \cdot \gamma_{glucose} dt \qquad (4\text{-}2)$$

When the operation is relatively free from fouling,

$$\sum W_{glucose} = V_R \cdot \gamma^{ss}_{glucose} + A_m \int_0^{t_{ss}} J_V \cdot \gamma_{glucose} dt + A_m \cdot J^{ss}_V \cdot \gamma^{ss}_{glucose} (\varphi - t_{ss}) \quad \text{.....(4- 3)}$$

The $\gamma^{ss}_{glucose}$, is the steady state glucose concentration, V_R the total volume of the ultrafiltration system, A_m membrane area, J_V the flux, t_{SS} the steady state time, J^{ss}_V the steady state flux. In continuous operation where the produced glucose solution is fed direct into the subsequent process, it could be difficult to integrate the equation 4-3 simultaneously as different membrane and operation conditions give different values of the produced glucose and the flux. However, by using the Simpson or the trapezoid rules to calculate the total glucose formed during unsteady state operation will simplify the calculations for Equation 4-2. In this study, the produced glucose solution was collected in a storage tank, weighed and assayed for concentration thus enabling assessment of the total weight of the glucose produced to be made.

Table 4- 7: Comparison summary of batch and continuous processes carried out in the Ultrafiltration System. T_R=55^{0}C, γ_{S_0} = 100 g/litre, and $\sigma_{E_0^{mix}}$ = 0.6 ml/litre.

	Batch	**Continuous**
Used starch	1.22 kg	2.32 kg
Clean glucose	0g	670g (61g/litre)
Un-separated glucose	842g (67g/litre)	781g (64g/litre)
Total glucose	842g	1450g
Operating time	15 hrs	8.33 hrs
Used Enzymes	7.32 ml	7.32 ml
Productivity	7.67	23.8

As shown in Table 4-7, the advantages of the continuous operation process over the batch process are clean glucose is instantaneously produced, and the productivity increases by 3 fold. This comparison study supports the fact that the continuous process is better than the batch process and can be confirmed by economy analysis taking into account all the respective costs.

4-4 CONCLUSION

Polysaccharides and protein permeation tests were carried out using 30 kD polysulfone hollow fibre membrane modules to determine the possibility of retaining high degree polysaccharides and amylase enzymes in the system. In these tests, it has been found that the 30 kD membrane did not completely reject the amylase enzymes as was confirmed by protein being detected in the permeate stream of the 30kD membrane. The protein was confirmed as the active amylase enzymes by carrying out an enzymes activity test. The 30 kD polysulfone hollow fibre membrane is able to retain high degree polysaccharides, and allows maintly glucose (>98%) to pass through. This result is contrary to the result found by Paolucci-Jeanjean *et el.*, [2000b] that the Termamyl enzyme was completely rejected by a 50 kD ceramic membrane. However, the result obtained here is supported by the findings of Gupta R., *et al.*, [2003] that the amylase enzymes varies in size from 10 to 210 kD. Due to these results, the protein permeation test was carried out using a 5 kD ceramic membrane, the same membrane material and manufacturer but with a different molecular weight cut off to the membrane used by Paolucci-Jeanjean *et el.*, [2000b]. The results showed that trace amount of proteins were detected in the permeate stream. However the protein that was detected in the permeate stream of the 5 kD ceramic membrane was not confirmed either as active amylases enzymes or

fractions of lyses enzymes due to the very low concentrations and further tests are necessary.

The use of the ultrafiltration system as a working system for continuous process of the SGLS to produce clean glucose solution has been confirmed. The results using w=10% of the starch milk, and the concentration of enzymes at 6ml/kg-substrate showed that the ultrafiltration system performed better when operated at low temperature and low applied pressure at 55^0C and 0.5 bars respectively, and have produced a steady state glucose concentration of ~64 g/litre and a constant flux at ~14.5 litre/m^2-h over 9 hours operation. The constant flux suggests that the ultrafiltration system is able to continuously produce the glucose, and the membrane is not significantly fouled over the period studied. The conditions given above may also lie within the critical flux region as suggested by the flux reaching a steady state after 3 hours operation and remaining constant thereafter. Additionally, extending the operation time will not decrease the flux but may require unproductive product to be removed, and further addition of the enzymes may be required. The productivity was also effectively increased by pre-heating of the substrate before being fed into the reactor as this strategy would increase the quantity of gelatinised starch.

The other importance process variables are the applied pressure and the temperature. The applied pressure is generally responsive for control of the concentration of glucose in the permeate stream. However, the upper limit of the critical flux must be determined so that the process can continuously produce glucose solution over long period of operation. The temperature effect has also found to affect the flux pattern by changing the dynamic viscosity and the hydraulic resistance kept at a constant pressure. The dynamic viscosity of the filtrate (medium) relies on the reaction rate, while the hydraulic resistance is a combination of the membrane resistance, the gel layer thickness, and the surface polarisation resistance. High

operating temperature will increase the dynamic viscosity but may also increase the thickness of the gel layer by increasing of the quantity of gelatinised starch in contact with the membrane

A comparison study of batch and continuous supports the hypothesis that continuous operation is better than the batch process as shown by higher productivity. Furthermore, continuous operation of the SGLS also produces a clean glucose solution, thus no further purification process is required.

After considering all results, future study of the ultrafiltration system for continuous production of clean and sterile glucose should be an economy analysis to compare conversional glucose production processes and the ultrafiltration system. A small molecular weight cut off membrane can also be used to improve the ability for retaining the active enzymes. It may also improve the long run operation performance. When a different membrane is going to be used, the applied pressure effects on the flux must be studied, hence the relationship of the applied pressure to the specific conversion can be obtained, and the system can be operated within the critical flux region.

CHAPTER 5:

IN-SITU GLUCOSE PRODUCTION AND PACKED BED BIOREACTOR FOR CELL FREE XANTHAN GUM PRODUCTION

5.0 INTRODUCTION

The glucose production in an ultrafiltration system discussed in Chapter 3, has been confirmed to be viable for production of a purified glucose solution. The strategies of low temperature SGLS in the ultrafiltration process discussed in Chapter 4 that offer pure and clean glucose may also serve as a basis for glucose pre-processing technology in biotechnology industries. The purpose of this study is to introduce a basic integration of glucose production by the ultrafiltration system with packed bed fermentation that is used for cell-free xanthan gum production. The packed bed fermentation will be used for development of the fed batch continuous recycle packed bed bioreactor. This new bio-reactor will be discussed briefly in Chapter 6 as a future study. The outcome of the process integration should be more efficient and reliable xanthan gum production without problems of relying to the quality and price of the glucose in the global market. It could also useful as a basis for continuous production of cell free xanthan gum from starch.

In this study, two main objectives are outlined; firstly is to compare parameters of biomass accumulation, glucose consumption and xanthan gum production using the glucose produced by the ultrafiltration system

called "in situ glucose production" and pure glucose purchased from a local chemical supplier, and secondly is to provide a basis for designing a new bioreactor used for continuous cell-free xanthan gum production. The continuous cell-free xanthan gum production will need further investigation and therefore it will not be included in this report.

5-1 WHY A NEW BIOREACTOR IS REQUIRED

Many attempts have been reported for optimising variables of xanthan gum fermentation, i.e. nutrient composition and feeding technique, temperature, pH, agitation, and adding antifoam [Evans *et al.* 1967; Davidson 1978; Souw & Demain, 1979; Vashitz & Sheintuch, 1991; Zhang & Greasham, 1999; Garcia-Ochoa *et al.* 1992, 1995; 1998; 2000; 2004; Casas *et al.* 2000; Lo Y.M. *et al.* 1997a; Amanullah *et al.* 1998; Letisse *et al.* 2001]. Some attempts have been made to use immobilised-cell cultures for production of xanthan gum [Yang et al. 1996; 1998] and other bacterial polysaccharides [Saude et al. 2002; Stavros et al. 2003]. All show some improvement in the area studied. Other substrates were also utilised [Glicksman, 1975; Charles and Radjai, 1977; El-Salam *et al.* 1993; Kalogiannis *et al.* 2003] but glucose is still the best in terms of product yield, supply, and quality [Leela and Sharma, 2000; Becker *et al.* 1998; Harding *et al.* 1995; Davidson, 1978]. Relatively, most of previous studies did not offer a significant price reduction of xanthan gum; therefore, this study will initiate new strategies to improve the xanthan gum processing and for significantly reducing the production cost.

Studying the conventional xanthan production, commercially available glucose powder will be diluted to 20-50g/litre and then sterilised together with other ingredients. The broth is fermented in a bioreactor by batch or continuous means and with several possible feeding techniques. Mixing is

the main problem in batch fermentation as the broth during production stage is very viscous. Agitation by mechanical stirrer would require a balance between the problems of cell disruption and oxygen transfer. Thus, it is suggested that the xanthan gum produced in the liquid phase should be continuously removed from the bioreactor. Furthermore, in the last few years, membrane processes have been increasingly used for concentrating high viscous broth [Pritchard, *et al.* 1995; Lo, *et al.* 1997b; Howell, *et al.* 1996]. Ultra-filtration was also reported to save up to 80% energy required for recovering of xanthan gum from fermentation [Lo, *et al.* 1997b]. This approach could solve the mixing problem by continuously remove the product and recycling the medium into the system but fouling by biomass may limit the application.

Giving the appropriate support, e.g. cotton wool and fabric, for micro-organisms growth may ensure a physical separation between the micro-organisms and the liquid phase containing nutrients and products. However, the specific xanthan productivity was reported lower in a Centrifugal Fibrous-Bed Bioreactor (CPBR) than in a STR because of relatively low cell viability (~60%) and oxygen transfer limitation in the CPBR [Yang et al. 1996]. Some xanthan gum is also required for cell adsorption onto the support [Yang et al. 1998], thus complete removal of xanthan gum would decrease the rate of cells adsorption and may increase fouling of the membrane. This suggests that only excess xanthan gum should be removed from bioreactor. The process could be effective by recycling medium across the membrane only during the production stage thereby avoiding membrane fouling caused by the cells.

The problem of oxygen transfer could require a new design of the bioreactor by simulating the natural environment of the *X. camprestris* where microbe is attached (e.g. cabbage plant). Therefore, bioreactor could be designed to allow free movement of liquid media and air passing through the

porous matrix (support) to ensure good contact with the cells that adsorb on the matrix support. This approach may improve oxygen transfer and microbes would continuously get fresh medium, hence this could increase reaction rate and also reduce mutation problems.

In this study, batch cell adsorptions on the packed and unpacked matrix supports were studied for cell-free xanthan gum fermentation using clean and purified glucose solution, controlled in-situ, and produced by the ultrafiltration process.

5-2. MATERIALS AND METHODS

5-2.1 Bacterial Strain

Xanthomonas campestris strain DSMZ (Deutsche Sammlung von Mikroorganismen und Zellkulturen GmbH) was used in this study. The dried pellet contained in a sterile glass ampoule was dehydrated in skimmed milk before streaking on the YDC agar plate. It was maintained in the YDC agar plate containing (g/litre) yeast extract 10, glucose 20, calcium carbonate 20, and agar-agar 20, pH 7.0 and was grown for 24 hours at 28^0C, and stored at 4^0C [Leela and Sharma, 2000 ; Chia and Lo , 2003]. The culture was transferred once in every two weeks to maintain good cell stability.

5-2.2 Inoculums Preparation

The seed culture of *Xanthomonas campestris* was prepared before fermentation process. This step is used to obtain the bacteria in a liquid environment (seed culture) before adding to the fermentation process in which the fermentation broth is liquid medium. 50 ml of the prepared culture

medium containing 10g/litre yeast extract, 20g/litre glucose, and 20g/litre calcium carbonate, adjusted to pH 7, was transferred into Erlenmeyer flasks, autoclaved, and then seeded with active colonies culture using a loop. The initial pH of each medium was adjusted to pH 7 by 1M NaOH solution. The Erlenmeyer flask was incubated at 200 rpm at 28 ^{O}C for 24 hours, and then was stored at 4 ^{O}C.

5-2.2 Preparation of Packed of Cotton Fibre

Cotton fibre was loosely packed into ϕ=5 mm tubes. The surface of the tube was finely slice to allow the cotton fibre in the middle of the tube is opened in contact with the medium and increases the oxygen transfer in the inner core of the packed cotton fibre. The tube with the packed cotton fibre was cut into 5 cm lengths.

5-2.3 Batch Fermentation of Packed and Unpacked Supports

25 ml medium in 125 ml Erlenmeyer flasks containing 30g/litre glucose solution produced by SGLS in the ultrafiltration process and the glucose purchased from a local chemical supplier, 3g/litre yeast extract, 2g/litre K_2HPO_4, and 0.1g/litre $MgSO_4.7H_2O$. Different packing strategies of cotton fibre were prepared as mention above. Unpacked and packed cotton fibres of 0.039 g-cotton per millilitre medium each were tested. The pH of the medium was initially adjusted to 7 by adding NaOH solution, and then was autoclaved. 2.5 ml seeding culture prepared as mention above was inoculated into 25 ml medium, and then flasks were incubated at 30^{o}C and 200rpm. Two flasks with packed and unpacked cotton fibre were taken everyday to measure the relative cell density and to recover the xanthan gum.

5-2.5 Cell Density Measurement and Xanthan Gum Recovery

The fermentation broth produced by the batch processes were diluted using distilled water to lower the viscosity, and then 20 ml aliquots were transferred into micro-centrifuge tubes. The micro-centrifuge tubes containing aliquots were centrifuged at 11,000 rpm for 30 minutes at 4 ^{0}C. After centrifugation, two fractions were formed, (1) supernatant containing xanthan gum and (2) biomass deposited as a pellet. Biomass pellets were weighed in pre-weighted micro-centrifuges tubes and the average value was used to show the relative performance of the cotton fibre in retaining the cells. Supernatants were mixed with 2/3 (v/v) isopropanol, re-centrifuged at 11,000 rpm for 45 minutes at 4 ^{0}C to completely precipitate xanthan gum before removing the solvent and water from the top portion. The precipitated xanthan gum collected from all samples was dried overnight in the oven at 50 – 60 ^{0}C in the pre-weighed micro-centrifuge tube. The concentration of xanthan gum was determined as the dry weight of xanthan gum per litre.

5-2.6 Glucose Analysis

Aliquots after dilution were filtered through a 0.2 μm using a syringe into vials. HPLC was used to determine glucose concentrations using the same procedure as described in Chapter 4.

5-3. RESULTS AND DISCUSSION

5-3.1 Sources of Glucose

Two experiments were conducted, using the glucose produced by SGLS in the ultrafiltration system, so called in-situ glucose production, and the glucose purchased from a local chemical supplier (Fisher Scientific). The

concentration of the depleted glucose, the biomass accumulation, and the xanthan gum production are shown in Fig 5-2 (c) and (d). As expected, results were effectively the same suggesting that the source of glucose for xanthan gum production was not affected by the method of the glucose production but the quality of glucose would affect xanthan gum production as indicated by many authors [Leela and Sharma, 2000; Becker *et al.* 1998; Harding *et al.* 1995;]. Nonetheless, in-situ glucose production could give different results of the xanthan gum quality if direct feeding of the produced glucose solution into bioreactor or mixing tank of bioreactor without prior sterilisation process is applied. This is due to the fact that unwanted reactions during sterilisation (e.g. Maillard reaction) may reduce the xanthan gum quality. As both glucose sources gave a significantly the same value of the measured variables (biomass accumulation, glucose consumption, and xanthan gum formation), and some difficulties were encounter in controlling contamination and also uncertainty of the quality of glucose produced in-situ, pure glucose purchased from the local chemical supplier (Fisher Scientific) was used to the rest of the experiments. The difficulties encountered when carrying out an integration process of the in situ glucose production and the xanthan gum fermentation studied in this experiment was occurred due to several batch fermentations were required to obtain the result which needs cleaning every time the system in fully integrated, however once the system has been fully working and run at a steady state, the integrated process was easy to control and free from contamination.

5-3.2 Glucose consumption

Lo *et al.* [1997a] and Amanullah *et al.* [1998] have proposed that sequence and simple pulse feeding of the glucose after nitrogen source has been exhausted in the growth phase would significantly improve xanthan gum production and reduce the time to reach the maximum xanthan gum production. Lo *et al.* [1997a] added 2.5% glucose solution after 34 hour

fermentation time while Amanullah *et al.* [1998] started adding by a single pulse after 30 hours. The glucose consumption pattern is shown in Fig. 5-1 and a comparison made in Fig 5-2(a). During the first 2 days fermentation, the glucose consumption was low, but from day 2 to day 4 the glucose concentration sharply decreased. After day 4 the concentration of glucose was very low and effectively became negligible after day 5. Sigmoid curves of the glucose consumption may suggest that inverse sigmoid feeding may be required during the growth phase but thereafter steady state feeding at an optimised glucose concentration should follow together with other nutrients for cells maintenance. These strategies may increase the productivity and could also be applicable for continuous fermentation.

5-3.2 Adsorption of Cells

Yang S-T *et al.* [1998] have studied different support materials and found that cotton terry cloth that has rough surfaces was the preferred material for cell adsorption. Cell adsorptions to cotton were also faster than polyester fibre. They also studied the adsorption kinetic of cells to fibres, and suggested a first order equation has been followed. Furthermore they also mentioned factors that affect cell adsorption. However, the packing strategy was not studied. In this work, cotton fibre at 0.039g/ml was used to determine the effectiveness of the relative cell adsorption and its effect on xanthan gum production by packed and unpacked strategies. Biomass measurements in the liquid medium would give relative adsorption of the cells by these two methods

Fig. 5-1 (a) and (b) show the results of batch fermentations by packed and unpacked support matrix of cotton fibre using 0.039 g-cotton/ml. Fig. 5-1 (d) shows the control experiment result of free-cells fermentation without the support matrix. Fig. 5-2 (a) (b) and (c) show the re-plots graph used for

comparison study side by side between the consumed glucose, the dry biomass concentration, and the xanthan gum concentration. As can be seen in Fig 5-2 (b), the relative cell adsorption after day 3 of batch fermentation was faster in the packed bed at < 0.25 g/litre biomass than unpacked cotton at < 0.37g/litre biomass, measured in the liquid medium. It gives approximately 78% and 67% reduction of the cell concentrations in the liquid medium by the packed and unpacked cotton fibres respectively compared to the cell-free fermentation. The reason could be due to the fact that the robustness of the packed porous matrix support has increased stability of the colonies in the inner core of the packed cotton fibre. After day 5, adsorption of the cell was relatively complete when taking into account the experimental error (< 0.05g/litre).

5-3.3 Xanthan Gum Production

As can be seen from the graphs in Fig. 5-1 and 5-2, Xantham gum production after day 4 (96 hours) obtained with free-cells fermentation was 19.5g/litre, whereas 15 g/litre xanthan gum were obtained by packed bed and 16 g/litre by unpacked bed cotton fibre. The reason for different xanthan gum production between cells-free xanthan gum fermentation, and fermentation by packed and unpacked cotton fibre could be because some xanthan gum product is trapped in the bed, giving a lower concentration in the liquid phase. The other reason could be due to low cell viability and oxygen transfer limitations in the inner core as reported for the Centrifugal Fibrous-Bed Bioreactor (CFBR) [Yang *et al.* 1996]. Yang *et al.* [1998] has also stated that immobilised cells could trap a large portion of the xanthan gum and could not easily be separated from the cells. Increasing operation time to 7 days showed that the packed bed, the unpacked bed, and the cell-free fermentations gave 21.1 g/litre, 20.8 g/litre, and 20.4 g/litre respectively which could be considered to be effectively the same taking into account experimental error.

Fig. 5-1(a): Packed Support Matrix

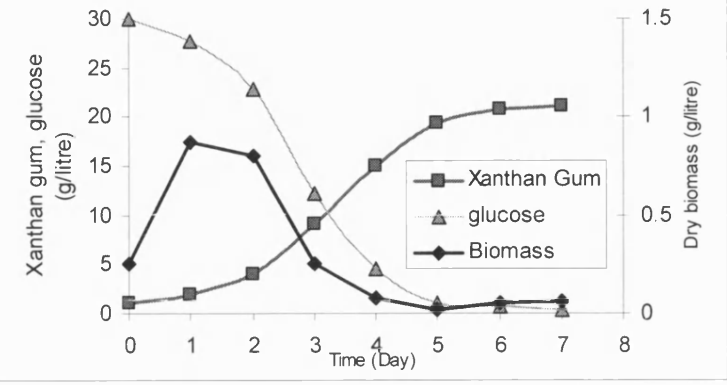

Fig. 5-1(b): Unpacked Support Matrix

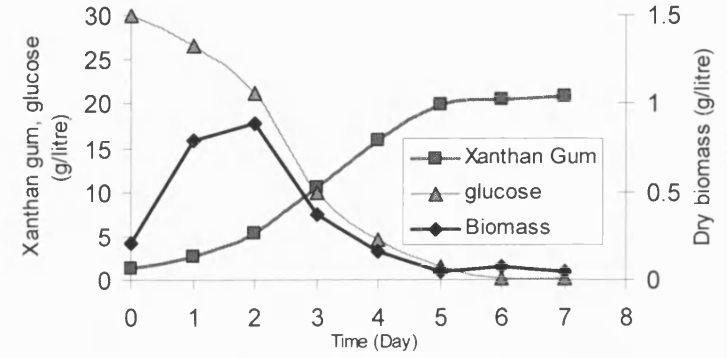

Fig. 5-1(c): Glucose by In-Situ Production

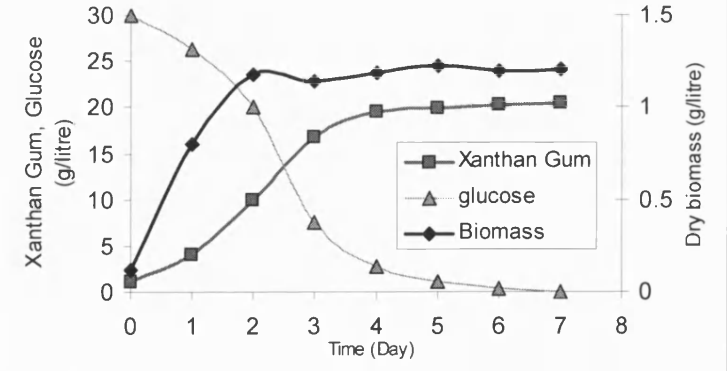

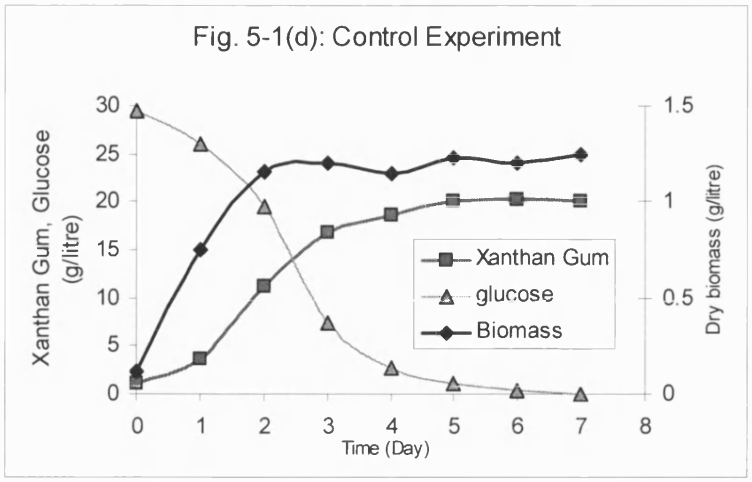

Fig. 5- 1: Curves of Xanthan gum, glucose, and biomass during Batch Fermentation. (a) Using packed matrix support and the glucose was purchased from Fisher Scientific, (b) Using unpacked matrix support and the glucose was purchased from Fisher Scientific (c) Free-cell fermentation using the glucose was produced in-situ and (d) Free cell fermentation (control experiment) using the glucose was purchased from Fisher Scientific.

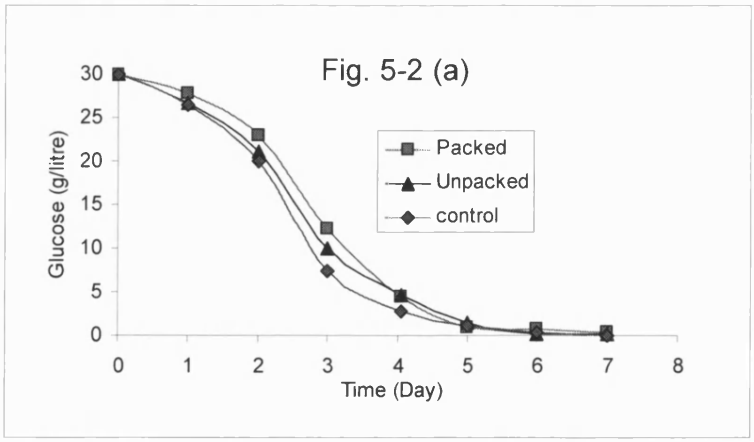

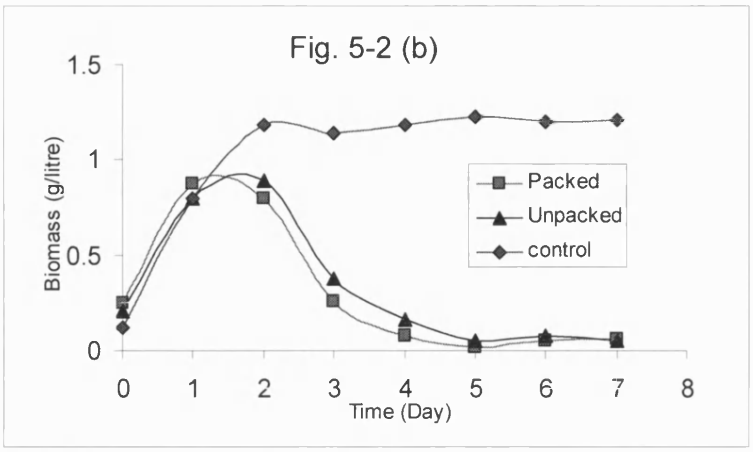

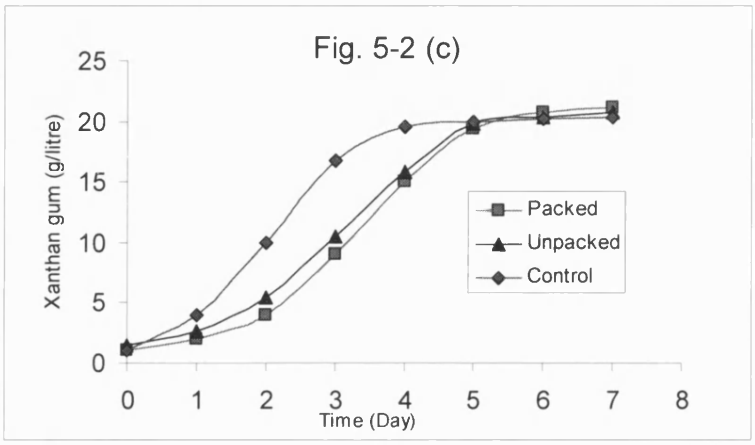

Fig. 5- 2: Comparison curves side by side for (a) glucose, (b) biomass and (c) xanthan gum.

5-4 CONCLUSION

Two sources of glucose, in-situ and pure glucose purchased from a local supplier were used for production of xanthan gum. It was found that both successfully produce xanthan gum with 68% glucose converted to xanthan gum over the period studied. Both sources of glucose also effectively showed the same monitored parameters (consumed glucose, biomass accumulation, and xanthan gum production) when treated by the same fermentation procedure. However, providing a clean process that

enable to eliminate contamination, direct feeding of in-situ glucose solution into bioreactor without prior sterilisation process should give a different result for the xanthan gum quality. This is due to the fact that the main purpose of sterilisation process in conversional process is to sterilise the medium. However, sterilisation will also produce complex by-products by un-wanted reactions that may reduce the xanthan gum quality. Therefore, comparison studies between sterilised and un-sterilised glucose is required for process integration between the glucose production in the ultrafiltration system and the continuous xanthan gum production to ensure xantham gum quality is maintained or improved..

Adsorption of the cells onto several different fibrous matrix supports was used by Yang *et al.* [1996:1998] but oxygen transfer limitations and cell viability reduced the specific productivity. The packing strategy was also not investigated. In this study, adsorption of the cells by different packing strategies of cotton fibre were investigated for cell-free xanthan gum production. The results have found that 0.039g/litre of unpacked and packed cotton fibres have completely adsorbed the cells after day 5 fermentation. The loosely packed bed cotton fibre in open surface tubes reported here could be the approach for development of a new bioreactor by permitting free movement of the nutrients and air.

5-5 FUTURE RESEARCH IN XANTHAN GUM PRODUCTION

As explained in the beginning of this work, xanthan gum production is one of applications that would benefit from glucose production by the SGLS in the ultrafiltration system. A simple integration of glucose production by the ultrafiltration system with conversional xanthan gum production could slightly reduce the production cost; however full control of the glucose quality is a huge advantage for this integration process.

In this chapter, the approach of integration of the glucose production in the ultrafiltration system and the xanthan gum production has been established and appears to be viable in terms of cost and process. The basic study of the bioreactor has been carried by Yang *et al.* [1996; 1998]. .However, future study will be needed on the bioreactor design for continuous production of cell-free xanthan gum. Although some problems have been reported such as cell mutation in continuous production, high viscosity limiting mass transfer, the literature review has outlined suggestions for overcoming these limitations. The proposal for a new bioreactor is discussed in Chapter 6.

CHAPTER 6:

CONCLUSION AND FUTURE STUDIES

6.0 CONCLUSION

The kinetic model and the optimisation of the SGLS of tapioca starch at a 1:1 ratio of α-amylase to Termamyl enzymes, and low temperature below 60^0C has been successfully studied. At the optimum condition, SGLS hydrolysis can convert by weight 65 % of tapioca starch to glucose. The viscosity of the SGLS was kept consistent below 2.2×10^{-3} pas throughout the hydrolysis. When the pH was monitored, the SGLS has self-regulated to the optimum pH particular to the hydrolysis time, thus optimising the enzymatic reactions particular to the pH required by the α-amylase and the AMG respectively.

The relative productivity of the SGLS was studied at different starch and enzymes concentrations and found that when the starch concentration is fixed to 100g/litre, the relative productivity was optimised at 0.6 ml/litre enzymes. Increasing the initial starch concentration and fixing the enzymes concentration would increase the relative productivity. However, at certain starch concentrations, the relative productivity was reduced which could be due to mass transfer limitations and the starch to water ratio is becoming insufficient [Tester and Sommerville 2000]. The relative productivity could be one of the useful tools for comparison and economy analysis studies when different systems and procedures are used. Studies of the enzyme activity at $T=55^0$C and one to one ratio of the amylase and AMG found that

high activity was reached when the enzymes concentration ranged between $0.6 \leq \sigma_{E_0^{mix}} < 0.9$ ml/litre and the starch concentration ranged between $100 \leq \gamma_{S_0} \leq 150$ g/litre.

The kinetic study of the SGLS that is based on the basic Michaelis-Menten kinetic Equation has a critical assumption used to mathematically derive the kinetic model, i.e. **"the balanced reactions of the gelatinisation and liquefaction and the gelatinisation is the limiting factor"**. Furthermore, the reaction temperature must be low, thus the saccharyfing enzymes (AMG) can be mixed and would react simultaneously. When the balance reaction between gelatinisation and liquefaction is assumed to occur during the SGLS hydrolysis, the intermediate substrate concentrations of the gelatinised and liquefied starches should be low, and considered negligible, thus the rate of the glucose formation will only rely on the gelatinisation rate or the saccharifying rate. Therefore the two reaction rates have produced two glucose formation models. The first model is based on the maximum production rate and the second model is based on the maximum glucose formation. As both the maximum production rate and the maximum glucose production are constant within certain conditions, both models should include a time function which decreases with the hydrolysis time. The time function models were also found to change with different enzymes and substrate concentrations; hence, the time functions that are coupled with the constant of the maximum glucose production and the maximum glucose formation which reduce with the hydrolysis time could represent the reduction of the enzymes activity. This is based on the fact that the enzymes activity changes with the enzymes and the starch concentrations. In order to calculate the glucose formation models, three parameters are required; (1) the maximum production rate, (2) the time to obtain half of the maximum glucose production, and (3) the maximum conversion.

To further evaluate the kinetic models, two new parameters of n and m are introduced which both depend on the concentration of the enzymes and the starch concentration. From the mathematical derivation shown in the kinetic model development, exp(n) represents the maximum production rate which is controlled by the concentration of the enzymes in the system, however the starch concentration must be sufficient to avoid mass transfer limitations and insufficient water to starch ratio [Tester and Sommerville 2000]. The value of m after transient phase (t/τ > ~1) that describes the enzymes activity is also affected by the starch concentration, making both the active enzymes and the starch concentration in the system affect the value of m. The experimental results has shown that high enzymes activity would give low value of m. The m value after the transient phase has also decreased with time, and the decreasing model follows the enzymes decay model. In this study, the value of m changes with time has been modelled, but the three unknown parameters of $k_S, k_g,$ and k_E are required. These three constants are calculated by the statistical methods of linearization least square analysis and non-linearization least square analysis. Finally, the kinetic of the glucose production has been successfully developed as shown in Fig. 3-14. A comparison of the developed glucose kinetic model that calculates the simulated glucose kinetic is verified by the experiment result, and the error was found to be less than 10%.

The temperature effect on the kinetic of the SGLS has been investigated. When the reaction temperature was increased from T=55 to 60^0C, the relative productivity and enzymes activity have increased by 24% and 50% respectively. Despite the increased of the productivity and the enzymes activity, reaction temperature cannot be increased more than 60^0C as it will limit the selection of the polymeric membranes, would increase the enzymes decay rate, and also increases viscosity of the reactant due to imbalanced reaction rates of the gelatinisation and liquefaction reactions.

Development of the ultrafiltration system was started with investigations of the membrane ability to separate between the product and the reactants. The permeate stream of the 30 kD polysulfone hollow fibre was analysed by the HPLC to determine the polysaccharides content and by the UV-visible spectrophotometer to scan the protein spectrum. The results found that the 30 kD polysulfone membrane module can retain most of the high degree polysaccharides and let pass the glucose with a purity >98% but the amylase enzymes were not completely rejected throughout the hydrolysis time. The enzymes permeation test carried out here is contrary with the result given by Paolucci-Jeanjean *et al.* [2000b] as they found that the Termamyl enzyme was completely rejected by a 50 kD ceramic membrane. However, the result here is supported by the work of Gupta R., *et al.*, [2003] that the amylase enzymes vary in size from 10 to 210 kD. To support the result that the 30 kD polysulfone membrane did not completely retain the amylase enzymes, a protein permeation test was carried out on a 5 kD ceramic membrane obtained from the same manufacturer and membrane material as was used by Paolucci-Jeanjean *et el.*, [2000b]. The protein permeation test result of the 5kD ceramic membrane showed that trace amounts of the protein spectrum was detected in the permeate stream. However, the protein spectrum detected was not confirmed as either active amylases or as a fraction of the lyses enzymes due to very low concentrations.

The ultrafiltration system used as a working system for the continuous process of the SGLS to produce clean glucose solution has been confirmed. The ultrafiltration system comprised a mixing tank, a pre-heating coil, a reaction tank, a settling tank, 30 kD polysulfone hollow fibre membrane module, and permeate tank together with pumps and controls. In this work, the result of w=10% starch milk, and the enzymes concentration at 6ml/kg-substrate showed that the ultrafiltration system has performed well when operated at low temperature of 55^0C and low applied pressure of 0.5 bars.

The permeate stream produced a steady state glucose concentration at 64 g/litre and at a constant flux of 14.5 litre/m^2-h over 9 hours operation. The constant flux suggests that the ultrafiltration system is able to continuously produce the glucose, and the membrane is not significantly fouled over the period studied. The conditions given above are still within the critical flux region as the flux has reached steady state after 3 hours operation, and the flux remained constant thereafter over the period studied. Additionally, extending the operation time would not decrease the flux but it would require the unproductive product to be removed, and addition of more enzymes may be required. The productivity has also increased by pre-heating of the substrate before feeding into the reactor as this strategy increases the amount of gelatinised starch in the system.

The other importance process variables are the applied pressure and the temperature. The applied pressure is generally responsive to control the concentration of glucose solution in the permeate stream. However, the upper limit of the critical flux must be determined; hence the process will run at steady state with constant residence time and will continuously produce certain glucose concentrations over long periods of operation. At a constant applied pressure, the temperature effect is found responsive on the flux rate pattern by changing the dynamic viscosity and the hydraulic resistance. The dynamic viscosity of the filtrate relies on the reaction rate while the hydraulic resistance may consist of the membrane resistance, and the gel layer and surface polarisation resistances. High operating temperature would increase the dynamic viscosity and it may also increase the gel layer resistance by increasing the gelatinised starch in contact with the membrane surface.

A comparison study of batch and continuous processes appears to support the proposal that continuous operation is better than the batch process. These facts were supported by fact that the continuous process has given high productivity and producing purified glucose. Increasing the

operation time of the continuous operation equivalent to the batch process may lead to an increase of productivity compared to the batch operation. Furthermore, as the continuous process of the SGLS using the ultrafiltration system produces pure glucose solution, no further purification process should be necessary.

Two sources of glucose, in-situ and pure glucose purchased from local chemical supplier have been tested for production of xanthan gum. Both sources have found successfully produce an effectively the same of the consumed glucose, the biomass accumulation and the xanthan gum production. The conversion of glucose to xanthan gum is ~68% over 120 hour fermentation time. Using the clean process that eliminates contamination, direct feeding of in-situ glucose solution into the bioreactor without prior sterilisation process is believed to give a better xanthan gum quality. This is due to the fact that the main purpose of the sterilisation process in conventional processes is to sterilise the medium. However, sterilisation will also produce complex by-products by un-wanted reactions that could impair the xanthan gum quality. Therefore, comparison studies between sterilised and un-sterilised glucose is needed to determine if integration between the glucose production in the ultrafiltration system and the continuous xanthan gum production is appropriate.

Adsorption of the cell onto several fibrous matrix supports were used by Yang *et al.* [1996:1998] but the oxygen transfer and the viability of the cells reduced the specific productivity. The packing strategy was also not investigated. In this study, adsorption of the cells by different packing strategies of the cotton fibre was investigated for cell-free xanthan gum production. The result found that 0.039g/litre of the unpacked and packed cotton fibre have effectively completed adsorbing the cells after day 5 of the fermentation. The loosely packed bed of the cotton fibre by the open surface

tube reported here could be a considerable advantage on development of the bioreactor by permiting free movement of the nutrients and air.

6.1. FUTURE STUDIES

The value of *m* has mathematically found its relationship as shown in Equation 3-49. However, the relationship uses an assumption that *m* is constant thus it does not change with hydrolysis time. This assumption might not be ideal as Equation 3-48 of $m = B\tau = \frac{k_2^{gel}}{(1-\alpha)}\tau$ shows that it depends upon the gelatinisation and the unproductive fraction. However, this Equation needs evaluations of the α value which changes with hydrolysis time. Moreover, the kinetic model of the glucose production uses the assumption that the first order gelatinisation rate velocity (k_2^{gel}) is constant throughout the hydrolysis as suggested by Tester and Sommerville [2000]. However, as a different system and process were used, the k_2^{gel} value could differ meaning that the low temperature kinetics of the gelatinisation reaction should be studied separately. A complete evaluation on those uncertainties should give the empirical relationship of *m* value with the parameters such as enzymes activity, starch concentration, and pH, which would change with hydrolysis time. Nevertheless, the value of *m* could correspond to the enzymes activity and the enzymes decay. By knowing exactly the relationship of *m* value, the future model of *m* value should be more universal and may simplify the model. The future model should reduce the number of unknown kinetic parameters, hence reducing the dependency on linearization least square analysis and non-linearization least square analysis as currently applied.

Future studies of the ultrafiltration system for continuous production of clean and sterile glucose should include an economic analysis to compare

conventional process and the ultrafiltration process for production of clean and sterile glucose. A small molecular weight cut off membrane may be helpful to improve the ability to retain the enzymes thus improving the quality of the produced glucose solution and could also improves long run operation performance. When a different membrane is used, the effect of applied pressure on the flux must be studied. This study will give the relationship of the applied pressure to the specific conversion. The system should also be operated within the critical flux region.

In this study, two strategies were introduced, (1) Settling tank used to retain unconverted starch and high degree polysaccharides, and (2) pre-heating of the substrate. Both approaches showed contribution to the success of the ultrafiltration system and the conversion rate. Therefore, a precipitation process and settling tank should be included in the SGLS. A pre-heating process that contributes in increased productivity should also be optimised., which also requires consideration of the gelatinisation reaction and the equipment used. These studies are required for scaling –up the ultrafiltration system, and should also help in sizing the down stream process.

The proposed bioreactor for the xanthan gum production is still in initial stage. Below is given a laboratory scale bioreactor setup, so called the fed batch continuous recycling packed bed bioreactor. Fig. 6.1 shows the schematic diagram of the proposed packed bed bioreactor. The packed bed bioreactor consists a column with the packed cotton fibre is arranged inside. Water is circulated through outer column to maintain the bioreactor temperature (e.g. 30^0C). Sterile air is introduced into the medium through a hole at the bottom of the reactor by a constant flow rate. Alternatively, the packed bed bioreactor may also be tested by using an improvise bioreactor as shown in Fig. 6.2.

Three operation stages are proposed; (1) cell growing stage (2) production stage and (3) product harvesting stage. Different flow rates of glucose should be studied to optimise the system. In first day, low glucose concentration of the media (1.5-2.5%) should be continuously recycled to enhance the cell growing. After day one (24 hours), the glucose is increased (2.5-5%) to enhance the xanthan gum production [Lo *et al.* 1997a; Amanullah *et al.* 1998]. After day 3, the product harvesting should begin as all cells should have effectively adsorbed onto the matrix support as indicated in the batch fermentation study. Adding an adsorption tower after the bioreactor may help to completely absorb the cells still in the nutrient phase. Harvesting the product can be done by a membrane filtration process and the fouling being reduced by the adsorption tower. The filtrate is re-circulated back to the mixing tank.

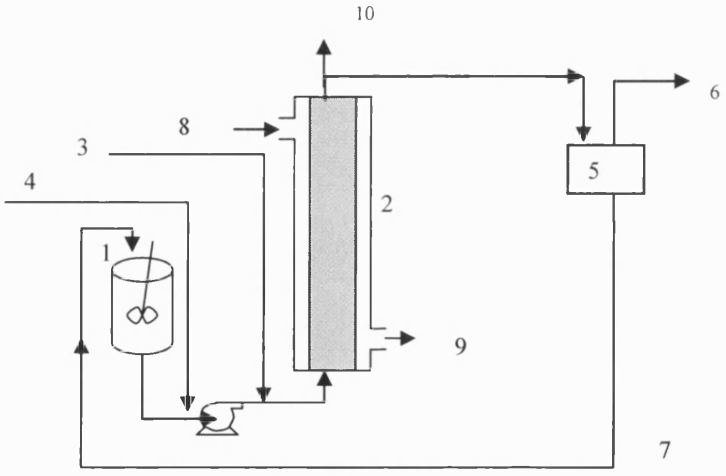

Fig. 6-1: Schematic Representation of Experiment setup. (1). Mixing tank with magnetic stirrer (2) Packed-bed bioreactor (3) Sterilized air (4) Inoculums (5) Membrane filter (6) Concentrated cell- free xanthan gum (7) Permeate substrate and medium recycled stream (8), (9). Water in and out and, (10) Air out.

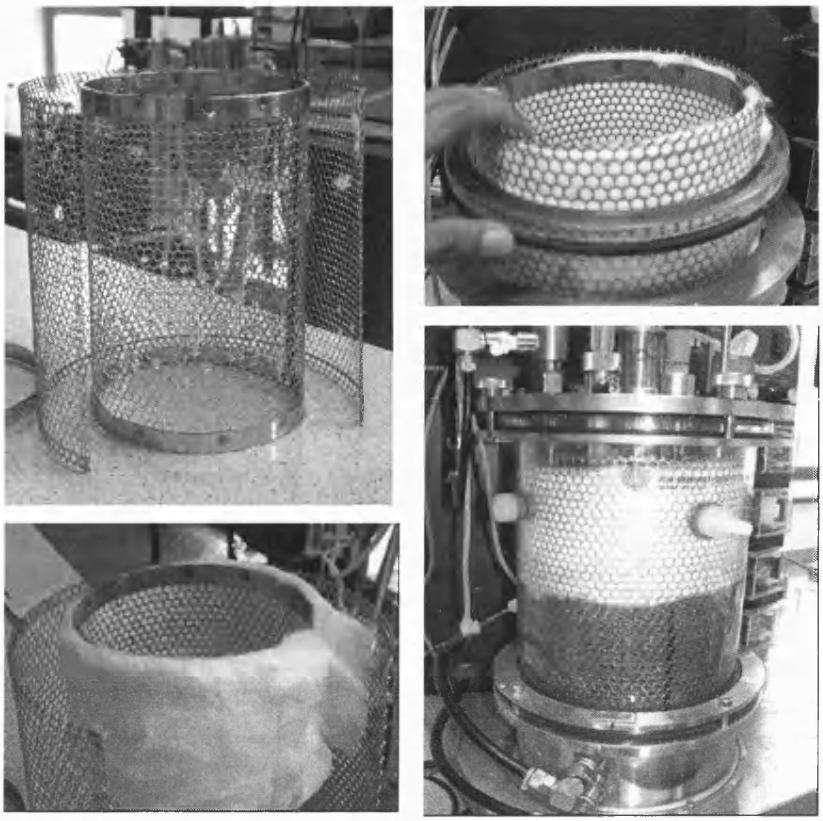

Fig. 6- 2: Example of the proposed bioreactor.

REFERENCES

Ahmet R. Özdural , D. Tanyolaç, Ismail H. B. M. Mutlu, C. Webb, [2003]; *Determination of apparent kinetic parameters for competitive product inhibition in packed-bed immobilised enzyme reactors,* Biochemical Engineering Journal, 14: 27-36.

Aimar P., C. Taddei, J.-P. Lafaille and V. Sanchez, [1988]; *Mass transfer limitations during ultrafiltration of cheese whey with inorganic membranes,* J. Membrane Sci., 38: 203-220.

Akerberg C, G. Zacchi, N. Torto, L. Gorton, [2000]; *A kinetic model for enzymatic wheat starch saccharification,* J. Chem. Technol. Biotechnol. 75: 306–314.

Akoum O., M. Y. Jaffrin, L-H Ding, [2005], *Concentration of Total Proteins by High Shear Ultrafiltration in a Vibrating Membrane Module*, Journal of Membrane Science, 247: 211-220.

Alavi S.H., K-H Chen , and S. S. H. Rizvi [2002]; *Rheological Characteristics of Intermediate Moisture Blends of Pregelatinized and Raw Wheat Starch*, *J. Agric. Food Chem. 50 :* 6740-6745

Amanullah A., Satti S., and Nienow A.W., [1998]: Enhancing *Xanthan Fermentations by Different Modes of Glucose Feeding*, *Biotechnol. Prog. 14:* 265-269

Atkinson B. and F. Mavituna [1991]; *Biochemical Engineering and Biotechnology Handbook,* 2nd. ed. Macmillan Publishers Ltd.

Atra R., G. Vatai, E. Bekassy-Molnar, A. Balint, [2005]; *Investigation of Ultra- and Nanofiltration for Utilisation of Whey Protein and Lactose,* Journal of Food Science, 67: 325-332.

Attafuah E., and G.M. Hall [1995]; *Preparation and evaluation of a low fouling ultrafiltration membrane made from a biopolymer*, Journal of Membrane Science, 108: 207-217.

Bailey J.E, D.F. Ollis [1986], Biochemical Engineering Fundamentals, 2nd ed., McGraw-Hill, New York. ISBN: 0070032122

Balows, A., and Trüper, H. G.,[1991]: *The Prokaryotes,* Springer-Verlag, NewYork.

Bayramoglu G., M. Yilmaz, M. Y. Arica [2004]; *Immobilisation of a thermostable α-amylase onto reactive membranes; kinetic characterisation and application to continuous starch hydrolysis*, Food Chemistry, 84: 591-599.

Becker A., Katzan F., Puhler A., and Ielpi L. [1998]: *Xanthan Gum biosynthesis and application: a biochemical/genetic prespective.* Applied Microbial Biotechnology 50:145-152.

Betlach, M.R., Capage D.H., Doherty D.H., Hassler R.A., Henderson N.M., Vanderslice R.W., Marrelli J.D., and Ward M.B., [1987]: *Genetically engineered polymers: Manipulation of xanthan gum biosynthesis*: 35-50. In Industrial Polysaccharides Genetic Engineering, Structure/Property Relations and Applications. M.Yalpani (ed.). Elsevier Science Publisher B.V., Amsterdam.

Blanch H. W., Papoutsakis E. T., and Stephanopoulos G., [1983]; *Foundations of Biochemical Engineering*, American Chemical Society, United States. ISBN: 0841207526.

Boom R.M., I.M. Wienk, T van den Boomgaard, C.A. Smolders, *Microstructures in phase-inversion membranes. Part 2. The role of a polymeric additive*, Journal of Membrane Science, 73: 277-292.

Brandama C., X.M. Meyer, J. Proth, P. Strehaiano, H. Pingaud [2003]; An original kinetic model for the enzymatic hydrolysis of starch during mashing, Biochemical Engineering Journal 13 : 43–52

Brotherton J.D., and Chau P.C., [1996]: *Modeling of Axial-Flow Hollow Fiber Cell Culture Bioreactors*, Biotechnol. Prog., 12 : 575-590

Buchtmann C, U. Kies, W-D. Deckwer, V. Hecht [1997]; *Performance of Three Phase Fluidized Bed Reactor for Quinoline Degradation on Various Supports at Steady State and Dynamic Conditions*, Biotechnology And Bioengineering, Vol. 56, No. 3.

Byong H. L., [1996]: *Fundamentals of Food Biotechnology*, VCH Publishers, Inc., United States.

Casas, J.A., V.E. Santos, F. Garcıa-Ochoa [2000], *Xanthan gum production under several operational conditions: molecular structure and rheological properties*, Enzyme and Microbial Technology 26: 282–291.

Charles, M. and Radjai M.K., [1977]: *Xanthan Gum from Acid Whey.* In Sandford

Chaturvedi B.K., AK. Ghosh, V. Ramachandhranb, M.K. Trivedi, M.S. HanTab, B.M. Misra [2001]; *Preparation, characterization and performance of polyethersulfone ultrafiltration membranes*, Desalination 133: 31-40.

Chen C., Huang Y.L., and Yang S.T., [2002]: *A fibrous-bed bioreactor for continuous production of developmental endothelial locus-1 by osteosarcoma cells*, Journal of Biotechnology Volume 97, Issue 1: 23-39.

Chia-Hua and Y.M. Lo: [2003]; *Characterization of xanthan gum biosynthesis in a centrifugal flux analysis*: Process Biochemistry 38: 1617-1625.

Chudacek M. W., and A.G. Fane, [1984]; *The dynamics of polarization in unstirred and stirred ultrafiltration,* J. Membrane Sci., 21 : 145-160.

Chiu T.Y and A.E. James [2005]; *Critical flux determination of non-circular multi-channel ceramic membranes using TiO_2 suspensions*, Journal of Membrane Science, Volume 254, Issues 1-2, 05, Pages 295-301

Dai Y., X. Jian, S. Zhang, M.D. Guiver [2001]; *Thermosable ultrafiltration and nanofiltration membrane from sulfonated poly (phthalazionone ether sulphone ketone)*, Journal of Membrane Science, 188: 109-203.

Davidson W. [1978]: *Production of polysaccharide by xanthomonas camprestris in continuous culture.* FEMS Microb Lett 3: 347-349.

De Vuyst, L., Vermiere, A., Van Loo, J., and Vandamme, E.J. [1987]: *Nutritional, physiological and process-technological improvements of xanthan gum fermentation process.* Mec. Fac. Landbouww. Rijkuniv. Gent. (52) : [1881-1900]

Dlmamini A.M., and Peiris P. S., [1997]: *Production of exopolysaccharide by pseudomonas sp. ATCC 31461 (Pseudomonas elodea) using whey as fermentation substrate*, Applied Microbiol Biotechnology 47: 52-57.

El-Salam A., Fadel M.A and Murad H. A., [1993]: *Bioconversion of sugarcane molasses into xanthan gum.* Journal of Biotechnology. 33:103-106.

Espinasse B., P. Bacchin, P. Aimar, [2002]; *On an experimental method to measure critical flux in ultrafiltration, Desalination*, 146: 9 l-96

Espinasse B., P. Bacchin, P. Aimar [2002]; *On an experimental method to measure critical flux in ultrafiltration*, Desalination 146: 9l-96.

Evans, C.G.T, Yeo, R.G. and Ellwood, D.C. [1967]: *Continuous culture studies on the production of extracellular polysaccharides by Xanthomonas juglandis.* In Berkeley, R.C.W., Gooday, G.W. and Ellwood, D.C. (pnyt.). *Microbial Polysaccharides and Polysaccharases:* 51-67. London: Academic Press Inc. (London) Ltd.

Feins M., and K. K. Sirkar, [2005]; *Novel Internally Staged Ultrafiltration for Protein Purificatio*, Journal of Membrane Science, 248: 137-148.

Field R.W., D. Wu, J.A. Howell, B.B. Gupta, [1995]; *Critical flux concept for microfiltration fouling*, J. Membr. Sci. 100: 259–272.

Flickinger F. C., and S. W. Draw., [1999]: *Encyclopedia of Bioprocess Technology: Fermentation,* vol 5 : 2706-2707

Fogarty W. M., and Kelly C. T., [1990]: *Microbial Enzymes and Biotechnology, second edition*, Elsevier Science Publishers Ltd., England. ISBN: 0853341850

Fu, J.-F., and Tseng Y.H., [1990]: *Construction of lactose-utilising Xanthomonas camprestris and production of xanthan gum from whey.* Applied Environment. Microbiol. (56): 919-923.

Fujii M, Kawamura Y. [1985]: *Synergistic action of a-amylase and glucoamylase on hydrolysis of starch.* Biotechnol Bioeng 27:260–265.

Gan Q, S.J. Allen, G. Taylor [2002]; *Design and operation of an integrated membrane reactor for enzymatic cellulose hydrolysis,* Biochemical Engineering Journal 12: 223–229.

Garcia-Ochoa, F., Santos, V.E, and Fritsch, A.P. [1992]: *Nutritional study of Xanthomonas campestris in xanthan gum production by factorial design of experiments.* Enzyme and Microbial Technology 14: 991-997.

Garcia-Ochoa, F., Santos, V.E, and Alcon A., [1995]: *Xanthan Gum Production: An unstructured Kinetic Model*, Enzyme and Microbial Technology 17: 206–217.

Garcia-Ochoa, F., Santos, V.E, and Alcon A., [1998]: *Metabolic Structured Kinetic Model for Xanthan Gum Production*, Enzyme and Microbial Technology 23: 75–82.

Garcia-Ochoa F., Go´mez Castro E., and Santos V.E. [2000]: *Oxygen transfer and uptake rates during xanthan gum production,* Enzyme and Microbial Technology 27: 680–690

Garcia-Ochoa, F., Santos, V.E, and Alcon A., [2004]: *Chemical Structured Kinetic Model for Xanthan Gum Production*, Enzyme and Microbial Technology 35: 284–292.

George A. B., [1997]: *Encyclopedia of Food and Color Additives*, volume III, CRC Press, Inc., United States.

Geremia R.A., Roux M., Ferreiro D. U., Dauphin-Dubous R., Lellouch A.C., and Ielpi L., [1999]: *Expression and biochemical characterization of recombinant AceA a bacterial α-mannosyltransferase*, Mol Gen Genet 261:933-940.

Giorno L, E. Drioli, G. Carvoli, A. Cassano, L. Donato [2001]; *Study of an Enzyme Membrane Reactor with Immobilized Fumarase for Production of L-Malic Acid,* Biotechnology And Bioengineering, Vol. 72, No. 1.

Glicksman, M., [1975]: *Gum Technology in the Food Industry.* New York: Academic Press Inc.

Godjevargova T., V. Konsulov, and A. Dimov, [1999]; *Preparation of an ultrafiltration membrane from the copolymer of acrylonitrile-glycidylmethacrylate utilised for immobilisation of glucose oxide*, Journal of Membrane Science 152: 235-240.

Goldberg I., and Williams R., [1991]: *Biotechnology and Food Ingredients*, Van Nostrand Reinhold, New York.

Gramer M.J., and Poeschl D.M., [1998]: *Screening Tool for Hollow-Fiber Bioreactor Process Development*, Biotechnol. Prog. 14: 203-209

Gupta R, P. Gigras, H. Mohapatra, V. K. Goswami, and B. Chauhan, [2003]; *Microbial α-amylases: a biotechnological perspective*, Process Biochemistry 38 :1599-1616.

Harding, N.E., Cleary, J.M. and Luis, L. [1995]: Genetics and Biochemistry of Xanthan Gum Production by *Xanthomonas campetris*. In. Hui, Y.H. and Khachatourians, G. *Food Technology Microorganisms:* 495-514. USA: John Wiley-VCH Inc.

Hashim M. A., (ed.], [1994]: *Bioproducts Processing – Technologies for the Tropics*, Institution of Chemical Engineers, UK.

Heertjes P.M., [1964]; *Filtration*, Trans. Inst. Chem. Eng., 42: T266-T274.

Hinkova A., I. Bohacenko, Z. Bubnik, M. Hrstkova, P. Jankovska, [2004]; *Mıneral Membrane filtration in refinement of starch hydrolysates,* Journal of Food Engineering, 61: 521-526

Houng J.Y., J.Y Chiou, K.C. Chen, [1992]; *Production of high maltose syrup using an ultrafiltration reactor,*Bioprocess Engineering. 8: 85.

Howell J.A, [1995]; *Sub-critical flux operation of microfiltration*, J. Membr. Sci. 107: 165-171.

Howell J.A.., Field R., and Wu D., [1996]: *Ultrafiltration of High-Viscosity Solutions: Theoretical Developments And Experimental Findings,* Chemical Engineering Science, Vol. 51, No. 9: 1405- 1415.

Hsu C. H., Martin Lo Y., [2003]: *Characterization of xanthan gum biosynthesis in a centrifugal,packed-bed reactor using metabolic flux analysis*, Process Biochemistry 00, : 1-9

Imeson and Alan, [1997]: *Thickening and Gelling Agents for Food*, 2nd edition, Blackie Academic and Professional, Great Britain.

Jean-Claude M G. T., Roland H F B. and Benedicte L T W., [1997]: *Production of xanthan gum by fermenting a feedstock containing a mixture of mannose and glucose*, Biotechnology Advances, Volume 15, Issue 1 , Page 267.

Jung B., [2004]; *Preparation of Hydrophilic polyacrylonitrile blend membranes for ultrafiltration*, Journal of Membrane Science, 229:129-136.

Kalogiannis S., Iakovidou G., Maria L. K.., Kyriakidis D.A., Skaracis G.N., [2003]: *Optimization of xanthan gum production by Xanthomonas campestris grown in molasses*, Process Biochemistry 00 :1-8

Kawai T, M. Nakamura, and K. Sugita [2001]; *High Conversion in Asymmetric Hydrolysis during Permeation through Enzyme-Multilayered Porous Hollow-Fiber Membranes*, Biotechnol. Prog. 17: 872-875.

Kerr, R.W. [1968]: *Chemistry and Industry of Starch.* New York: Academic Press Inc. Publishers.

Kennedy J. F., Jones P. B. SA, [1982]: *Factors affecting microbial growth and polysaccharide production during the fermentation of xanthomonas cmprestris culture.* Enzyme microbial technology 4: 39-43.

Kennedy, J.F. and Bradshaw, I.J. [1984]: *Production, properties and application of xanthan gum*, Prog. Ind. Microbial, 19: 319-371.

Kevin S. and Munir C., [1992]: *Hydrolysis of liquefied corn starch in a membrane reactor,* Biotechnology and Bioengineering, Volume 39, Issue 9: 960-967.

Khayet M, C.Y. Feng, K.C. Khulbe and T. Matsuura [2002]; *Preparation and characterisation of polyvinylidene fluoride hollow fibre membranes for ultrafiltration*, Polymer 43: 3879-3890.

Kimmerla K., and H. Strathmann [1990]; *Analysis of the structure determining process of phase inversion membranes*, Desalination 79: 283-203.

Kirchoff G.S.C., [1811]; Acad. Imp. Sci. St. Petersbourg, Memoires. 4: 27.

Konsula Z., M. Liakopoulou-Kyriakides, [2004]; *Hydrolysis of Starch by the action of an α-amylase from Bacillus subtilis*, Process Biochemistry, 39: 1745-1749.

Koops G.H., J.A.M. Nolten, M.H.V. Mulder, C.A. Smolders, [1994]; *Integrally Skinned Polysulfone Hollow Fibre Membrane for Pervaporation*, Journal of Applied Polymer Science, 54: 385-404.

Krishnaiah D., and Rosalam S., [2002]; *Potential of High Value Added Agro Based Commercial Products in Borneo,* Borneo Research Council – Seventh Biennial International Conference, 15-18 July, Universiti Malaysia Sabah.

Kumar N., and Das D., [2000]: *Production and purification of α- amylase from hydrogen producing Enterobector cloacae IIT-BT 08*, Biprocess Engineering 23: 505-208.

Lai J.-Y., F.-C. Lin, C.-C. Wang, [1996]; *Effect of non-solvent additives on the porosity and morphology of asymmetric TPX membrane*, Journal of Membrane Science, 118: 49-61.

Lee B.H., [1996]: *Fundamentals of Food Biotechnology*, VCH Publishers, Inc. United States.

Lee W.J, and B-R Min [1999]; *Improvement in Particle Separation by Hollow Fiber Flow Field-Flow Fractionation and the Potential Use in Obtaining Particle Size Distribution,* Anal. Chem. 71:3446-3452

Leela J. K., and Sharma G., [2000]: *Studies on xanthan production from xanthomonas camprestris*, Bioprocess Engineering 23: 687-689.

Letisse F, P. Chevallereau, J.L. Simon and N. D.Lindley [2001]: *Kinetic analysis of growth and xanthan gum production with Xanthomonas camprestris on sucrose, using sequentially consumed nitrogen sources*, Applied Microbioil Biotechnol, 55: 417-422.

Li S-G, G.H. Koops, M.H.V. Mulder, T.V.D. Boomgaard, C.A. Smolders, [1994]; *Wet spinning of integrally skinned hollow fiber membranes by a modified dual-bath coagulation method using a triple orifice spinneret,* J. Membr. Sci. 94: 329–340.

Lim L.H, D. G. Macdonald, G. A. Hill, [2003]; *Hydrolysis of starch particles using immobilized barley α-amylase,* Biochemical Engineering Journal 13: 53–62

Lindqvist K., and E. Liden, [1997]; *Preparation of Alumina Membranes by Tape casting and Dip Coating,* Journal of the Eupopean Ceramic Society 17: 359-366.

Linko Y. Y., and Javanainen P., [1996]: *Simultaneous Liquefaction, Saccharification and Lactic Acid fermentation on barley starch*, Enzyme and Microbial Technology, 19: 118-123.

Linton JD, [1990]: *The relationship between metabolite production and the growth efficiency of the producing organism.* FEMS Microbiol Rev 75: 1-18.

Liu Y., G.H. Koops, and H. Strathmann, [2003]; *Characterization of morphology controlled polyethersulfone hollow fibre membranes by the addition of polyethylene glycol to the dope and bore liquid solution*, Journal of Membrane Science, 223:187-199.

Lo Y.M., Yang S. T., Min D. B., [1996]: *Kinetic and feasibility studies of ultrafiltration of viscous xanthan gum fermentation broth*, Journal of Membrane Science 117: 237-249.

Lo Y. M., Yang S. T., and Min D. B, [1997a]: *Effects of Yeast Extract and Glucose on Xanthan Production and cells Growth in Batch Culture of Xanthomonas Camprestris*, A:I. Microbiol Biotechnol, 47: 689-694.

Lo Y.M., Yang S.T., and Min D.B., [1997b]: *Ultrafiltration of Xanthan Gum Fermentation Broth: Process and Economic Analyses*, Journal of Food Engineering, Volume 31, Issue 2 , February 1997, Pages 219-236

Loeb S., and S. Sourirajan, [1963]; *Sea water demineralization by means of an osmotic membranes*, Adv. Chem. Ser. 38: 117.

López-Ulibarri R., and Hall G.M., [1997]: *Saccharification of cassava flour starch in a hollow-fiber membrane reactor*, Enzyme and Microbial Technology Volume 21, Issue 6, 1 : 398-404.

Luong, J.H.T., Mulchandani, A. and Leduy, A. [1998]. *Kinetics of biopolymers synthesis: a revisit.* Enzyme and Microbial Technology 10: 326-333.

Luyten J., J. Cooymans, C. Smolders, S. Vercauteren, E.F. Vansart, R. Leysen, [1997]; Shaping of multilayer ceramic membranes by dip coating, J. Eur. Ceram. Soc. 17: 273.

Mahon H.I., [1966]; *Permeability separatory apparatus and membrane element, method of making the same and process utilizing the same,* US Patent 3,228,876, Dow Chemical.

Malaisamy R, D. R. Mohan, and M. Rajendran [2002]; *Polyurethane and Sulfonated Polysulfone Blend Ultrafiltration Membranes*, J. Col. and Interface Sci. 254: 129-140.

Malik V.S., and PSridhar, [1992]: *Industrial Biotechnology*, Oxford and IBH Publishing Co. Pvt. Ltd., New Delhi.

Marchal L. M., A. M. J. van de Laar, E. Goetheer, E. B. Schimmelpennink, J. Bergsma, H. H. Beeftink, J. Tramper [1999], *Effect of Temperature on the Saccharide Composition Obtained after α-Amylolysis of Starch*, Biotechnology and Bioengineering, Vol. 63, No. 3.

MacGregor A. W, S. L. Bazin and S. W. Schroeder, [2002]; *Effect of Starch Hydrolysis Products on the Determination of Limit Dextrinase and Limit Dextrinase Inhibitors in Barley and Malt*, Journal of Cereal Science 35: 17–28

Martin Lo Y., D. Cao, S. Argin-Soysal, J. Wang, T-S Hahm, [2005]; *Recovery of protein from poultry processing wastewater using membrane ultrafiltration*, Bioreource Technology 96: 687-698.

Meindersma G.W, J. Augeraud, F.H.P. Vergossen [1997]; *Separation of a biocatalyst with ultrafiltration or filtration after bioconversion*, Journal of Membrane Science 125: 333-349.

Montesinos T., and Navarro J.M., [2000]: *Role of the maltose in the simultaneous-saccharificationfermentation process from raw wheat starch and saccharomyces cervisiae,* Bioprocess engineering 23: 319-322.

Moraine, R.A, and Rogovin, P, [1971]: *Xanthan biopolymer production at increased concentration by pH control*, Biotechnol. Bioeng,(13): 381-391.

Nagpal S, S. Chuichulcherm, L. Peeva, and A. Livingston [2000]; *Microbial Sulphate Reduction in a Liquid–Solid Fluidized Bed Reactor*, Biotechnology and Bioengineering, Vol. 70, No. 4.

Nakajima M., T. Shoji, H. Nabetani [1992]; Process Bio chem, *A forced flow membrane enzyme reactor for sucrose inversion using molasses* 27:155.

Nakao S., T. Nomura and S. Kimura, [1984]; *Characteristics of macromolecular gel layer formed in tubular ultrafiltration membrane*, AIChE. J., 25: 115-124.

Noordman T.R., A. de Jonge, J.A Wesselingh, W.Bal, M.Dekker, E.Ter Voorde, S.D. Grijpma, [2002]; *Application of fluidised particles as turbulence promoters in ultrafiltration improvement of flux and rejection*, Journal of Membrane Science 208: 157-169.

Ozbek B, S. Yuceer, [2001]; *α-Amylase inactivation during wheat starch hydrolysis process*, Process Biochemistry 37: 87–95

Pala P, S. Datta, and P. Bhattacharya, [2002]; *Multi-enzyme immobilization in eco-friendly emulsion liquid membrane reactor—a new approach to membrane formulation,* Separation and Purification Technology 27: 145–154

Paolucci-Jeanjean D., Melleville M.P., Rios G.M., [1999]: *Nadine Zakhia, Why on Earth Can People Need Continuous Recycle Membrane Reactors for Starch Hydrolysis? Starch/Stärke* 51 1, p. 25.

Paolucci-Jeanjean D., Belleville M.P., Zakhia N., Rios G.M., [2000a]*: Kinetics of Cassava Starch Hydrolysis with Termamyl® Enzyme,* Biotechnology And Bioengineering, Vol. 68, No. 1.

Paolucci-Jeanjean D., Melleville M.P., Rios G.M., and Zakhia N., [2000b]: *The effect of enzyme concentration and space time on the performance of a continuous recycle membrane reactor for one-step starch hydrolysis*, Biochemical Engineering JournalVolume 5, Issue 1, : 17-22

Paolucci-Jeanjean D., Melleville M.P., Rios G.M., and Zakhia N., [2000c]: *Kinetics of continuous starch hydrolysis in a membrane reactor,* Biochem. Eng. Journal, Volume 6, Issue 3: 233-238

Paolucci-Jeanjean D., M-P Belleville and G. M. Rios, [2001]; *A comprehensive study of the loss of enzyme activity in a continuous membrane reactor – application to starch hydrolysis,* Journal of Chemical technology and Biotechnology 76:273-278

Papi1 R. M., Ekateriniadou1 L.V., Beletsiotis E., Typas M.A., and Kyriakidis D.A, [1999]: *Xanthan gum and ethanol production by Xanthomonas campestris .and Zymomonas mobilis from peach pulp*, Biotechnology Letters 21: 39–43, 39

Perea A and U. Ugalde [1996]; *Continuous hydrolysis of whey proteins in a membrane recycle reactor*, Enzyme and Microbial Technology Volume 18, Issue 1: 29-34.

Phillips G.O., Wedlock, D.J. and Williams, P.A., [1986]: *Gums and Stabilisers for the Food Industry 3*, Elsevier Applied Science Publishers Ltd., London

Pons, A, Dussap, C.G., and Gros, J.B. [1989]: Modelling Xanthomonas Camprestris batch fermentation in bubble column. Biotechnol. Bioeng. (33): 394-405.

Pollock and Thorn, [1987]: A method of increasing xanthan gum production and decorating the product, US patent number 233019A2.

Porter M.C. [1972]; Industrial Engineering Chem. Production Res. Develop., 11(3): 234.

Prazeres D.M.F and J. M. S. Cabral [1994]: *Enzymatic membrane bioreactors and their applications,* Enzyme and Microbial Technology Volume 16, Issue 9: 738-750.

Pritchard M., Howell J.A., Field R.W., [1995]: *The ultrafiltration of viscous fluids*, Journal of Membrane Science 102: 223-235

Qin J-J., M. H. Oo, Y. Li; [2005]; *Development of high flux polyethersulfone hollow fibre ultrafiltration membrane from a low critical solution temperature dope via hypochlorate treatment*, Journal of Membrane Science, 247: 137-142.

Rakib S., M. Sghyar, M. Rafiq, A. Larbot, L. Cot, [2001]; *New porous ceramics for tangential filtration*, Sep. Purif. Technol. 25: 385.

Reeve, [1992]; *A., Starch Hydrolysis: Process and Equipment*, Worldwide technology, Production and Application, VCH Publisher UK, Ltd.

Rosalam S. and England R., [2004]: *Critical Review of Membrane Bioreactor Systems Used for Continuous Production of Hydrolysed Starch*, Chem. Biochem. Eng. Q. 18 (2): 73-76

Sablani S.S., M.F.A. Goosena, R. Al-Belushi, M. Wilf, [2001]; *Concentration polarization in ultrafiltration and reverse osmosis: a critical review*, Desalination 141: 269-289

Saffaj N, S. Alami Younssi, A. Albizane, A. Messouadi, M. Bouhria, M. Persin, M. Cretin, A. Larbot, [2004]; *Preparation and characterization of ultrafiltration membranes for toxic removal from wastewater*, Desalination 168: 259-263.

Saroja N. R., and Rudrapatnam N.T [2000]: *In Vitro amylolytic degradation of natural and graft copolymerised cassava and potato starch*, Eur Food Res Technol, 211: 411- 414.

Saude, N., Chèze-Lange, H., Beunard, D., (2002): *Alginate production by Azotobacter Vinelandii in a membrane bioreactor.* Process Biotechnology 38: 273-278.

Schreyer H.B, and R. W. Coughlin [1999]; *Effects of Stratification in a Fluidized Bed Bioreactor During Treatment of Metalworking Wastewater*, Biotechnology And Bioengineering, Vol. 63, No. 2.

Schwartzberg H. G., and Rao M. A., [1990]: *Biotechnology and Food Process Engineering*, Marcel Dekker, Inc., United States.

Seffaja N., S. Alami Younsi, M. Persinb, M. Cretin, A. Albizanea, and A. Larbot [2005]; *Processing and characterization of TiO2/ZnAl2O4 ultrafiltration membranes deposited on tubular support prepared from Moroccan clay*, Ceramics International 31: 205–210.

Sims A. K and C. Munir [1992]: *Hydrolysis of liquefied corn starch in a membrane reactor*, Biotechnology and Bioengineering, Volume 39, Issue: 960-967.

Slominska L., and A. Grzeskowiak-Przywecka, [2004]; *Study on the Membrane Filtration of Starch Hydrolysates,* Desalination 162: 255-261.

Smith, C. L., R. W. Pike, and P. W. Murrill, [1970]; *Formulation and Optimisation of Mathematical Models,* International Textbook Company, The Haddon Crafsmen, Inc., Scranton, Pennsylvania. ISBN: 0700222456

Smith J.W. and D.H. King [1975]; *Electrochemical wall mass transfer in liquid particulate systems,* Cal. J. Chem. Eng. 53: 41-47

Smolders C.A., A.J. uvers, R.M. Boom, I.M. Wienk, [1992]; *Microstructure in phase-inversion membrane. Part 1. Formation of microvoids,* Journal of Membrane Science, 73: 259-275.

Souw P, Demain AL [1979], *Nutritional studies on xanthan gum production by xanthomonas camprestris NRRL B1459.* Appl Environment Microbiol 37: 1186-1192.

Stavros Kalogiannis, Gesthimani ,I, Maria L.K, Dimitrios A.K and George, N.S: (2003): *Optimization of xanthan gum production by Xanthomonas campestris grown in molasses*, 39: 249-256.

Sutherland, I.W. [1977]: Microbial Exopolysaccharide Synthesis. Dlm. Sandford, P. A. and Laskin, A. *Extracellular Microbial Polysaccharides*: 40-57. USA: American Chemical Society.

Tait MI, Sutherland IW, Sturman [1986], C. Effect of growth conditions on the production, composition and viscosity of *Xanthomonas campestris* exopolysaccharide. J Gen Microb 132:1483–92.

Terashima M., Hosono M., and Katoh S., [1997]: *Functional roles of protein domains on rice α- amylase activity.* Appl Microbiol Biotechnol, 47: 364-367.

Tester R.F., and M. D. Sommerville [2000]; *Swelling and Enzymatic Hydrolysis of Starch in Low Water Systems, Journal of Cereal Science* 33: 193–203.

Van Gestel T., C. Vandecasteele, A. Buekenhoudt, C. Dotremont, J. Luyten, R. Leysen, B. Van der Bruggen, G. Maes, [2002]; *Alumina and titania multilayer membranes for nanofiltration: preparation, characterization and chemical stability*, J. Membr. Sci. 207: p73.

Van't Hof J.A., A.J. Reuvers, R.M. Boom, H.H.M. Rolevink, C.A. Smolders, [1992]; *Preparation of Asymmetric Gas Separation Membranes with High Selectivity by a Dual-Bath Coagulation Method*, Journal of Membrane Science, 70: 17-30

Vashitz O, Sheintuch M [1991], Analysis of polymer synthesis rates during steady state growth of x.camprestris. Biotechnol Bioeng 37: 383-385.

Vedpal S. M. and Sridhar P., [1992]: *Industrial Biotechnology*, Oxford and IBH Publishing Co. Pvt. Ltd., New Delhi.

Vilker V., C.K. Colton, K.A. Smith and D.L. Green, [1984]; *The osmotic pressure of concentrated protein and lipoprotein solutions and its significance to ultrafiltration*, J. Membrane Sci., 20:63-77.

Weiss, R.M. and Ollis, D.F, [1980]: *Extracellular microbial polysaccharides. Substrate, biomass, and product kinetic equations for batch xanthan gum fermentation.* Biotechnol. Bioeng (22): 859-873.

Weir M.R., E.Rutinduka,C.Detellier,C.Y. Feng, Q.Wang,T.Matsuura, R. Le VanMao, [2001]; *Fabrication, characterization and preliminary testing of all*

inorganic ultrafiltration membrane made of a naturally occurring sepiolite clay mineral, J. Membr. Sci. 182: p41.

Wienk I.M., H.A. Teunis, T. van den Boomgaard, C.A. Smolders, [1993]; A *New Spinning Technique for Hollow Fibre Ultrafiltration Membranes*, Journal of Membrane Science 78: 93-100.

Wijmans J.G., S. Nakao, J.W.A. Van den Berg, F.R. Troelstra and C.A. Smolders, [1985]; *Hydrodynamic resistance of concentration polarization boundary layers in ultrafiltration,* J. Membrane Sci., 22 :117-135.

Wijmans J.G., S. Nakao and C.A. Smolders, [1984] *Flux limitation in ultrafiltration: osmotic pressure model and gel layer model,* J. Membrane Sci., 20: 615-622.

Wu D., J.A. Howell, R.W. Field, [1999]; *Critical flux measurement for model colloids*, J. Membr. Sci. 152: 89–98.

Xu Z-K, L-Q Shen, Q. Yang, F. Liu, S-H Wang, and Y-Y Xu [2003]; *Ultrafiltration hollow fibre membranes from poly(ether imide): preparation, morphologies, and properties,* Journal of Membrane Sci. 223: 105-118.

Yang S. T, Lo Y. M. and Min, D. B., [1996]: *Xanthan Gum Fermentation by Xanthomonas campestris Immobilized in a Novel Centrifugal Fibrous-Bed Bioreactor.* Biotechnology Progress 12: 630-637.

Yang S. T., Lo Y.M., and Chattopadhyay D., [1998]: *Production of Cell-Free Xanthan Fermentation Broth by Cell Adsorption on Fibers.* Biotechnology Progress 14: 259-264.

Yasunishi A, M. Fukuma, K. Muroyama [1988]: *Wall-to-liquid mass transfer in packed and fluidised beds with gas-liquid co-current up-flow*, J. Chem. Eng. Jpn. 21: 522-528.

Yoo S. D., and Harcum S. W. [1999], *Xanthan gum production from waste sugar beet pulp*, Bioresource Technology Volume 70, Issue 1 , Pages 105-109

Yoshida T., and Tanner R.D., [1993]: *Bioproducts and Bioprocess 2*, Springer-Verlag Berlin Heidelberg, Germany.

Yoshikatsu Murooka and Tadayuki Imanaka, *Recombinant Microbes for Industrial and Agricultural Applications*, Marcel Dekker, Inc., United States, 1994.

Zhang and Greasham, [1999]: *Chemically defined media for commercial fermentations*, Applied Microbiol Biotechnol, 51: 407-421.

Zhang S., X. Jian, Y. Dai, [2005], *Preparation of Sulfonated poly (phthalazionone ether sulphone ketone) composite nanofiltration membrane,* Journal of Membrane Science, 246: 121-126.

APPENDIX 1

A STANDARD CALIBRATION CURVE FOR GLUCOSE DETERMINATION BY HPLC

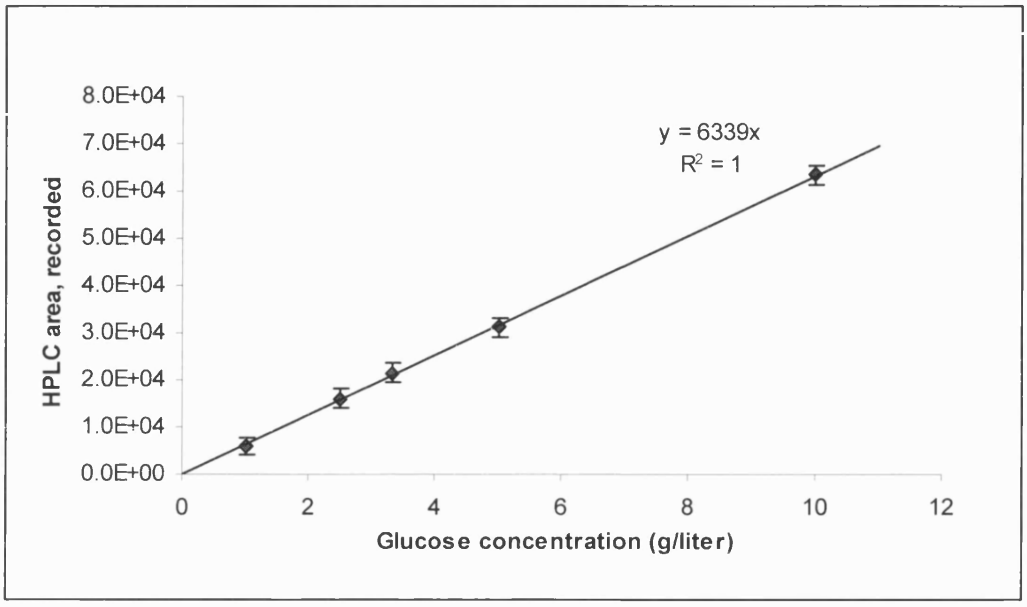

APPENDIX 2

ERROR ESTIMATION OF THE SAMPLING AND THE FLOW RATE DURING EXPERIMENTS.

1. *Error estimation for glucose concentration measurements*

Possible error by a single injection of the sample to HPLC: ± 0.5

Number of repeated injection per sample : 3

Error estimated from the glucose standard curve:

$= \pm 0.5/3$

$= \pm 0.17$ g/litre

Standard curve error : ± 0.17 g/litre

Dilution factor : 10 (increases possible error)

No of experiment repeated : 3 (reduce the error)

Accumulated Error : $\pm 0.17x10/3$

± 0.56g/litre

The accumulation error for the glucose concentration for the whole analysis is $\gamma_{glucose} \pm 0.56$ g/litre.

2. *Estimation Error for the flux (permeate) measurement*

$$\text{Flux} = \frac{\text{Flow rate}}{\text{Membrane area}}$$

Since the membrane area is a fixed value given by the manufacturer, assuming that the area has a significantly very small to compare to the

membrane area thus the possible flux error at the particular time will be only come from the permeate flow rate measurement.

$$\text{Permeate flow rate} = \frac{\text{Volume of sample}}{\text{Time is required to collect 20 ml sample}}$$

As the sample collection done by fixing the volume to collect 20 ml of the sample, thus the sample volume is the main factor of the possible flux error.

Error of the volume of the collected permeate stream = ± 0.5 ml
Number of experiment repeated = 3 (reduces possible error)
The average measurement error = $\pm 0.5/3$ = ± 0.17 ml or that was approximately 0.83%.

Since the flow rate of the permeate stream depends upon the time required to collect 20 ml of the sample thus the possible flux error that relates to the flow rate also changes with the time required to collect 20 ml sample. Low flux will give less error while high flux will give high possible error. The error calculated here is the highest possible error given by a high flux during the experiment.

$$\text{The possible flow rate error} = \frac{V \pm \delta V}{t_{20ml}}$$

Where V= volume of samples = 20 ml, δV = 0.17ml, and t_{20ml} time is required to collect 20 ml sample. In this study, the highest flow rate error was given when TMP = 1 bar and the lowest time recorded was 17.16s.

$$\text{The highest flow rate error} = \frac{V \pm 0.17}{17.16} = F \pm 0.01 \text{ ml/s} = F \pm 0.036 \text{ litre/h}$$

The experiment error also relates to the membrane surface area, increasing the membrane surface will reduce the experimental error. The membrane area used was 0.1 m^2 thus,

$$\text{The highest flux error} = \pm\frac{0.036}{0.1}$$

$$= F \pm 0.036\ \frac{litre}{m^2 \cdot h}$$

APPENDIX 3

RELATED LISTS OF PUBLISHED, SUBMITTED, WAITING LIST, PROCEEDINGS, AND PRESENTATIONS

JOURNALS

1. Rosalam S, R. England, *Critical Review of Membrane Bioreactor Systems Used for Continuous Production of Hydrolysed Starches*, Chem. Biochem Eng. Q. 18(2) 73-76 (2004).
2. Rosalam S. & England R. *Review of Xanthan Gum from Unmodified starches by Xanthomonas comprestris sp.* Enzyme and Microbial Technology (2005). Article in Press.
3. Rosalam S. & England R. *Review of the Transport Mechanism and Preparations of the Membrane in the Ultrafiltration Process, Article waiting for submission.*
4. Rosalam S. & England R. *Starch Hydrolysis by Low Temperature Simultineous, Gelatinisation, Liquefaction And Saccharification (SGLS), Submitted to* Chem. Biochem Eng. Q (2005).
5. Rosalam S. & England R. *The Kinetic of Gelatinisation, Liquefaction, and Saccharification Reactions (SLGS),* Submitted to Process Biochemistry (2005) – Part 1.
6. Rosalam S. & England R. *Optimisation of the Simultineous, Gelatinisation, Liquefaction and Saccharification (Sgls).* Submitted to Process Biochemistry, (2005) – Part 2.
7. Rosalam S.& England R. *Ultrafiltration for Continuous Separation of Glucose Solution By Simultineous Gelatinisation Liquefaction And Saccharification (SGLS)-Part 1.(waiting for submission).*
8. Rosalam S. & England R.: *Effects of the Applied Pressure, Temperature and Pre-Heating Process on the Simultineous Gelatinisation Liquefaction and*

Saccharification (SGLS) in the Ultrafiltration System-Part 2. (Waiting for submission)

9. Rosalam S. & England R.: *In-Situ Glucose Production and a Packed Bed Strategy for Cell Free Xanthan Gum Production – (waiting for submission)*

.

PROCEEDINGS

1. Rosalam S., & R. England (2003): *How the practical process is developed for continuous production of high grade xanthan gum from unmodified starch*, Proceedings of International Conference on Chemical and Bioprocess Engineering, pp. 980-985, Malaysia.
2. Rosalam S., A. Bono, B. Arifin, D.Krisnaiah, M. Rajin (2003): *Effects of Different Carbon Sources in Xanthan Gum Production in Batch Culture.* Proceedings of International Conference on Chemical and Bioprocess Engineering, pp. 1033-1038, Malaysia.
3. Rosalam S., S. Abang, B. Arifin, D. K. and L. C. Ling, *Rheological Characteristics of Hydrolysed Tapioca Starch,* International Conference on Chemical and Bioprocess Engineering, August 27-29th 2003: vol.(1):483-487.

PRESENTATIONS

1. Euro Membrane (2004), Sept 28-Oct first, Hamburg Germany. *Continuous and Simultaneous Acting of Gelatinisation, Liquefaction, and Saccharification in the Hollow Fibre Membrane Reactor System.*(Poster presentation)
2. The young engineer competition (SET) (Dec 2003), *Continuous and Simultaneous Gelatinisation, Liquefaction, and Saccharification in a Hollow Fiber Membrane Reactor System,* House of Common, London (Poster Competition).

3. Fermentation and Bio-processing Conference, 18 & 19 April 2002, Melbourne Australia. *Kinetics of Xanthan Gum Production Using Hydrolysed Tapioca Starch as the Carbon Source.* (Oral presentation).
4. International K-Starch 2001 Conference, Kota Kinabalu, Sabah, Malaysia. *Enhancement of Pure Culture Fermentation Process of Xanthan Gum Using Xanthomonas Comprestris*. (Invited speaker)